The Systematics and Evolution of Neotropical Bellflowers

(Campanulaceae: Lobelioideae)

A dissertation presented

by

Laura Penelope Lagomarsino

to

The Department of Organismic and Evolutionary Biology

in partial fulfillment of the requirements

for the degree of

Doctor of Philosophy

in the subject of Biology

Harvard University

Cambridge, Massachusetts

June 2015

© 2015 Laura Penelope Lagomarsino

All rights reserved.

Dissertation Advisor: Professor Charles C. Davis

Laura Penelope Lagomarsino

The Systematics and Evolution of Neotropical Bellflowers (Campanulaceae: Lobelioideae)

Abstract

The Andean mountain chains of South America are home to exceptionally high levels of biodiversity, including one-sixth of all plant species. Among them, the 550 species in the Neotropical bellflower clade (Campanulaceae: Lobelioideae) represent one of the single largest endemic radiations. In this dissertation, I perform a series of studies, ranging from alpha taxonomy to phylogenetic comparative biology, to understand this group's evolution.

In Chapter 1, I resolve phylogenetic relationships of the Neotropical bellflowers from five plastid DNA regions using maximum likelihood and Bayesian inference. This phylogeny greatly improves the resolution within this group and highlights the need for taxonomic revisions. My results demonstrate that the majority of species of *Centropogon*, *Burmeistera*, and *Siphocampylus* together form a primarily mainland Neotropical clade, collectively termed the centropogonids. Within the centropogonids, I identify high support for the monophyly of *Burmeistera* and the polyphyly of *Centropogon* and mainland *Siphocampylus*. Caribbean *Siphocampylus*, however, group with other Caribbean lobelioid species. Ancestral character state reconstruction identifies a dynamic pattern of fruit evolution within the centropogonids, which underscores the difficulty of diagnosing broad taxonomic groups on the basis of fruit type. Finally, we identify that the centropogonids form a Pan-Andean radiation with broad habitat diversity, which sets the stage for a subsequent chapter in my thesis (Chapter 4).

In Chapters 2 and 3, I describe four species of centropogonids as new to science. In Chapter 2, two species of *Burmeistera* from the Cordillera de Talamanca are described: *B. serratifolia* Lagom. & D. Santam., endemic to Panama, and *B. monroi* D. Santam. & Lagom., from both Panama and Costa Rica. These species are included in a dichotomous key to all Central American species of *Burmeistera*. In Chapter 3, I describe two species of *Siphocampylus* from the Central Andes of Peru and Bolivia: *S. antonellii* Lagom. & D. Santam., endemic to high elevation grasslands of Calca, Peru, and *S. siberiensis* Lagom. & D. Santam., endemic to cloud forests of Cochabamba, Bolivia. Both species are robust shrubs that produce tubular pink flowers that are likely pollinated by hummingbirds.

In Chapter 4, I use the Neotropical bellflowers as a model system to understand the triggers of rapid diversification in the Andes. I explore the interaction of abiotic and biotic factors by applying a series of diversification models that incorporate orogeny, climate, and biological trait evolution to a time-calibrated phylogeny of the group. Here, I demonstrate that speciation rates rose with increasing Andean elevation, while extinction decreased during global cooling. Of these, climate appears to have played the more important role, which I attribute to preadaptation to cool climates. Biotic traits that facilitate plant-animal mutualisms, specifically fruit type and pollination syndrome, additionally enhanced diversification rates. These results suggest that, while the Andes acted as a species pump for this lineage, a synergistic interaction of abiotic and biotic factors underlies its rapid diversification, which culminated in one of the fastest plant radiations documented to date: the centropogonids. This study underscores the complex interplay of ecological and historical determinants in generating the world's biodiversity.

Finally, in Chapter 5, I use comparative methods to explore shifts between vertebrate pollination syndromes in the centropogonid clade. Such shifts, which are often associated with convergent floral phenotypes, are invoked as key factors underlying floral diversification in angiosperms. Using phylogenetic principal components analyses, I show that, despite morphological similarities between these pollination syndromes, centropogonid flowers adapted to pollination by bats and by hummingbirds fall into separate regions of morphospace. I further document the repeated evolution of pollination syndromes: the clade is ancestrally hummingbird pollinated, and bat pollination has evolved independently fourteen times, with nine reversions to hummingbird pollination. An obligate relationship with sicklebill hummingbirds, characterized by extremely curved bills, evolved only once. While the evolution of floral morphology has been dynamic in this clade, there is no difference in diversification rate in hummingbird and bat pollinated linages. These results suggest that specialized pollination syndromes are not evolutionary dead-ends. Instead, shifts between vertebrate pollinators may have greatly facilitated the maintenance of an ancestrally high diversification rate among centropogonid species.

Table of Contents

Title Page i

Copyright Page ii

Abstract iii

Table of Contents vi

List of Figures ix

List of Tables xi

Acknowledgements ---

Chapter I: Phylogeny, Classification, and Fruit Evolution of the Species-Rich Neotropical Bellflowers (Campanulaceae: Lobelioideae)

- 1.1 Abstract 2
- 1.2 Introduction 3
- 1.3 Materials and Methods 13
- 1.4 Results 18
- 1.5 Discussion 25
- 1.6 Acknowledgements 40
- 1.7 References 41

Chapter II: Two New Species of *Burmeistera* (Campanulaceae: Lobelioideae) from the Cordillera de Talamanca of Costa Rica and Panama, with a Key to the Central American Species

- 2.1 Abstract 49
- 2.2 Introduction 50
- 2.3 Materials and Methods 52
- 2.4 Taxonomic Treatment 53
- 2.5 Dichotomous Key 62

2.6 Acknowledgements 66

2.7 References 67

Chapter III: Two new species of *Siphocampylus* (Campanulaceae: Lobelioideae) from the Central Andes

3.1 Abstract 71

3.2 Introduction 72

3.3 Materials and Methods 73

3.4 Taxonomic Treatment 74

3.5 References 88

Chapter IV: The abiotic and biotic drivers of rapid diversification in the Andes

4.1 Abstract 92

4.2 Introduction 93

4.3 Materials and Methods 97

4.4 Results 102

4.5 Discussion 108

4.6 Acknowledgements 116

4.7 References 116

Chapter V: The repeated evolution of vertebrate pollination syndromes in a recently diverged Andean plant clade

4.1 Abstract 127

4.2 Introduction 129

4.3 Materials and Methods 135

4.4 Results 141

4.5 Discussion 153

4.6 Acknowledgements 164

4.7 References 165

Appendix A: Supporting material for Chapter I 172

Appendix B: Supporting material for Chapter IV 192

Appendix C: Supporting material for Chapter V 211

Appendix D: Lectotypification of Peruvian Campanulaceae names associated with collections made by Augusto Weberbauer

D.1 Abstract 222

D.2 Introduction 223

D.3 Typification 224

D.4 Acknowledgements 228

D.4 References 229

List of Figures

1.1 Floral diversity of *Burmeistera, Centropogon,* and *Siphocampylus*. 5

1.2 Fruit diversity of *Burmeistera, Centropogon,* and *Siphocampylus* 6

1.3 Five locus plastid phylogeny of Neotropical Lobelioideae 21

1.4 Bayesian stochastic character mapping of fruit evolution 35

2.1 Illustration of *Burmeistera monroi* 55

2.2 *Burmeistera monroi*, photographs from field collections 56

2.3 Illustration of *Burmeistera serratifolia* 60

3.1 Illustration of *Siphocampylus antonellii* 75

3.2 Photographs of *Siphocampylus antonellii* 76

3.3 Closest relatives of *Siphocampylus antonellii* 79

3.4 Illustration of *Siphocampylus siberiensis* 82

3.5 Photographs of *Siphocampylus siberiensis* 84

3.6 Closest relatives of *Siphocampylus siberiensis* 86

4.1 Growth form diversity in Neotropical bellflowers 96

4.2 Diversification of Neotropical bellflowers 104

5.1 Flowers of species representing the various pollination syndromes present in the centropogonid clade 130

5.2 Phylogenetic principal components analysis of floral morphology 145

5.3 Bayesian stochastic character mapping of pollination syndrome evolution 148

A.1 Five locus plastid phylogeny of Neotropical Lobelioideae inferred using MrBayes, excluding gap regions 173

A.2 Five locus plastid phylogeny maximum likelihood phylogram 175

of Neotropical Lobelioideae

A.3 Maximum likelihood ancestral character reconstruction of fruit evolution 178

B.1 Time-calibrated phylogeny of Neotropical Campanulaceae, including representatives of Lobelioideae and Campanuloideae 193

B.2 Diversification rate analysis using BAMM 196

B.3 Posterior distributions of trait-dependent speciation, extinction, transition, and net diversification rates as estimated by BiSSE 198

C.1 Depiction of measurements of floral traits taken herbarium specimens 212

C.2 Maximum likelihood reconstruction of pollination syndromes in the centropogonid clade. 213

List of Tables

1.1 Comparison of the phylogenetic results from this study with the subgeneric classification of *Burmeistera*, *Centropogon,* and *Siphocampylus* 10

1.2 Summary statistics of plastid data sets 19

3.1 Differences between *Siphocampylus antonelli*, *S. elfriedii*, and *S. parvifolius* 80

4.1 Net diversification rates in the fastest species radiations in the Tree of Life, including the centropogonids 109

5.1 Model comparison for the BiSSE analyses for bat and hummingbird taxa, with mean parameter estimates for each model 141

5.2 Average values for each quantitative floral trait used in comparative analyses for all species within a pollination syndrome 142

5.3 Loadings of each trait for the first three PC axes from a phylogenetic principal components analysis of floral morphology 144

5.4 Average PC values for all species within each pollination syndrome for the first four PC axes 146

5.5 Number of transitions between pollination syndromes in the centropogonid clade 147

5.6 Correlation between quantitative floral characters from phylogenetic generalized linear model and BayesTraits 151

5.7 Mean corrected Akaike information criterion (AICc) weights representing the relative likelihood of each fitted model of trait evolution 153

A.1 Taxa sampled in the five-locus plastid study of Neotropical Lobelioideae, with voucher information, country of origin, and GenBank accession numbers 179

A.2 Fruit coding for character state reconstruction 186

B.1 Divergence time estimation to assess sensitivity to dating method, calibration selection, and branch length heterogeneity 199

B.2 Trait codings for the four traits used in BiSSE analyses 200

B.3 Paleoenvironmental-dependent diversification analyses using paleoaltimetry and Cenozoic climate data 204

B.4 Model comparison for the four BiSSE analyses presented in Chapter IV 206

B.5 Correlated evolution of binary traits using BayesTraits 209

B.6 Model comparison for the two diversity-dependence analyses presented, with mean parameter estimates for each model 210

C.1 Trait values of floral characters for all species sampled 214

C.2. Results of analysis of correlated floral trait evolution using Bayesian MCMC 218

Acknowledgements

There are so many people thank after the long slog of a dissertation. I have no idea where to begin, and I'm sure I will miss someone, but here it goes….

Thank you, Chuck, for being a positive, supportive advisor. Thank you for telling me to "follow my bliss" in my first year of graduate school, and for sticking by me as I did just that, even when it was difficult and even when the revisions were seemingly endless. I have learned a great deal about the process of science and academia from you; I'm excited to fledge the nest and try it out on my own, and hope I am half as excited about my work as you are when I reach your career stage. I have to extend my thanks here to Sarah Mathews here, too. For a good year and a half, you were just as much my advisor as Chuck. I grew substantially as a scientist during that time. You taught me to be critical of my own work and how to write elegantly and convincingly. But you were also a great mentor, and your advice over coffee, sprinkled with tough love and lessons in perseverance, got me through a tough time; for that, I am most grateful.

Obrigado and tack to Alexandre Antonelli for a good many things: for encouraging me to work with Neotropical lobelioids and for sending me those first samples to get my research off the ground; for suggesting that Daniel would make a good field assistant in Costa Rica, and for the support you gave us a couple when we got married three years later; for inviting me to Sweden to participate in your *totally awesome* research group; for your careful comments that significantly improved two of my chapters; and for being an inspiration in work-life balance, even while your career is taking off so successfully. I am excited to begin my postdoctoral career with you.

Thank you to my committee members, of course. Your insights into my project clarified my thinking at many junctures. Brian, thank you for the constant reminders that my plants are more than DNA sequences, but are, more importantly, living, breathing organisms interacting with other organisms and their environment. Thank you, Naomi, for making me question assumptions that I didn't even realize I had and for being so friendly and encouraging while doing so. And thank you, Scott, for being supportive and available so frequently and for helping me find my place in the broader context of phylogenetic biology. I wish I could have had more meetings with each of you.

I have been so honored to be part of a broader botanical community in the Harvard University Herbaria. Thank you to all herbarium denizens that I had the pleasure of calling colleagues in the last six years, but a few special shout-outs are in order: Thank you, Kanchi Ghandi, for the nomenclatural advice and all those conversations in the kitchen. Thank you, Dave Boufford, for sharing your botanical knowledge, scary stories about our future town, and your cooking skills (I really did enjoy the sushi!). Thank you (on my part, as well as on behalf of all those type specimens) to Walter Kittredge, for helping me to become a more careful botanist and taxonomist than I was before I took up residence in your office. Thank you, Anthony Brach; I'm sure my collections are in the best of hands. Thank you, Michaela Schmull, for helping me navigate sometimes-opaque rules. Gracias, Gustavo Romero, for being supportive and interested. Thanks to the ladies at the library, especially Gretchen Wade, Judy Warnement, and Lisa DeCesare (those exhibits were so fun to put together!). Thank you, Barry Tomlinson, for teaching me to "ask the plant." And a huge thanks and accompanying belly laugh to Emily Wood; the

herbarium hasn't been the same since you graced the Cape with your presence in your well-deserved retirement.

Within the herbarium, I am very happy to have been a member of Charles Davis' dynamic lab. Thanks to everyone who has shared that experience with me: Liming Cai, Jeff DaCosta, Rachel Engstrand, Keith Gaddis, Matt Klooster, Daniel Park, Kylee Peterson, Brad Ruhfel, Charlie Willis, Wenheng Zhang, and all our short-term visitors. Special thanks go out to Simone Cappellari, for being such a uniting and positive force in the lab; to Hanno Schaefer, from whose example I learned dedication and how to be constructively critical; to Tallen Xi, the only lab member whose time completely overlapped with mine and whose computer prowess saved me tons of time; to Joel Nitta, for bringing more ferns into my life and for being a great office mate; to Beth Forrestel, an honorary Davis Lab member and a careful, exacting scientist who I look up to earnestly; and to Luke Nikolov— we started as labmates and ended up the best of friends.

I'm also honored to have been an associated member of Alexandre Antonelli's group during my dissertation. Through this venue, I met many inspiring scientists who I now consider my friends and colleagues, among them Christine Bacon, Fernanda Carvahlo, Fabien Condamine, Suzette Flantua, Carina Hoorn, Daniele Silvestro, and Alexander Zizka. Thanks to every one of you— you are some of the smartest and kindest people I know. I hope we continue to have productive and positive relationships.

I was lucky to visit many herbaria throughout the world and perform fieldwork in four countries during my dissertation; countless people aided me in these endeavors. Thank you to the curators and staff at the following herbaria for your hospitality and for permitting me to use your precious resources: the New York Botanical Garden (NY), the

Missouri Botanical Garden (MO), the University of Gothenburg (GB), the Herbario Nacional de Bolivia (LPB), the Herbario Forestal Martín Cardenas (BOLV), the Herbario del Oriente de Bolivia (USZ), the Instituto Nacional de Biodiversidad in Costa Rica (INB), the Museo Nacional in Costa Rica (CR), the University of Panama (PMA), the herbarium of the Smithsonian Tropical Research Institute, Panama (SCZ), Universidad Mayor de San Marcos in Peru (USM), and the Universidad Nacional Agraria La Molina in Peru (MOL). I met so many fantastic herbarium curators who were more than gracious during these visits, including: Alfredo Fuentes, Mireya Correa, Barry Hammel, Carmen Galdames, Michael Grayum, J. Francisco Morales, Toby Kellogg, Ron Leisner, Scott Mori, Michael Nee, Claes Persson, Peter Stevens, and Nelson Zamora. My fieldwork was aided by many botanists whose long hours and tireless effort resulted in fantastic herbarium specimens; thanks especially go to John Janovec (and Papa Pepe!), Moises Mendoza, and Daniel Santamaría-Aguilar, who accompanied me during all of my collections, only sometimes putting his life in danger in the pursuit of Campanulaceae. Thanks also to the permitting agencies in Costa Rica, Panama, Peru, and Bolivia.

I also benefitted from many generous funding sources. The National Science Foundation has supported me through both a Graduate Research Fellowship and a Doctoral Dissertation Improvement Grant (DEB-1210401). I also received grants from many sources including: the Arnold Arboretum, the American Society of Plant Taxonomists, the Botanical Society of America, the Explorers Club, the Department of Organismic and Evolultionary Biology (OEB) at Harvard, the Organization for Tropical Studies, and the Rockefeller Center for Latin American Studies at Harvard. I want to

extend my gratitude to each of these funding sources; my dissertation would not have been possible without the help.

The administrative staff in OEB helped with administration of these grants and fellowships, but more importantly, made sure that the department ran like a well-oiled machine; it has been a real pleasure to work with you all. Thank you specificlly to Krista Carmichael, Becky Chetham, Paul Dwyer, Jeanette Everitt, Donna Gadbois, Jason Green, Alex Hernandez-Siegel, Bridget Power, Peg Richards (you are the absolute best!), Damari Rosado, Anna Salvato, and Geoff Tierney. A special shout-out goes to Chris Preheim, who had the graduate students' backs during my entire stay at Harvard, and who definitely knows the ins-and-outs of the university better than anyone; you are already missed.

My experience in graduate school was made much richer by my relationships with many other botanists and evolutionary biologists. Atop this list is Robbin Moran; thank you, Robbin, for our many deeply enjoyable conversations about plant morphology and for your so-bad-they're-good botany jokes— I hope there are still many more caminatas waiting for us in Costa Rica. Stacey Combes, you were the best mentor I could have hoped for: supportive, understanding, and California-casual. Chelsea Specht, thank you for my passion for tropical plants and for leading me into this fulfilling career path; I hope we can find a space to work together again in the future. Nathan Muchhala, thanks for your helpful insights into the amazing plants I study and for challenging my evolutionary perspective with your ecological one; working with you as a postdoc is going to be a lot of fun. Luke Mahler, you have no idea how much you inspired me as a young graduate student, and you continue to do so. Christine Bacon, I consider you a

mentor and a friend, but you're also a world-class scientist; I want to be like you when I grow up. And thanks to a set of plant biologists who are a few rungs ahead of me in this crazy ladder of academia: Julien Bachelier, Madelaine Bartlett, Amanda Grusz, Beth Forrestel, Jesse Hollister, Ben Hunter, Rachel Jabaily, Ricardo Kriebel, Juan Losada, Tanya Renner, and Cathy Rushworth. Watching your careers and lives unfold has been such a pleasure and, also, very reassuring; I'm learning from each of you along the way, even if we don't speak often enough. And to Inanna Carter, an honorary botanist and my first student: you were such a pleasure to mentor. You are effervescent and beautiful (inside and out), your positivity is contagious, and you are in complete control of your future— I know you will go far and be happy in whatever you do.

And thanks to all the amazing OEB graduate students, past and present: what a great assembly of students the department has put together! In particular, it was an honor getting to know the following folks: Chris Baker, Leonora Bittleston, Jasmin Camacho, Glenna Clifton (I wish we could have made it to one more brewery), Jake Cohen (and I am so deeply sorry for Cajetas), Carolyn Eng, Ben Ewen-Campen, Kara Felich, Danny Haelewaters, Miriam Johnston, Tamsin Jones, Emily Kay, Evan Kingsley, Steve Kloosterman, Francheso Molina, Talia Moore, Zachary Morris, Martha Muñoz, Jon Sanders, and Prashant Sharma. Of course, thanks to my Harvard Phylogenetics Journal Club breathren, some of whom became good friends: Chris Laumer, Bruno de Medeiros, Tauana Cunha, Julia Cosgrove, Caitlin Baker, Beka Buckman, Kadeem Gilbert, Patrick Gorring, Allison Shultz, and everybody else— good luck making and using trees! A few OEB grad students are especially dear to me. Ambika Kamath: you are one of the most sincere, well-reasoned human beings that I know; I am certain I will continue reading

your popular science writing for years to come and nodding my head in fervent agreement with almost everything you put out there (and thanks for taking on Mandarina and giving her a better life than we ever did!). Chris Laumer: thanks for nerding out with me about trees and worms (and more than once, their penises); your academic passion shines through everything, and your current professional and personal success makes me so happy. Anjan Bhullar: you are an intimidating academic role model if there ever was one, but you are also a dedicated and insightful friend, and I thank you so much for committing to me so wholly— but let's never drink whiskey together again. To Becky Povilus, you and I know a secret that others don't: plants really are the best; thank goodness there are Botany meetings every year so that we can catch up regularly! To Luke Nikolov, I would be a different person today if I hadn't met you in Barry's class. Thanks for all the coffees, beers, banitsas, and gossip sessions; I can't wait to explore major European cities and sleepy beach towns with you and Philip in the upcoming years. Finally, thanks to my amazing cohort: Melissa Adams, Raymond Ko, Jingyi Yu, Brian Arnold, Shane Campbell-Staton, Heather Olins, Zack Lewis, Liz Sefton, Didem Sarikaya, and Dipti Nayak. You are all amazing and success is waiting each and every one of you. To Brian (and by extension, Jesse and Ben): your friendship shaped me in my first three years of graduate school and I had so much fun. To Heather, Zack, and Shane, thanks for your balanced perspectives and friendship throughout our time at Harvard. And finally, to the ladies I'm going to miss the most, but who I know will form a core set of friends in my future: Didem, Dipti, and Liz. Didem, your impeccable work-life balance has been almost as important in my development as your constant teachings in pop culture; let's continue to work and play together for many more years. Dipti, I'm sure you get this a

lot, but you are the smartest and most well rounded person I know; let's drink many craft beers and cubanos in the future, and please keep sending me podcast recommendations. And Liz, thanks for always being available and accommodating, even when it's inconvenient; your generous friendship and hilarious, spot-on sense of humor have been assuring constants during the last six years and I can't wait to explore more of the world with you and Tim.

And finally, thanks to the people who have supported me from the beginning: my family. I have been all too absent in the last six years, but hope I can spend more time with you now that I am done with my thesis. Thanks, Dad, for teaching me to love learning and to love nature while I was growing up, and for encouraging me in the career path I have chosen. Thanks, Grandma and Grandpa, for supporting me along the way and for giving me a love of the world in all its splendid diversity and of deep, reflective conversation. Thanks, Brian, for being a great brother who deserves only the best, and to Jessica, for meeting that criterion. Gracias, Jerry and Mary Caye, for being the biggest supporters of Daniel and me (and for impromptu dances in your living room). Thank you to Mark, John, Chris, Gina, Ken, Liana, Elias, Bob, Lizz, Sally, Richard, Mike, and Joe—Lagomarsino family get-togethers are what I most looked forward to in the precious, limited time I had in California during my Ph.D. Gracias a mi familia Tica: Damaris, Mercedes, Diego, Valentina, Tacha, Gabriela, Gabriel, y Reinaldo, por aceptarme calurosamente como familia. Thanks to Susie, Don, and Katherine, for being so present and supportive. And, to my Grandma Penny: I know you would have been so proud; I miss you and love you.

And, to Daniel, my husband and the best botanist I know: muchas gracias por todo. I don't have words (in English or Spanish) to express my love and gratitude for you. You have been faithfully by my side since we collected that first *Burmeistera* in 2010, and it's been a joy travelling the world and digging into herbaria with you ever since. You have taught me more about plants and taxonomy than anyone, but more importantly, you are my perfect complement and make me so happy, even on my worst days. I can't wait to see where the future takes us.

Para mi mejor amigo y esposo, mi colega y colaborador, mi apoyo principal durante esta disertación: Daniel.

Y, también para las plantas tan bellas que nos unieron.

Chapter I:

Phylogeny, Classification, and Fruit Evolution of the Species-Rich Neotropical Bellflowers (Campanulaceae: Lobelioideae)

The contents of this chapter are reprinted from Lagomarsino LP, Antonelli A, Muchhala N, Timmerman A, Mathews S, Davis CC. Phylogeny, Classification, and Fruit Evolution of the Species-Rich Neotropical Bellflowers (Campanulaceae: Lobelioideae). *American Journal of Botany* 101(12): 2097-2112. Copyright 2014 with permission from the Botanical Society of America.

1.1 Abstract

The species-rich Neotropical genera *Centropogon*, *Burmeistera*, and *Siphocampylus* represent more than half of the diversity in the subfamily Lobelioideae (Campanulaceae). They exhibit remarkable morphological variation in floral morphology and habit. Limited taxon sampling and phylogenetic resolution, however, obscures our understanding of relationships between and within these genera. Here, I inferred a phylogeny from five plastid DNA regions (*rpl32-trnL*, *ndhF-rpl32*, *rps16-trnK*, *trnG-trnG-trns*, rbcL) using maximum likelihood and Bayesian inference. Ancestral character reconstructions were applied to infer patterns of fruit evolution. My results demonstrate that the majority of species of *Centropogon*, *Burmeistera*, and *Siphocampylus* together form a primarily mainland Neotropical clade, collectively termed the centropogonids. Caribbean *Siphocampylus*, however, group with other Caribbean lobelioid species. We find high support for the monophyly of *Burmeistera* and the polyphyly of *Centropogon* and mainland *Siphocampylus*. The ancestral fruit type of the centropogonids is a capsule; berries have evolved independently multiple times. This plastid phylogeny greatly improves the phylogenetic resolution within Neotropical Lobelioideae, and highlights the need for taxonomic revisions in the subfamily. Inference of ancestral character states identifies a dynamic pattern of fruit evolution within the centropogonids, underscoring the difficulty of diagnosing broad taxonomic groups on the basis of fruit type. Finally, we identify that the centropogonids, *Lysipomia*, and *Lobelia* section *Tupa* form a Pan-Andean radiation with broad habitat diversity. This clade is a prime candidate for investigations of Neotropical biogeography and morphological evolution.

1.2 Introduction

The bellflower family, Campanulaceae Juss., is cosmopolitan in its distribution and includes ~2,300 species in 84 genera (Lammers 2007b). Members of the family share at least three putative synapomorphies: laticifers, stamens attached to the disc of the ovary, and epigynous flowers (Lammers 2004, 2007a). Additionally, plants are usually herbaceous with alternate, estipulate leaves and five-merous, protandrous flowers with various forms of secondary pollen presentation. Five subfamilies are recognized: Campanuloideae Burnett, Lobelioideae Burnett, Cyphioideae Walp., Nemacladoideae Lammers, and Cyphocarpoideae Miers. The largest of these is Lobelioideae, which includes ~1,200 species, and is characterized by species with resupinate, zygomorphic flowers, connate stamens, and styles with brush hairs that facilitate secondary pollen presentation by a pump and piston mechanism (Erbar and Leins 1995; Leins and Erbar 2006). Lobelioideae are ecologically diverse, ranging from northern temperate herbs and small aquatics to the giant tropical pachycaul rosettes, cliff succulents, and epiphytes that comprise the canonical Hawaiian island radiation (Givnish et al. 2009). Lobelioideae are widely distributed, but absent from the Arctic, Middle East, and large regions of central Asia (Stevens 2003). Some Lobelioideae are well-known for their horticultural importance in temperate latitudes, including *Lobelia cardinalis* L., *L. siphilitica* L, and *L. erinus* L. The majority of species, however, are native to tropical regions, with the highest diversity in the New World tropics (Lammers 2007b).

Approximately half of all Lobelioideae species fall within three exclusively Neotropical genera: *Centropogon* C. Presl (~210 spp.), *Burmeistera* Triana (~100 spp), and *Siphocampylus* Pohl (~230 spp) (Lammers 2007b). Previous studies have suggested that these genera form a clade (Antonelli, 2008, 2009; Knox et al., 2008), which has been informally named the "CBS

clade" (Batterman and Lammers [2004]). After the cosmopolitan and polyphyletic *Lobelia* L. (Antonelli 2008, 2009; Lammers 2011), these are the three largest genera within the Lobelioideae. Species in *Burmeistera*, *Centropogon*, and *Siphocampylus* are distinguished by their shrubby habit and entire corolla tubes, which are neither fenestrate nor dorsally cleft, as in many species of *Lobelia*. The lone exception is *Siphocampylus* section *Macranthi* E. Wimm. subsection *Hemisiphocampylus* (A. DC.) E. Wimm., whose species possess fenestrate corollas. The corolla lobes in *Centropogon*, *Siphocampylus*, and *Burmeistera* are either monomorphic or, if dimorphic, the dorsal pair are larger than the ventral three (Lammers 2002). The staminal tube almost always extends beyond the corolla, with the anther tube frequently bearing a tuft of hair on the ventral side (Figure 1.1). Most species are scandent or erect suffruticose shrubs and subshrubs. However, plants can be hemiepiphytes (e.g., many species of *Burmeistera*), herbs (e.g., *C. coccineus* [Hook.] Regel ex B.D. Jacks.), xerophytes with substantial woody bases (e.g., *Siphocampylus smilax* Lammers), or very rarely trees (e.g., *Siphocampylus tunarensis* Zahlbr.). Like many other woody species of Lobelioideae, all species of *Centropogon* and *Siphocampylus* whose cytology has been studied are tetraploid ($n = 14$), though chromosome numbers have never been reported for *Burmeistera* species (Lammers 1993). Genera have been distinguished primarily by fruit type: species of *Burmeistera* and *Centropogon* produce berries (Figure 1.2B-F), while species of *Siphocampylus* produce capsules (Figure 1.2A). *Burmeistera* is further distinguished on the basis of several characters, including: ebracteolate pedicels, an inflated corolla opening (Figure 1.1A), a dilated anther orifice, and isodiametric seeds (Lammers 1998; Muchhala and Lammers 2005). Aside from fruit type, there are no characters that readily distinguish *Centropogon* and *Siphocampylus*; their morphology overlaps in nearly every vegetative and reproductive character. As a result, specimens are often misfiled between these

two genera in herbarium collections. Additionally, character overlap has caused many species to be described as ambiguously placed between the two genera, particularly when fruit information is missing (e.g., *Centropogon dubius* [Zahlbr.] E. Wimm.). A major goal of our study is to determine if fruit type is a useful taxonomic character for delineating these large Neotropical Lobelioideae genera.

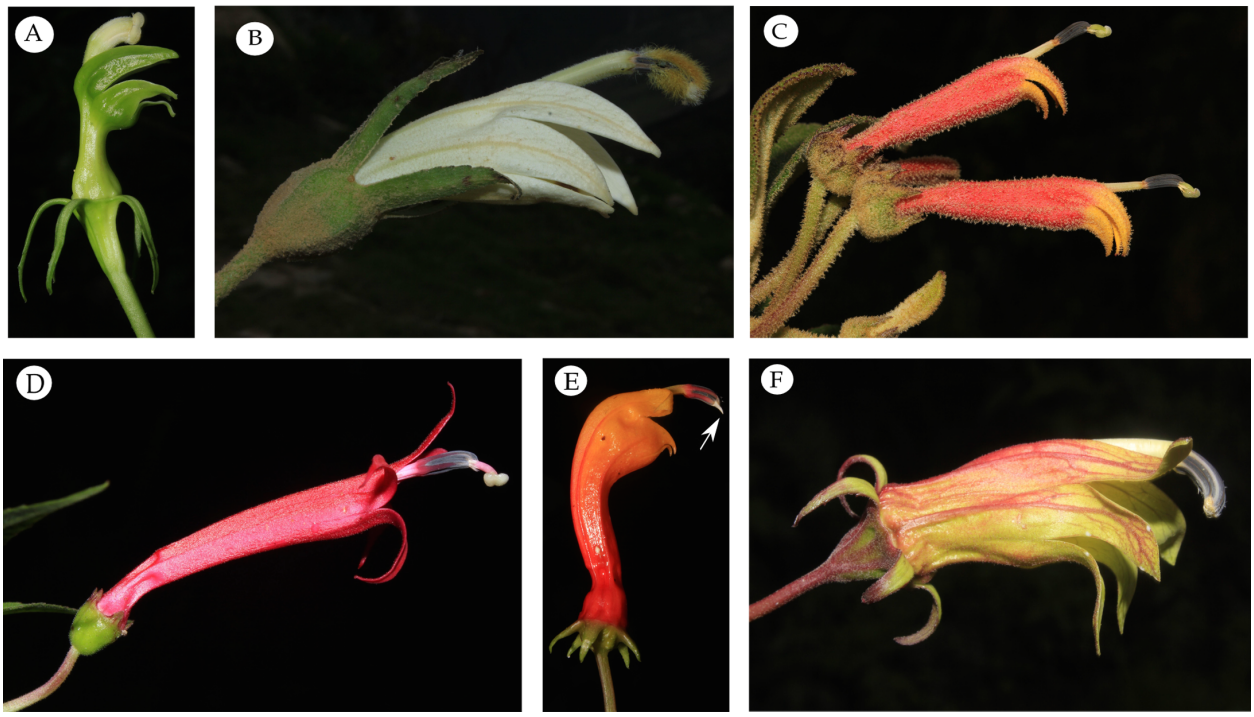


Figure 1.1. Floral diversity of *Burmeistera, Centropogon,* and *Siphocampylus*, the majority of whose species we informally designate at the centropogonids. A) *Burmeistera tenuiflora* Donn. Sm. (burmeisterid); **B)** *C. dombeyanus* E. Wimm. (peruvianid); **C)** *C. macbridei* Gleason (brevilimbatid); **D)** *C. leucocarpus* McVaugh (colombianid); **E)** *C. yungasensis* Britton (eucentropgonid); **F)** *Siphocampylus rusbyanus* Britton. (Photos: L. Lagomarsino)

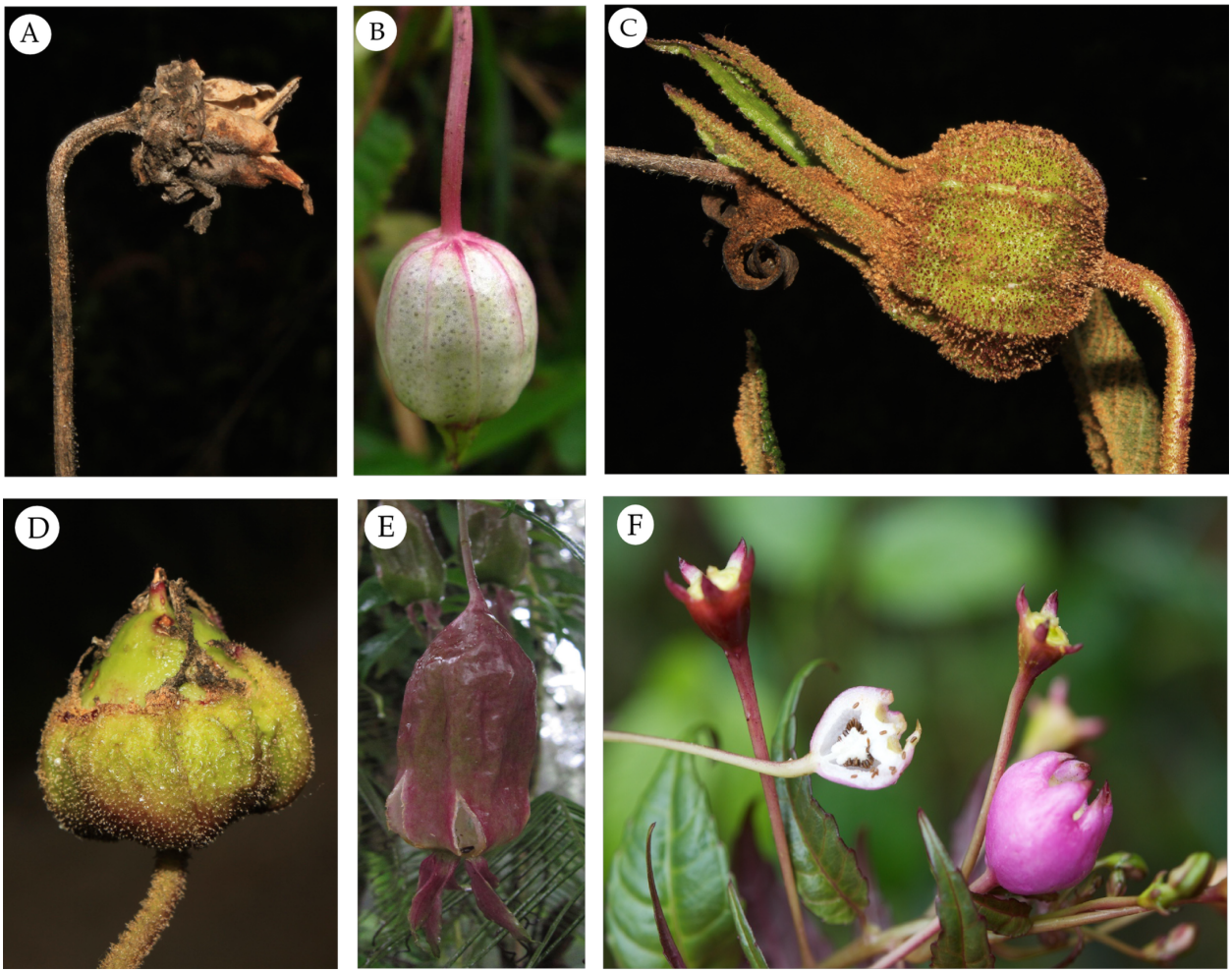


Figure 1.2. Fruit diversity of *Burmeistera, Centropogon,* and *Siphocampylus*, the majority of whose species we informally designate at the centropogonid clade. A) Capsule of *Siphocampylus corynoides* E. Wimm.; **B)** Berry of *Centropogon coccineus* (Hook.) Regel ex B.D. Jacks. (colombianid); **C)** Berry of *C. viriduliforus* E. Wimm. (peruvianid); **D)** Berry of *C. weberbaueri* Zahlbr. (brevilimbatid)*;* **E)** Berry of *B. vulgaris* E. Wimm. (burmeisterid); **F)** Berry of *B.* aff. *minutiflora* Garzón & Gonzalez (burmeisterid). (Photos: A–E: L. Lagomarsino; F: A. Antonelli)

The more than 540 species of *Burmeistera, Centropogon*, and *Siphocampylus* exhibit a high degree of morphological variation, particularly in floral form, habit, and fruit type. Together, their high species diversity, striking morphological variation, and relatively recent origin (estimated to be ~5-12 My; [Givnish et al., 2009; Antonelli, 2009]) make the group particularly interesting for studies of species diversification. Factors that have likely contributed to their diversification include pollinator interactions and climatic and geological events (particularly the orogeny of the Andes; see below). Variation in floral morphology is associated with diverse pollinator interactions: *Centropogon* and *Siphocampylus* species are primarily adapted to a variety of hummingbird pollinators (Knox et al., 2008) (Figure 1.1C-E), though bat-pollination is relatively common (Figure 1.1B, F). With the exception of one documented hummingbird-pollinated species, however, *Burmeistera* species are almost exclusively bat-pollinated (Muchhala 2006b). Floral morphology in these species and the pollinators that they attract (Stein 1992; Muchhala 2006b) are consistent with classical descriptions of pollination syndromes (Baker, 1961; Faegri and van der Pijl, 1979; Fenster et al., 2004) . For example, the hummingbird pollinated *Burmeistera rubrosepala* (E. Wimm.) E. Wimm. (Muchhala 2006b) and *Centropogon valerii* Standl. (Colwell et al. 1974) have flowers that are typical of species pollinated by hummingbirds–they lack odor, are brightly colored (red, pink, orange), and have narrow corolla openings. *Centropogon granulosus* Presl. and many other members of *Centropogon* section *Centropogon* Benth. & Hook. (Stein 1992) (Figure 1.1E), on the other hand, have abruptly curved corollas and inflorescences that allow for perching, as is typical of species pollinated by sicklebill hummingbirds. Many *Burmeistera* species (Muchhala 2006b) and *C. nigricans* Zahlbr. (Muchhala and Thomson 2009) are generally pale in color, produce a strong skunk-like odor, and open at night, like most bat-pollinated species. At least two species,

S. sulfureus E. Wimm. (Sazima et al., 1994) and *B. tenuiflora* Donn. Sm. (Muchhala 2003), are effectively pollinated by both bats and hummingbirds, and produce flowers that are intermediate between hummingbird and bat pollination syndromes. Flower length is highly variable in these three genera and varies from less than 1 cm in *B. minutiflora* Garzón and F. Gonzalez (Garzón Venegas et al., 2012) to more than 8 cm in *C. nigricans*. In the latter, long flowers are an adaptation to specialized pollination by the bat species *Anoura fistulata* Muchhala, Mena-Valenzuela & Albuja (Muchhala and Thomson 2009), which has the longest tongue protrusion known among mammals (Muchhala 2006a).

Centropogon, *Burmeistera*, and *Siphocampylus* are a mostly continental radiation, ranging from southern Mexico through northern Argentina, with a handful of species occurring in the Caribbean region. These genera have a broad ecological amplitude, occurring from mid-montane cloud forests (the majority of species) to lowland tropical rainforests (e.g., *C. cornutus* [L.] Druce, *C. tessmannii* E. Wimm.), seasonally dry subtropical forest (e.g., *S. orbignianus* A. DC., *S. smilax* Lammers), and high elevation grasslands (e.g., *S. jelskii* Zahlbr., *C. ferrugineus* [L.f.] Gleason). *Burmeistera* is distributed from Guatemala through northern Peru; *Centropogon* is distributed from southern Mexico to Bolivia and Brazil, with two species in the Lesser Antilles; and *Siphocampylus* is distributed from Costa Rica to Argentina, and in the Greater Antilles. These genera form an especially conspicuous element in the cloud forest understories of montane regions of South America, particularly in the Andes. As a result of extensive plant diversification, the Andean cordilleras, where Neotropical lobelioids are most abundant, are the richest of the global biodiversity hotspots (Myers et al., 2000). In a survey of various Andean angiosperm lineages, *Burmeistera* was found to have the highest speciation rate of all groups examined (Pennington et al., 2010, Table S1). The Andean orogeny is thought to have stimulated

diversification in numerous groups (Antonelli et al., 2009; Bell and Donoghue, 2005; Hughes & Eastwood, 2006; Madriñán et al., 2013; Smith and Baum, 2006; von Hagen and Kadereit, 2003; Winkworth and Donoghue, 2005), the ultimate causes of which are attributed to a variety of factors (Luebert and Weigend 2014). The Miocene (~5-12 My) diversification of *Centropogon*, *Burmeistera*, and *Siphocampylus* (Antonelli 2009) is similarly consistent with the hypothesis that Andean orogeny was a major factor promoting diversification.

Many scholars have expressed frustration with the existing classifications of *Burmeistera*, *Centropogon*, and *Siphocampylus*, particularly in the latter two genera (e.g., Lammers, 1998, 2007a; McVaugh, 1949). Wimmer's treatments for Lobelioideae in Das Pflanzenreich (Wimmer 1943, 1953, 1968) constitute the most recent monograph these three genera. Wimmer divided each genus into a series of hierarchical divisions, including sections, subsections, greges (singular: grex), subgreges, and series. This work often relies on single, seemingly arbitrary characters and narrow species concepts to define taxa. An outline of the classification by Wimmer (1943), including his refinements (Wimmer 1953, 1968), is presented in Table 1.1. McVaugh (1949) substantially improved on the taxonomy of *Centropogon* by erecting new sections and recircumscribing existing taxa using a combination of characters. McVaugh's concept of *Centropogon*, plus an additional section described in Lammers (1998), is preferred by current taxonomists of Lobelioideae (Batterman and Lammers, 2004; Lammers 1998, 2002) (Table 1.1). There has been no substantial taxonomic revision within *Siphocampylus* or *Burmeistera* since Wimmer (1943, 1953, 1968), though a systematic treatment of Colombian species of *Burmeistera* is in progress (Garzón Venegas and González 2012). Lammers (1998, 2004) suggested that the monophyly of genera and subgenera would remain dubious until a broad phylogenetic analysis is conducted.

Table 1.1. Comparison of the phylogenetic results from this study with the subgeneric classification of *Burmeistera*, *Centropogon,* and *Siphocampylus* largely following Wimmer. Subgeneric classifications of Wimmer (1943, 1953, 1968), McVaugh (1949), and Lammers (1998) shown for *Centropogon*. N/A denotes insufficient taxon sampling to determine phylogenetic status; ***** denotes a monotypic taxon.

Table 1.1 (Continued).

Genus	Section	Subsection	Grex	Phylogenetic Status
Burmeistera Triana				
	Imberbes nom. Invalid. (=Burmeistera)			Non-monophyletic
		Genuinae E. Wimm.		Non-monophyletic
		Aequilatae E. Wimm.		N/A
	Barbatae E. Wimm.			Non-monophyletic
Siphocampylus Pohl				
	Macrosiphon Wimm.			
		Hemisiphocampylus Wimm.		Non-monophyletic
		Siphocampylus (A. DC.) E. Wimm.		Non-monophyletic
			Ectropici E. Wimm.	Non-monophyletic
			Verticillati E. Wimm.	Non-monophyletic
			Umbellati E. Wimm.	Non-monophyletic
			Botryoides E. Wimm.	Non-monophyletic
			Dissitiflori E. Wimm.	Non-monophyletic
		Byrsanthes (Presl) E. Wimm.		N/A
	Brachysiphon Wimm.			Non-monophyletic
		Secundiflori E. Wimm.		Non-monophyletic
		Altofissi E. Wimm.		Non-monophyletic
			Barbiceps E. Wimm.	Non-monophyletic
			Cremochilus E. Wimm.	Monophyletic*
		Megastomi E. Wimm.		Non-monophyletic
		Megalandri E. Wimm.		N/A
Centropogon Presl (sensu Wimmer)				
	Centropogon Benth. & Hook.			Monophyletic
		Corymboides E. Wimm.		Non-monophyletic
			Campylobotrys E. Wimm.	Non-monophyletic
			Amplifolii Zahlb.	Monophyletic
		Botryoides E. Wimm.		Non-monophyletic
		Axillares Gleason		Monophyletic
	Siphocampyloides Benth & Hook			Non-monophyletic
		Brevilimbati E. Wimm.		Non-monophyletic
			Formosi E. Wimm.	Non-monophyletic
			Stellato-tomentosi Gleason	Non-monophyletic
		Macranthi Wimm.		Non-monophyletic
			Lehmannioides Wimm.	Non-monophyletic
			Mandonioides E. Wimm.	Non-monophyletic
Centropogon (infrageneric taxonomy sensu McVaugh and Lammers)				
	Centropogon Benth & Hook			Monophyletic
	Siphocampyloides Benth & Hook			Non-monophyletic
		Brevilimibatii E. Wimm.		Non-monophyletic
		Peruviani McVaugh		Non-monophyletic
	Wimmeriopsis McVaugh 1949			Non-monophyletic
		Falcati McVaugh		Non-monophyletic
		*Colombian*i McVaugh		Non-monophyletic
	Burmeisteroides McVaugh 1949			Non-monophyletic
	Niveopsis Lammers			Monophyletic*

Phylogenetic analyses of the Neotropical Lobelioideae, however, remain limited despite their remarkable floral diversity and broad ecological amplitude. Three previous studies have attempted to reconstruct relationships within and among *Burmeistera, Centropogon*, and *Siphocampylus* using molecular data (Antonelli, 2008, 2009; Knox et al., 2008). These studies suggested that together these genera form a clade, but that the two largest genera, *Centropogon* and *Siphocampylus*, are not monophyletic. *Burmeistera* was found to be monophyletic, consistent with the presence of numerous putative morphological synapomorphies (see above). These were important findings, but of the roughly 530 species in these genera, only 41 (Knox et al. 2008) and 14 (Antonelli 2008) species were included, respectively. Nonetheless, their results suggested that many of the subgeneric taxa of Wimmer and McVaugh are non-monophyletic. *Centropogon* section *Centropogon*, however, was found to be monophyletic in both studies; it is characterized by scale-like concrescent hairs on the tips of the ventral anthers (Figure 1.1E, arrow). Both studies also resolved *Lysipomia* Kunth, a genus of minute, occasionally suffrutescent herbs restricted to the high Andes, as sister to *Burmeistera, Centropogon*, and *Siphocampylus*. Despite these discoveries, however, much of the phylogeny remains uncertain due to low taxon sampling and the lack of phylogenetic resolution, especially along the spine of the tree. This presents a substantial obstacle for understanding how i) fruit characters inform classification, ii) floral morphology has evolved, and iii) biogeographic history has influenced evolution in the group.

Here, we present a greatly revised phylogeny of *Centropogon*, *Burmeistera*, and *Siphocampylus* and its close relatives, based on five plastid DNA regions (*rpl32-trnL*, *ndhF-rpl32*, *rps16-trnK*, *trnG-trnG-trns, rbcL*). Our phylogeny includes nearly six times more species than the most comprehensive published phylogeny (Knox et al. 2008). This sampling covers

most of the taxonomic, morphological, and geographical variation in these genera. It provides a strong starting point for recircumscription of taxa, and sheds insight on the evolution of fruit type, a trait that is taxonomically, ecologically, and evolutionarily important. Finally, our study lays the foundation for future investigations into the pattern of floral diversification and biogeography in this charismatic and conspicuous group.

1.3 Materials and Methods

***Taxon selection*—**Members of all subdivisions of Wimmer's taxonomy within *Centropogon*, *Burmeistera*, and *Siphocampylus*, were sampled, including more than one species from eleven of his fourteen subsections and all thirteen of his greges. Multiple individuals representing distinct populations were sampled in widespread and/or morphologically variable species. Additionally, multiple close relatives, sensu Antonelli (2008), were sampled, including five species of *Lysipomia* and three of the four species of the hexploid Chilean *Lobelia* section *Tupa* (G. Don.) Benth (Lammers 2000). The majority of species we sampled are Neotropical. Two species of Campanuloideae, *Campanula medium* L. and *Triodanis perfoliata* (L.) Nieuwl., were used as outgroups to root the phylogeny (Antonelli 2008). The majority of specimens were collected in the field by A.A., A.T., L.L., and N.M. during trips in Bolivia, Brazil, Colombia, Costa Rica, Ecuador, Panama, Peru, and the United States. Leaf tissue was preserved using silica gel and vouchers were deposited in various herbaria. Leaf fragments were extracted from dried herbarium specimens when Wimmer's subsections/greges were not represented by field collections. In total, 268 individuals were included. Ninety-three, 105, and 41 individuals represent *Siphocampylus*, *Centropogon*, and *Burmeistera*, respectively. Table A.1 contains a list of species with associated collection information and GenBank accession numbers.

***Molecular methods*—**Genomic DNA was extracted from leaf tissue using the Qiagen DNeasy kit (Qiagen, Valencia, California, USA). Rapidly evolving plastid markers were initially tested by L.L. in ten phylogenetically diverse Lobelioideae using primers discussed in Shaw et al. (2007). Species for this preliminary analysis were selected according to the phylogenetic trees in Antonelli (2008) and Knox et al. (2008), and included: *B. cyclostigmata* Donn. Sm., *B. vulgaris* E. Wimm., *S. umbellatus* (Kunth.) G. Don., *S. westinianus* Pohl, *C. cornutus* (L.) Druce, *C. granulosus*, *C. ferrugineus* (L.f.) Gleason, *C. costaricae* (Vatke) McVaugh, *Lysipomia muscoides* Hook f., and *Lobelia laxiflora* Kunth. We selected the four markers that showed the most variation: *rpl32-trnL*, *ndhF-rpl32*, *rps16-trnK*, and *trnG-trnG-trns*. The use of low copy nuclear markers, which provides an important test of plastid phylogenies (Sang, 2002; Small et al., 2004), was attempted, but was not successful. *waxy* (Mason-Gamer et al., 1998) showed little sequence variation, while *LFY* (Howarth and Baum 2005), *cam* (Johansen 2005), *NIA* (Howarth and Baum 2002, 2005), and *rpb2* (Denton et al., 1998) exhibited complex duplication history, which posed challenges for correct orthology assessment (data not shown). Additionally, the internal transcribed spacer from the nuclear ribosomal DNA (nrITS), a marker commonly used in plant phylogenetics, produced sequences with many multiple overlapping peaks, indicating multiple copies in our focal taxa (data not included). Moreover, aligned nrITS sequences did not yield reliable topologies in a preliminary phylogenetic analysis; they differed greatly from the plastid markers and contradicted previously published phylogenies (Knox et al 2008; Antonelli 2008, 2009). Explanations for these problems include duplication of tandem arrays, incomplete homogenization, misleading signal from concerted evolution following hybridization or introgression, and the presence of pseudogenes (Álvarez and Wendel 2003). Chloroplast capture

is an additional mechanism by which our plastid phylogeny would contradict with a nuclear phylogeny (Rieseberg and Soltis 1991; Soltis et al 1991).

PCR amplification of the plastid markers used the following reaction mixture with the Qiagen Taq DNA polymerase kit (Qiagen, Valencia, CA): 1X CoralLoad Buffer, 0.4 mM MgCl2, 0.2 mM dNTPs, 0.4 μM forward primer, 0.4 μM reverse primer, 0.4 U Taq polymerase, for a final volume of 10 μL. The following thermocycler protocol was used: 7 min at 94°C, followed by 35 cycles of 1 min at 60°C, 1 min at 49°C (*rpl32-trnL*, *ndhF-rpl32*, *rps16-trnK*) or 55°C (*trnG-trnG-trnS*), 2 min at 72°, with a 10 min at 72°C. Amplification products were subsequently visualized on 1.5% agarose gels.

PCR products were Sanger sequenced at Functional BioSciences (http://functionalbio.com) and Genewiz (http://www.genewiz.com/). Chromatograms were checked for quality, assembled into contigs, and edited using Geneious v6.1.8 (www.geneious.com). Sequences of *rbcL* from previous molecular phylogenetic analyses (Knox et al 2008, Antonelli 2008, 2009) were obtained from GenBank and included for species that overlapped with our sampling. With the exception of these *rbcL* sequences, all molecular data were newly generated for this study. Alignments were inferred using MUSCLE (Edgar 2004) as implemented in Geneious and then edited manually. Gaps were coded using gapcode.py v2.1 (Richard Ree, personal communication; http://www.bioinformatics.org/~rick/software.html) based on the method of Simmons and Ochoterena (2000). Individual markers did not show discordant relationships (>70 maximum likelihood bootstrap percentage [BP]) and were combined and analyzed simultaneously.

***Phylogenetic Analysis*—**PartitionFinder v1.1.1 (Lanfear et al., 2012) was used to determine an appropriate data partitioning scheme from potential partitions that were defined a

priori (in this case, each plastid locus), as well as the best fitting model of molecular evolution for each partition, using the Bayesian Information Criterion. Maximum likelihood (ML) analyses of the optimally partitioned data were performed using RAxML v7.7.5 (Stamatakis et al, 2008; Stamatakis, 2006). The GTRGAMMA model of sequence evolution was determined to be the best fitting model for each nucleotide partition. The MK model of character evolution for a binary state (Lewis 2001) was determined to be the best model for the gap partition. The search for an optimal Maximum Likelihood tree was combined with a rapid bootstrap analysis of 1,000 replicates. After an initial RAxML run, RogueNaRok (Aberer et al., 2013) was used to prune unstable taxa from the analysis. Each of the 18 excluded individuals lacked sequences for at least two of the four non-coding plastid markers. The resulting taxon sampling was used in all analyses presented. The RAxML analysis was repeated with this reduced taxon sampling scheme. All RAxML analyses were performed on the Harvard Odyssey 2.0 cluster (http://rc.fas.harvard.edu/).

Two phylogenetic analyses with the reduced taxon sampling were conducted using Bayesian inference (BI). The first was a partitioned analysis in MrBayes v3.2.2 (Altekar et al. 2004; Ronquist et al. 2012) performed on the CIPRES cluster (http://www.phylo.org/). The parameters of each of the partitions were the same as in the ML analysis. Rate heterogeneity, base frequencies, and substitution rates across partitions were unlinked. The analysis was allowed to run for 100 million generations across eight independent runs each with four chains, sampling every 10,000 generations. Convergence of the chains across runs was explored in Tracer v1.5 (Rambaut and Drummond 2003) and convergence of topologies and clade stability were confirmed using AWTY (Nylander et al., 2008). The first 25% of the trees from all runs were excluded as burn-in before making a majority-rule consensus of the 7,500 posterior

distribution trees using the "sumt" function. This analysis was repeated with identical parameters but excluding gap characters to confirm that these characters did not bias the results (Figure A.1).

We performed a second BI analysis on CIPRES using PhyloBayes, implementing a mixture model using CAT (Lartillot and Philippe 2004). This analysis was performed with two independent chains on the partitioned molecular data using a different CAT-GTR model for each partition, with gap data excluded. The analysis was allowed to run until the maxdiff value was 0.1, and the minimum effective size was 50. Convergence parameters were calculated after excluding the first 500 generations, and assessed using Tracer.

***Alternative Topology Testing*—**We utilized the approximately unbiased (AU) test (Shimodaira 2002) to examine alternative suboptimal topologies. Three phylogenetic hypotheses based on Wimmer's (1953) taxonomy that were not supported in our analyses were tested: i) the monophyly of *Centropogon*, ii) the monophyly of *Siphocampylus*, and iii) the monophyly of mainland *Siphocampylus* (i.e., excluding the Caribbean subsection *Hemisiphocampylus*). Additionally, two hypotheses based on fruit evolution were tested: i) monophyly of species with capsular fruits and ii) monophyly of species with berry fruits. Topologies conforming to these hypotheses were created in Mesquite v2.5 (Maddison and Maddison 2011) and used to perform constrained phylogenetic analyses in RAxML using the settings described above. The per-site likelihood scores were calculated in RAxML (-f g option) from the constrained and unconstrained ML topologies. The AU test was performed using the site-likelihoods and the relltest function in scaleboot (Shimodaira, 2008) in R v3.0.2 (R Core Team, 2013).

***Fruit Evolution*—**Fruit evolution was explored via Bayesian stochastic character mapping (Bollback 2006). All taxa were coded as berry (0) or capsule (1), from specimens or the

literature (Table A.2). Before performing the stochastic character mapping, the optimal ML tree, trimmed to include only the clade containing *Centropogon*, *Burmeistera*, mainland *Siphocampylus*, *Lysipomia*, and *Lobelia* section *Tupa,* was made ultrametric using the chronoPL function in the ape package (Paradis et al. 2004) in R. This implements the penalized likelihood method of Sanderson (Sanderson 2002). Ancestral state reconstructions were initially performed using standard maximum likelihood methods using the equal rates ("ER") and all-rates-different ("ARD") models using the ace function. A likelihood-ratio test was subsequently performed to determine the optimal model. Ancestral character states were then estimated from 1,000 iterations of Bayesian stochastic character mapping under the optimal model ("ER") using the make.simmap function in the phytools package (Revell 2012). The Q transition matrix was fixed at the most likely values, i.e., the empirical Bayes method (Q = "empirical"). This analysis calculated ancestral states at each node as the marginal posterior probabilities for both character states, which relies on the ultrametric RAxML topology.

1.4 Results

Characteristics of the plastid dataset—The final concatenated matrix included 7,282 bp of aligned sequence data and 207 gap characters for 268 individuals from 199 species. Two hundred thirty-nine individuals from 172 species of *Centropogon*, *Burmeistera*, and *Siphocampylus* are represented; this is approximately one-third of the described species in these genera. Table 1.2 contains the summary statistics for the individual markers and for the coverage of each marker in our dataset.

Table 1.2. Summary statistics of plastid data sets.

Locus	Total length (bp)	# of var char	# pars inform. Char	# Gap Char	% Coverage
ndhF-rpl32	1,623	589	361	67	87.7
rpl32-trnL	1,083	878	522	51	97.0
rps16-trnK	1,188	656	439	63	98.9
trnG-trnG-trnS	1,694	759	434	24	80.2
rbcL	3,821	404	165	3	12.7

***Phylogenetic reconstructions, topology congruence, and taxonomic implications*—**The results of each of the three phylogenetic analyses were largely congruent (Figure 1.3). None of the relationships that differed between trees were well-supported (i.e., >80BP or PP), and any differences below this threshold were generally restricted to closely related taxa. All data matrices are deposited in the Dryad repository (doi:10.5061/dryad.8t4gp).

Centropogon, *Siphocampylus*, and *Burmeistera* do not form a clade. Five species of *Siphocampylus* form a paraphyletic grade that fall outside of the "CBS clade" with high support (BP = 100, Bayesian posterior probability percentage [PP] = 100 [PP from MrBayes]/100 [PP from PhyloBayes]) (Figure 1.3). All species in this grade are included in Wimmer's *Siphocampylus* subsection *Hemisiphocampylus*, which comprises all and only Caribbean species of *Siphocampylus*. This grade is most closely related to the pantropical weed *Hippobroma longiflora* (L.) G. Don., which is native to Jamaica, and to the Caribbean endemic *Lobelia martagon* Hitchc.

We refer to the newly identified clade that includes all species of *Centropogon*, *Burmeistera*, and mainland *Siphocampylus* as the centropogonids (Figure 1.3, arrow; BP= 96,

PP=100/100). *Siphocampylus fulgens* Hort., is well-supported (BP= 80, PP=98/100) as sister to the rest of the centropogonids. As has been the case in previous phylogenetic analyses of the centropogonids (Antonelli 2008; Knox et al. 2008), branch lengths separating species were short (Figure 1.3, inset phylogram; Figure A.2). However, unlike previous analyses, moderate to high support values were estimated along the majority of the backbone, and often towards the tips of the phylogeny (Figure 1.3).

Among the focal genera, *Burmeistera* is the only monophylyetic genus (BP= 100, PP=100/100) (Figure 1.3). *Centropogon* and *Siphocampylus* are polyphyletic with respect to one another (Figure 1.3). Moreover, subgeneric taxa in all three genera are largely not monophyletic. The exceptions are *Centropogon* section *Centropogon* and the monotypic taxa highlighted in Table 1.1. Members of *Centropogon* form at least seven clades that are broadly distributed within the centropognid clade. Most *Centropogon* species (89%) belong to five subclades that correspond to morphologically cohesive units, which reflect currently accepted taxonomy sensu McVaugh (1949). These five well-supported subclades, which we characterize in detail in the Discussion, are: i) the brevilimbatiids (BP= 98, PP=100/100), ii) the peruvianids (BP= 85, PP=100/100), iii) the colombianids (BP= 93, PP=96/99), iv) the burmeisterids (including the entire genus *Burmeistera*) (BP= 87, PP=100/100) and v) the eucentropogonids (BP= 95, PP=100/100). The eucentropogonids can be further divided into three subclades, which closely reflect the classification of Stein (1987a). In contrast, species of *Siphocampylus* are scattered throughout the phylogeny and most species do not fall into well-supported, morphologically coherent clades.

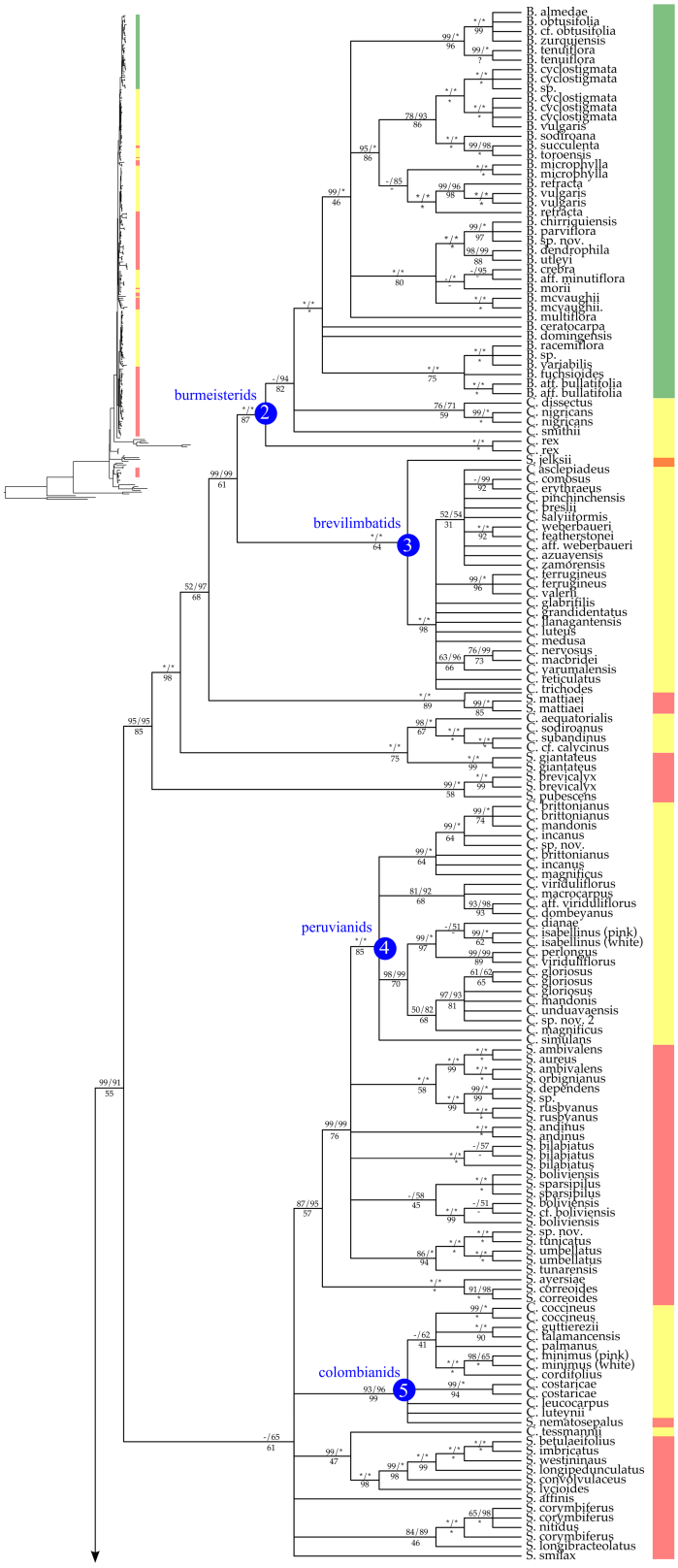


Figure 1.3. Five locus plastid phylogeny of Neotropical Lobelioideae

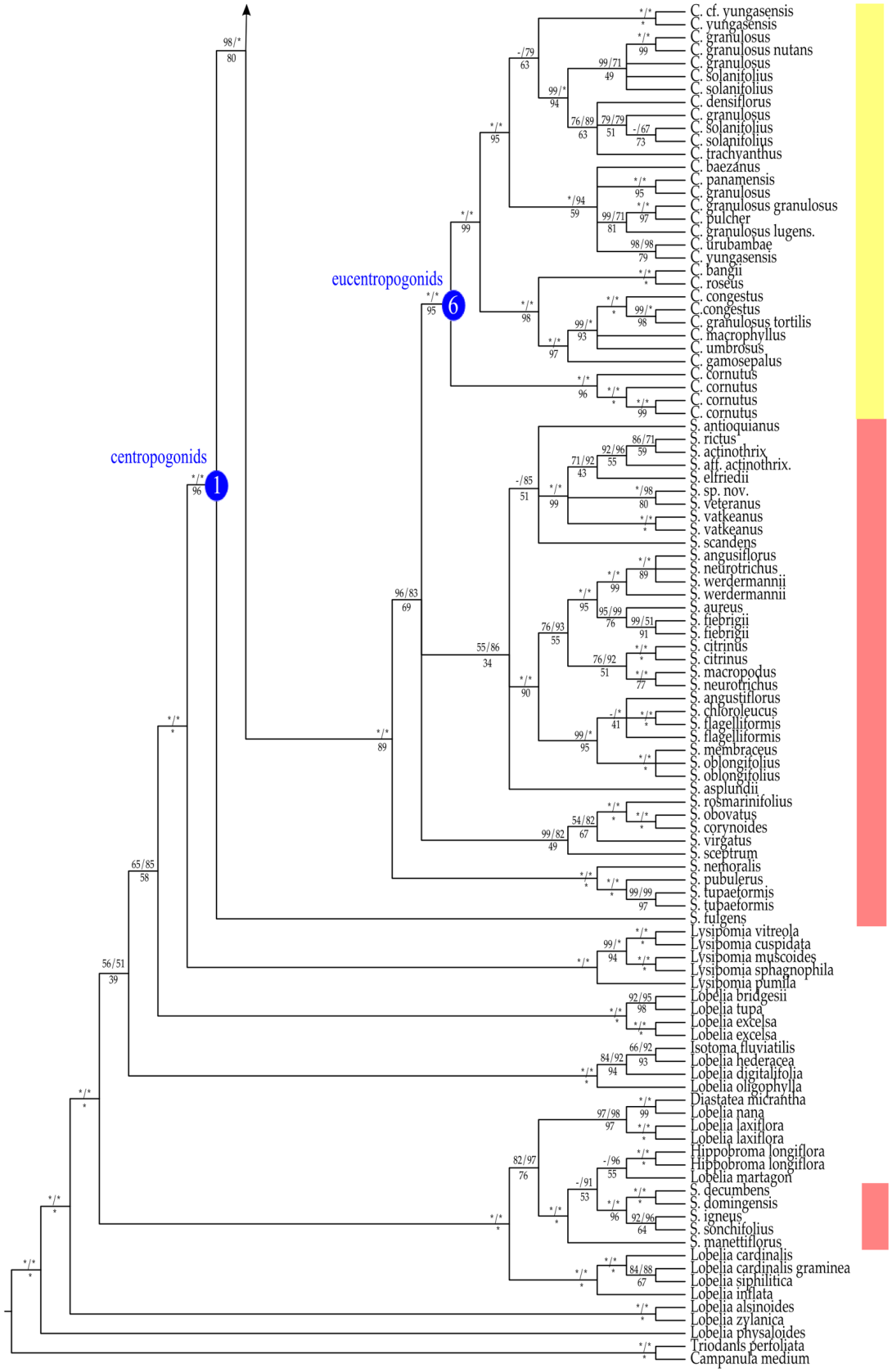


Figure 1.3 (Continued).

Figure 1.3 (Continued). Five locus plastid phylogeny of Neotropical Lobelioideae. Bayesian posterior probabilities (MrBayes / PhyloBayes) shown above branches. Maximum likelihood bootstrap support values shown below branches. * indicates highest possible support value; - indicates that the branch was not supported in the relevant analysis. The phylogram, depicting branch lengths, is inset (see also Figure A.2 for full phylogram with tip labels and scale bar). Species of *Burmeistera*, *Centropogon*, and *Siphocampylus* are color coded green, yellow, and **Figure 1.3 (Continued).** red, respectively, in the rectangles at right in both the cladogram and phylogram. Nodes with blue circles at nodes in the cladogram correspond to the six well-supported subclades described in detail in the text: 1) centropogonids; 2) burmeisterids; 3) brevilimbatids; 4) peruvianids; 5) colombianids; and the 6) eucentropogonids.

AU tests rejected the monophyly of i) *Centropogon* and ii) *Siphocampylus* ($P < 0.01$ and $P < 0.01$ respectively). They additionally rejected the monophyly of iii) mainland *Siphocampylus* (i.e., the monophyly of *Siphocampylus* when excluding the more distantly related Caribbean *Siphocampylus* in subsection *Hemisiphocampylus*) ($P < 0.01$).

We find the large cosmopolitan genus *Lobelia* to be polyphyletic. Members of the genus form a series of lineages including species of *Diastatea* Scheidw., *Hippobroma* G. Don., *Isotoma* (R. Br.) Lindl. and *Siphocampylus*, which are successively sister to the *Lysipomia* plus centropogonid clade (Figure 1.3). These findings corroborate previous studies (Antonelli 2008; Knox 2014). This highlights that additional phylogenetic efforts within *Lobelia* will be important since this genus represents more than a third of the species within the subfamily Lobelioideae, yet remains sparsely sampled. Lammers' (2011) revision of *Lobelia* will provide an important starting point for further targeted phylogenetic sampling to facilitate future reclassification.

Lysipomia is monophyletic (BP=100, PP=100/100) and placed sister to the centropogonids with high support (BP= 100, PP=100/100) (Figure 1.3), agreeing with the results of Antonelli (2008, 2009) and Knox et al. (2008). Within *Lysipomia*, the monophyly of subgenus *Lysipomia* (A. DC.) E. Wimm. is supported (BP=100, PP=100/100), but subgenus *Rhizocephalum* (Wedd.) E. Wimm. is paraphyletic.

The hexaploid ($n = 21$) species that constitute *Lobelia* section *Tupa* (Lammers and Hensold 1992; Lammers 1993, 2000), the Chilean lobelias, form a well supported clade (BP=100, PP= 100/100) that is moderately to weakly placed as sister to the centropogonids plus *Lysipomia* (BP= 58, PP=65/85; Figure 1.3). This clade collectively represents a broad pan-Andean distribution spanning temperate and tropical latitudes. Knox et al. (2008) similarly placed the Chilean lobelias sister to the centropogonids plus *Lysipomia*. Antonelli (2008) placed

them as more distantly related to the centropogonids, but with low support.

***Fruit evolution*—**Bayesian stochastic character mapping demonstrated that the ancestral fruit type of centropogonids is unequivocally capsular (PP=100; Figure 1.4). These results were corroborated by our maximum likelihood character state reconstruction (Figure A.3). On average, 12.2 transitions between character states were estimated on the phylogeny of the ((centropogonid, *Lysipomia*), *Lobelia* section *Tupa*) clade. Of these, 7.5 were from capsule to berry and 4.7 were transitions from berry to capsule. On average, 26.1% percent of the branch space (i.e., including branch lengths) is reconstructed as the berry state and 73.9% as the capsule state. The monophyly of capsular and berry fruited species was rejected by the AU test ($P < 0.01$ and $P < 0.01$ respectively).

1.5 Discussion

We present the first well-resolved, densely sampled phylogeny of *Burmeistera*, *Centropogon*, and *Siphocampylus*. Our plastid phylogeny greatly improves on prior taxon sampling efforts by including ~33% of the species in the centropogonid genera; previous studies have included at most ~8% (Knox et al. 2008). Our results indicate that the taxonomy of the centropogonids does not, for the most part, reflect evolutionary relationships. In lieu of proposing a new formal classification for the group, we discuss the existing classification of the centropogonids in light of our new phylogeny. We then discuss the dynamic pattern of fruit evolution in centropogonids, and suggest future directions for investigating Andean biogeography.

***Systematics*—**

Intergeneric phylogeny and taxonomy—The well-supported placement (BP=100, PP=100/100) of the Caribbean-endemic *Siphocampylus* subsection *Hemisiphocampylus* in a clade with other Caribbean lobeloids, including *Lobelia martagon* and *Hippobroma longiflora*, renders the CBS clade sensu Batterman and Lammers (2004) non-monophyletic (Figure 1.3). Despite their shared Caribbean distribution, members of this clade exhibit diverse morphologies: species of *Siphocampylus* subsection *Hemisiphocampylus* are suffrutescent subshrubs with reddish flowers, while *Hippobroma longiflora* (L.) G. Don. is a low weedy rosette plant with white flowers with long, narrow tubular corollas. These phylogenetic results provide strong support for taxonomic separation of the Caribbean *Siphocampylus* from mainland centropogonids. Species of subsection *Hemisiphocampylus* have traditionally been circumscribed within *Siphocampylus* largely on the basis of their shared Caribbean distribution. However, they also differ notably from other *Siphocampylus* in possessing a fenestrate corolla, and they have a generally lower vegetative stature. Further phylogenetic and morphological sampling are required before names can be applied to the species of *Siphocampylus, Hippobroma*, and *Lobelia* that constitute this clade.

Our newly discovered mainland centropogonid clade is not reflected in any previous classification. Our phylogeny renders the two tribes within subfamily Lobelioideae (Wimmer 1943, 1953, 1968), the berry fruited Delisseeae Rchb. (=Bacciferae E. Wimm.) and the capsular fruited Lobelieae Presl., non-monophyletic, a result that corroborates the reconstruction of fruit type within the subfamily by Givnish *et al.* (2009). This suggests that tribal circumscriptions of Lobelioideae have been misled by an over reliance on the single character of fruit type. This is not unique to the Lobelioideae; the classification schemes of several large tropical angiosperm clades have been guided by fruit type, only to have elements of these schemes shown to be non-

monophyletic by subsequent molecular phylogenetic systematics (e.g., Melastomataceae Juss. [Clausing et al., 2000], Malpighiaceae Juss. [Davis et al., 2001; Davis and Anderson, 2010], and Verbenaceae J. St.-Hil. [Marx et al., 2010]). In the case of Lobelioideae, a major overhaul of the tribal classification within the subfamily is necessary, as recognized previously by Lammers (Lammers 2004, 2007a, 2011).

We determined that *Burmeistera* form a well-supported clade, which confirms previous findings (Antonelli 2008, 2009; Knox et al. 2008). *Burmeistera* was originally described by Triana (1854), and his concept for the genus has been retained and subsequently refined (Wimmer 1943, 1953, 1968; Wilbur 1975; Nash 1976; Jeppesen 1981; Stein 1987b). Species in the genus are characterized by several putative synapomorphies, including: an inflated corolla opening, a dilated anther orifice, and isodiametric seeds. In the past, many species of *Centropogon* and *Siphocampylus* have been placed in *Burmeistera* because of their superficial similarity due to convergent evolution in floral morphology (e.g., many species of *Centropogon* section *Burmeisteroides* McVaugh, and the former *Burmeistera* section *Aequilatae* E. Wimm., now placed in *Siphocampylus* [Stein, 1987b]).

Our findings indicate that generic concepts of *Centropogon* and *Siphocampylus* are problematic. This discrepancy between taxonomy and phylogeny we identify likely results from the fact that fruit type was the basis for circumscription of each genus: *Centropogon* have berries and *Siphocampylus* have capsules. Many students of Lobelioideae have questioned the utility of fruit type in distinguishing these two genera due to the wide overlap of non-fruit characters (Gleason 1921; Stein 1987b; Lammers 1998). Whereas previous studies have documented the non-monophyly of *Centropogon* and *Siphocampylus* (Antonelli 2008, 2009; Knox et al. 2008), our results provide much greater detail on the extent to which these genera are polyphyletic.

Siphocampylus are the least resolved: its species fall into at least 11 distantly related clades. *Centropogon* fall into six well-supported clades and one grade constituting at least two separate clades (Figure 1.3).

Infrageneric Phylogeny and Taxonomy—Most previously circumscribed subgenera in *Burmeistera, Centropogon,* and *Siphocampylus* are polyphyletic. We discuss this finding in the context of two important contributions to the taxonomy of lobelioids: Wimmer's (1943, 1953, 1968) comprehensive monograph of the Lobelioideae, and McVaugh's refinements to Wimmer's classification of *Centropogon* (McVaugh 1949). Together, these works form the basis of the currently accepted classification in these genera (Lammers 1998, 2002, 2007b). In the following section, we consider the classification within each genus, and denote non-monophyletic genera when necessary with parentheses.

"Siphocampylus"— The 11 subclades of *Siphocampylus* we identified are not well resolved with respect to each other. Moreover, the species that constitute each of these clades are not easily characterized by morphology, distribution, or ecology, even in cases where clade support is high. Refining the placement of the constituent subclades of *Siphocampylus* remains fertile ground for future investigation. When this information is combined with detailed morphological investigations, we anticipate a clearer direction for dividing this group into monophyletic subunits.

Burmeistera—The monophyly of *Burmeistera* is well supported here (BP=100, PP=100/100) (Figure 1.3) and in previous studies (Antonelli 2008, Knox et al 2008). Within *Burmeistera*, however, Wimmer's two sections are not monophyletic (Table 1.1). Those sections, "*Imberbes"* nom. invalid (section *Burmeistera* sensu Lammers 1998) and *Barbatae* E. Wimm. are based on anther hair type (glabrous or sparsely pubescent, versus barbate). This character

appears to have a complex evolutionary history in this clade and should not be used alone to delineate taxa in *Burmeistera*.

"Centropogon"—Among the at least eight lineages of *Centropogon*, only one of Wimmer's taxa, section *Centropogon*, is monophyletic (Table 1.1). Five of these *Centropogon* subclades form the basis of our subsequent discussion because they can be delineated by morphology and exhibit reasonable overlap with currently accepted taxonomies (McVaugh 1949; Lammers 1998). We refer to these well-supported subclades informally as the brevilimbatids (BP= 64, PP=100/100), eucentropogonids (BP= 95, PP=100/100), peruvianids (BP= 85, PP=100/100), colombianids (BP= 99, PP=93/96), and burmeisterids (BP= 87, PP=100/100) (Figure 1.3). All clade names are derived from previous taxonomies (McVaugh 1949; Wimmer 1943).

The burmeisterids—The burmeisterid clade includes *Burmeistera* plus a grade of robust, green-flowered *Centropogon* species that fall into at least two separate lineages, which are successively sister to *Burmeistera*. These *Centropogon* species are placed in two greges of *Centropogon* section *Siphocampyloides* Benth. & Hook. subsection *Macranthi* E. Wimm. by Wimmer. In McVaugh (1949), they are placed in *Centropogon* section *Burmeisteroides* Gleason.

The burmeisterids occur from Guatemala to northern Peru. They share an inflated corolla opening, which has previously been recognized as a defining trait for *Burmeistera*. This represents a potential synapomorphy for the entire burmeisterid clade. Additionally, burmeisterid species tend to have robust, green flowers, many of which are known to be pollinated by long-tongued bats (Muchhala 2006b; Muchhala and Potts 2007; Muchhala and Thomson 2009). The grade of *Centropogon* species (Figure 1.2B) differs from *Burmeistera* (Figure 1.1A) in their erect, soft-woody shrub habit, larger flowers, constricted anther orifice, and seeds that are

slightly longer than wide. The morphology of berries within burmeisterids is quite variable (e.g., Figure 1.2E-F).

Species within McVaugh's section *Burmeisteroides* fall into at least two distinct and distantly related clades, the burmeisterids and the peruvianids. This is an example where the classification groups distantly related species using features that appear to have evolved convergently. Both clades include shrubby species with large, cream-colored or greenish flowers, with wide openings and large anthers that produce abundant pollen. This combination of characters is widely accepted as part of the bat pollination syndrome (e.g., Fleming et al., 2009), which likely arose than once within the centropogonids (L. Lagomarsino, in prep.).

The brevilimbatids—The brevilimbatids are sister to the burmeisterids and include two subclades: the capsular-fruited *S. jelksii,* and a second, well-supported (BP=98, PP=100/100) subclade including numerous berry-fruited *Centropogon* species. The berry-fruited brevilimbatids largely comprise species from Wimmer's *Centropogon* section *Siphocampyloides* subsection *Brevilimbatii* grex *Stellato-tomentosi*. This grex is not monophyletic as it also includes species that we place separately in the peruvianid clade (see below). Additionally, the glabrous species we place in the brevilimbatid clade (i.e., *C. valerii*, *C. grandidentatus* [Schltdl.] Zahlbr., and *C. trichodes* E. Wimm.) include some, but not all, of Wimmer's subsection *Brevilimbatii* E. Wimm. grex *Formosi* E. Wimm. This grex is also non-monophyletic, with numerous members belonging in our colombianid clade (see below). Within McVaugh's taxonomy, the berry-producing brevilimbatid clade corresponds closely to *Centropogon* section *Siphocampyloides* subsection *Brevilimbatii*. However, glabrous species in the brevilimbatid clade were placed elsewhere by McVaugh in his *Centropogon* section *Wimmeriopsis* McVaugh subsection *Falcati* McVaugh.

The berry-fruited brevilimbatids are scandent plants of mostly exposed areas with a uniform floral form. They possess long, narrow, orange corolla tubes with falcate, narrowly triangular yellow lobes and steel grey anthers that are glabrous or sparsely pubescent (Figure 1.1C). Berries in these species are leathery (Figure 1.2D). Most species have leaves, stems, and corollas that are covered in tawny, branched trichomes. *Siphocampylus jelskii*, the sister to the rest of the brevilimbatids, differs in its capsular fruit and growth from, which is characterized by tall stems with large terminal leaf rosettes, much like species of *Espeletia* Mutis ex Bonpl. (Asteraceae), which also occur in high altitude Andean grasslands (e.g., páramo and puna). In addition, its large greenish flower with wide opening is more similar to the burmeisterids then the rest of the brevilimbatids. While *S. jelskii* shares these aspects of its floral morphology with the burmeisterids, it overlaps in its high elevation habitat with the rest of the brevilimbatids, many of which prefer habitats above treeline.

The peruvianids—The peruvianids mainly comprise taxa from Wimmer's *Centropogon* section *Siphocampyloides* subsection *Macranthi* grex *Mandonioides* E. Wimm., and to a lesser extent from his subsection *Brevilimbatii* grex *Stellato-tomentosi* E. Wimm. Most peruvianids were placed in *Centropogon* section *Siphocampyloides* subsection *Peruvianii* by McVaugh. However, one species from outside McVaugh's subsection *Peruvianii* falls into this clade: *C. incanus* (Britton) Zahlbr. (section *Burmeisteriodes*, see discussion above). *Centropogon dianae* Lammers, the only species of the monotypic section *Niveopsis* Lammers (Lammers 1998), is deeply nested within the peruvianids.

The peruvianids are tall (> 3 m), robust shrubs of the central Andes of Peru and Bolivia. They frequently have branched trichomes, and both vegetative surfaces and flowers emit a musky odor. They have large, sturdy flowers with corollas of various colors. The corolla lobes

are usually narrowly triangular and falcate (Figure 1.1B), but these can sometimes be deltate and decurved (e.g., *C. dianae*). Anther connectives bear dense, long, simple hairs. They produce the largest berries among the centropogonids (Figure 1.2C).

The colombianids—The colombianids encompass part of Wimmer's *Centropogon* section *Siphocampyloides* subsection *Brevilimbatii* grex *Formosii*, with the exception of *Siphocampylus nematosepalus* (Donn. Sm.) E. Wimm., which he placed in *Siphocampylus* section *Macrosiphon* E. Wimm. subsection *Siphocampylus* (A. DC.) E. Wimm. grex *Dissitiflori* E. Wimm. Remaining members of grex *Formosii* occur throughout the centropogonid phylogeny, rendering it non-monophyletic. In McVaugh's treatment, the colombianids correspond closely to *Centropogon* section *Wimmeriopsis* subsection *Colombiani* McVaugh with two exceptions. His treatment did not extend to *Siphocampylus*, and so could not have included *S. nematosepalus* (which we place among the colombianids). Also, we place *C. tessmannii* E. Wimm., which McVaugh included in subsection *Colombiani*, outside of the colombianids.

The colombianids are restricted to premontane and montane regions of Central America and the adjacent Chocó region of Colombia. Members of this clade are scandent or climbing vines, either woody or herbaceous, with a small stem diameter and leaves with pronounced dentation. The corolla is always long-tubular and bright pink or red, with narrowly triangular lobes that are usually erect or spreading, (Figure 1.1D). Fruit form is variable: berries and capsules are both present, and berries are either dry-leathery or fleshy with a thin exocarp (Figure 1.2B). Due to its fruit type, *S. nematosepalus* is not currently placed in the same genus as the rest of the colombianids. However, despite it being the only member of its clade that produces capsules, the rest of its morphology is otherwise very similar to other colombianid species.

The eucentropogonids—The eucentropogonid clade corresponds completely to Wimmer's and McVaugh's section *Centropogon,* which was elevated to subgeneric rank and renamed *Centropogon* (Wilbur 1976). The most recent monograph and taxonomic revision of this clade was by Stein (1987a). The name eucentropogonid comes from their taxonomic history: *Centropogon* section *Centropogon* was originally described as section *Eucentropogon,* but the International Code of Botanical Nomenclature no longer allows this naming convention, as detailed in Article 21.3.

The eucentropogonids' primary characteristic is a cornute scale-like appendage of concrescent hairs at the base of the two lower anthers (Figure 1.1E, arrow), a trait that functions in their pollination biology. Flowers, which are oriented vertically, are often abruptly curved (Figure 1.1E) and are frequently arranged in erect terminal inflorescences. This is likely to be an adaptation for pollination by sicklebill hummingbirds (*Eutoxeres*: Phaethornidae; Stein 1992). Plants are vegetatively glabrous or sparsely pubescent and occur at low elevations relative to the rest of the centropogonids, which occur more broadly from sea level to ~1500 m.

Based on our sampling, the eucentropogonids can be subdivided into three subclades. One consists solely of the widespread, though morphologically homogenous *Centropogon cornutus*, whose monophyly is strongly supported (BP=96, PP=100/100). It is a scandent subshrub with light pink, moderately curved corollas that grows at low elevations, including in the Amazon basin. Although it is a single species, branch lengths between individuals are amongst the longest within the ingroup (Figure A.2), suggesting that there may be cryptic species within this group. The second subclade (BP=95, PP=100/100) corresponds largely to Wimmer's grex *Campylobotrys* E. Wimm. (and completely to Stein's subsection of the same name). These are vining subshrubs of low to mid-elevations with corollas with tubes that are are extremely

curved and tend to be red in color (Fig 1E). The corollas have bright yellow deltate lobes; the dorsal pair are strongly recurved, and the ventral three are reflexed. The most common and widespread species of this clade is *Centropogon granulosus*, which we find is not monophyletic (Figure 1.3). The third subclade (BP=98, PP=100/100) consists of species that are placed in various greges of Wimmer's section *Centropogon*, but whose membership corresponds exactly to Stein's subsection *Amplifolii*. These species are erect clonal herbs with bright pink flowers having extremely curved corolla tubes. They grow in wet soils at low to mid elevations. When they occur at lower elevations, they frequently develop extrafloral nectaries between calyx lobes, thought to attract ants as defense against herbivory (Stein 1992).

***Fruit Evolution*—**The lability of fruit evolution in the centropogonids is striking. Stochastic character mapping shows that the ancestor of the centropogonids was capsular, with an average of 7.5 more recent origins of berries (Figure 1.4). While the majority of transitions are from capsule to berry, on average 4.7 reversions from berry to capsule are inferred, suggesting that fruit evolution is not unidirectional in the centropogonids. Two of these inferred reversals, representing the independent evolution of capsules in *S. jelskii* and *S. nematosepalus*, are supported very strongly in our reconstructions. Given the homoplasy in fruit type, it is unlikely that fruit types are homologous across the centropogonids. In this regard, it is not surprising that the gross morphology of berries is quite variable among centropogonids. They can be dry and leathery with a rounded distal end (e.g., the brevilimbatids; Figure 1.2D), round with opaque, juicy mesocarp and a leathery, ribbed exterior (e.g., in the eucentropogonids and peruvianids; Figure 1.2C), somewhat inflated with spongy mesocarp (e.g., *B. toroensis* Wilbur; Figure 1.2F), much inflated and thin-walled, lacking a fleshy mesocarp (e.g., *B. vulgaris*) (Figure 1.2E), or oblong with thin exocarp and viscous pericarp (Figure 1.2B).

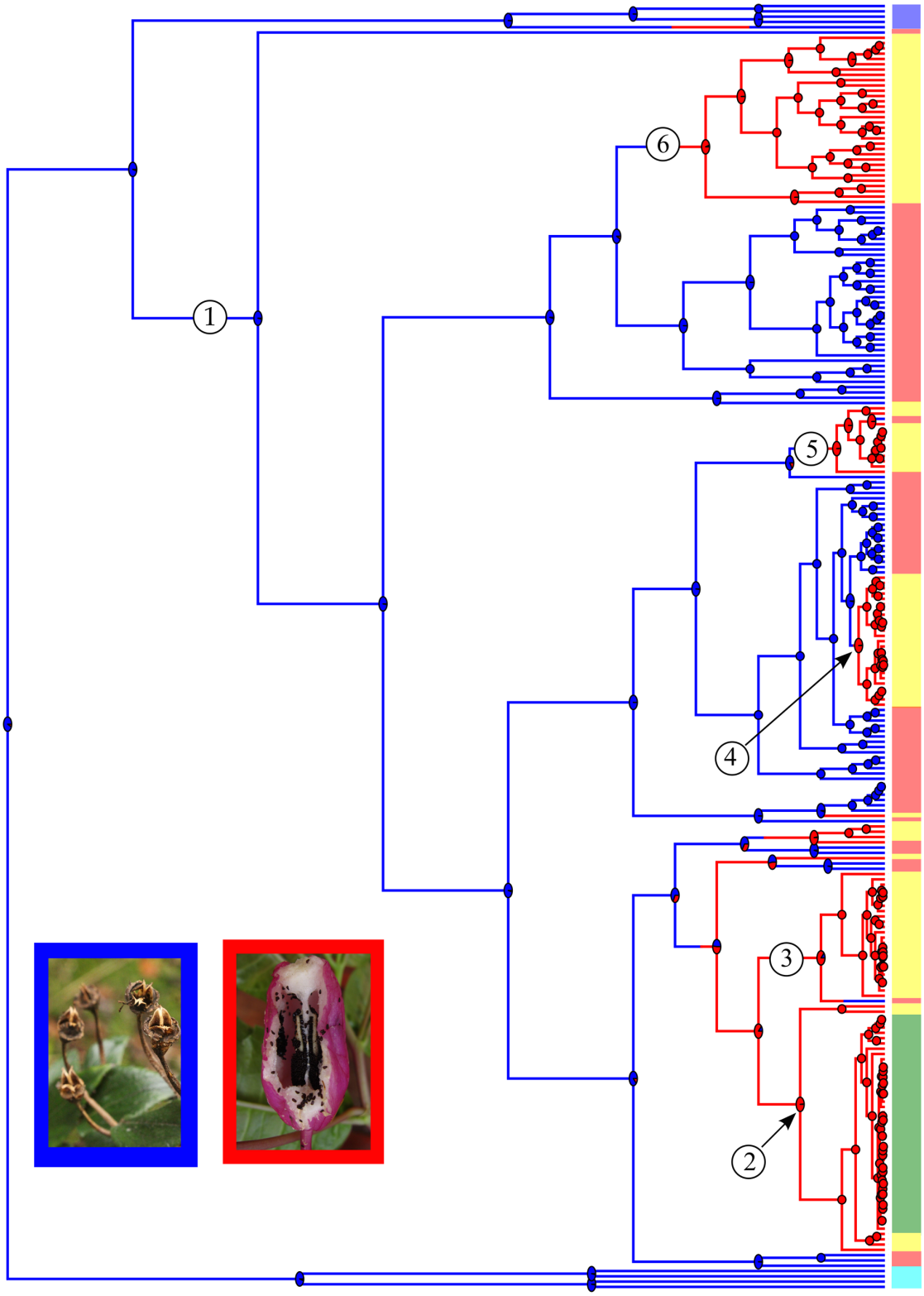


Figure 1.4. Bayesian stochastic character mapping of fruit evolution.

Figure 1.4 (Continued). Bayesian stochastic character mapping of fruit evolution. Pie charts at nodes represent ancestral states that were calculated as the marginal posterior probability of capsule (blue) and berry (red). White circles at internodes or indicated by arrows correspond to the six subclades we define in the text, numbered according to Figure 1.3: 1) centropogonids; 2) burmeisterids; 3) brevilimbatids; 4) peruvianids; 5) colombianids; and the 6) eucentropogonids. Bars to the right of the phylogeny are color-coded according to taxon: *Lysipomia* (purple), *Centropogon* (yellow), *Siphocampylus* (red), *Burmeistera* (green), and *Lobelia* section *Tupa* (light blue). Photos of representative fruits are *Siphocampylus ayersiae* Lammers (capsule) and *Burmeistera toroensis* Wilbur (berry). (Photos: L. Lagomarsino)

In contrast, capsule morphology within the centropogonids is not very diverse: they are bilocular and open apically via two valves (Figure 1.2A). This suggests that the ancestral, centropogonid-type capsule was modified in various ways to form a fleshy, animal-dispersed berry.

More broadly within Capanulaceae, Givnish *et al.* (2009) demonstrate that fleshy fruits have evolved in at least six distantly related clades outside of the centropogonids. Our analysis is consistent with this broader view that fruit evolution is particularly labile in Campanulaceae, but our results suggest that patterns of fruit evolution may be far more dynamic. An in-depth morphological and developmental survey of fruits in Campanulaceae would aid in characterizing fruit evolution in the family. This could be coupled with powerful molecular developmental genetics to determine the genes underlying the independent, potentially distinct developmental transitions between fruit type, both within the closely related centropogonids and the more distantly related Campanulaceae. The FRUITFULL MADS-box gene lineage may be of particular interest in this endeavor (Knapp and Litt, 2013; Litt et al., 2013; Pabón-Mora and Litt, 2011).

More generally, transitions between fleshy and dry fruits have been important in angiosperm evolution. It is thought that the evolution of fleshy fruit may be an adaptation to facilitate animal dispersal in forest understories (Gentry, 1982; Givnish et al., 2005), including within Campanulaceae (Givnish 2009). Some of our data are consistent with this hypothesis. For example, capsular taxa in the centropogonids (i.e., *Siphocampylus*) tend to occur in exposed environments, either above tree line, in shrubland, or on cliffs. Additionally, *Burmeistera*, all of which produce berries, occur exclusively in forest interiors. There are also specific cases of contrasting fruit type in sister lineages that support this hypothesis: *S. jelskii* (brevilimbatid) and *S. nematosepalus* (colombianid), both of which represent reversals from berries to capsules

(Figure 1.4), occur above tree line whereas their closest berry-fruited relatives tend to occur in forest interiors. Also, berry-producing *C. tessmannii* grows in lowland tropical rainforest interior, while its capsular-fruited sister group consists of species that all grow on exposed montane cliffs in Brazil. This pattern is not universal, however. Many berry-fruited *Centropogon* species occur in exposed or disturbed habitat (e.g., a small number of baccate brevilimbatids can grow in páramo, and many species only occur in exposed, open areas, including *C. coccineus*, *C. granulosus*, and *C. smithii* E. Wimm.). Regardless, these observations suggest that a combination of elevation, precipitation, and habitat type may have greatly influenced fruit evolution within the centropogonids, suggesting that the group may provide an additional test of the correlation between fleshy fruits and forest understories first proposed by Gentry (1982) and tested across monocots by Givnish et al. (2005).

Biogeography: a Neotropical, primarily Andean radiation—The centropogonids are part of a larger Neotropical radiation that includes *Lysipomia* and *Lobelia* section *Tupa*. *Lysipomia* and the centropogonids together represent a tropical, primarily Andean component of this radiation that is estimated to be approximately 15-18 My (Antonelli 2009; Givnish et al., 2009), although the two groups have markedly different natural histories. The centropogonids, whose crown group is estimated to be ~5-12 My (Antonelli, 2009; Givnish et al., 2009), are shrubby, robust cloud-forest plants. *Lysipomia*, whose crown group is estimated to be ~11 My (Antonelli, 2009), in contrast, are diminutive herbs with extreme adaptations to the highest elevations of the Andes. If we expand our phylogenetic view to also include the closely related, species-poor *Lobelia* section *Tupa,* this clade forms a mainly pan-Andean radiation that encompasses both tropical and temperate ecosystems. Within this larger clade, *Lysipomia* represents an extremely derived morphology, specialized to its high-elevation habitat. *Lobelia*

section *Tupa* share many similarities with the centropogonids, despite their occurrence in temperate latitudes of the southern Andes of central Chile. These similarities include their suffrutescent habit and tendency towards red, long-tubular corollas, typical of hummingbird pollinated plants. These traits are likely pleisiomorphic within the centropogonids, and are shared with the species that is sister to the rest of the centropogonid clade, *Siphocampylus fulgens*. An in-depth analysis to determine the origin of the progenitor of this Andean-centered radiation will be possible when additional taxa have been sampled.

Given their myriad growth forms and extreme floral diversity, the centropogonids are one of the most dramatic primarily Andean radiations in angiosperms. Many other Andean plant groups (e.g., *Lupinus* L. [Hughes and Eastwood, 2006], *Valeriana* L. [Bell and Donoghue, 2005], *Vasconella* Walp. [Antunes Carvalho and Renner, 2012], and *Puya* Molina [Jabaily and Sytsma, 2013]) are thought to have radiated rapidly in a similar timeframe as the centropogonids, within the last 10 My, likely in response to a combination of the last phases of Andean orogeny, climate fluctuations, and biotic interactions (e.g., with pollinators) (Luebert and Weigend 2014). To our knowledge, fine-scale phylogenetic relationships of these clades have remained largely unresolved, which hinders focused biogeographical investigation. Our robust centropogonid phylogeny is the foundation for a unique investigation of fine-scale patterns of diversification and niche evolution in this hotspot of biodiversity. The importance of centropogonids in this regard results from their exceptional breadth of habitat diversity compared to many other Andean plant groups.

The future inclusion of phylogenetic data from the nuclear genome will undoubtedly improve our understanding of evolution within the centropogonids, especially in light of polyploidization within this young (<12 Ma), rapidly diversifying clade. Fortunately, the

acquisition of genomic-scale nuclear data is quickly becoming feasible in non-model organisms (Grover et al. 2012, Weitemier et al. 2014), including within Asterales, which includes Campanulaceae (Mandel et al. 2014). Along these lines, owing to their rapid radiation it seems possible that incomplete lineage sorting has lead to gene tree-species tree discordance within the centropogonids. Future effort should explore the effect of this phenomenon with additional data by applying phylogenetic reconstruction methods that utilize coalescent methods (e.g, Liu et al. 2009).

1.6. Acknowledgements

The authors would like to thank the collection and export permitting agencies in Bolivia, Brazil, Colombia, Costa Rica, Ecuador, Panama, and Peru. The Smithsonian Tropical Research Institute in Panama and the Organization for Tropical Studies in Costa Rica additionally helped to facilitate permitting. Field assistance for L.L.'s collections was provided by M. Mendoza (Bolivia), J. Janovec (Peru), and, in particular, D. Santamaría Aguilar (Costa Rica, Panama, Bolivia, Peru). Additional samples were provided by C. Bacon. T. Lammers identified many specimens used in this study. The following herbaria kindly allowed the use of their collections: A, CR, GB, GH, INB, LPB, MO, MOL, NY, PMA, SCZ, USM, and USZ. Funding for this project was provided by a National Science Foundation Doctoral Dissertation Improvement Grant to C.D. and L.L. (DEB-1210401), a Deland Award from the Arnold Arboretum, an Exploration Fund Grant from the Explorer's Club, and student research grants from the Botanical Society of America, the American Society of Plant Taxonomists, and the David Rockefeller Center for Latin American Studies at Harvard University. Comments on the draft by L. Nikolov

and D. Santamaría Aguilar improved this manuscript. Z. Xi and E. Forrestel provided advice on analytical methods.

1.7 References

Aberer, A. J., D. Krompass, and A. Stamatakis. 2013. Pruning rogue taxa improves phylogenetic accuracy: an efficient algorithm and webservice. Syst. Biol. 62:162–6.

Altekar, G., S. Dwarkadas, J. P. Huelsenbeck, and F. Ronquist. 2004. Parallel Metropolis coupled Markov chain Monte Carlo for Bayesian phylogenetic inference. Bioinformatics 20:407–15.

Álvarez, I., and J. F. Wendel. 2003. Ribosomal ITS sequences and plant phylogenetic inference. Mol. Phylogenet. Evol. 29:417–434.

Antonelli, A. 2009. Have giant lobelias evolved several times independently? Life form shifts and historical biogeography of the cosmopolitan and highly diverse subfamily Lobelioideae (Campanulaceae). BMC Biol. 7:82.

Antonelli, A. 2008. Higher level phylogeny and evolutionary trends in Campanulaceae subfam. Lobelioideae: Molecular signal overshadows morphology. Mol. Phylogenet. Evol. 46:1–18.

Antonelli, A., J. A. A. Nylander, C. Persson, and I. Sanmartín. 2009. Tracing the impact of the Andean uplift on Neotropical plant evolution. Proc. Natl. Acad. Sci. U. S. A. 106:9749–9754.

Antunes Carvalho, F., and S. S. Renner. 2012. A dated phylogeny of the papaya family (Caricaceae) reveals the crop's closest relatives and the family's biogeographic history. Mol. Phylogenet. Evol. 65:46–53.

Baker, H. G. 1961. The adaptation of flowering plants to nocturnal and crepusclar pollinators. Q. Rev. Biol. 36:64–73.

Batterman, M. R. W., and T. G. Lammers. 2004. Branched foliar trichomes of Lobelioideae (Campanulaceae) and the infrageneric classification of Centropogon. Syst. Bot. 29:448–458.

Bell, C. D., and M. J. Donoghue. 2005. Phylogeny and biogeography of Valerianaceae (Dipsacales) with special reference to the South American valerians. Org. Divers. Evol. 5:147–159.

Bollback, J. P. 2006. SIMMAP: stochastic character mapping of discrete traits on phylogenies. BMC Bioinformatics 7:88.

Clausing, G., K. Meyer, and S. S. Renner. 2000. Correlations among fruit traits and evolution of different fruits within Melastomataceae. Bot. J. Linn. Soc. 133:303–326.

Colwell, R. K., B. J. Betts, P. Bunnell, F. L. Carpenter, and P. Feinsinger. 1974. Competition for the nectar of *Centropogon valerii* by the hummingbird *Colibri thalassinus* and the flower-piercer *Diglossa plumbea*, and its evolutionary implications. Condor 76:447–452.

Davis, C. C., and W. R. Anderson. 2010. A complete generic phylogeny of Malpighiaceae inferred from nucleotide sequence data and morphology. Am. J. Bot. 97:2031–48.

Davis, C. C., W. R. Anderson, and M. J. Donoghue. 2001. Phylogeny of Malpighiaceae: Evidence form chloroplast ndhF and trnL-F nucleotide sequences. Am. J. Bot. 88:1830–1846.

Denton, A. L., B. L. McConaughy, and B. D. Hall. 1998. Usefulness of RNA Polymerase II coding sequences for estimation of green plant phylogeny. Mol. Biol. Evol. 15:1082–1085.

Edgar, R. C. 2004. MUSCLE: multiple sequence alignment with high accuracy and high throughput. Nucleic Acids Res. 32:1792–7.

Erbar, C., and P. Leins. 1995. Portioned pollen release and the syndromes of secondary pollen presentation in the Campanulales-Asterales complex. FLORA 190:323–338.

Faegri, K., and L. van der Pijl. 1979. The Principles of Pollination Ecology. 3rd ed. Oxford: Pergamon Press.

Fenster, C. B., W. S. Armbruster, P. Wilson, M. R. Dudash, and J. D. Thomson. 2004. Pollination Syndromes and Floral Specialization. Annu. Rev. Ecol. Evol. Syst. 35:375–403.

Fleming, T. H., C. Geiselman, and W. J. Kress. 2009. The evolution of bat pollination: A phylogenetic perspective. Ann. Bot. 104:1017–1043.

Garzón Venegas, J., and F. González. 2012. Five new species and three new records of *Burmeistera* (Campanulaceae-Lobelioideae) from Colombia. Caldasia 34:309–324.

Garzón Venegas, J., F. González, and J. M. Vélez Puerta. 2012. *Burmeistera minutiflora* (Campanulaceae-Lobelioideae), a new species from the high Andes of Antioquia (Colombia) with the smallest flowers in the genus. An. del Jardín Botánico Madrid 69:243–246.

Gentry, A. H. 1982. Patterns of Neotropical plant species diversity. Pp. 1–84 *in* M. K. Hecht, B. Wallace, and G. T. Prance, eds. Evolutionary Biology. Springer US, Boston, MA.

Givnish, T. J., K. C. Millam, A. R. Mast, T. B. Paterson, T. J. Theim, A. L. Hipp, J. M. Henss, J. F. Smith, K. R. Wood, and K. J. Sytsma. 2009. Origin, adaptive radiation and

diversification of the Hawaiian lobeliads (Asterales: Campanulaceae). Proc. R. Soc. B Biol. Sci. 276:407–416.

Givnish, T. J., J. C. Pires, S. W. Graham, M. a McPherson, L. M. Prince, T. B. Patterson, H. S. Rai, E. H. Roalson, T. M. Evans, W. J. Hahn, K. C. Millam, A. W. Meerow, M. Molvray, P. J. Kores, H. E. O'Brien, J. C. Hall, W. J. Kress, and K. J. Sytsma. 2005. Repeated evolution of net venation and fleshy fruits among monocots in shaded habitats confirms a priori predictions: Evidence from an ndhF phylogeny. Proc. R. Soc. B Biol. Sci. 272:1481–1490.

Gleason, H. A. 1921. A rearrangement of the Bolivian species of *Centropogon* and *Siphocampylus*. Bull. Torrey Bot. Club 48:189–201.

Howarth, D. G., and D. a Baum. 2005. Genealogical evidence of homoploid hybrid speciation in an adaptive radiation of *Scaevola* (Goodeniaceae) in the Hawaiian Islands. Evolution (N. Y). 59:948–61.

Howarth, D. G., and D. A. Baum. 2002. Phylogenetic utility of a nuclear intron from nitrate reductase for the study of closely related plant species. Mol. Phylogenet. Evol. 23:525–528.

Hughes, C., and R. Eastwood. 2006. Island radiation on a continental scale: Exceptional rates of plant diversification after uplift of the Andes. Proc. Natl. Acad. Sci. U. S. A. 103:10334–10339.

Jabaily, R. S., and K. J. Sytsma. 2013. Historical biogeography and life-history evolution of Andean *Puya* (Bromeliaceae). Bot. J. Linn. Soc. 171:201–224.

Jeppesen, S. 1981. Lobeliaceae. Pp. 9–170 *in* G. Harling and B. Sparre, eds. Flora of Ecuador, No 14. Swedish Natural Science Research Council.

Johansen, L. B. 2005. Phylogeny of *Orchidantha* (Lowiaceae) and the Zingiberales Based on Six DNA Regions. Syst. Bot. 30:106–117.

Knapp, S., and A. Litt. 2013. 2. Fruit- An Angiosperm Innovation. *in* G. B. Seymour, M. Poole, J. J. Giovannoni, and G. A. Tucker, eds. The Molecular Biology and Biochemistry of Fruit Ripening. Blackwell Publishing Ltd., Oxford, UK.

Knox, E. B. 2014. The dynamic history of plastid genomes in the Campanulaceae sensu lato is unique among angiosperms. Proc. Natl. Acad. Sci., doi: 10.1073/pnas.1403363111.

Knox, E. B., A. M. Muasya, and N. Muchhala. 2008. The predominantly South American clade of Lobeliaceae. Syst. Biol. 33:462–468.

Lammers, T. G. 2004. Campanulaceae. Pp. 78–80 *in* N. Smith, S. A. Mori, A. Henderson, and D. W. Stevenson, eds. Flowering plants of the Neotropics. Princeton University Press, in association with The New York Botanical Garden.

Lammers, T. G. 2007a. Campanulaceae. Pp. 26–56 *in* K. Kubitzki, J. W. Kadereit, and C. Jeffrey, eds. The Families and Genera of Vascular Plants. Springer-Verlag, Berlin.

Lammers, T. G. 1998. Review of the neotropical endemics *Burmeistera*, *Centropogon*, and *Siphocampylus* (Campanulaceae: Lobelioideae), with description of 18 new species and a new section. Brittonia 50:233–262.

Lammers, T. G. 2011. Revision of the Infrageneric Classification of *Lobelia* L. (Campanulaceae: Lobelioideae). Ann. Missouri Bot. Gard. 98:37–62.

Lammers, T. G. 2002. Seventeen new species of Lobelioideae (Campanulaceae) from South America. Novon 12:206–233.

Lammers, T. G. 2007b. World Checklist and Bibliography of Campanulaceae. Royal Botanic Gardens, Kew.

Lanfear, R., B. Calcott, S. Y. W. Ho, and S. Guindon. 2012. Partitionfinder: Combined selection of partitioning schemes and substitution models for phylogenetic analyses. Mol. Biol. Evol. 29:1695–1701.

Lartillot, N., and H. Philippe. 2004. A Bayesian mixture model for across-site heterogeneities in the amino-acid replacement process. Mol. Biol. Evol. 21:1095–109.

Leins, P., and C. Erbar. 2006. Secondary pollen presentation syndromes of the Asterales — a phylogenetic perspective. Bot. Jahrbücher 127:83–103.

Lewis, P. O. 2001. A likelihood approach to estimating phylogeny from discrete morphological character data. Syst. Biol. 50:913–925.

Litt, A., M. Strahl, E. McCarthy, R. Meyer, and N. Pabón-Mora. 2013. The role of FRUITFULL genes in the fruit development in Solanaceae. *in* Botany. New Orleans, LA, USA.

Luebert, F., and M. Weigend. 2014. Phylogenetic insights into Andean plant diversification. Front. Ecol. Evol. 2:1–17.

Maddison, W. P., and D. R. Maddison. 2011. Mesquite: a modular system for evolutionary analysis.

Madriñán, S., A. J. Cortés, and J. E. Richardson. 2013. Páramo is the world's fastest evolving and coolest biodiversity hotspot. Front. Genet. 4:1–7.

Marx, H. E., N. O'Leary, Y.-W. Yuan, P. Lu-Irving, D. C. Tank, M. E. Múlgura, and R. G. Olmstead. 2010. A molecular phylogeny and classification of Verbenaceae. Am. J. Bot. 97:1647–63.

Mason-Gamer, R. J., C. F. Weil, and E. A. Kellogg. 1998. Granule-bound starch synthase: structure, function, and phylogenetic utility. Mol. Biol. Evol. 15:1658–73.

McVaugh, R. 1949. Studies in South American Lobelioideae (Campanulaceae) with special reference to Colombian species. Brittonia 6:450–493.

Muchhala, N. 2003. Exploring the boundary between pollination syndromes: Bats and hummingbirds as pollinators of *Burmeistera cyclostigmata* and *B. tenuiflora* (Campanulaceae). Oecologia 134:373–380.

Muchhala, N. 2006a. Nectar bat stows huge tongue in its rib cage. Nature 444:701–2.

Muchhala, N. 2006b. The pollination biology of *Burmeistera* (Campanulaceae): Specialization and syndromes. Am. J. Bot. 93:1081–1089.

Muchhala, N., and T. G. Lammers. 2005. A New Species of *Burmeistera* (Campanulaceae: Lobelioideae) from Ecuador. Novon 15:176–179.

Muchhala, N., and M. D. Potts. 2007. Character displacement among bat-pollinated flowers of the genus *Burmeistera*: Analysis of mechanism, process and pattern. Proc. R. Soc. B Biol. Sci. 274:2731–2737.

Muchhala, N., and J. D. Thomson. 2009. Going to great lengths: Selection for long corolla tubes in an extremely specialized bat-flower mutualism. Proc. R. Soc. B Biol. Sci. 276:2147–2152.

Myers, N., R. A. Mittermeier, C. G. Mittermeier, G. A. B. Fonseca, and J. Kent. 2000. Biodiversity hotspots for conservation priorities. Nature 403:853–858.

Nash, D. L. 1976. Campanulaceae. Pp. 396–431 *in* D. L. Nash and J. V. A. Dieterle, eds. Floral of Guatemala. Fieldiana, Botany.

Nylander, J. a a, J. C. Wilgenbusch, D. L. Warren, and D. L. Swofford. 2008. AWTY (Are We There Yet?): a system for graphical exploration of MCMC convergence in Bayesian phylogenetics. Bioinformatics 24:581–3.

Pabón-Mora, N., and A. Litt. 2011. Comparative anatomical and developmental analysis of dry and fleshy fruits of Solanaceae. Am. J. Bot. 98:1415–36.

Paradis, E., J. Claude, and K. Strimmer. 2004. APE: Analyses of Phylogenetics and Evolution in R language. Bioinformatics 20:289–290.

Pennington, R. T., M. Lavin, T. Sarkinen, G. P. Lewis, B. B. Klitgaard, and C. E. Hughes. 2010. Contrasting plant diversification histories within the Andean biodiversity hotspot. Proc. Natl. Acad. Sci. 107:13783–13787.

Rambaut, A., and A. J. Drummond. 2003. Tracer.

Revell, L. J. 2012. phytools: an R package for phylogenetic comparative biology (and other things). Methods Ecol. Evol. 3:217–223.

Ronquist, F., M. Teslenko, P. van der Mark, D. L. Ayres, A. Darling, S. Höhna, B. Larget, L. Liu, M. a Suchard, and J. P. Huelsenbeck. 2012. MrBayes 3.2: efficient Bayesian phylogenetic inference and model choice across a large model space. Syst. Biol. 61:539–42.

Sanderson, M. J. 2002. Estimating absolute rates of molecular evolution and divergence times: A penalized likelihood approach. Mol. Biol. Evol. 19:101–109.

Sang, T. 2002. Utility of low-copy nuclear gene sequences in plant phylogenetics. Crit. Rev. Biochem. Mol. Biol. 37:121–47.

Sazima, M., I. Sazima, and S. Buzato. 1994. Nectar by day and night: *Siphocampylus sulfureus* (Lobeliaceae) pollinated by hummingbirds and bats. Plant Syst. Evol. 191:237–246.

Shaw, J., E. B. Lickey, E. E. Schilling, and R. L. Small. 2007. Comparison of whole chloroplast genome sequences to choose noncoding regions for phyogenetic studies in angiosperms: the tortoise and the hare III. Am. J. Bot. 94:275–288.

Shimodaira, H. 2002. An approximately unbiased test of phylogenetic tree selection. Syst. Biol. 51:492–508.

Shimodaira, H. 2010. scaleboot: Approximately unbiased p-values via multiscale bootstrap.

Simmons, M. P., and H. Ochoterena. 2000. Gaps as characters in sequence-based phylogenetic analyses. Syst. Biol. 49:369–81.

Small, R. L., R. C. Cronn, and J. F. Wendel. 2004. Use of nuclear genes for phylogeny reconstruction in plants. Aust. Syst. Bot. 17:145–170.

Smith, S. D., and D. A. Baum. 2006. Phylogenetics of the florally diverse Andean clade Iochrominae (Solanaceae). Am. J. Bot. 93:1140–1153.

Stamatakis, A. 2006. RAxML-VI-HPC: maximum likelihood-based phylogenetic analyses with thousands of taxa and mixed models. Bioinformatics 22:2688–90.

Stamatakis, A., P. Hoover, and J. Rougemont. 2008. A rapid bootstrap algorithm for the RAxML Web servers. Syst. Biol. 57:758–71.

Stein, B. A. 1992. Sicklebill hummingbirds, ants, and flowers: Plant-animal interactions and evolutionary relationships in Andean Lobeliaceae. Bioscience 42:27–33.

Stein, B. A. 1987a. Synopsis of the genus *Burmeistera* (Campanulaceae: Lobelioideae) in Peru. Ann. Missouri Bot. Gard. 74:494–496.

Stein, B. A. 1987b. Systematics and evolution of Centropogon subgenus Centropogon (Campanulaceae-Lobelioideae). Washington University.

Team, R. C. 2013. R: A language and environment for statistical computing. Vienna, Austria.

Triana, J. J. 1854. Nuevos jeneros i especies de plantas para la flora neo-granadina. Pp. 13–14 *in* Imprenta del Neo-Granadino. Bogotá.

Von Hagen, K., and J. Kaderelt. 2003. The diversification of *Halenia* (Gentianaceae): Ecological opportunity versus key innovation. Evolution (N. Y). 57:2507–2518.

Wilbur, R. L. 1975. A synopsis of the Costa Rican species of Burmeistera (Campanulaceae: Lobelioideae). Bull. Torrey Bot. Club 102:225–231.

Wilbur, R. L. 1976. A synopsis of the Costa Rican species of the genus Centropogon Presl (Campanulaceae, Lobelioideae). Brenesia 8:59–84.

Wimmer, F. E. 1968. Campanulaceae-Lobelioideae supplementum et Campanulaceae-Cyphiodeae. Pp. 815–1024 *in* S. Danert, ed. Das Pflanzenreich IV.276c. Akademie-Verlag, Berlin.

Wimmer, F. E. 1953. Campanulaceae-Lobelioideae, II. Teil. Pp. 261–814 *in* R. Mansfeld, ed. Das Pflanzenreich IV.276b. Akademie-Verlag, Berlin.

Wimmer, F. E. 1943. Campanulaceae-Lobelioideae. I. Teil. Pp. 1–260 *in* R. Mansfeld, ed. Das Pflanzenreich IV.276b. Wilhem Engelmann, Leipzig.

Winkworth, R., and M. J. Donoghue. 2005. Viburnum phylogeny based on combined molecular data: Implications for taxonomy and biogeography. Am. J. Bot. 92:653–666.

Chapter II:

Two New Species of *Burmeistera* (Campanulaceae: Lobelioideae) from the Cordillera de Talamanca of Costa Rica and Panama, with a Key to the Central American Species

The contents of this chapter are reprinted from Lagomarsino LP, Santamaría-Aguilar DA, Muchhala N. Two New Species of *Burmeistera* (Campanulaceae: Lobelioideae) from the Cordillera de Talamanca of Costa Rica and Panama, with a Key to the Central American Species. *Systematic Botany* 40(3): XXX–XXX [in press]. Copyright 2015 with permission from the American Society of Plant Taxonomists.

2.1 Abstract

Two new species of *Burmeistera* (Campanulaceae: Lobelioideae) from the Cordillera de Talamanca are described, illustrated, and discussed with reference to similar species. One species, *B. serratifolia*, is endemic to Panama, while the second, *B. monroi*, is known from both Panama and Costa Rica. Additionally, these species are included in a dichotomous key to all Central American species of *Burmeistera*.

2.2 Introduction

Burmeistera Triana, with ~120 species, is the fourth largest genus of Lobelioideae in the family Campanulaceae (Lammers 2007). Species are found in the understory of cloud forests from Guatemala through northernmost Peru, but are absent in Belize, El Salvador, and Nicaragua. The highest species diversity of *Burmeistera* occurs in the northern Andes of Colombia and Ecuador (McVaugh 1949; Jeppesen 1981; Garzón Venegas et al. 2014). The genus comprises herbaceous to suffruticose plants that are terrestrial or hemi-epiphytic. As in all Lobelioideae, *Burmeistera* is characterized by protandrous flowers: anthers are fused into an anther tube which releases pollen through the initial male phase as the style elongates within; the stigma then emerges from this tube, unfolds, and becomes receptive (Erbar and Leins 1995; Leins and Erbar 2006). Flowers are typically green or dark maroon and adapted to bat pollination, although some are yellow or pink, and at least one species is known to be hummingbird pollinated (Muchhala 2006b). Fruits are berries, which are often inflated or brightly colored and spongy.

Burmeistera is a subclade of the centropogonids, a clade that also includes the large Neotropical genera *Centropogon* C. Presl and *Siphocampylu*s Pohl (Lagomarsino et al. 2014). This clade is unique within Lobelioideae for the combination of its Neotropical distribution, woody habit and corolla tube that is entire, neither fenestrate nor dorsally cleft (Lammers 2002; Muchhala and Lammers 2005). Unlike in *Centropogon* and *Siphocampylus*, the monophyly of *Burmeistera* is strongly supported (Antonelli 2008; Knox et al. 2008; Lagomarsino et al. 2014). Morphological synapomorphies of *Burmeistera* include a dilated anther orifice and seeds that are much longer than broad (Lammers 1998). Additionally, most species of *Burmeistera* have ebracteolate pedicels (Lammers 1998). At least two lineages of green-flowered, bat-pollinated *Centropogon* species are successively sister to *Burmeistera*; together, this clade is known as the

burmeisterids and is defined morphologically by a ventricose, inflated corolla throat (Lagomarsino et al. 2014) (e.g., Figure 2.3).

Burmeistera is a taxonomically difficult genus (Wilbur 1975, 1976). This is in part due to the wide overlap of characters between species and morphological variation within species, such as in the widespread *B. cyclostigmata* Donn. Sm. and *B. vulgaris* E. Wimm. The last comprehensive taxonomic treatment of the genus was Wimmer's monograph of Lobelioideae for Engler's Das Pflanzenreich (Wimmer 1943), though the infrageneric taxonomy established in Wimmer (1943) does not reflect evolutionary relationships (Muchhala and Lammers 2005; Knox et al. 2008; Lagomarsino et al. 2014). Although a new infrageneric taxonomy is still outstanding, taxonomic knowledge of *Burmeistera* has substantially improved since Wimmer's treatment. There are now floristic treatments for the genus for most countries in which it occurs, including Guatemala (Nash 1976), Costa Rica (Wilbur 1975), Panama (Wilbur 1976, 1981), Colombia (ongoing), Ecuador (Jeppesen 1981), and Peru (Stein 1987). The ongoing floristic treatment of Colombia alone has resulted in the description of at least 10 new species and several range extensions (Garzón Venegas and González 2012; Garzón Venegas et al. 2012, 2013, 2014). Additionally, recent research on the pollination biology of *Burmeistera* has resulted in the description of new species (Muchhala and Lammers 2005; Muchhala and Pérez 2015) and a better understanding of the ecology and evolution of the group (Muchhala 2003, 2006a,b, 2007; Muchhala and Potts 2007).

The Cordillera de Talamanca, shared between Costa Rica and Panama, is home to 21 species of *Burmeistera*, the highest species diversity outside of the Andean mountains. This mountain range stretches 320 km from the vicinity of San José and Cartago, Costa Rica to just beyond the Costa Rica-Panama border (Janzen 1983). The flora of the Cordillera de Talamanca,

which has strong phytogeographical affinities with the Northern Andes (Gentry 1982; Kappelle et al. 1992), is extremely diverse, particularly at mid-elevation. Important habitats in the Talamanca mountain range include cloud forests, oak forests, bogs, and the westernmost páramos (Luteyn 1999). A large portion of this cordillera is protected by the Parque Internacional La Amistad (PILA), a UNESCO World Heritage Site shared between Costa Rica and Panama.

Here, we describe two new species of *Burmeistera* native to the Cordillera de Talamanca: *B. monroi* and *B. serratifolia*. We also provide a key to all known species of *Burmeistera* native to Central America.

2.3 Materials and methods

Herbarium specimens, including types, of Central American *Burmeistera* were examined at A, CR, GH, INB, MO, NY, PMA, and SCZ (herbarium abbreviations and throughout follow Thiers [2013]). Additional type specimens were accessed from the Global Plants Initiative website (http://plants.jstor.org/). Material was examined under a Leica StereoZoom 5 binocular microscope. Terminology in the taxonomic treatment and dichotomous key largely follows Wilbur (1975, 1976, 1981). The dichotomous key is adapted from Wilbur (1975, 1976, 1981) and includes the countries of occurrence for each species in parentheses (COL: Colombia; CR: Costa Rica; ECU: Ecuador; G: Guatemala; H: Honduras; P: Panama); these data were obtained from herbarium specimens, as well as from the Tropicos database (http://www.tropicos.org/).

2.4 Taxonomic treatment

Burmeistera monroi D. Santam. & Lagom., sp. nov.— TYPE: PANAMA. Bocas del Toro: Ridges leading to Río Teribe, NE most ridge of Cerro Fábrega ridge, 09°09'07"N 082°51'52"W, 2,900 m, 07 Mar 2006 (fl), *A. K. Monro & S. Knapp 5225* (holotype: PMA!; isotype: BM!).

Terrestrial herb 0.6–1 m in height, with ascending branches, producing white latex; branches 1.5–3 mm in diameter, fistulose, reddish to purple in living material, drying yellowish, indumentum villose with septate trichomes, internodes 1.8–5.5 cm long. Leaves distichous or spirally arranged; petiole 0.4–1.6 cm long, villose; blade 4.9–12.1 × 2.5–3.4 cm, elliptic or narrowly elliptic, apex acuminate, base cuneate, margin dentate, 2 short teeth per cm, round or very minutely triangular; venation semicraspedodromous, with 6–12 pairs of lateral nerves, flat and barely visible on the adaxial surface, elevated on the abaxial surface; adaxial surface glabrous; abaxial surface pubescent, especially over the veins. Flowers solitary in the axils of distal leaves, pedicels 1.9–5.7 cm long, ebracteolate, straight, villose, bearing septate trichomes; hypanthium 3–4.7 × 3–5 mm, globose or hemispheric at anthesis, sparsely pubescent, green or green with dark purple; calyx lobes 2.3–5 × 1.2–1.5 mm, oblong to lanceolate with acute or obtuse apex, one central vein, the margins entire or dentate with 2–5 teeth per side, sometimes with marginal ciliate trichomes, glabrous on the adaxial surface, sparsely pubescent on the abaxial surface, erect or slightly recurved; corolla 22–25 mm long, green grading into dark purple or brownish externally, purple and green internally, sparingly to moderately short pubescent externally, glabrous internally, throat not ventricose at anthesis; corolla tube 14–16 × 2–3 mm, straight in anthesis; corolla lobes deflexed-falcate, narrowly linear, with an acute apex,

dorsal lobes 8–12 × 1.5–2 mm, lateral lobes 5–7 × 1–1.2 mm, ventral lobe 4–6 × 1–1.2 mm; filament tube 18–21 × 1–1.8 mm, straight, completely glabrous, reddish-purple in living material, exserted between the dorsal corolla lobes 2–3 mm beyond the corolla; anther tube ca. 5–8 × 2–3 mm, purple, largely glabrous, but with appressed sparse pubescence in the suture between individual anthers, the two ventral anthers ca. 5 mm long, with penicillate white hairs at the apex but otherwise glabrous, the three dorsal anthers ca. 6 mm long, glabrous throughout. Berries 0.5 × 0.7 cm when immature (dried), 0.8 × 0.9 cm when mature (dried), globose, inflated, color unknown; seeds 0.5–0.8 mm long, light brown, elliptic. Figures 2.1–2.2.

Additional Specimens Examined— COSTA RICA. Puntarenas: Parque Internacional La Amistad, sendero al Valle del Silencio, sector entre el albergue y la línea divisora de aguas, 09°04'00"N, 82°59'00"W, 2,100–2,200, 20 Feb 2006 (fl & fr), *D. Santamaría 3909* (GH, INB); Parque Internacional La Amistad. Casa Coca, punto 11, 09°05'61"N, 82°58'66"W, 2,550 m, 04 Apr 2011 (fl & fr). *A. K. Monro & D. Santamaría 6986* (BM, GH, INB, MO); Parque Internacional La Amistad. Tararia. Valle del Silencio, 09°06'61"N, 82°58'03"W, 2,500 m, 01 Sep 2001 (fl), *E. Alfaro & O. Esquivel 3716* (MO).

PANAMA. Bocas del Toro: Cordillera de Talamanca, headwaters of the Río Culubre, 6 airline km NW of the peak of Cerro Echandi on the Costa Rican-Panamanian international border, 2,450–2,600 m, 02–03 March 1984 (fl & fr), *G. Davidse et al 25196* (CR, DUKE[image]).



Figure 2.1. Illustration of *Burmeistera monroi.* A) Habit with flower buds, flower, and fruit. **B)** Flower in female phase. All drawings by L. Lagomarsino based on *A. K. Monro 7142.*



Figure 2.2. *Burmeistera monroi*, photographs from field collections. A) Habit. **B)** Flower in female phase, lateral view. **C)** Flower in female phase, frontal view with detail of stigma and anthers. **D)** Flower in male phase, lateral view. **E)** Flowering branch with developing fruits. **F)** Abaxial leaf surface. All photos are of *A. K. Monro 7142* except D, which is of *A. K. Monro 6986.* Photos by A. K. Monro.

Distribution and Habitat— *Burmeistera monroi* is restricted to the Parque Internacional La Amistad, where it is found on both the Costa Rican and Panamanian sides of this protected area. It grows in cloud forests on the Caribbean slope of the Cordillera de Talamanca between 2,100–2,900 m. The elevational range occupied by *Burmeistera monroi* is high for its genus, though not exceptional.

Phenology— Specimens of *Burmeistera monroi* were collected in flower in February–April and September. All except the September collections were also in fruit. This suggests a long flowering season, but phenology in the rest of the year is unknown.

Etymology— It is an honor to dedicate this new species to the British botanist Alexandre K. Monro (1968–), investigator at the Kew Royal Botanic Gardens in London and world authority of Urticaceae. Monro has led many botanical expeditions into the Cordillera de Talamanca and Parque Internacional La Amistad in Costa Rica and Panama that have substantially increased our understanding of the biodiversity in this species-rich region. During one of these trips, Monro collected the type specimen of the species that we describe here in his honor.

Notes— *Burmeistera monroi* is distinguished by its straight, narrow, sparsely pubescent corolla with narrowly linear corolla lobes and a non-ventricose throat. It is most similar to *B. nigropilosa* Luteyn ex Garzón & F. González from Antioquia, Colombia (Garzón Venegas and González 2012), but can be distinguished by its glabrous to sparsely-pubescent, smooth leaves (versus densely pubescent, bullate leaves), ebracteolate pedicels (versus bracteolate), dark purple or brown corolla tube that grades distally to green (versus green), and whitish and sparse corolla pubescence (versus dark or hyaline and dense).

Among Central American species, *Burmeistera monroi* is most similar to *B. chirripoensis* Wilbur, from which it can be distinguished by its dark purple to brown corolla tube grading into green (versus green), the corolla throat that is not ventricose (versus ventricose), and largely glabrous anthers (versus densely pubescent throughout). It is also similar to *B. virescens* (Benth.) Benth. & Hook. f. ex Hemsl. from relatively low elevations, ca. 500 –2000 m, in Guatemala and Honduras due to its narrow corolla tube, but can be readily distinguished by its villose stems (versus glabrous or puberulent), elliptic or narrowly elliptic leaves (versus oblong-elliptic to ovate), globose to hemispheric hypanthium at anthesis (versus obconic), corolla throat that is not ventricose (versus ventricose), and corolla tube that is dark purple to brown grading into green

(versus green). *Burmeistera monroi* is vegetatively similar to *B. estrellana*, but differs in its corolla that is not ventricose (versus ventricose) with linear lobes (versus deltoid).

Burmeistera monroi is among three known species of *Burmeistera* in Central America with inflated fruits. The other species are *B. vulgaris* and *B. glauca* (E. Wimm.) Gleason. The former, *B. vulgaris*, is a widespread species that is readily distinguished from *B. monroi* by its ventricose corolla throat (versus not ventricose) and cylindric hypanthium (versus globose or hemispheric). The latter, *B. glauca*, can be distinguished from *B. monroi* by its hemi-epiphytic to epiphytic habit (versus terrestrial), glabrous corolla (versus sparsely to moderately pubescent), and oblong-ovoid berry (versus globose).

Burmeistera monroi is also among few species of its genus that does not have a ventricose corolla throat (as in e.g., *B. serratifolia*, Fig. 2.3D), thought to be an adaptation to bat pollination in some species (Muchhala 2006b). This species' corolla morphology (a long, straight corolla tube with falcate corolla lobes and a non-ventricose throat) is quite similar to the brevilimbatid subclade of *Centropogon* (Lagomarsino et al. 2014), which includes the hummingbird-pollinated *C. valerioi* Standl. (Colwell et al. 1974) and *C. ferrugineus* (L. f.) Gleason from Costa Rica; these species are easily distinguished from *B. monroi* by their more robust, scandent subshrub habit (versus terrestrial herb less than 1 m in height), generally bright orange corolla tubes with yellow limb (versus brown grading into green), and a constricted anther orifice (versus dilated). The pollinator of *B. monroi* is unknown.

Burmeistera serratifolia Lagom. & D. Santam., sp. nov.— TYPE: PANAMA. Chiriquí: Ridges above and to W of Quebrada Alemán, trail to town of Fortuna, 08º45′N, 82º13′W, 1,200–1,500 m, 13 Aug 2000 (fl), *S. Knapp & J. Mallet 9226* (holotype: PMA!; isotype: SCZ!).

Epiphytic herb producing white latex; branches 2.5–3 mm in diameter, fistulose, sparsely puberulent with simple trichomes, internodes 1.5–3 cm long. Leaves spirally arranged; petiole 0.6–1.5 cm long, sparsely pubescent; blade 10.2–15 × 1–1.7 cm, narrowly oblong-lanceolate, apex acuminate, base cuneate, sometimes slightly decurrent and asymmetric, margin strongly irregularly serrate, 15–17 conspicuous triangular teeth per cm; venation semicraspedodromous, lateral nerves 13–20 per side, flat and little visible on the adaxial surface, elevated on the abaxial surface; adaxial surface glabrous; abaxial surface glabrous except on the veins, which are pubescent. Flowers solitary in the axils of upper leaves, which are sometimes reduced in size compared to mature leaves not associated with flowers; pedicels 7–11.2 cm long, straight or slightly curved towards the apex, ebracteolate, glabrous or very sparsely pubescent, the trichomes not septate; hypanthium 9–11 × 2–4 mm, campanulate at anthesis, glabrous or very sparsely pubescent with simple trichomes; calyx lobes 3–4.5 × 1–4.5 mm, oblong-lanceolate to triangular with acute apex, with one almost indistinct central vein, margins serrate, with 3–5 teeth per side, glabrous on both surfaces, straight or slightly curved; corolla ca. 21–40 mm long, green, glabrous on all surfaces, throat ventricose; tube 5–11 × 2–4.5 mm, straight; lobes oblong, falcate, with an acuminate or acute apex, dorsal lobes 13–15 × 3.5–5 mm, lateral lobes ca. 14 × 4 mm, ventral lobe ca. 14 × 2 mm; filament tube ca. 31 × 1.1 mm, straight in the proximal half and curved towards the distal end, glabrous except towards the apex where it is strigose, exserted between the pair of dorsal lobes ca. 15 mm; anther tube ca. 5 × 3 mm, glabrous or minutely

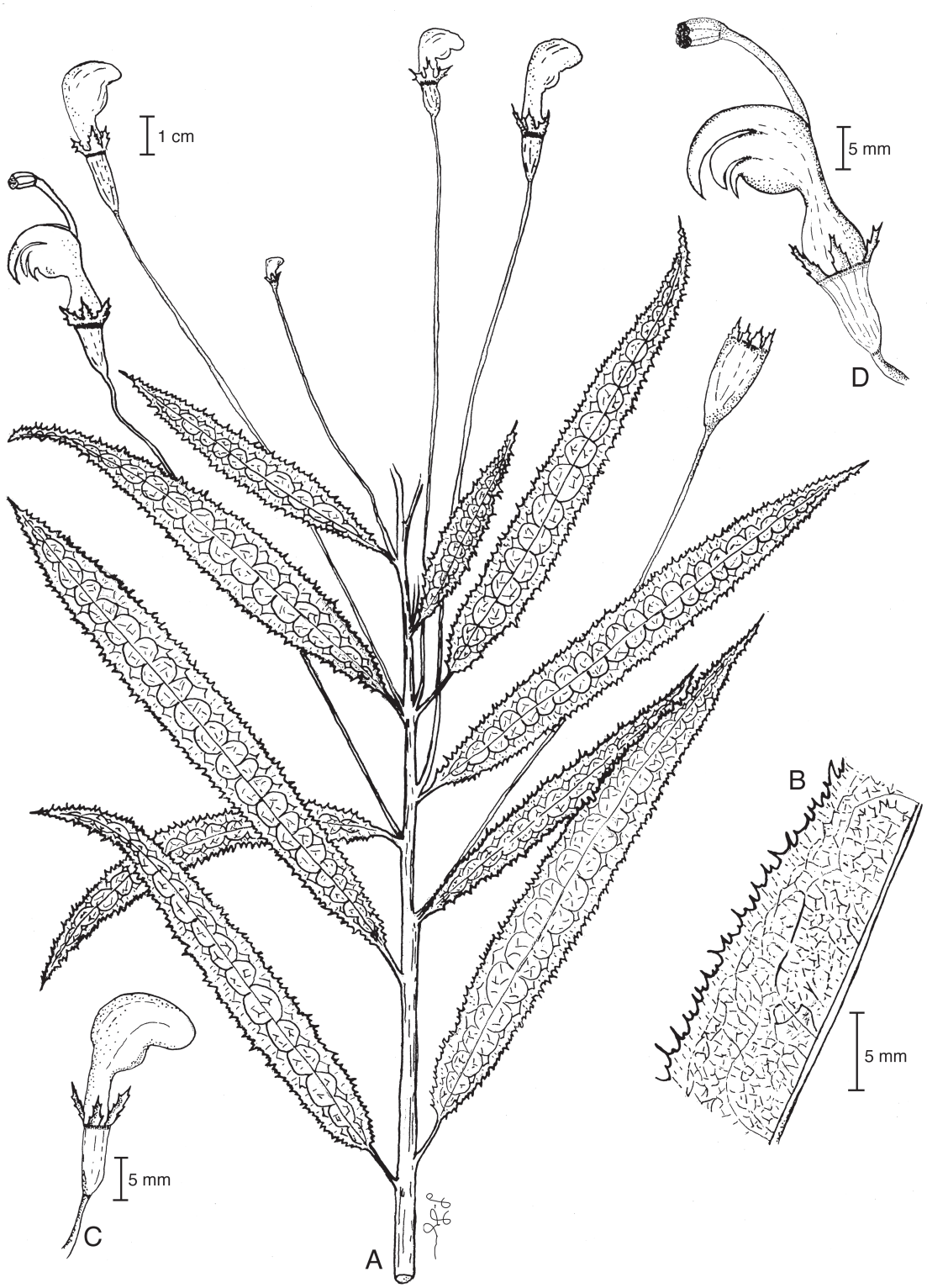


Figure 2.3. Illustration of *Burmeistera serratifolia*. A) Habit with flower buds, flower, and fruit. **B)** Detail of leaf margin and venation. **C)** Flower bud. **D)** Flower in male phase. All drawings by L. Lagomarsino based on the holotype.

pubescent, the two ventral anthers ca. 3–4 mm long, glabrous throughout, the three dorsal anthers ca. 5 mm long, glabrous throughout. Berries 1.8 × 0.6 cm (possibly not mature), more or less cylindrical, calyx lobes persistent, glabrous; seeds not seen. Seedlings produce very finely divided leaves (information from label). Figure 2.3.

Distribution and Habitat— *Burmeistera serratifolia* is endemic to Panama, where it grows in premontane and montane forests on the Caribbean slope of the Cordillera de Talamanca between 1,200–1,500 m in elevation. It is only known from the type, collected in the Reserva Forestal Fortuna, Chiriquí, Panama.

Phenology— Flowers and fruits were collected from *Burmeistera serratifolia* in August, but phenology is otherwise unknown.

Etymology—This species' epithet refers to the characteristic serrate leaf margins of this species.

Notes— This species is exceptional for its oblong-lanceolate leaves with strongly serrate margins. *Burmeistera serratifolia* is most similar to *B. chiriquiensis* Wilbur from western Panama and eastern Costa Rica, with which it shares its oblong-lanceolate leaves; it can be distinguished by its prominently and irregularly serrate leaf margins with more than 15 conspicuous teeth/cm (versus shallowly dentate leaf margins with one to two inconspicuous teeth/cm), secondary and tertiary venation that is easily distinguished and reticulate (versus secondary and tertiary venation that is not prominent), acuminate leaf apex (versus caudate), pedicel 7.0–11.2 cm long (versus ca. 3 cm long), campanulate hypanthium (versus obconic), filament tube 30 mm long (versus 23 mm long), and the glabrous tips of the ventral anthers (versus densely pilose). *Burmeistera intii* Gómez-Laur. & L.D. Gómez also has oblong-lanceolate leaves; however, they are less than 8 cm long (versus 10–15 cm in *B. serratifolia*).

Burmeistera silencioensis Wilbur (ined.), which is soon to be validly published in conjunction with the Manual de las Plantas de Costa Rica, also produces elongate leaves. However, *B. serratifolia* can be distinguished from this entity, which would also belong near the third couplet of the key below, by its irregularly serrate leaf margins (versus serrulate), acute leaf apices (versus acuminate to caudate), sepals with serrate margins (versus inconspicuously serrulate), and filament tube exserted 1.5 cm beyond the corolla (versus included or exserted less than 5 mm). The following specimens of *B. silencioensis* from Costa Rica and Panama were examined to compare to *B. monroi*: *A. K. Monro 7117* (INB), *D. Santamaría-Aguilar 9093* (INB), and *T. Antonio 1608A* (DUKE [image]). It is not our intention to validly publish this species name here.

Among Central American species, *Burmeistera serratifolia* shares its finely divided juvenile leaves only with *B. mcvaughii* Wilbur, from which it is readily distinguished by its long-lanceolate leaves with serrate margins bearing more than 15 teeth/cm (versus elliptic with serrulate to denticulate margins bearing 6–8 teeth/cm) and campanulate hypanthium (versus obconic). Additionally, two specimens currently identified as *B. dendrophila* (*L. E. Skog 4056* [MO] and *B. Hammel 6199* [MO]) also produce finely divided young leaves, though this does not appear to be common in this species.

2.5 Dichotomous Key

DICHOTOMOUS KEY TO THE CENTRAL AMERICAN SPECIES OF *BURMEISTERA*

1. Leaves > 5 times longer than wide.
    2. Leaves distichously arranged, ≤ 8 cm long; dorsal corolla lobes long-acuminate, > 4 times as long as the lateral and ventral lobes……...……...……...…...……. *B. intii* (CR)
    2. Leaves spirally arranged, ≥ 10 cm long; dorsal corolla lobes acute, < 1.5 times as long as the lateral and ventral lobes

3. Leaf margins weakly dentate, 1–2 teeth per cm; venation pattern not readily apparent; pedicels ca. 3 cm long; filament tube not exserted from corolla tube……..……..... *B. chiriquiensis* (CR,P)

3. Leaf margins strongly serrate, 15+ teeth/cm; venation semicraspedodromous; pedicels > 6 cm long; filament tube exserted from corolla tube > 1 cm…….. *B. serratifolia* (P)

1. Leaves < 5 times longer than wide

4. Corolla < 1.5 cm long

5. Corolla pink or green; filament tube ≤ 9 mm long…….…….*B. kirkbridei* Wilbur (P)

5. Corolla bright yellow; filament tube ≥ 10 mm long……..….*B. parviflora* E. Wimm. ex Standl. (CR, P)

4. Corolla > 2 cm long

6. Corolla throat not ventricose ……..……..……..... *B. monroi* (CR, P)

6. Corolla throat ventricose

7. Plants climbing, sometimes hemiepiphytic; branches arching to pendent; leaves distichously arranged.

8. Leaf margins lobed, undulate. ……...*B. quercifolia* Gómez-Laur. & L.D. Gómez (CR)

8. Leaf margins crenate-serrate, flat

9. Stems densely spreading-hirsute

10. Cauline trichomes terete, tawny or reddish purple; pedicels and hypanthia glabrous ……..……..……*B. almedae* Wilbur (CR, P)

10. Cauline trichomes flattened, tawny; pedicels and hypanthia pubescent ……...……. *B. obtusifolia* E.Wimm. (CR, P)

9. Stems glabrous, or with only a few scattered trichomes

11. Anthers externally pilose with golden trichomes……..…….. ……...*B. microphylla* Donn. Sm. (CR, P, COL)

11. Anthers externally glabrous

12. Leaves 2.7–5 (–8) × 1.2–2.5 cm; petioles 0.4–0.7 cm long; flowers 30–35 mm long; hypanthium cylindric; berries oblong-ovoid, 3–6 cm long ……..…… *B. glauca* (P)

12. Leaves 5–9.5 × 2.5–3.9 cm; petioles 0.7–1 cm long; flowers 45–55 mm long; hypanthium obconic; berries globose, 0.9–1.1 cm long……
……..…….*B. zurquiensis* Wilbur (CR)

7. Plants climbing or terrestrial; branches erect; leaves spirally arranged

13. Hypanthium at anthesis obconic, acute-tapering at the base with the sides strongly divergent

14. Leaves with conspicuously denticulate, serrulate, or crenate margins, with ≥ 6 teeth/cm

15. Leaf margin subentire to coarsely and irregularly dentate or crenate; corolla lobes sublinear to linear, 6 × 1.5 mm ……..……...…. *B. virescens* (G, H)

15. Leaf margin denticulate or serrulate; corolla lobes falcately oblong to deltoid, 5–13 × 3–4 mm ……..……. *B. mcvaughii* (P)

14. Leaf margins entire to inconspicuously serrulate, with ≤ 4 teeth per cm.

16. Calyx lobes > 6 mm long (up to 20 mm), equaling or longer than the hypanthium……..……..... *B. tenuiflora* Donn. Sm. (CR, P)

16. Calyx lobes < 4 mm long, shorter than the hypanthium

17. Corolla lobes greatly recurved; calyx lobes 1–1.5 mm long ..…...……...
……..…….……*B. toroensis* Wilbur (P)

17. Corolla lobes erect or deflexed; calyx lobes > 2 mm long

18. Distal leaves not markedly reduced, not giving the impression of a bracteate raceme, the flowers obviously borne singly

19. Corolla lobes sublinear to linear..……..…. *B. virescens* (G, H)

19. Corolla lobes falcate and deltoid

20. Leaf apex acute to short-acuminate, tertiary venation indistinct; filament tube exserted more than 1 cm beyond the corolla, largely glabrous, but distally puberulent…….*B. dendrophila* E.Wimm. (P)

20. Leaf apex long-acuminate, tertiary venation distinct; filament tube exserted less than 1 cm beyond the corolla or included, pubescent throughout… ……..……..*B. estrellana* E. Wimm. (CR)

18. Distal leaves that bear flowers greatly reduced, giving the impression of a bracteate raceme

21. Pedicels > 7 cm long……...…….……...…*B. utleyi* (P)

21. Pedicels < 6 cm long

22. Leaves and corolla puberulent; flowers ca. 40 mm long

……...…….....……...…… *B. chirripoensis* (CR)

22. Leaves glabrous, the corolla glabrous to inconspicuously puberulent; flowers ca. 30 mm long…….…. *B. morii* Wilbur (P)

13. Hypanthium at anthesis cylindric to campanulate or urceolate, somewhat rounded at the base with the sides more or less parallel

23. Leaves with conspicuously denticulate or serrulate margins

24. Stems puberulent with several-celled, yellowish-white hairs; pedicels 7–8 cm long; hypanthium 7.5 × 2 mm; anthers externally sparsely pubescent, naked at tips……...

……..……...……..……...……... *B. crebra* McVaugh (CR)

24. Stems inconspicuously puberulous to glabrate; pedicels 3–4 cm long; hypanthium 4-5 × 3–4 mm; anthers externally appressed-pilosulose, pilose-fringed at tips……...

……...……...…….. *B. hammelii* Wilbur (P)

23. Leaves with shallowly crenate-serrate or inconspicuously serrulate margins

25. Calyx lobes ≤ 5 mm long.

26. Corolla moderately to densely puberulous; berry red……. *B. dukei* Wilbur (P)

26. Corolla glabrous or occasionally sparsely puberulous; berry white or greenish turning black

27. Upper corolla lobes ≥ 18 mm long and the 2 lateral lobes 12–14 mm long; corolla dark red; anthers externally glabrous …...… *B. darienensis* Wilbur (P)

27. Upper corolla lobes < 12 mm long and the 2 lateral lobes ca. 7 mm long; corolla greenish; anthers externally puberulous……… *B. pirrensis* Wilbur (P)

25. Calyx lobes > 5 mm long

28. Two ventral anthers densely bearded; leaves (except the most distal) ≥ 5 cm wide……..……..…… *B. panamensis* Wilbur (P)

28. Two ventral anthers sparingly fringed apically or glabrous; leaves mostly < 5 cm wide

29. Corolla predominantly purplish or green with a deep suffusion of maroon or dark purple; hypanthium and calyx lobes purplish, drying dark purple or black; berry fleshy and with a thick wall, 1–2 (–3) × 1–2 (–2.5) cm……..... ……*B. cyclostigmata* (CR, P, COL, ECU)

29. Corolla green or bronze; hypanthium and calyx lobes green, drying green or stramineous (rarely suffused with purple or maroon); berry greatly inflated with a thin, bladdery wall, 2.5–5 × 2–4 cm…..……. *B. vulgaris* (CR, P)

2.6 Acknowledgements

The authors would like to thank the following herbaria for use of their collections and facilities: A, CR, GH, INB, MO, NY, PMA, and SCZ. We additionally would like to acknowledge the help of the following individuals: Carmen Galdames and Eric K. O. Hattori scanned herbarium specimens for study, Carlos Maldonado drew preliminary line illustrations, Alexandre Monro allowed us to use his photos of living specimens of *B. monroi*, and Kanchi Gandhi provided nomenclatural advice. This research was supported by student grants to L.P.L. from the Explorer's Club, the Rockefeller Center for Latin American Studies at Harvard University, the American Society of Plant Taxonomists, and a National Science Foundation Doctoral Dissertation Improvement Grant (DEB-1210401). Drafts of this manuscript were substantially improved at various stages by comments from Charles C. Davis, Michael Grayum, Barry Hammel, an anonymous reviewer, Associate Editor Ricarda Riina, and Editor-in-Chief.

2.7 References

Antonelli, A. 2008. Higher level phylogeny and evolutionary trends in Campanulaceae subfam. Lobelioideae: Molecular signal overshadows morphology. Mol. Phylogenet. Evol. 46:1–18.

Erbar, C., and P. Leins. 1995. Portioned pollen release and the syndromes of secondary pollen presentation in the Campanulales-Asterales complex. FLORA 190:323–338.

Garzón Venegas, J., and F. González. 2012. Five new species and three new records of *Burmeistera* (Campanulaceae-Lobelioideae) from Colombia. Caldasia 34:309–324.

Garzón Venegas, J., F. González, and J. M. Vélez Puerta. 2012. *Burmeistera minutiflora* (Campanulaceae-Lobelioideae), a new species from the high Andes of Antioquia (Colombia) with the smallest flowers in the genus. An. del Jardín Botánico Madrid 69:243–246.

Garzón Venegas, J., J. L. Luteyn, and F. González. 2014. A new species of *Burmeistera* (Campanulaceae, Lobelioideae) from the Western Cordillera of Colombia. Novon A J. Bot. Nomencl. 23:165–170.

Garzón Venegas, J., J. M. Vélez Puerta, and F. González. 2013. Three new species of *Burmeistera* (Campanulaceae-Lobelioideae) from Colombia. Brittonia 65:119–127.

Gentry, A. H. 1982. Neotropical floristic diversity: Phytogeographical connections between Central and South America, Pleistocene climatic fluctuations, or an accident of the Andean orogeny? Ann. Missouri Bot. Gard. 69:557–593.

Janzen, D. H. 1983. Costa Rican Natural History. University of Chicago Press, Chicago.

Jeppesen, S. 1981. Lobeliaceae. Pp. 9–170 *in* G. Harling and B. Sparre, eds. Flora of Ecuador, No 14. Swedish Natural Science Research Council.

Kappelle, M., A. M. Cleef, and A. Chaverri. 1992. Phytogeography of Talamanca montane Quercus forests, Costa Rica. J. Biogeogr. 19:299–315.

Knox, E. B., A. M. Muasya, and N. Muchhala. 2008. The predominantly South American clade of Lobeliaceae. Syst. Biol. 33:462–468.

Lagomarsino, L. P., A. Antonelli, N. Muchhala, A. Timmermann, S. Mathews, and C. C. Davis. 2014. Phylogeny, classification, and fruit evolution of the species-rich Neotropical bellflowers (Campanulaceae: Lobelioideae). Am. J. Bot. 101:2097–2112.

Lammers, T. G. 1998. Review of the neotropical endemics *Burmeistera*, *Centropogon*, and *Siphocampylus* (Campanulaceae: Lobelioideae), with description of 18 new species and a new section. Brittonia 50:233–262.

Lammers, T. G. 2002. Seventeen new species of Lobelioideae (Campanulaceae) from South America. Novon 12:206–233.

Lammers, T. G. 2007. World Checklist and Bibliography of Campanulaceae. Royal Botanic Gardens, Kew.

Leins, P., and C. Erbar. 2006. Secondary pollen presentation syndromes of the Asterales — a phylogenetic perspective. Bot. Jahrbücher 127:83–103.

Luteyn, J. L. 1999. Paramos: A checklist of plant diversity, geographical distribution, and botanical literature. New York Botanical Garden Press, Bronx, N.Y.

McVaugh, R. 1949. Studies in South American Lobelioideae (Campanulaceae) with special reference to Colombian species. Brittonia 6:450–493.

Muchhala, N. 2007. Adaptive trade-off in floral morphology mediates specialization for flowers pollinated by bats and hummingbirds. Am. Nat. 169:494–504.

Muchhala, N. 2003. Exploring the boundary between pollination syndromes: Bats and hummingbirds as pollinators of *Burmeistera cyclostigmata* and *B. tenuiflora* (Campanulaceae). Oecologia 134:373–380.

Muchhala, N. 2006a. Nectar bat stows huge tongue in its rib cage. Nature 444:701–2.

Muchhala, N. 2006b. The pollination biology of *Burmeistera* (Campanulaceae): Specialization and syndromes. Am. J. Bot. 93:1081–1089.

Muchhala, N., and T. G. Lammers. 2005. A New Species of *Burmeistera* (Campanulaceae: Lobelioideae) from Ecuador. Novon 15:176–179.

Muchhala, N., and M. D. Potts. 2007. Character displacement among bat-pollinated flowers of the genus *Burmeistera*: Analysis of mechanism, process and pattern. Proc. R. Soc. B Biol. Sci. 274:2731–2737.

Nash, D. L. 1976. Campanulaceae. Pp. 396–431 *in* D. L. Nash and J. V. A. Dieterle, eds. Floral of Guatemala. Fieldiana, Botany.

Stein, B. A. 1987. Synopsis of the genus *Burmeistera* (Campanulaceae: Lobelioideae) in Peru. Ann. Missouri Bot. Gard. 74:494–496.

Thiers, B. 2013. Index Herbariorum: A global directory of public herbaria and associated staff. The New York Botanical Garden.

Wilbur, R. L. 1975. A synopsis of the Costa Rican species of *Burmeistera* (Campanulaceae: Lobelioideae). Bull. Torrey Bot. Club 102:225–231.

Wilbur, R. L. 1981. Additional Panamanian species of *Burmeistera* (Campanulaceae: Lobelioideae). Ann. Missouri Bot. Gard. 68:167–171.

Wilbur, R. L. 1976. Family 183. Campanulaceae (Flora of Panama). Ann. Missouri Bot. Gard. 63:593–655.

Wimmer, F. E. 1943. Campanulaceae-Lobelioideae. I. Teil. Pp. 1–260 *in* R. Mansfeld, ed. Das Pflanzenreich IV.276b. Wilhem Engelmann, Leipzig.

Chapter III:

Two new species of *Siphocampylus* (Campanulaceae: Lobelioideae) from the Central Andes

3.1 Abstract

Two species of *Siphocampylus* (Campanulaceae: Lobelioideae) from the Central Andes of Peru and Bolivia are described, illustrated, and discussed with reference to related species. One species, *S. antonellii*, is endemic to high elevation grasslands of Calca, Peru, while the second, *S. siberiensis*, is endemic to cloud forests of Cochabamba, Bolivia. Both species are robust shrubs that produce tubular pink flowers that are likely pollinated by hummingbirds.

3.2 Introduction

While the subfamily Lobelioideae Burnett (1835: 942) of Campanulaceae Jussieu (1789:163) is cosmopolitan in its distribution, more than half of its ~1200 species are restricted to the Neotropics (Lammers 2007). Most of these species (~550/680) belong to the Andean-centered centropogonid clade, which comprises *Burmeistera* Triana (1854: 13) (~120 species), *Centropogon* C. Presl (1836: 48) (~210 species), and the mainland species of *Siphocampylus* Pohl (1831: 104) (~220 species). This clade is unique within Lobelioideae for its combination of Neotropical distribution, woody habit, entire corolla tube (i.e., neither fenestrate nor dorsally cleft), and floral adaptation to pollination by either hummingbirds or nectar bats (Lammers 2002; Muchhala and Lammers 2005; Lagomarsino et al. 2014). Within the centropogonid clade, *Siphocampylus* can further be distinguished by its capsular (vs. baccate) fruit. The genus, however, is not monophyletic (Antonelli 2008; Knox et al. 2008): in addition to the Caribbean species, which are distantly related to the centropogonid clade, its mainland species form at least 11 subclades that are polyphyletic with respect to the berry-producing *Centropogon* (Lagomarsino et al. 2014). This result is not surprising given the high degree of character overlap between *Centropogon* and *Siphocampylus,* which has frequently resulted in the incorrect filing of material in herbaria (Gleason 1921; Lammers 1998) and the occasional description of a new species to the incorrect genus or of uncertain placement (e.g., C. dubius [Zahlbr.] Wimmer [1943: 196] for both scenarios) (Gleason 1921). The non-monophly of these genera is largely due to the dynamic evolution of fruit-type within the clade; fleshy fruits have evolved approximately eight times from dry-fruited ancestors, likely as a result of migration to densely forested habitats (Givnish et al. 2005, 2009; Lagomarsino et al. 2014). While further phylogenetic information is necessary to begin to re-delimit generic boundaries to reflect

evolutionary relationships within Neotropical Lobelioideae, *Siphocampylus* species are easily identified to genus within the confines of the current classification system, especially when fruiting material is available. Despite its non-monophyly, *Siphocampylus* remains a conspicuous, if poorly studied, component of the cloud forests and high elevation grasslands that comprise much of the tropical Andean global biodiversity hotspot (Myers et al. 2000). Future taxonomic and phylogenetic work focused on the centropogonid clade will undoubtedly result in the description of many new species and discovery of new clades defined by synapomorphies.

Here we describe two new species of hummingbird-pollinated *Siphocampylus*. Type specimens for both species were included in the most recent molecular phylogeny of the centropogonid clade, which is based on five plastid markers and includes relatively dense taxon sampling that spans all recognized taxonomic divisions, geographical occurrences, and morphological variation within Neotropical Lobeloideae (Lagomarsino et al. 2014). The phylogeny provides the information necessary to discuss these new species in relation to their closest evolutionary relatives. We additionally discuss similarities and differences of the species placed closely to their relatives in the most recent monograph of *Siphocampylus* (Wimmer 1943, 1953, 1968).

3.3 Materials and methods

Field collections focused on Campanulaceae were conducted in Bolivia in November–December, 2011 and in Peru in November–December, 2013. Species identification and description of new species as a result of this research utilized many taxonomic works for reference (Gleason 1921; Wimmer 1937, 1943, 1953, 1968; Lammers 1998; León and Lammers

2006) and collections at the following herbaria: A, BOLV, GB, GH, LPB, MO, MOL, NY, SMF, and USZ. Herbarium acronyms here and throughout follow the *Index Herbariorum* (Thiers 2013).

3.4 Taxonomic Treatment

Siphocampylus antonellii **Lagom. & D. Santam.,** ***sp. nov.*** (Figs. 1–2)

Type:— PERU. Cusco: Calca, Lares, Calle entre Amaparaes y Suyo, Arriba de Amaparaes, 12°58'902"S, 077°50'W, 3799 m, 10 December 2012 (fl), *L. Lagomarsino, D. Santamaría, J. Wells, F. Farro 400* (holotype: A!; isotype: GB!, MO!, NY!).

Shrub 1.5 m tall, branching 20 cm above the base, with soft wood; branches 0.2–0.6 cm in diameter, solid and fistulose, light brown to reddish purple in living material, glabrescent or white-tomentose; internodes 0.2–1.0 cm long; latex white. Leaves spirally arranged, distributed evenly along the branches, producing lemon-like odor; petiole 0.1–0.5 cm long, sometimes subsessile, villous, the trichomes whitish, adaxially canaliculate, abaxially rounded to triangular; lamina 3.8–5.2 × 0.3–0.55 cm, linear-oblanceolate, not rugose, appearing glabrous but densely pubescent with diminutive, whitish, stellate to echinoid trichomes; base attenuate to decurrent, sometimes with uneven sides; apex acuminate; margin sinuate, subentire, or diminutively dentate, 11–25 teeth per side, rounded to uncinate, sometimes appearing as a glandular callosity; venation reticulate, with 5–10 pairs of lateral nerves, ascending, impressed or indistinct adaxially, flat abaxially. Flowers solitary, axillary, generally towards the apex of branch; pedicel 3.0–5.0 cm long, straight for almost the entire length, but curved below the hypanthium, cylindrical or flattened, densely pubescent, bibracteolate; calyx lobes 5, 0.7–1.6 × 0.1–0.12 cm, linear-oblanceolate, margins diminutively dentate with 3–5 teeth per side, densely pubescent on both



Figure 3.1. Illustration of *Siphocampylus antonellii*. A) Flowering branch. **B)** Leaf, abaxially, including detail of leaf margin and stellate hairs that cover surface. **C)** Staminate-phase flower, including bibracteolate pedicel, with detail of sepal and stellate hairs that cover the outer corolla surface. **D)** Longitudinal section of a pistillate-phase flower, showing the insertion of staminal

Figure 3.1 (Continued) tube to corolla, style and stigma as situated relative to the stamens, and bilocular ovary with axile placentation. **E)** Corolla lobe detail. **F)** Detail of anther tube, including apical hairs on ventral anthers, and stigma. Drawing by Bobbi Angel from the type.

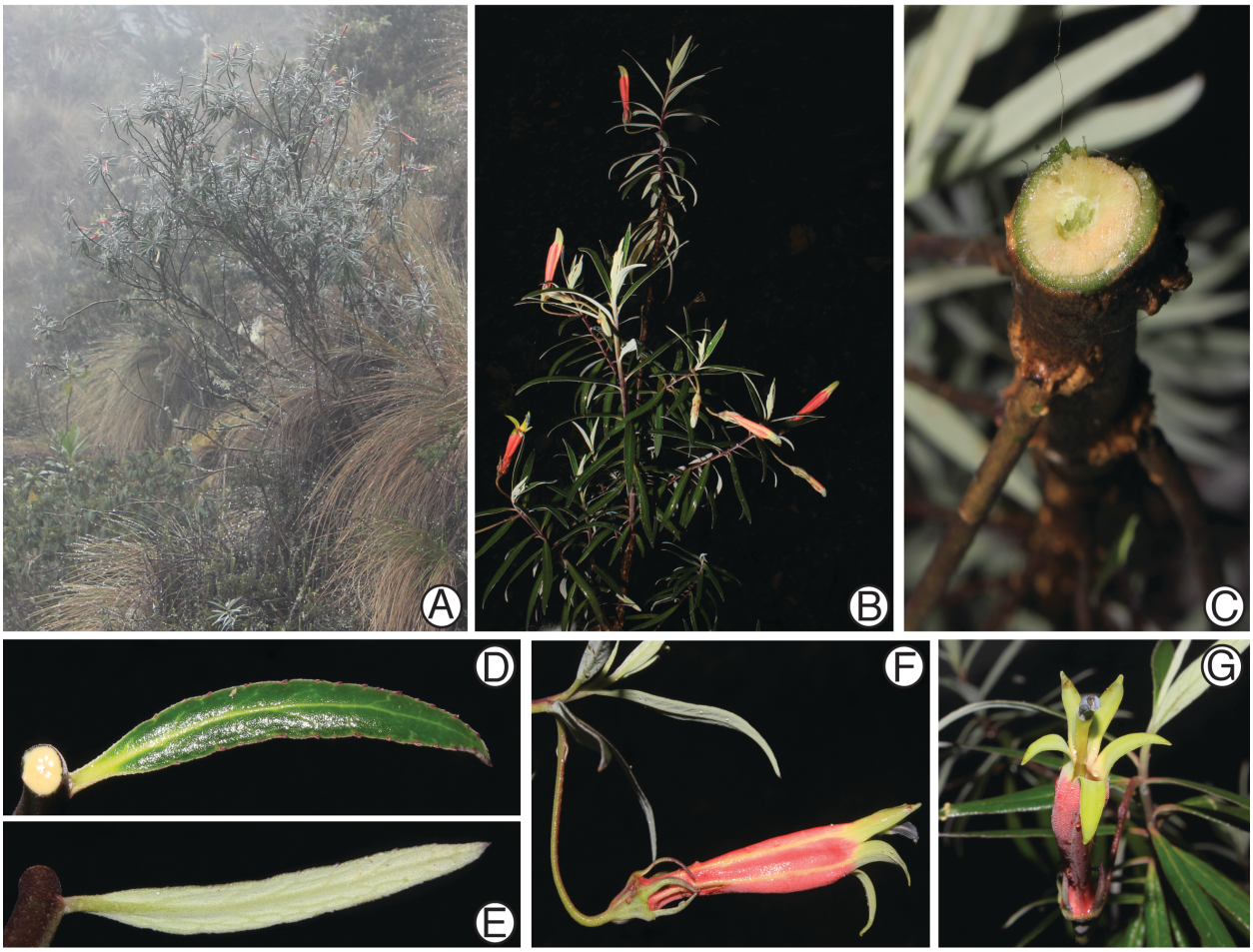


Figure 3.2. Photographs of *Siphocampylus antonellii*. A) Habit and high-elevation grassland (pajonál) habitat. **B)** Flowering branch. **C)** Cross-section of stem showing woody habit. **D)** Adaxial leaf surface. **E)** Abaxial leaf surface. **F)** Lateral view of flower in staminate phase. **G)** Anterior view of a flower, showing corolla aperture. All photos of the type collection, taken in the field by L. Lagomarsino.

Distribution and habitat:— *Siphocampylus antonellii* is endemic to Peru, where it grows on rocky slopes in puna habitat at ~3800 m in elevation. It is only known from the type collection.

Phenology:— Individuals were collected in flower in December; the rest of the phenology of this species remains unknown.

Etymology:— It is an honor to name this attractive species for Dr. Alexandre Antonelli (1978–), a biogeographer and phylogeneticist at the University of Gothenburg. Antonelli has made many important contributions to our understanding of the movement of Neotropical biodiversity through space and time, and to the evolution of various taxa, including Lobelioideae. His efforts in the latter inspired the first author to study *Centropogon*, *Siphocampylus*, and *Burmeistera*.

Discussion:— *Siphocampylus antonellii* is most similar to *S. elfriedii* Wimmer (1935: 75) (Figure 3.3C) and *S. parvifolius* Wimmer (1937: 463), both of which are also endemic to Peru. These species share a shrubby habit (Figure 3.2A), generally high elevation occurrence ([1050–] 2100–3620 m), bibracteolate pedicels (Figure 3.1C, 3.2F), pink or pinkish-purple corolla tubes with yellow-green lobes (Figures 3.2F–G, 3.3C), glabrous anthers (except at the apex of the ventral anthers) (Figures 3.1F, 3.3C), and turbinate ovaries (Figures 3.1C, 3.2F, 3.3C). Both *S. antonellii* and *S. elfriedii* produce echinoid trichomes, following Batterman & Lammers 2004. However, *S. antonellii* can be easily distinguished by the differences enumerated in Table 3.1 and by the agreeable lemon-like smell that it emits.

Following Wimmer (1936), this new species is most similar to *S. nobilis* Wimmer (1929: 12) and *S. rosmarinifolius* Don (1834: 704), also endemic to Peru. These species all share linear leaves, turbinate ovaries, and narrow corolla lobes. However, these two species have glabrous

sepals and corolla (vs. pubescent in *S. antonellii*), ebracteolate, glabrous pedicels (vs. bibractolate and pubescent), and different corolla colors: reddish orange with yellow lobes in *S. rosmarinifolius* and purple in *S. nobilis* (following Wimmer 1936, 1953) (vs. pink with yellow-green lobes [Figure 3.2F]). *Siphocampylus nobilis* can be further separated by its vining habit (vs. shrubby), its long, narrow leaves (6.0–8.0 × 0.2–0.3 vs. 3.8–5.2 × 0.3–0.55 cm), and its glabrous branches, leaves, pedicels, and hypanthium (vs. pubescent [Figure 3.1]). *Siphocampylus rosmarinfolius* can be further separated by its longer leaves (8.0–11.5 cm vs. 3.8–5.2 cm), the rugose, glabrous adaxial leaf surface (vs. not rugose and pubescent), and revolute leaf margins (vs. not revolute).

Molecular phylogenetic analysis places *S. antonellii* in a well-supported clade that includes *S. veteranus* Wimmer (1924: 264), *S. vatkeanus* Zahlbruckner (1897: 377) (Figure 3.3A, D), *S. elfriedii* (Figure 3.3C)*, S. rictus* Lammers (1998: 239), and *S. actinotrix* Wimmer (1924: 253) (Figure 3.3C); within this clade, *S. antonellii* is sister to *S. veteranus* (Lagomarsino et al. 2014). This clade as a whole is composed of generally tall, woody shrubs with turbinate ovaries. The placement of *S. elfriedii* in this clade is not surprising, as it is quite similar to *S. antonellii* (see above). However, it is more difficult to find similarities with the remaining species. They species in this clade can be easily distinguished from *S. antonellii* by a series of putative adaptations to pollination by bats: long pedicels (7.0–15 cm), wide corolla apertures, and longer corollas (3.2–5.0 cm) that are generally dull in color (either green, cream-colored, white or yellowish, sometimes mottled with reddish pigmentation) (Figure 3.3A–B). Additionally, these species have longer leaves (6.0–13.5 cm vs 3.8–5.2 cm) and a glabrous or only sparsely pubescent corolla (but with echinoid-stellate pubescence in *S. actinothrix* [Figure 3.3B]).



Figure 3.3. Closest relatives of *Siphocampylus antonellii*, based on molecular phylogeny of Lagomarsino et al (2014). A) Flower of *Siphocampylus veteranus*. **B)** Flower of *Siphocampylus actinothrix*. **C)** Flower of *Siphocampylus elfriedii*. **D)** Cross-section of main stem of *S. veteranus*, showing a much more robust habit than *S. antonellii*, but similar wood structure. All photos taken in the field by L. Lagomarsino. **A and D.** *L. Lagomarsino et al. 388*, **B.** *L. Lagomarsino et al. 403*, **C.** *L. Lagomarsino et al. 387*.

Table 3.1. Differences between *Siphocampylus antonellii*, *S. elfriedii*, and *S. parvifolius*.

	S. antonellii	*S. elfriedii*	*S. parvifolius*
Leaf shape	Linear-oblanceolate	Lanceolate	Lanceolate to oblanceolate
Leaf size	3.8–5.2 × 0.3–0.55 cm	5.0–7.4 × 1.1–1.9 cm	2.0 × 0.5 cm
Leaf margin	Margin sinuate, subentire, or diminutively dentate	Denticulate	Weakly crenulate
Sepal length	0.7–1.6 cm	0.7–1.4 cm	0.3 cm
Sepal margin	Diminutively dentate	Denticulate	Entire or diminutively denticulate
Corolla length	(2.8–) 3.9–5.1 cm	3.9–4.6 cm	3.4 cm
Corolla indument	Pubescent	Pubescent	Glabrous
Dorsal corolla lobe length	1.0–1.6 cm	0.9–1.2 cm	1.1–1.4 cm
Ventral corolla lobe length	1.4–1.9 cm	0.5–1 cm	0.9–1.2 cm
Reference sheets	*L. Lagomarsino 400* (GH)	*L. Lagomarsino* 387 (GH); *J. L. Luteyn & M. L. Lebrón-Luteyn 6395* (MO); *F. W. Pennell 13841* (GH); *T. Plowman & E. W. Davis 5126* (GH); *J. West 7045* (GH)	*R. D. Metcalf 30469* (A)

Siphocampylus siberiensis* Lagom. & D. Santam., *sp. nov. (Figs. 4–5)

Type:— BOLIVIA. Cochabamba: Carrasco, En la entrada para Sunchal, cerca a rótulo "Unidad Educativa Manulea Gandarillas," 17°47'267"S, 064°47'669"W, 2668 m, 18 December 2011 (fl & fr), *L. Lagomarsino, D. Santamaria & J. M. Mendoza 241* (holotype: USZ; isotype: A!).

Multi-stemmed shrub 3–4 m tall, branched, all branches arising from a single point at ground level, with soft wood, the bark suberose; branches 0.4–0.6 cm in diameter, fistulose, the youngest parts purple, brown when mature (greyish to whitish in dry material), glabrescent to tomentose; internodes 0.9–1.7 cm long; latex white. Leaves spirally arranged and generally clustered at the

apex of branches, leaving prominent leaf scar after falling; petiole 0.3–0.7 cm long, glabrescent to tomentose with whitish trichomes, winged, adaxially canaliculate, abaxially more or less triangular with two ribs; leaf blade 10.5–19.5 × 2.9–4.6 cm, oblanceolate, adaxially tomentose and abaxially densely pubescent, the pubescence principally on the veins, trichomes simple, the base decurrent; apex acuminate; margin doubly dentate and ciliate, 75–95+ teeth per side, the teeth triangular; venation reticulate with 16–21 pairs of lateral nerves, lightly ascendant, impressed adaxially and elevated abaxially. Flowers solitary, axillary, generally towards branch apex; pedicel 4.5–9.4 cm long, straight, cylindrical, densely pubescent; bracteoles absent; hypanthium 0.5–0.8 × 0.3–0.4 cm, hemispherical, tomentose; calyx lobes 5, (0.8–) 1.0–1.4 × (0.2–) 0.3 cm, narrowly triangular, the margins ciliate, entire, pubescent on both surfaces, erect or recurved, the apex acuminate; corolla 3.5–3.8 cm long, completely pink, diminutively pubescent on both surfaces; corolla tube 0.9–2.2 × 0.7–0.8 cm, cylindrical for its entire length, a little wider towards the apex than at the base, straight at anthesis; corolla lobes 5, narrowly triangular, slightly falcate, the margins ciliate, the apex acute to acuminate, the two dorsal lobes 1.5 cm long, the two lateral lobes 1.4 cm long, the ventral lobe 1.4 cm long, staminal tube 3.0–3.8 × 0.1–0.2 cm, straight, sparsely pubescent, pink, exserted between the two dorsal lobes; anther tube 0.8–0.9 × 0.2–0.3 cm, gray in living material, glabrous except in the sutures between anthers, which are densely pubescent, the trichomes white, ventral anthers 0.6–0.8 cm long, penicillate at the apex, the trichomes white, the dorsal anthers 0.7–1.0 cm long, penicillate at the apex, the trichomes white. Fruit capsule, 5.0 × 1.0–1.2 cm, ca. 15-lobed, with external ridges, the calyx persistent; seeds not seen.



Figure 3.4. Illustration of *Siphocampylus siberiensis.*

Figure 3.4 (Continued). Illustration of *Siphocampylus siberiensis.* A) Flowering branch, showing the persistent leaf scars and developmental procession of distal flower at anthesis to basal capsular fruit. **B)** Flower in pistillate phase, including detail of sepal with pubescence. **C)** Corolla lobe detail, including marginal pubescence. **D)** Longitudinal section of a pistillate phase flower, showing the insertion of staminal tube to corolla, style and stigma as situated relative to the stamens, and bilocular ovary with axile placentation. **E)** Anther tube in staminate-phase flower. **F)** Capsule with lobes and ridges. Drawing by Bobbi Angel from the type.

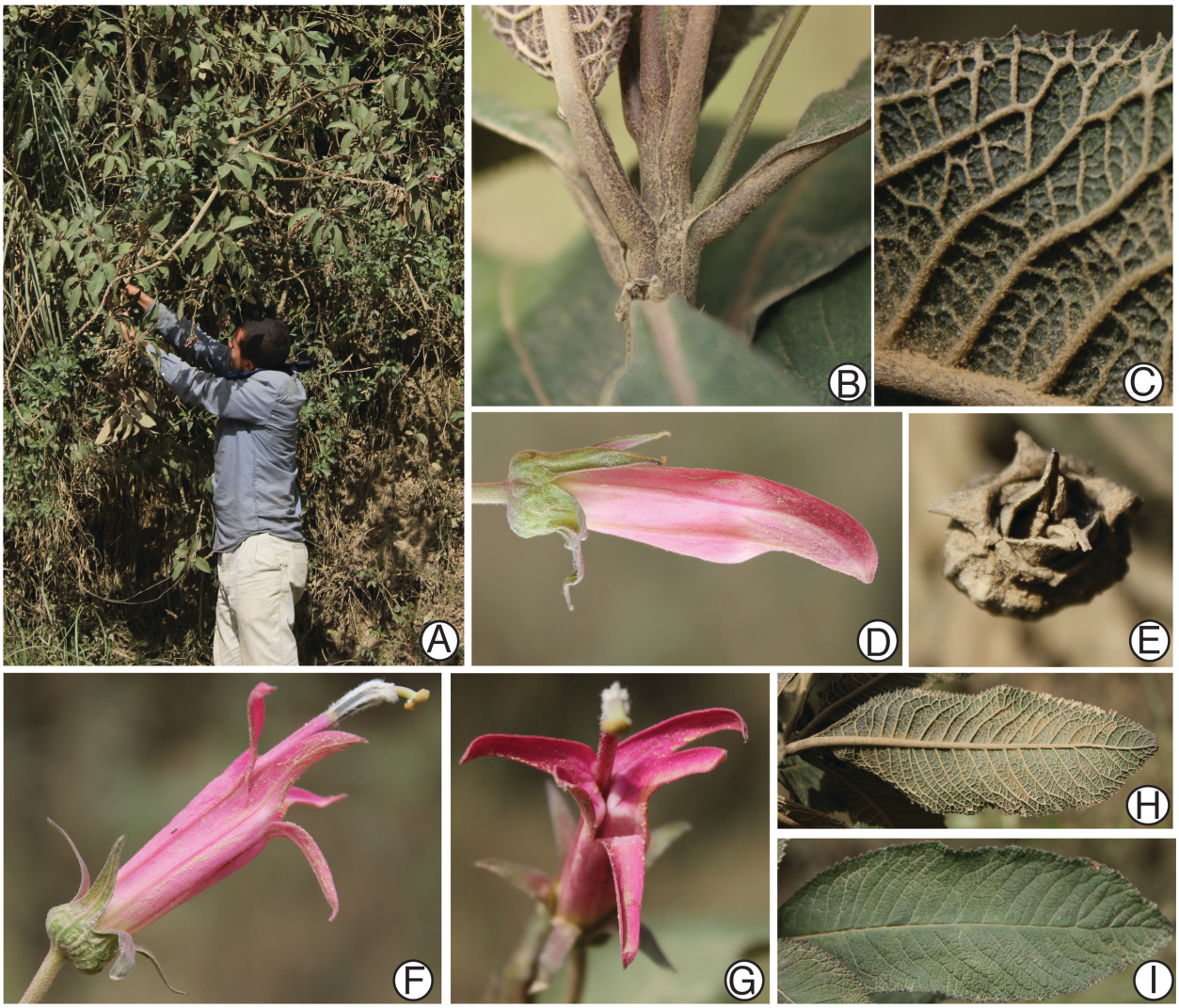


Figure 3.5. Photographs of *Siphocampylus siberiensis.* A) Habit. **B)** Detail of young stem. **C)** Detail of leaf margin and venation on abaxial leaf surface. **D)** Flower bud. **E)** Capsule. **F)** Lateral view of flower in pistillate phase. **G)** Anterior view of corolla, showing corolla aperture. **H)** Abaxial leaf surface. **I)** Adaxial leaf surface. All photos of the type collection, taken in the field by L. Lagomarsino.

Distribution and habitat:— *Siphocampylus siberiensis* is endemic to Bolivia, where it has been collected at the edge of the road at ca. 3700 m in elevation in cloud forest. It is only known from the type locality.

Phenology:— Individuals were collected in flower and fruit in December; the rest of the phenology of this species remains unknown.

Etymology:— The specific epithet of this species refers to the type locality, the Serranía de Siberia, a mountain range at the limit between the Cochabamba and Santa Cruz departments in Bolivia.

Discussion:— *Siphocampylus siberiensis* can be recognized by its shrubby habit with multiple stems arising from a single point; leaves aggregated at the apex of branches (Figure 3.4A); conspicuous venation (especially on the abaxial leaf surface) (Figures 3.4A, 3.5C); solitary flowers borne in the axil of leaves (Figure 3.4A); light pink corolla with a tube that is cylindrical for its entire length (i.e., not basally constricted) (Figures 3.4B, D, 3.5F); anther tube that is densely pubescent in the sutures between individual anthers (Figures 3.4E, 3.5F); and fruits that are both ribbed and lobed (Figures 3.4F, 3.5E).

Molecular phylogenetic analysis places *S. siberiensis* in a clade that includes *S. tunarensis* Zahlbruckner (1897: 376), *S. tunicatus* Zahlbruckner (1898: 189), and *S. umbellatus* (Kunth) Don (1834: 702); this clade is closely related to *S. boliviensis* Zahlbruckner (1891: 443) and *S. sparsipilus* Wimmer (1924: 388) (Lagomarsino et al. 2014; Lagomarsino et al. unpub.) (Figure 3.5, 3.6). These species are all restricted to the Central Andes of Peru and Bolivia, with the exception of *S. umbellatus*, whose range also extends to Brazil. This clade is composed of robust shrubs or trees that are exceptionally tall for the centropogonid clade (Figures 3.5A, 3.6E–F), or rarely scandent subshrubs (*S. sparsipilus* and some collections of *S. boliviensis*), with

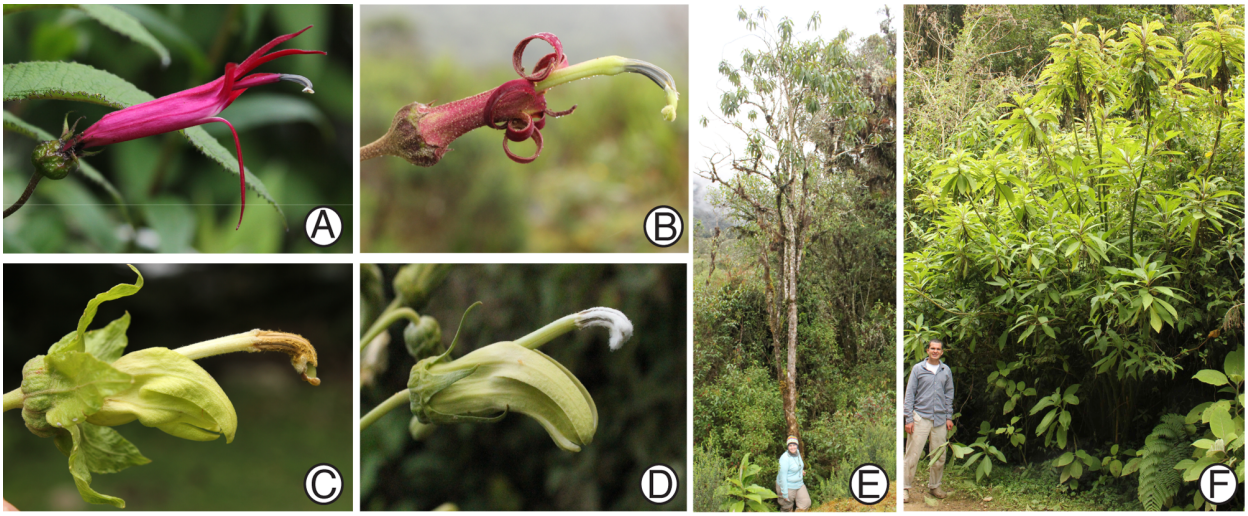


Figure 3.6. Closest relatives of *Siphocampylus siberiensis*, based on molecular phylogeny of Lagomarsino et al (2014). A) Flower of *Siphocampylus boliviensis*. **B)** Flower of *Siphocampylus tunarensis*. **C)** Flower of *Siphocampylus tunicatus*. **D)** Flower of *Siphocampylus umbellatus*. **E)** Habit of *Siphocampylus tunarensis*. **F)** Habit of *Siphocampylus tunicatus*. All photos taken in the field by L. Lagomarsino (A–D, F) and D. Santamaría-Aguilar (E). **A.** *L. Lagomarsino et al. 239*, **B and E.** *L. Lagomarsino et al. 232*, **C and F.** *L. Lagomarsino et al. 235*. **D.** *L. Lagomarsino et al. 193.*

ebracteolate pedicels, a shallow, hemispherical hypanthium (turbinate in *S. tunarensis*), and leaves that leave prominent scars after falling (Figure 3.4A) with dentate margins and reticulate venation that is conspicuous on both surfaces, but especially the abaxial surface (Figures 3.4A, 3.5C). Both bright pink (*S. siberiensis*, *S. boliviensis*, *S. sparsipilus*) and dull colored (*S. tunarensis*, *S. tunicatus*, *S. umbellatus*) corollas are represented in this clade. This color variation,

which is associated with different gross corolla morphologies, likely reflects adaptation to different pollinators (hummingbirds and bats, respectively) (Figures 3.5F–G, 3.6A–D).

Even though they are not the most closely related species, the pink, narrow flowers *S. siberiensis* most closely resemble those of *S. boliviensis* and *S. sparsipilus*. However, the latter two species can be easily distinguished by their corollas that are constricted at the base (vs. not constricted) and much rounder ovary (vs. flattened at top). The other species in the immediate clade that includes *S. siberiensis* differ in their dull reddish (*S. tunarensis* [Figure 3.6B]) or whitish-green (*S. tunicatus* [Figure 3.6C], *S. umbellatus* [Figure 3.6D]) corollas (vs. bright pink in *S. siberiensis*). *Siphocampylus tunicatus* and *S. siberiensis* are sister species that are vegetatively very similar, though their flowers are markedly different (Figures 3.4, 3.5, 3.6C, F). In addition to its green corolla, the former can be distinguished by its longer sepals (2.0–2.8 cm [Figure 3.6C] vs. [0.8–] 1.0–1.4 cm [Figures 3.4B, D, 3.5F]) that are leaf-like (vs. not leaf-like) and its wider hypanthium (1.5–2.0 vs. 0.3–0.4 cm) (Figure 3.6C). *Siphocampylus tunarensis* can be separated by its linear, markedly revolute corolla lobes (Figure 3.6B) (vs. narrowly triangular and not revolute [Figures 3.4B, 3.5F–G]) and short sepals (0.2–0.4 cm [Figure 3.6B] vs. 1.0–1.4 cm [Figure 3.5F]). Furthermore, while *S. siberiensis* is a robust shrub 3–4 m tall, *S. tunarensis* can grow to be a very tall tree (>10 m) with a diameter of more than 30 cm and is possibly one of the largest species of Campanulaceae in the Americas (Figure 3.6E).

The species that is most superficially similar to *S. siberiensis*, *S. boliviensis*, is placed in the same couplet as *S. macrostemon* de Candolle (1839: 403) in the dichotomous key to the members of the genus in Wimmer (1953). This is a markedly different species that can be distinguished by its subsessile leaves (vs. pedicels 0.3–0.7 cm long) that are smaller (5–8 × 1.31.5 cm vs. 10.5–19.5 × 2.9–4.6 cm) and sparsely pubescent on the adaxial surface (vs.

tomentose), minutely dentate leaf margins (vs. doubly dentate and ciliate), shorter pedicels (2.6–4.2 cm vs. 4.5–9.4 cm) that are bracteolate (vs. ebracteolate), and glabrous corolla (vs. pubescent). The other species most closely related to *S. siberiensis* fall into many disparate taxonomic units within the current classification scheme of the genus. This makes it difficult to place this new species in the context of Wimmer's taxonomy; this is likely due to this treatment's reliance on single, often arbitrary characters to designate groups.

The measurements of the calyx and corolla in parenthesis correspond to *E. Fernández et al 3583* (MO). Based on label information, this specimen has white corolla, but otherwise corresponds to the species concept for *S. sibieriensis* presented here.

Additional specimens examined: BOLIVIA: Cochabamba, Carrasco, Siberia, 17°48'11"S 064°46'12"W, 2900 m, 16 Apr 2005 (fl), *E. Fernández et al 3583* (MO).

3.5 References

Antonelli, A. 2008. Higher level phylogeny and evolutionary trends in Campanulaceae subfam. Lobelioideae: Molecular signal overshadows morphology. Mol. Phylogenet. Evol. 46:1–18.

Batterman, M. R. W., and T. G. Lammers. 2004. Branched foliar trichomes of Lobelioideae (Campanulaceae) and the infrageneric classification of Centropogon. Syst. Bot. 29:448–458.

Burnett, G. T. 1835. Outlines of Botany. J. and C. Adlaed, London.

De Candolle, A. P. 1839. Prodromus Systematis Naturalis Regni Vegetabilis. Treuttel & Wurts, Paris.

De Jussieu, A. L. 1789. Genera Plantarum secundum ordines naturales disposita. Barrois, Viduam Herissant et Theophilum, Paris.

Don, G. 1834. A General History of the Dichlamydeous Plants. J.G. and F. Rivington, London.

Givnish, T. J., K. C. Millam, A. R. Mast, T. B. Paterson, T. J. Theim, A. L. Hipp, J. M. Henss, J. F. Smith, K. R. Wood, and K. J. Sytsma. 2009. Origin, adaptive radiation and

diversification of the Hawaiian lobeliads (Asterales: Campanulaceae). Proc. R. Soc. B Biol. Sci. 276:407–416.

Givnish, T. J., J. C. Pires, S. W. Graham, M. a McPherson, L. M. Prince, T. B. Patterson, H. S. Rai, E. H. Roalson, T. M. Evans, W. J. Hahn, K. C. Millam, A. W. Meerow, M. Molvray, P. J. Kores, H. E. O'Brien, J. C. Hall, W. J. Kress, and K. J. Sytsma. 2005. Repeated evolution of net venation and fleshy fruits among monocots in shaded habitats confirms a priori predictions: Evidence from an ndhF phylogeny. Proc. R. Soc. B Biol. Sci. 272:1481–1490.

Gleason, H. A. 1921. A rearrangement of the Bolivian species of *Centropogon* and *Siphocampylus*. Bull. Torrey Bot. Club 48:189–201.

Knox, E. B., A. M. Muasya, and N. Muchhala. 2008. The predominantly South American clade of Lobeliaceae. Syst. Biol. 33:462–468.

Lagomarsino, L. P., A. Antonelli, N. Muchhala, A. Timmermann, S. Mathews, and C. C. Davis. 2014. Phylogeny, classification, and fruit evolution of the species-rich Neotropical bellflowers (Campanulaceae: Lobelioideae). Am. J. Bot. 101:2097–2112.

Lammers, T. G. 1998. Review of the neotropical endemics *Burmeistera*, *Centropogon*, and *Siphocampylus* (Campanulaceae: Lobelioideae), with description of 18 new species and a new section. Brittonia 50:233–262.

Lammers, T. G. 2002. Seventeen new species of Lobelioideae (Campanulaceae) from South America. Novon 12:206–233.

Lammers, T. G. 2007. World Checklist and Bibliography of Campanulaceae. Royal Botanic Gardens, Kew.

León, B., and T. Lammers. 2006. Campanulaceae endémicas del Perú. Rev. Peru. Biol. 13:237–241.

Muchhala, N., and T. G. Lammers. 2005. A New Species of *Burmeistera* (Campanulaceae: Lobelioideae) from Ecuador. Novon 15:176–179.

Myers, N., R. A. Mittermeier, C. G. Mittermeier, G. A. B. Fonseca, and J. Kent. 2000. Biodiversity hotspots for conservation priorities. Nature 403:853–858.

Pohl, J. B. E. 1831. Plantarum Brasiliae icones et descriptiones hactenus ineditae. Jussu et auspiciis Francisci Primi, imperatoris et regis augustissimi. Antonii Strauss, Vienna.

Presl, C. B. 1836. Prodromus Monographiae Lobelacearum. Filiorum Theophili Haase, Prague.

Thiers, B. 2013. Index Herbariorum: A global directory of public herbaria and associated staff. N.

Triana, J. J. 1854. Nuevos jeneros i especies de plantas para la flora neo-granadina. Pp. 13–14 *in* Imprenta del Neo-Granadino. Bogotá.

Wimmer, F. E. 1937. Campanulaceae. *in* J. F. Macbride, ed. Flora of Peru.

Wimmer, F. E. 1968. Campanulaceae-Lobelioideae supplementum et Campanulaceae-Cyphiodeae. Pp. 815–1024 *in* S. Danert, ed. Das Pflanzenreich IV.276c. Akademie-Verlag, Berlin.

Wimmer, F. E. 1953. Campanulaceae-Lobelioideae, II. Teil. Pp. 261–814 *in* R. Mansfeld, ed. Das Pflanzenreich IV.276b. Akademie-Verlag, Berlin.

Wimmer, F. E. 1943. Campanulaceae-Lobelioideae. I. Teil. Pp. 1–260 *in* R. Mansfeld, ed. Das Pflanzenreich IV.276b. Wilhem Engelmann, Leipzig.

Wimmer, F. E. 1935. Lobelioideae Novae. II. Repert. Specierum Nov. Regni Veg. 38:75–87.

Wimmer, F. E. 1924. Lobelioideae. II. Repert. Specierum Nov. Regni Veg. 19:211–265.

Wimmer, F. E. 1929. Studien zu einer Monographie der Lobelioïdeen (Lobelioïdeae IV). Repert. Specierum Nov. Regni Veg. 26:1–20.

Zahlbruckner, A. 1898. Campanulaceae. *in* C. E. O. Kuntze, ed. Revisio generum plantarum: vascularium omnium atque cellularium mularum secundum leges nomeclatura. A. Feliz, Leipzip.

Zahlbruckner, A. 1891. No Title. Ann. des Kais. Naturhistorischen Hofmuseums 6:443.

Zahlbruckner, A. 1897. Revisio Lobeliacearum Boliviensium hucusque cognitarum. Bull. Torrey Bot. Club 24:371–388.

Chapter IV:

The abiotic and biotic drivers of rapid diversification in the Andes

4.1 Abstract

Abiotic and biotic factors both contribute to rapid radiations, but their relative contributions are seldom examined. We explore this interaction by applying diversification models that incorporate orogeny, climate, and biological trait evolution to the Andean-centred Neotropical bellflowers. We demonstrate that speciation rates rose with increasing Andean elevation, while extinction decreased during global cooling. Of these, climate appears to have played the more important role, which we attribute to preadaptation to cool climates. Biotic traits facilitating plant-animal mutualisms, in particular fruit type and pollination syndrome, were key to further enhancing diversification rates. These results suggest that, while the Andes acted as a driver of speciation for this lineage, a synergistic interaction between ecological and environmental factors underlies its rapid diversification, which culminated in one of the fastest plant radiations documented to date: the centropogonids. Our study underscores the complex interplay of ecological and historical determinants in generating the world's biodiversity.

4.2 Introduction

Species-rich rapid radiations are a conspicuous ecological and evolutionary phenomenon in the Tree of Life. Clades that have undergone such diversification are often documented in insular environments, including islands (Baldwin and Sanderson 1998; Lapoint et al. 2014), lakes (Wagner et al. 2012), and mountains (Hughes and Eastwood 2006; McGuire et al. 2014). Though they represent a small fraction of total terrestrial land surface, mountains are home to the greatest number of these rapidly diversifying groups (Madriñán et al. 2013; Hughes and Atchison 2015). The processes underlying such mountain radiations remain elusive, yet understanding the associated richness patterns is critical, especially in the context of global change. Of particular importance is the world's most species-rich biodiversity hotspot, the tropical Andes, which stretch from Venezuela to northern Argentina along the western coast of South America. These mountains are home to ~15% of all flowering plant species, half of which are endemic to the region (Myers et al. 2000). The origin of this biodiversity (e.g, Hughes & Eastwood 2006; Hutter *et al.* 2013; Madriñán *et al.* 2013; McGuire *et al.* 2014) is even more stunning considering the recency of mountain uplift: more than 60% of the current elevation of the tropical Andes was attained within the last 10 million years (Myr) (Gregory-Wodzicki 2000). Although the onset of this orogeny dates to the Paleocene and Eocene (66–33.9 Myr), exceptionally rapid surface uplift occurred during the late Miocene (~10-6 Myr) and early Pliocene (~4.5 Myr) (Garzione et al. 2008; Hoorn et al. 2010; Mulch et al. 2010). Such mountain building is thought to generate species diversity in a variety of ways, including by increasing environmental heterogeneity, affecting local and regional climate, facilitating the immigration of new species, and creating island-like ecological opportunity for adaptive radiation (Hoorn et al. 2013). The role of the rise of the Andes in the origination of biodiversity is evident in clades as diverse as birds (McGuire et

al. 2014), butterflies (Elias et al. 2009), and angiosperms (Hughes and Eastwood 2006; Madriñán et al. 2013; Givnish et al. 2014). In addition to their recent and rapid diversification, many of these groups display remarkable phenotypic diversity, as exemplified by the Andean lupines, whose growth forms range from herbs to shrubs and trees (Hughes and Eastwood 2006).

Identifying the causes of rapid radiations is a major goal in ecology and evolutionary biology. While some authors argue that abiotic processes are the main drivers of regional patterns of diversification (Peters 2008), others argue that species ecology is more important (Smith et al. 2014). However, rapid diversification is undoubtedly the product of both abiotic and biotic factors acting on different spatial and temporal scales (Benton 2009), though their individual contributions have proven difficult to assess within a single clade (but see Ezard *et al.* 2011 for a compelling example), and a tendency to explain a given diversity pattern with a single process persists. For Andean radiations, molecular divergence time estimates contemporaneous with geological activity have been cited as evidence that mountain building facilitated diversification (Hughes and Eastwood 2006; McGuire *et al.* 2014). Rapid Neotropical plant diversification has also been attributed to specialized pollination relationships with hummingbirds (Givnish *et al.* 2014) and to shifts between pollination syndromes (Kay *et al.* 2005). However, many factors, both abiotic and biotic, are likely to impact the diversification process in these and other groups.

Here, we seek to untangle the ecological and historical factors that have contributed to the generation of Andean megadiversity using the Neotropical bellflowers as a model system. The Neotropical bellflowers (Campanulaceae: Lobelioideae) are an Andean-centred clade of ~600 morphologically and ecologically diverse species. The group was recently resolved into three well-supported subclades: the Chilean lobelias (*Lobelia* section *Tupa*; 4 species) of the

temperate southern Andes; the páramo and puna endemic *Lysipomia (*50 species); and the centropogonid clade of primarily cloud forest endemics (*Centropogon*, *Burmeistera*, and *Siphocampylus*; ~550 species) (Lagomarsino et al. 2014). *Lyispomia* are diminutive herbs, while the other subclades are robust and mostly woody. The centropogonids are particularly diverse in their growth form: most species are vining plants with woody bases, but herbs, shrubs, and trees are all represented (Figure 4.1). Similar phenotypic diversity is also apparent in two traits that facilitate plant-animal interactions: fruit type and floral morphology. Abiotically dispersed capsules characterize ~40% of the species, while the remaining species produce fleshy, animal-dispersed berries, which evolved at least seven times from capsular ancestors (Lagomarsino et al. 2014). Floral morphology is also highly variable. *Lysipomia* produces small, white flowers that are indicative of invertebrate pollination, while both the Chilean lobelias and the centropogonids produce robust flowers that are usually vertebrate pollinated. Flowers in the centropogonid clade are particularly diverse (Figure 4.2) and principally adapted to pollination by hummingbirds and nectar bats (Muchhala & Potts 2007). Moreover, centropogonid flowers can be found in almost every colour, and range from less than 1 cm to more than 10 cm in length.

Owing to their broad Andean distribution and remarkable floral and fruit diversity, the Neotropical bellflowers represent a model group to examine the interaction of abiotic and biotic factors that trigger rapid mountain radiations. To accomplish this goal, we develop and apply novel statistical models to explicitly investigate the influence of geology, climate, and ecological traits on species diversification using the first well-sampled time-calibrated phylogeny of the group.

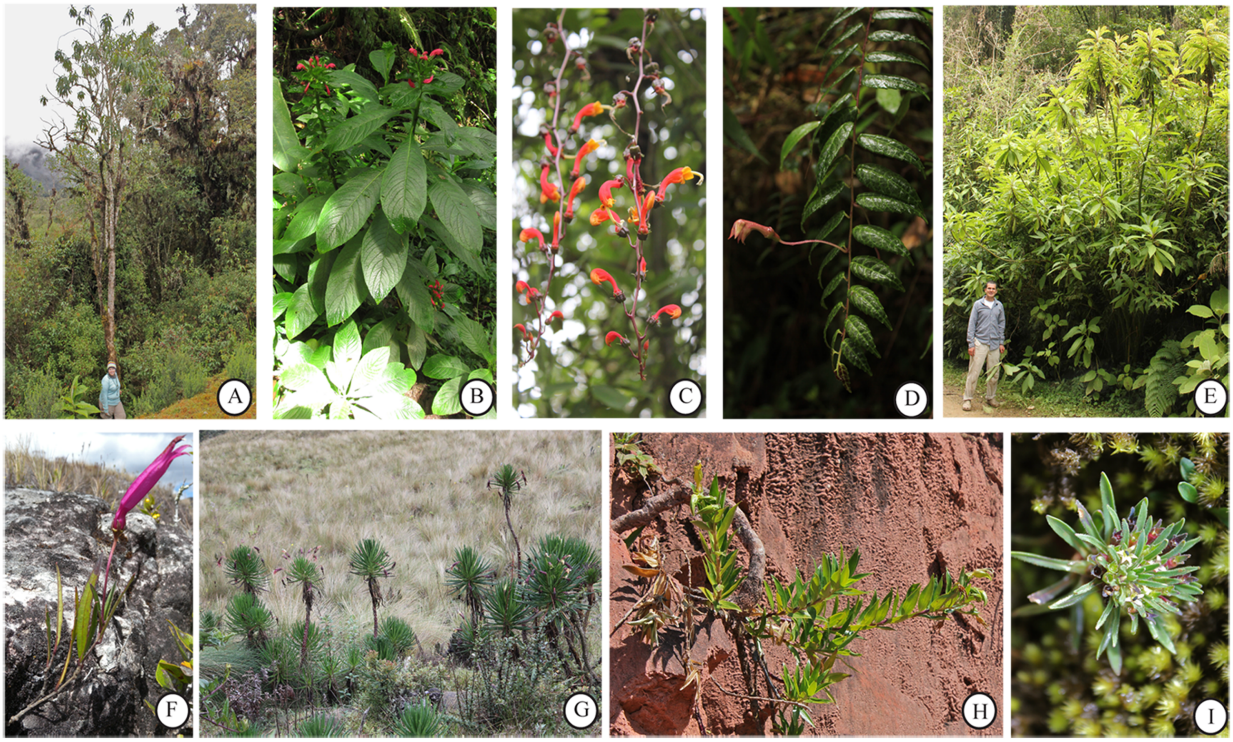


Figure 4.1. **Growth form diversity in Neotropical bellflowers. A)** *Siphocampylus tunarensis* Zahlbr., a tree ~7–10 m. **B)** *Centropogon congestus* Gleason, a clonal herbaceous species of wet soil, ~1.5 m. **C)** *Centropogon pulcher* Zahlbr., a hanging vine. **D)** *Burmeistera* sp., a hemi-epiphytic herb. **E)** *Siphocampylus tunicatus* Zahlbr., a tall shrub, with individual stems ~5 m tall, arising from a single point. **F)** *Siphocampylus williamsii* Rubsy, a plant producing a small number of narrow aerial stems arising from a xylopodium, or underground tuber-like stem. **G)** *Siphocampylus jelskii* Zahlbr., a giant rosette shrub with elongated stems, each ~1–2 m tall apparently clonal, growing in high altitude grasslands. **H)** *Siphocamplus smilax* Lammers, a xerophyte with a densely woody stem (likely water-storing) growing in sandstone. **I)** *Lysipomia muscoides* Hook f., a minute rosette herb growing among moss in puna habitat. Photos by L. Lagomarsino (B–E, G, H), D. Santamaría-Aguilar (A), and A. Fuentes (F).

4.3 Materials and Methods

Species and molecular dataset

One-third of Neotropical bellflower species were sampled, including all four species of *Lobelia* section *Tupa*, five of the ~40 species of *Lysipomia*, and 191 species of the ~550 species of the centropogonid clade (Figure B.1). Our sampling includes representatives from all taxonomic subdivisions of *Centropogon*, *Burmeistera*, and *Siphocampylus* (Lagomarsino et al. 2014). We assembled a concatenated molecular matrix that includes seven plastid regions totalling 11,990 base pairs (bp). Taxon sampling, molecular methods for newly generated sequences, and alignment protocols followed Lagomarsino *et al.* (2014). Outgroup sampling includes broad representation across Lobelioideae. Nine representatives of Campanuloideae were used as outgroups to root the phylogeny and provide appropriate nodes for fossil calibration.

Phylogenetics and dating

Phylogenies were inferred using maximum likelihood and Bayesian inference as implemented in RAxML 8.0 (Stamatakis 2014) and BEAST 2.1.3 (Bouckaert et al. 2014). Four calibrations points were used to estimate divergence times: *i)* the fossil seed of †*Campanula paleopyramidalis* as a minimum age constraint of 16 Myr for the most recent common ancestor of *C. pyramidalis* and *C. carpatica*; *ii)* a geological maximum age constraint of 29.8 Myr, which corresponds to the age of the oldest island of the Hawaiian Ridge, Kure (Clague 1996), for the crown group of the endemic Hawaiian clade (*Brighamia, Cyanea, Clermontia*, and *Delissea*); and *iii+iv)* two secondary age constraints from Bell *et al.* (2010): 41–67 Myr ago for crown group Campanulaceae, and 28–56 Myr ago for crown group Campanuloideae.

The optimal RAxML tree was dated using penalized likelihood in treePL (Smith and O'Meara 2012) with hard minimum and maximum age constraints. Confidence intervals were generated using 1,000 RAxML bootstrap trees. We then simultaneously inferred phylogenetic relationships and divergence times using both relaxed uncorrelated lognormal and exponential clock models in BEAST. A lognormal prior (mean of 1.5 and standard deviation of 1.0) was assigned to the fossil calibration age of 16 Myr, a uniform prior was assigned to the geological age constraint at 29.8 Myr (maximum hard bound), and normal priors were placed on the two secondary age constraints (mean age of 56.0 Myr and standard deviation of 8.3 Myr for Campanulaceae; mean age of 43.0 Myr and standard deviation of 8.0 Myr for Campanuloideae). The dated tree from treePL was specified as the starting tree in each of eight separate BEAST runs, which were conducted for 10 million generations of Markov chain Monte Carlo (MCMC). Convergence was assessed using effective sample size (ESS) values of the runs, and the maximum clade credibility tree, including credibility intervals (CI) for ages and posterior probabilities (PP) for node support, was assembled.

Robustness of age estimates was assessed by removing one or a series of calibration points. The following sets of calibration points were used for this purpose: *i)* the root age secondary constraint only; *ii)* the fossil and root age secondary constraint; and *iii)* the fossil and both secondary age constraints. Divergence time estimation can be sensitive to branch length variation, which is potentially influenced by growth form (Smith and Donoghue 2008). Since they are generally herbaceous and have longer internal branches than their woody relatives, we removed *Lysipomia* entirely, and re-estimated molecular divergence times to determine if these differences impacted results. These sensitivity analyses collectively demonstrated that our estimated ages are robust to dating method, calibration points, and branch length heterogeneity:

the 95% CIs of the re-estimated ages overlap with the 95% CIs from the BEAST analysis that we use for diversification analyses (see also Table B.1).

Trait categorization

Species traits were obtained from a variety of sources, including: GBIF (http://www.gbif.org/), Tropicos (http://www.tropicos.org/), herbarium specimens, taxonomic literature, and field collections. Type specimens for nearly all 594 species, many of which were not represented in our phylogenetic sampling but were used to account for sampling biases in our analyses, were consulted using the JSTOR Global Plants database (http://plants.jstor.org/). We scored four binary traits related to the biology and geographic occurrence of all Neotropical bellflower species for our diversification analyses: *i)* fruit type (berry or capsule), *ii)* pollinator type (vertebrate or invertebrate), *iii)* elevation (median species occurrence <1900m versus >1900m), and *iv)* presence/absence in the Andes. Pollinator type was coded according to classical morphological definitions of pollination syndromes. Specimen locality data determined the cutoff between high and low elevation. We calculated the median elevation for each species, and used the global median as our cut-off for diversification analyses. All trait data are provided in Table B.2 and in Figure 2.

Diversification analyses

We applied a series of birth-death models to quantify the effects of abiotic and biotic correlates of speciation and extinction in Neotropical bellflowers. We assured robustness of our results in a variety of ways. First, to accommodate phylogenetic uncertainty (except in the case of the diversity-dependent analyses, which are computationally intensive), we conducted our

analyses across 500 randomly sampled trees from the BEAST posterior distribution (outgroups removed). Second, we implemented a sampling fraction to account for unsampled species diversity. We also applied a sampling fraction to account for any sampling bias in trait space for BiSSE analyses. Third, for each of our diversification analyses, except for those using Bayesian Analysis of Macroevolutionary Mixture (BAMM 2.2.2), we selected the best fitting model by computing the corrected Akaike Information Criterion (AICc) based on the log-likelihood and the number of free parameters for each model. The model supported by the lowest AICc was considered best if it was at least two ΔAIC units better than the model with the second lowest score. We also used likelihood ratio tests (significant at $P<0.05$) to estimate support for the best-fitting model when compared to rival models.

Time-dependent diversification

We used BAMM to estimate speciation and extinction rates through time and to identify shifts in diversification rate (Rabosky *et al.* 2014). We accounted for incomplete taxon sampling by applying clade-specific sampling probabilities in each of the three principal Neotropical bellflower subclades: the Chilean lobelias (1.0), *Lysipomia* (0.12), and the centropogonids (0.35). We ran BAMM with four reversible jump MCMC chains, each for five million generations. ESS values were used to assess convergence. The posterior distribution was used to estimate the configuration of the diversification rate shifts, and alternative diversification models were compared using Bayes factors. Results were analysed and plotted using the R package *BAMMtools* 2.0.2 (Rabosky et al. 2014).

Paleoenvironment-dependent diversification

We tested the effect of past environmental change on the diversification of Neotropical bellflowers using birth-death models that allow speciation and extinction rates to vary according to a quantitative, time-dependent environmental variable (Condamine et al. 2013), i.e., the global Cenozoic temperature profile (Zachos et al. 2008) and the paleoaltitude of the Andes. The latter was compiled for this study from numerous references (Garzione et al. 2006, 2008, 2014; Ehlers and Poulsen 2009; Leier et al. 2013). The R package *pspline* was used to interpolate a smooth line for each environmental variable. This smooth line was sampled during each birth-death modelling process to give the value of the paleoenvironmental variable at each time point. Speciation and/or extinction rates were then estimated as a function of these values along the dated phylogenies according to the parameters of the following models. For both temperature and Andean elevation, we developed and applied four models in which the paleoenvironment-dependency was exponential (Table B.3): *i)* speciation rate varies with the environmental variable and no extinction; *ii)* speciation rate varies with the environmental variable and extinction rate is constant; *iii)* speciation rate is constant and extinction rate varies with the environmental variable; and *iv)* speciation and extinction rates both vary with the environmental variable. We repeated these models with linear dependence on the environmental variable (Table B.3).

Trait-dependent diversification

We modelled the impact of traits on the diversification of Neotropical bellflowers by concurrently estimating their impact on speciation, extinction, and transition rates using Binary State-Speciation and Extinction (BiSSE, Maddison *et al.* 2007). For each of the four traits described above (Andean occurrence, elevation, pollination syndrome, and fruit type), we

evaluated eight BiSSE diversification models of increasing complexity in which speciation, extinction, and transition rates were allowed to either vary or remain equal between traits (Table B.4). Analyses were performed using the R package *diversitree* 0.7-6 (FitzJohn 2012). Once the best-fitting model was selected, CIs for each parameter were estimated for the tree. We used an exponential prior following FitzJohn (2012), and began the MCMC with the ML estimates. We ran MCMC for 20,000 generations and applied a burn-in of 2000 steps. We then computed the net diversification rates for each trait based on the combined speciation and extinction rate estimates. Finally, to determine if these traits were correlated, pairwise trait comparisons were performed across a random sampling of 500 trees from the posterior distribution in both a ML and Bayesian framework in BayesTraits v2.0 (Pagel and Meade 2006). Significance of binary trait dependence was assessed against a rival model where these traits evolved independently using likelihood ratio tests (ML) and Bayes Factors of the harmonic mean of likelihood values.

Diversity-dependent diversification

We applied models that allow speciation and extinction to vary according to the number of lineages in the phylogeny. Using the R package DDD v2.7 (Etienne et al. 2012), we built two models: *i)* speciation declines with diversity with no extinction, and *ii)* speciation declines with diversity with extinction present. The initial carrying capacity was set to the current species diversity, and the final carrying capacity was estimated according to the model and corresponding parameters.

4.4 Results

Molecular phylogeny and divergence time estimation

The final concatenated alignment comprised seven loci (~12,000 bp) sequenced for 275 species (Dryad: http://dx.doi.org/###). The concatenated Bayesian phylogenetic analysis using the best-fitting partitioning scheme yielded a highly resolved and strongly supported tree compatible with the ML tree and previously published results (Lagomarsino et al. 2014). Sequence divergence, particularly in the centropogonid clade, was low as reflected by the shallow branching pattern toward the tips. Despite short internal branches, indicative of a recent radiation, the phylogeny is well supported: 66% of nodes are recovered with high support (PP>0.90). Our results support the monophyly of the subfamilies Campanuloideae and Lobelioideae and the Neotropical bellflowers (the centropogonids, *Lysipomia*, and Chilean lobelias) with maximum nodal support (PP=1).

Results of the dating analyses are presented in Figure 4.2 (see Figure B.1 for the 95% CI for each node). Similar estimates were obtained using different dating methods and with alternative calibration scenarios and settings. The results were also robust to potential biases such as long internal branch lengths, possibly attributed to growth form variation (Table B.1). Based on the molecular divergence time estimates from BEAST and treePL, we place the origin of the extant Neotropical bellflowers diversity in the Miocene, ~17.1 Ma (95% CI 14.32–20.32 Ma). We further found that the crown groups of their three main subclades – Chilean lobelias, *Lysipomia*, and the centropogonids – originated 1.45 Myr (95% CI 0.42–2.78 Myr), 11.87 Myr (CI 9.00–15.24 Myr), and 5.02 Myr (CI 3.95–6.13 Myr), respectively (Figure 4.2, Figure B.1). All branching events in the most species-rich clade, the centropogonids, occur in the Plio-Pleistocene (5.3-0 Myr).

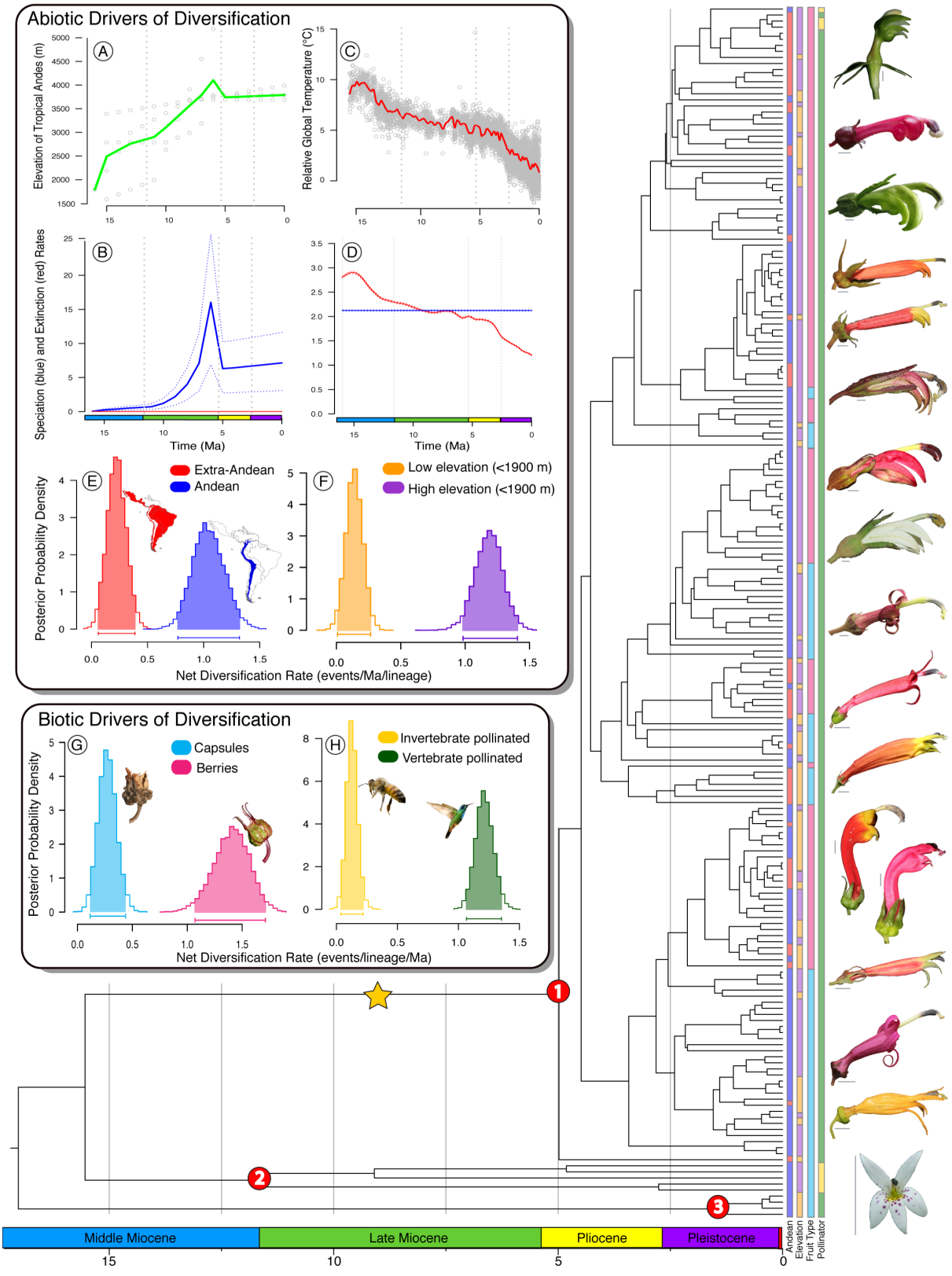


Figure 4.2. Diversification of Neotropical bellflowers (Campanulaceae: Lobelioideae).

Figure 4.2 (Continued). A time-calibrated species-level phylogeny shows the *ca.* 5 Ma age of the largely Andean centropogonid clade (~550 species, node 1), whose origin is associated with a significant increase in diversification rate (yellow star). *Lysipomia* (~50 species) and Chilean *Lobelia* (4 species) are indicated (nodes 2 and 3, respectively). Representative floral diversity shown at right illustrates the striking phenotypic diversity in the clade (see Figure 4.1 for comparable growth form diversity); scale bars equal 0.5 cm. Diversification models examining the abiotic correlates of this rapid diversification include average paleoaltitude of the tropical Andes through time **(A)** and global temperatures through time **(C)** (Zachos et al. 2008). Grey dots in **(A)** and **(C)** represent individual data points utilized to create the curves. Results from these models show inferred speciation (blue) and extinction (red) rates through time under paleoaltitude **(B)** and paleotemperature **(D)** models. Additional diversification analyses using BiSSE demonstrate the effect of two abiotic traits on net diversification rate: Andean occurrence [E; extra-Andean (red) vs. Andean (blue)] and elevation [**F**; low elevation, <1900 m (orange) vs. high elevation, >1900 m (purple)]. The biotic correlates of this rapid diversification were examined using additional BiSSE analyses: fruit type [**G**; dry capsules (light blue) vs. fleshy berries (pink)] and pollinator type [**H**; invertebrate (yellow) vs. vertebrate (green). All trait scorings are color-coded to the right of phylogeny. Outgroups were removed, and taxon names omitted due to space constraints. All photos by L. Lagomarsino.

Diversification analyses

The time-dependent diversification analysis strongly rejected constant diversification. Our BAMM analyses indicate that Neotropical bellflowers underwent a significant shift in net diversification rate coinciding with the recent origin of the centropogonid subclade (~5 Myr), which includes 550 of the 600 species (Figure 4.2, Figure B.2). The BAMM analysis further provide evidence for a 3.7-fold increase in diversification rate (1.83 versus 0.5 events/Myr/lineage); net diversification rate is similarly high using the alternative metric of Magallón and Sanderson (2001) (0.82 to 1.15 events/Myr/lineage under high [ε=0.90] and low [ε=0] extinction, respectively). As illustrated in Figure B.2B, the diversification rate for the centropogonid clade is much higher than its background rate.

Using a newly developed paleoenvironment-dependent diversification model that explicitly accommodates the effect of changing environment through the course of diversification (Figure 4.2A), we find that the speciation rates in the Neotropical bellflowers are positively dependent on the paleoaltitude of the Andes, while extinction rates are not effected (Figure 4.2B, Table B.3). Applying this model, we reconstruct a continuous increase in speciation rate beginning at ~12 Myr (mid-Miocene) and peaking at ~5 Myr (early Pliocene). This coincides with the maximum paleoaltitude of the Andes (>4000 m), at which point we infer an unprecedented ~15 speciation events/Myr/lineage for Neotropical bellflowers. Because of the potential significance of this result, we ran additional analyses implementing a trait-dependent diversification model using BiSSE. We implemented two models to estimate the effect of the Andes on the diversification rates; namely, we categorized the Neotropical bellflower species into Andean and extra-Andean and by their elevational distribution (high elevation [>1900 m] versus low elevation). The best-fitting model for these BiSSE analyses inferred significantly

higher speciation rate for Andean species and for species occurring at high elevation (Figure 4.2E-F, Table B.4), respectively. The similar results from these BiSSE analyses are likely partially explained by the correlated nature of elevational distribution and Andean occurrence that we identified in BayesTraits; this correlation is not surprising given that the Andes represent the most topographic relief across the Neotropical bellflowers' range (Table B.5). Altogether, these results are consistent with an important role of Andean uplift as a speciation trigger for Neotropical bellflowers.

Using the same paleoenvironmental birth-death model, but instead incorporating relative global temperature proxies that span the last ~20 million years of the Cenozoic (Zachos et al. 2008), we demonstrate a significant influence of climate change on Neotropical bellflower diversification (Figure 4.2D). In contrast to Andean orogeny, which influenced primarily speciation, the best fitting paleoclimatic model indicates that climate change only had a significant impact on extinction. Beginning ~15 Myr (mid-Miocene), extinction rates decreased dramatically towards the present as a function of global temperature (Figure 4.2D, Table B.3). Moreover, comparison of likelihood scores for these paleoenvironment-dependency analyses demonstrates that paleoclimate had a more pronounced effect on diversification than paleoaltitude, despite their similarity in magnitude (Table B.3).

Additional BiSSE analyses demonstrate that various clade-specific biotic traits influence diversification rates in Neotropical bellflowers. These traits showed uncorrelated evolution with respect to one another, and with both the abiotic factors discussed above (Table B.5). The best models, as supported by both AIC and likelihood ratio tests (Table B.4), infer higher net diversification rates in lineages with the following character states (Figure 4.2, Figure B.3): fleshy fruits (vs. dry fruits, Figure 4.2G), and vertebrate pollination syndromes (vs. invertebrate

pollination syndromes, Figure 4.2H). These traits acted differently on the two components of diversification: fleshy fruits confer lower extinction rates than capsules, while species pollinated by vertebrates have higher speciation rates than invertebrate-pollinated species. In total, we examined the effect of four traits on diversification rates in the Neotropical bellflowers; our results demonstrate their relative importance, in decreasing order, as follows: pollination syndrome, fruit type, Andean presence, and elevation (Table B.4). These results suggest that biotic traits are key to the rapid diversification in Neotropical bellflowers.

Finally, our diversity-dependent analysis inferred that the group has not reached diversity equilibrium; the estimated carrying capacity (i.e., number of species potentially sustained in the clade) far exceeds the current extant diversity of the clade (Table B.6).

4.5 Discussion

The Andean biodiversity hotspot is famous for its high species richness (Myers *et al.* 2000) and the rapid diversification rates that characterize many of its emblematic clades (e.g. Hughes & Eastwood 2006; Madriñán *et al.* 2013, Hughes & Atchison 2015). Although numerous studies have documented this pattern, few studies have attempted to test and dissect the precise causes of this megadiversity (but see Hutter *et al.* 2013). Our study tackles this issue using a multi-pronged, interdisciplinary approach that paves the way for future inquiry.

The impact of Andean orogeny and climate change on species diversification

We find that the Neotropical bellflowers are an ideal model system to investigate the origins of Andean megadiversity. Within this morphologically diverse clade, a shift to increased diversification rates on the branch subtending the centropogonid subclade resulted in an Andean-

centered radiation with ~550 extant species. The diversification rate for the centropogonids, estimated to be between 0.82–1.83 events/Myr/lineage, makes them one of fastest species radiations reported to date (Table 4.1), with average overall rates of speciation exceeding canonical groups ranging from *Espeletia* (Madriñán et al. 2013) and hummingbirds (McGuire et al. 2014) in the Andes to the silverswords (Baldwin and Sanderson 1998) and Drosophilidae of Hawaii (Lapoint et al. 2014).

Table 4.1. Net diversification rates in the fastest species radiations in the Tree of Life, including the centropogonids. Rates of diversification as calculated using the statistic of Magallón and Sanderson (2001) under low, medium, and high estimated extinction (ε) for the centropogonid clade (yellow) rank ordered with rates from other published rapid radiations. All rates in events/Ma/lineage. Estimates are derived from reported ages and species richness from the relevant literature cited. When possible, 95% confidence intervals for ages are reported, except in cases where sufficient data was unavailable.

Table 4.1 (Continued).

Clade	Area	Organism	Species #	Age (CI)	r (ε=0)	r (ε=0.5)	r (ε=0.9)
Dianthus (carnations) (Valente et al. 2010)	Eurasia	plant	200	1.5 (0.9-2.1)	3.07 (2.12–5.12)	2.88 (2.06–4.80)	1.99 (1.42–3.32)
African cichlids (Salzburger et al. 2005)	East African Lakes	fishes	1800	2.4 (1.22-4.02)	2.83 (1.69-5.76)	2.71 (1.62 - 5.34)	2.14 (1.28-4.22)
Lupinus (Hughes and Eastwood 2006)	Andes	plant	81	1.47 (1.18-1.76)	2.52 (2.10-3.14)	2.33 (1.95-2.90)	1.46 (1.22-1.82)
Neo-astragalus (clade F) (Scherson et al. 2008)	Andes	plant	90	1.89 (1.71–2.07)	2.04 (1.84–2.23)	1.87 (1.70–2.06)	1.19 (1.08–1.31)
Zosterops (Moyle et al. 2009)	Widely distributed	birds	80	1.84 (1.40–1.89)	2.0 (1.95–2.63)	1.85 (1.80–2.44)	1.16 (1.13–1.52)
Neo-astragalus (clade G) (Scherson et al. 2008)	Andes	plant	15	0.98 (0.79–1.17)	2.06 (1.72–2.55)	1.82 (1.52–2.26)	0.84 (0.70–1.04)
Gentianella (Hagen and Kadereit 2001)	Andes	plant	170	1.6–3.0*	1.48–2.78	1.39–2.6	0.94–1.77
Paussus (ant-nest beetles) (Moore and Robertson 2014)	Madagascar	insects	86	2.6 (1.7-3.6)	1.45 (1.04-2.21)	1.34 (0.97-2.05)	0.85 (0.61-1.29)
Centropogonids (this study)	Andes	plant	556	5.02 (3.95-6.13)	1.12 (0.91-1.42)	1.06 (0.87-1.35)	0.79 (0.65-1.00)
Espeletiinae (Madriñán et al. 2013)	Andes	plant	120	4.04 (2.42-5.92)	1.01 (0.69– 1.69)	0.944 (0.64–1.58)	0.62 (0.42–1.04)
AMC clade *Drosophila* (Lapoint et al. 2014)	Hawaii	insect	91	4.40 (3.45–11.82)	0.94 (0.35–1.2)	0.88 (0.33–1.12)	0.58 (0.22–0.74)
Inga (Richardson et al. 2001)	Neotropics	plant	300	5.9 (2.0–13.4)	0.85 (0.37–2.5)	0.8 (0.35–2.36)	0.57 (0.25–1.69)
Ruschioideae (Klak et al. 2003)	South Africa	plant	1,563	3.8–8.7	0.7–1.75	0.73–1.68	0.58–1.31
Bee hummingbirds (McGuire et al. 2014)	Andes	birds	36	5	0.58	0.53	0.29
Silversword alliance (Baldwin and Sanderson 1998)	Hawaii	plants	28	5.2 (4.4–6.0)	0.51 (0.44–60)	0.46 (0.40–0.54)	0.24 (0.21–0.29)
Costus subgenus *Costus* (Kay et al. 2005)	Neotropics	plant	51	1.5–7.1	0.46–2.16	0.42–1.98	0.24–1.16
Hawaiian lobeliads (Givnish et al. 2009)	Hawaii	plants	126	13.6 (10.49–16.71)	0.30 (0.25–0.39)	0.28 (0.23–0.37)	0.19 (0.15–0.24)
Hawaiian Drosophilidae (Lapoint et al. 2014)	Hawaii	insect	1000	25.15 (23.9–27.46)	0.25 (0.23–0.26)	0.24 (0.22–0.25)	0.18 (0.17–0.19)
Plethodon, *glutinosus* group (Kozak et al. 2006)	North America	amphibian	30	8–11	0.24–0.34	0.22–0.31	0.12–0.16
Hummingbirds (all) (McGuire et al. 2014)	Neotropics	bird	338	22.4 (20.3–24.7)	0.23 (0.21–0.25)	0.22 (0.20–0.24)	0.16 (0.14–0.17)

In addition, our analyses provide key insights into the abiotic and biotic drivers of exceptionally rapid diversification in the Andes. Using macroevolutionary diversification models that incorporate geological data, we demonstrate, for the first time to our knowledge, that fine scale orogeny resulted in increased diversification rates. Specifically, we demonstrate that the final stages of mountain building are strongly associated with the origin and rise of prolific speciation rates in the Neotropical bellflowers (Figure 4.2B, Table B.3). These speciation rates peaked at a remarkable ~15 event/Myr/lineage, concurrent with the highest past elevation of the Andes. Although not sustained, this maximum exceeds the highest speciation rates reported in plants, including in the Mediterranean carnations (2.2–7.6 speciation events/Myr/lineage; Valente *et al.* 2010) and Andean lupines (2.49–3.72 speciation events/Myr/lineage; Hughes & Eastwood 2006). These results corroborate the shift to faster speciation rates that was detected by BAMM during the period of final Andean uplift.

Furthermore, BiSSE analyses bolster our findings that the Andes in general are a major driver of species diversification in this clade: Andean taxa have significantly higher net diversification rates than extra-Andean taxa (Figure 4.2E, Figure B.3, Table B.4) and species diversification is faster at higher elevations (>1900 m) (Figure 2F, Figure B.3, Table B.4). Although not specifically addressed by the models we employed, it is likely that elevated diversification rates correlated with changes in paleoaltitude were also influenced by increases in geographic area and formation of microhabitats associated with the expanding Andean landscape. Overall, this supports the montane species pump hypothesis, which has been previously invoked to explain Andean megadiversity. This hypothesis posits that high montane diversity can be explained by elevated diversification rates as a result of habitat heterogeneity,

and has been supported in some Andean clades (Sedano and Burns 2010), but not others (Hutter et al. 2013)

Past climate change has also independently influenced diversification rates in the Neotropical bellflowers. Our paleotemperature-dependency analysis shows that, while speciation rates remained high but constant, extinction rates are significantly correlated with past temperature. Consequently, extinction rates were lowest during the coolest intervals, and have generally been declining since the origin of the Neotropical bellflowers, a result that is particularly striking in today's world of anthropogenic change. Although our proxy of climate change is global, it is almost certain that cooling since the mid-Miocene has affected the Andes, especially at mid-to-high elevations where Neotropical bellflowers are most diverse (Hoorn *et al.* 2010).

Indeed, a comparison of likelihood scores reveals that climate change appears to have had a stronger impact on diversification in Neotropical bellflowers than paleoaltitude. We hypothesize that Neotropical bellflowers likely evolved their tolerance to cool habitats in southern, perhaps temperate regions of South America, similar to where Chilean lobelias now occur, prior to major tropical Andean uplift. This climatic preadaptation may explain their northward expansion and decreased extinction rates as this clade exploited cooler niches associated with the rising Andes. These results significantly progress our understanding of the abiotic determinants that have triggered Andean diversification, and collectively indicate that orogeny and especially climate are key contributors to increases in net species diversification rate in Neotropical bellflowers that have acted on different components of net diversification.

Biotic traits that facilitate mutualisms are associated with elevated rates of net diversification

In addition to orogeny and climate change, our trait dependent analyses point to a potentially bigger role of species ecology in influencing species diversification in Neotropical bellflowers. Specifically, we identify that mutualistic interactions with seed dispersers and pollinators promote diversification. Here, we demonstrate that bird-dispersed berries and vertebrate-pollinated flowers are associated with significantly higher rates of diversification than their counterparts (Figure 4.2G–H, Figure B.3, Table B.4). Species with berries have a net diversification rate that is ~3.5 times higher than in capsular species, whose seeds are abiotically dispersed (Figure 4.2G; Figure B.3). As in other groups, fleshy fruits in Neotropical bellflowers are generally associated with densely forested habitats (Lagomarsino et al. 2014). It is likely that the relative success of berry-fruited clades was due to animal dispersal in a complex, changing environment with increasing forest cover. The repeated evolution of berries may have promoted diversification by increasing dispersability relative to their capsular ancestors, thus facilitating allopatric speciation via long distance dispersal (Willis et al. 2014).

Pollination by vertebrates appears to have played an even bigger role in species diversification than animal dispersal. Here, we see a ~6-fold increase in diversification rate relative to invertebrate pollination (Figure 4.2H; Figure B.3; Table B.4). Vertebrate pollinators, namely hummingbirds and bats, are hypothesized to be more effective pollinators than invertebrates in part because they can carry higher pollen loads over longer distances (Fleming et al. 2009). The increased speciation rates among vertebrate-pollinated taxa (Figure B.3, Table B.4) are a likely result of floral isolation, which allows closely related species to share pollinators (Muchhala 2003). In support of this, many Neotropical bellflowers have sympatric

distributions that appear to have been facilitated by either pollinator shifts (Muchhala 2006) or character partitioning of floral traits (Muchhala and Potts 2007).

Altogether, our analyses of biotic traits indicate that ecological factors, particularly mutualisms with other species, constitute additional triggers of net diversification rate in Neotropical bellflowers, as has been demonstrated in extra-Andean plant groups (Lutzoni and Pagel 1997; Weber and Agrawal 2014). This effect of species ecology is especially pronounced within the centropogonid subclade, in which more than half of the species are vertebrate pollinated and/or produce berries, and in which diversification rates are particularly elevated (Figure B.2). Our results demonstrate that diversity-dependent processes did not govern diversification, which suggests that the clade is in its early phases of diversification and is not bounded by ecological limits.

A synergy of abiotic and biotic factors drives Andean diversification

Although the interplay between abiotic and biotic drivers has long been recognized as fundamental for regulating diversity, progress toward understanding their interaction has been slow. Our study provides important insights in this regard. In the context of Andean biodiversity, dramatic geological and environmental transformations characterized the matrix in which lineages and their mutualists diversified. We demonstrate that orogeny and especially climate facilitated the rapid radiation of Neotropical bellflowers. Our results also indicate that key differences in biotic traits, including fruit dispersal and especially pollination syndrome, confer enhanced diversification capacity among closely related species co-occurring in the same rapidly changing environment. Indeed, our trait-dependent analyses indicate that these biotic traits may be the most important factor underlying the rapid diversification of Neotropical bellflowers.

Here, we hypothesize that preadaptation, especially with regard to exploitation of cooler climates as the tropical Andes rose, allowed this clade to achieve its broader distribution. This, in turn, precipitated mutualistic interactions, especially involving vertebrate pollinators, with groups showing similarly high Andean diversity (e.g., hummingbirds), further increasing diversification. We argue that the Andes, and the habitat heterogeneity created by their orogeny, acted as a montane species pump across many clades, but it is an additive interaction of ecological and environmental factors that underlies this region's megadiversity.

More generally, rapid plant diversification in the world's montane regions are frequently a product of island-like ecological opportunity following mountain uplift, further stimulated by evolutionary innovation (e.g., perenniality, vertebrate pollination) (Hughes and Eastwood 2006; Hughes and Atchison 2015). Our analyses demonstrate that this model likely applies to Neotropical bellflowers, which display extreme morphological and ecological diversity (Figures 4.1, 4.2)— a hallmark of plant evolution on islands. However, why are the Andes more diverse than other montane systems? It is likely that the receny of Andean orogeny partially explains this phenomenon: many clades may still be in the early phases of explosive radiation and thus are not yet greatly impacted by extinction. In addition, the Andes are characterized by deeply dissected topography including some of the steepest environmental gradients known (Hughes and Atchison 2015). These characteristics almost certainly enhance the island-like nature of this system and further intensify ecological opportunity and are shared with the Hengduan Mountains (Favre et al. 2014), another of the world's biodiversity hotspots (Myers et al. 2000). We are likely to gain insight into why the Andes are so diverse by comparing its clades' diversification histories with those in other such mountain hotspots. Our framework, including the integration of climatic, paleoaltimetry, and trait data, can be used towards this end.

4.6 Acknowledgements

I would like to thank members of the Davis and Antonelli research groups for helpful feedback and Suzette Flantua, Elisabeth Forrestel, Carina Hoorn, Daniel Santamaría-Aguilar, and Zhenxiang Xi for insightful conversations. The directors and curators at the following herbaria provided important access to their collections: BOLV, CR, GB, GH, INB, LPB, MO, MOL, NY, PMA, SCZ, SMF, and USZ. Funding was provided by a National Science Foundation Doctoral Dissertation Improvement Grant DEB-1210401 to L.P.L. and C.C.D. and from the Department of Organismic and Evolutionary Biology, the Botanical Society of America, the American Society of Plant Taxonomists, the Arnold Arboretum's Deland Award, the Explorer's Club, and the Rockefeller Center for Latin American Studies to L.P.L.

4.7 References

Baldwin, B. G., and M. J. Sanderson. 1998. Age and rate of diversification of the Hawaiian silversword alliance (Compositae). Proc. Natl. Acad. Sci. U. S. A. 95:9402–9406.

Bell, C. D., D. E. Soltis, and P. S. Soltis. 2010. The age and diversification of the angiosperms re-revisited. Am. J. Bot. 97:1296–1303.

Benton, M. J. 2009. The Red Queen and the Court Jester: Species diversity and the role of biotic and abiotic factors through time. Science 323:728–732.

Bouckaert, R., J. Heled, D. Kühnert, T. Vaughan, C. H. Wu, D. Xie, M. a. Suchard, A. Rambaut, and A. J. Drummond. 2014. BEAST 2: A software platform for Bayesian evolutionary analysis. PLoS Comput. Biol. 10:1–6.

Clague, D. 1996. Growth and subsidence of the Hawaiian-Emperor volcanic chain. Pp. 35–50 *in* A. Keast and S. Mille, eds. The Origin and Evolution of Pacific Island Biotas, New Guinea to Eastern Polynesia: Patterns and Processes. SPB Academic Press, Amsterdam.

Condamine, F. L., J. Rolland, and H. Morlon. 2013. Macroevolutionary perspectives to environmental change. Ecol. Lett. 16:72–85.

Ehlers, T. A., and C. J. Poulsen. 2009. Influence of Andean uplift on climate and paleoaltimetry estimates. Earth Planet. Sci. Lett. 281:238–248.

Elias, M., M. Joron, K. Willmott, K. L. Silva-Brandão, V. Kaiser, C. F. Arias, L. M. Gomez Piñerez, S. Uribe, a V. Z. Brower, a V. L. Freitas, and C. D. Jiggins. 2009. Out of the Andes: Patterns of diversification in clearwing butterflies. Mol. Ecol. 18:1716–1729.

Etienne, R. S., B. Haegeman, T. Stadler, T. Aze, P. N. Pearson, A. Purvis, and A. B. Phillimore. 2012. Diversity-dependence brings molecular phylogenies closer to agreement with the fossil record. Proc. R. Soc. B Biol. Sci. 279:1300–1309.

Ezard, T. H. G., T. Aze, P. N. Pearson, and A. Purvis. 2011. Interplay between changing climate and species' ecology drives macroevolutionary dynamics. Science 332:349–351.

Favre, A., M. Päckert, S. U. Pauls, S. C. Jähnig, D. Uhl, I. Michalak, and A. N. Muellner-Riehl. 2014. The role of the uplift of the Qinghai-Tibetan Plateau for the evolution of Tibetan biotas. Biol. Rev. 90:na/na.

FitzJohn, R. G. 2012. Diversitree: Comparative phylogenetic analyses of diversification in R. Methods Ecol. Evol. 3:1084–1092.

Fleming, T. H., C. Geiselman, and W. J. Kress. 2009. The evolution of bat pollination: A phylogenetic perspective. Ann. Bot. 104:1017–1043.

Garzione, C. N., D. J. Auerbach, J. Jin-Sook Smith, J. J. Rosario, B. H. Passey, T. E. Jordan, and J. M. Eiler. 2014. Clumped isotope evidence for diachronous surface cooling of the Altiplano and pulsed surface uplift of the Central Andes. Earth Planet. Sci. Lett. 393:173–181.

Garzione, C. N., G. D. Hoke, J. C. Libarkin, S. Withers, B. MacFadden, J. Eiler, P. Ghosh, and A. Mulch. 2008. Rise of the Andes. Science 320:1304–1307.

Garzione, C. N., P. Molnar, J. C. Libarkin, and B. J. MacFadden. 2006. Rapid late Miocene rise of the Bolivian Altiplano: Evidence for removal of mantle lithosphere. Earth Planet. Sci. Lett. 241:543–556.

Givnish, T. J., M. H. J. Barfuss, B. Van Ee, R. Riina, K. Schulte, R. Horres, P. a Gonsiska, R. S. Jabaily, D. M. Crayn, J. A. C. Smith, K. Winter, G. K. Brown, T. M. Evans, B. K. Holst, H. Luther, W. Till, G. Zizka, P. E. Berry, and K. J. Sytsma. 2014. Adaptive radiation,

correlated and contingent evolution, and net species diversification in Bromeliaceae. Mol. Phylogenet. Evol. 71:55–78.

Givnish, T. J., K. C. Millam, A. R. Mast, T. B. Paterson, T. J. Theim, A. L. Hipp, J. M. Henss, J. F. Smith, K. R. Wood, and K. J. Sytsma. 2009. Origin, adaptive radiation and diversification of the Hawaiian lobeliads (Asterales: Campanulaceae). Proc. R. Soc. B Biol. Sci. 276:407–416.

Gregory-Wodzicki, K. M. 2000. Uplift history of the Central and Northern Andes: A review. Geol. Soc. Am. Bull. 112:1091–1105.

Hoorn, C., V. Mosbrugger, A. Mulch, and A. Antonelli. 2013. Biodiversity from mountain building. Nat. Geosci. 6:154.

Hoorn, C., F. P. Wesselingh, H. ter Steege, M. A. Bermudez, A. Mora, J. Sevink, I. Sanmartín, A. Sanchez-Meseguer, C. L. Anderson, J. P. Figueiredo, C. Jaramillo, D. Riff, F. R. Negri, H. Hooghiemstra, J. Lundberg, T. Stadler, T. Särkinen, and A. Antonelli. 2010. Amazonia through time: Andean uplift, climate change, landscape evolution, and biodiversity. Science 330:927–931.

Hughes, C. E., and G. W. Atchison. 2015. The ubiquity of alpine plant radiations: From the Andes to the Hengduan Mountains. New Phytol., doi: 10.1111/nph.13230.

Hughes, C., and R. Eastwood. 2006. Island radiation on a continental scale: Exceptional rates of plant diversification after uplift of the Andes. Proc. Natl. Acad. Sci. U. S. A. 103:10334–10339.

Hutter, C. R., J. M. Guayasamin, and J. J. Wiens. 2013. Explaining Andean megadiversity: the evolutionary and ecological causes of glassfrog elevational richness patterns. Ecol. Lett. 16:1135–44.

Kay, K. M., P. A. Reeves, R. G. Olmstead, and D. W. Schemske. 2005. Rapid speciation and the evolution of hummingbird pollination in Neotropical Costus subgenus *Costus* (Costaceae): Evidence from nrDNA ITS and ETS sequences. Am. J. Bot. 92:1899–1910.

Klak, C., A. Khunou, G. Reeves, and T. Hedderson. 2003. A phylogenetic hypothesis for the Aizoaceae (Caryophyllales) based on four plastid DNA regions. Am. J. Bot. 90:1433–1445.

Kozak, K. H., D. W. Weisrock, and A. Larson. 2006. Rapid lineage accumulation in a non-adaptive radiation: Phylogenetic analysis of diversification rates in eastern North American woodland salamanders (Plethodontidae: Plethodon). Proc. R. Soc. B Biol. Sci. 273:539–546.

Lagomarsino, L. P., A. Antonelli, N. Muchhala, A. Timmermann, S. Mathews, and C. C. Davis. 2014. Phylogeny, classification, and fruit evolution of the species-rich Neotropical bellflowers (Campanulaceae: Lobelioideae). Am. J. Bot. 101:2097–2112.

Lapoint, R. T., K. N. Magnacca, and P. M. O'Grady. 2014. Phylogenetics of the Antopocerus-Modified Tarsus clade of Hawaiian *Drosophila*: Diversification across the Hawaiian Islands. PLoS One 9:e113227.

Leier, A., N. McQuarrie, C. Garzione, and J. Eiler. 2013. Stable isotope evidence for multiple pulses of rapid surface uplift in the Central Andes, Bolivia. Earth Planet. Sci. Lett. 371-372:49–58.

Lutzoni, F., and M. Pagel. 1997. Accelerated evolution as a consequence of transitions to mutualism. Proc. Natl. Acad. Sci. U. S. A. 94:11422–11427.

Maddison, W. P., P. E. Midford, and S. P. Otto. 2007. Estimating a binary character's effect on speciation and extinction. Syst. Biol. 56:701–710.

Madriñán, S., A. J. Cortés, and J. E. Richardson. 2013. Páramo is the world's fastest evolving and coolest biodiversity hotspot. Front. Genet. 4:1–7.

Magallón, S., and M. J. Sanderson. 2001. Absolute diversification rates in angiosperm clades. Evolution (N. Y). 55:1762–1780.

McGuire, J. A., C. C. Witt, J. V Remsen, A. Corl, D. L. Rabosky, D. L. Altshuler, and R. Dudley. 2014. Molecular phylogenetics and the diversification of hummingbirds. Curr. Biol. 24:910–916.

Moore, W., and J. A. Robertson. 2014. Explosive adaptive radiation and extreme phenotypic diversity within ant-nest beetles. Curr. Biol. 24:1–5.

Moyle, R. G., C. E. Filardi, C. E. Smith, and J. Diamond. 2009. Explosive Pleistocene diversification and hemispheric expansion of a "great speciator". Proc. Natl. Acad. Sci. U. S. A. 106:1863–1868.

Muchhala, N. 2003. Exploring the boundary between pollination syndromes: Bats and hummingbirds as pollinators of *Burmeistera cyclostigmata* and *B. tenuiflora* (Campanulaceae). Oecologia 134:373–380.

Muchhala, N. 2006. The pollination biology of *Burmeistera* (Campanulaceae): Specialization and syndromes. Am. J. Bot. 93:1081–1089.

Muchhala, N., and M. D. Potts. 2007. Character displacement among bat-pollinated flowers of the genus Burmeistera: Analysis of mechanism, process and pattern. Proc. R. Soc. B Biol. Sci. 274:2731–2737.

Mulch, A., C. E. Uba, M. R. Strecker, R. Schoenberg, and C. P. Chamberlain. 2010. Late Miocene climate variability and surface elevation in the central Andes. Earth Planet. Sci. Lett. 290:173–182. Elsevier B.V.

Myers, N., R. A. Mittermeier, C. G. Mittermeier, G. A. B. Fonseca, and J. Kent. 2000. Biodiversity hotspots for conservation priorities. Nature 403:853–858.

Pagel, M., and A. Meade. 2006. Bayesian analysis of correlated evolution of discrete characters by reversible-jump Markov chain Monte Carlo. Am. Nat. 167:808–825.

Peters, S. E. 2008. Environmental determinants of extinction selectivity in the fossil record. Nature 454:626–629.

Rabosky, D. L. 2014. Automatic detection of key innovations, rate shifts, and diversity-dependence on phylogenetic trees. PLoS One 9:e89543.

Rabosky, D. L., M. Grundler, C. Anderson, P. Title, J. J. Shi, J. W. Brown, H. Huang, and J. G. Larson. 2014. BAMMtools: An R package for the analysis of evolutionary dynamics on phylogenetic trees. Methods Ecol. Evol. 5:701–707.

Richardson, J. E., R. T. Pennington, T. D. Pennington, and P. M. Hollingsworth. 2001. Rapid diversification of a species-rich genus of neotropical rain forest trees. Science 293:2242–2245.

Salzburger, W., T. Mack, E. Verheyen, and A. Meyer. 2005. Out of Tanganyika: Genesis, explosive speciation, key-innovations and phylogeography of the haplochromine cichlid fishes. BMC Evol. Biol. 5:17.

Scherson, R. A., R. Vidal, and M. J. Sanderson. 2008. Phylogeny, biogeography, and rates of diversification of New World *Astragalus* (Leguminosae) with an emphasis on South American radiations. Am. J. Bot. 95:1030–1039.

Sedano, R. E., and K. J. Burns. 2010. Are the Northern Andes a species pump for Neotropical birds? Phylogenetics and biogeography of a clade of Neotropical tanagers (Aves: Thraupini). J. Biogeogr. 37:325–343.

Smith, B. T., J. E. McCormack, A. M. Cuervo, M. J. Hickerson, A. Aleixo, C. D. Cadena, J. Pérez-Emán, C. W. Burney, X. Xie, M. G. Harvey, B. C. Faircloth, T. C. Glenn, E. P. Derryberry, J. Prejean, S. Fields, and R. T. Brumfield. 2014. The drivers of tropical speciation. Nature 515:406–409.

Smith, S. A., and M. J. Donoghue. 2008. Rates of molecular evolution are linked to life history in flowering plants. Science 322:86–89.

Smith, S. A., and B. C. O'Meara. 2012. treePL: Divergence time estimation using penalized likelihood for large phylogenies. Bioinformatics 28:2689–2690.

Stamatakis, A. 2014. RAxML version 8: A tool for phylogenetic analysis and post-analysis of large phylogenies. Bioinformatics 30:1312–1313.

Valente, L. M., V. Savolainen, and P. Vargas. 2010. Unparalleled rates of species diversification in Europe. Proc. R. Soc. B Biol. Sci. 277:1489–1496.

Von Hagen, K. B., and J. W. Kadereit. 2001. The phylogeny of *Gentianella* (Gentianaceae) and its colonization of the southern hemisphere as revealed by nuclear and chloroplast DNA sequence variation. Org. Divers. Evol. 1:61–79.

Wagner, C. E., L. J. Harmon, and O. Seehausen. 2012. Ecological opportunity and sexual selection together predict adaptive radiation. Nature 487:366–369.

Weber, M. G., and A. A. Agrawal. 2014. Defense mutualisms enhance plant diversification. Proc. Natl. Acad. Sci. U. S. A. 111:16442–16447.

Willis, C. G., J. C. Hall, R. Rubio de Casas, T. Y. Wang, and K. Donohue. 2014. Diversification and the evolution of dispersal ability in the tribe Brassiceae (Brassicaceae). Ann. Bot. 114:1675–1686.

Zachos, J. C., G. R. Dickens, and R. E. Zeebe. 2008. An early Cenozoic perspective on greenhouse warming and carbon-cycle dynamics. Nature 451:279–83.

Chapter V:

The repeated evolution of vertebrate pollination syndromes in a recently diverged Andean plant clade

5.1 Abstract

Specialized biotic interactions, including those involving plants and their mutualistic pollinators, are often invoked to explain high species diversity. Pollination syndromes are inferred from suites of floral traits that are thought to be adaptive for the attraction and utilization of particular groups of pollinators. They are particularly useful for investigating biotic interactions at macroevolutionary scales, especially in large tropical groups where few large-scale pollination studies have been conducted. Here, we document the dynamic evolution of hummingbird and bat pollination syndromes in the centropogonids (Campanulaceae: Lobelioideae), an Andean-centered clade of ~550 angiosperm species whose rapid diversification was recently attributed to their association with vertebrate pollinators. Using phylogenetic principal components analysis, we demonstrate that flowers hypothesized to be adapted to pollination by hummingbirds and by bats, respectively, fall into separate regions of morphospace. This supports our use of pollination syndromes, which are further corroborated by ecological studies in this clade. We then document the repeated evolution of pollination syndromes: the centropogonids are ancestrally hummingbird pollinated, and bat pollination has evolved, on average, 14 times independently, with an average of nine reversions to hummingbird pollination. We further demonstrate a broad pattern of correlated evolution of key floral traits within these pollination syndromes. Finally, we detect no apparent difference in diversification rates between bird- and bat-pollinated lineages. These results collectively suggest that floral morphological diversity associated with pollination syndromes is very evolutionarily labile, likely as a result of selective pressures imposed by different pollinators. Moreover, they suggest that specialized pollination syndromes, such as hummingbird and bat pollination, are not evolutionary dead-ends. Instead, I hypothesize that

shifts between vertebrate pollinators have greatly facilitated the maintenance of an ancestrally high diversification rate among centropogonid species via speciation by floral isolation.

5.2 Introduction

The tropical Andes are home to more than 15% of all angiosperms species and encompass the world's most species-rich biodiversity hotspot. Specialized relationships with pollinators and shifts between different pollinator classes are a commonly invoked factor to explain this high level of biodiversity (Antonelli and Sanmartín 2011). The >550 species in the centropogonid clade of Neotropical bellflowers (Campanulaceae: Lobelioideae) are an ideal system to explore the effect of specialized pollination syndromes on Andean evolution (Fig. 5.1). This morphologically and ecologically diverse group, including the genera *Centropogon*, *Siphocampylus*, and *Burmeistera*, originated approximately five million years ago and is one of the fastest Andean radiations reported to date (Lagomarsino et al., in revision). Their exceptional diversification appears to have been driven by a complex interplay of both abiotic and biotic drivers, including Andean uplift, climate change, and biological traits facilitating plant-animal interactions (Lagomarsino et al, in revision). Among these factors, a relationship with vertebrate pollinators seems to be one of the most important drivers: lineages pollinated by vertebrates (i.e., hummingbirds or bats) have a net diversification rate that is six times higher than invertebrate pollinated lineages. This connects with a larger body of literature suggesting that specialized relationships and shifts between pollinators may stimulate diversification. For example, pollination by hummingbirds, which total more than 300 species, has been shown to be associated with increased rates of diversification in numerous plant lineages (Kay et al. 2005; Givnish et al. 2014; Tripp and McDade 2014). More broadly, there is some support for a link between specialized pollination and high species diversity, especially in the tropics (Eriksson and Bremer 1992; Hodges et al. 1995; Dodd et al. 1999; Vamosi and Vamosi 2011).

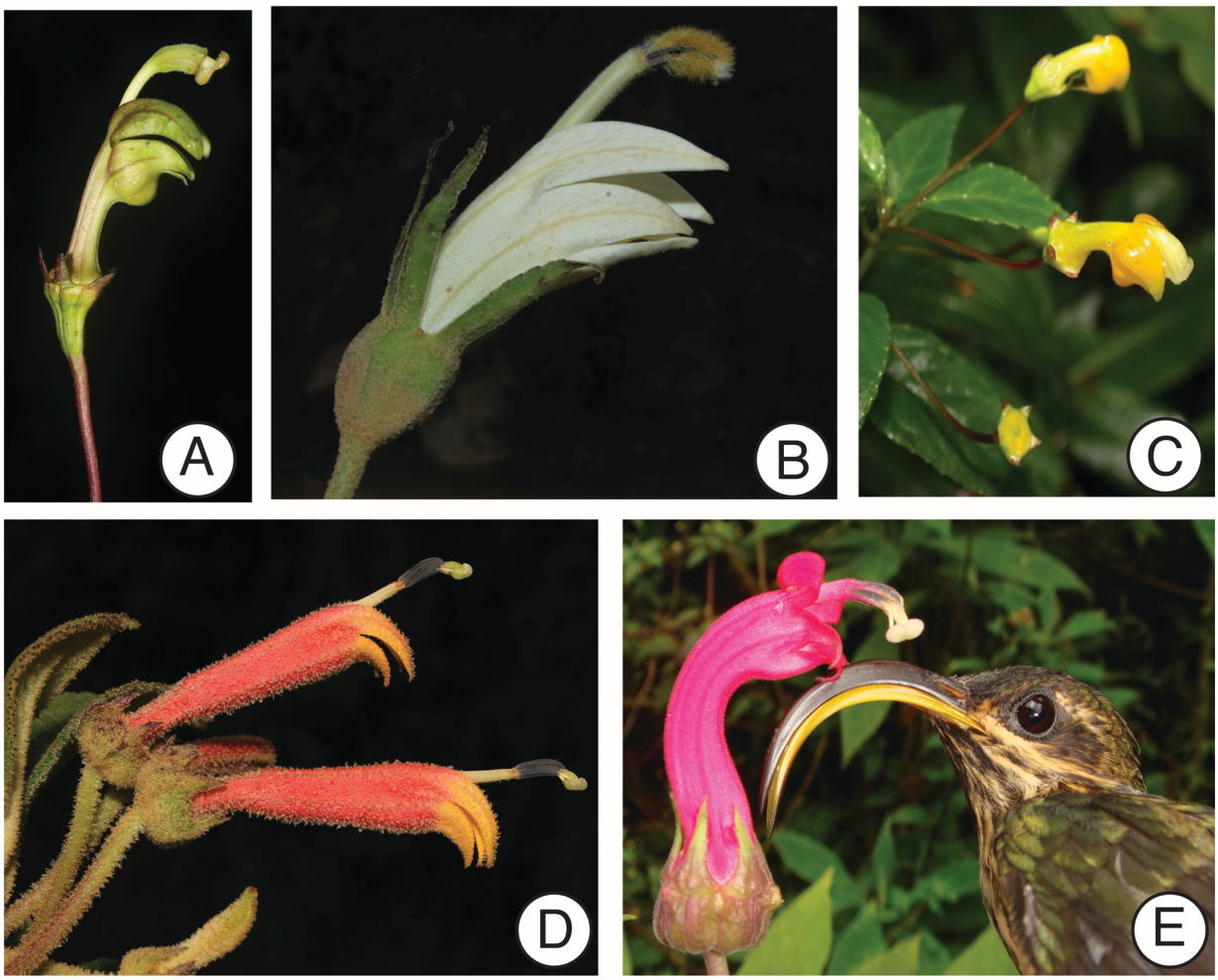


Figure 5.1. Flowers of species representing the various pollination syndromes present in the centropogonid clade. A) *Burmeistera cyclostigmata* Donn. Sm., a bat pollinated species. B) *Centropogon dombeyanus* E. Wimm., a bat pollinated species. C) *Burmeistera parviflora* E. Wimm. ex Standley, a putatively insect pollinated species. D) *Centropogon macbridei* Gleason, a straight-bill hummingbird pollinated species. E). *Centropogon umbrosus* E. Wimm., shown with *Eutoxeres condamini*, its sicklebill hummingbird pollinator. Photos A, B, and D by L. Lagomarsino, C by Barry Hammel, and E by Christopher Witt.

Such specialist pollination systems are often invoked as key factors underlying floral diversification in angiosperms (Darwin 1862; Grant and Grant 1965; Faegri and van der Pijl 1979; Fenster et al. 2004; Rosas-Guerrero et al. 2014). Pollination syndromes, or integrated suites of reproductive characters that match flowers to functional pollinator groups (Faegri and van der Pijl 1979; Fenster et al. 2004), are prima facie evidence of the importance of pollinators as agents of natural selection. An underlying assumption of the pollination syndrome concept is that each functional pollinator group (e.g., birds, bees, moths) exerts different selective pressures on plant species, leading to divergent floral morphologies in closely related plants with different pollinators and convergent floral morphology in distantly related plants that share pollinators (Fenster et al. 2004). The floral characters associated with a particular pollination syndrome ensure effective pollination visitation by the corresponding functional group, increasing the probability of successful reproduction for the plant. Studies have consistently shown that pollination syndromes can predict pollinator visitation accurately (Pauw 2006; Lázaro et al. 2008; Tripp and Manos 2008; Martén-Rodríguez et al. 2009; Danieli-Silva et al. 2012). Moreover, a recent global meta-analysis supported the pollination syndrome concept, and showed that the ability to predict effective pollinator by floral morphology is especially accurate in tropical regions, particularly in species that depend on pollination for reproduction (Rosas-Guerrero et al. 2014).

Despite this empirical support, the pollination syndrome concept is not without controversy. Some studies have found evidence against pollination syndromes (Ollerton 1996; Waser et al. 1996; Johnson and Steiner 2000), while others have found mixed evidence (Smith et al. 2008; Fenster et al. 2009). One of the most comprehensive studies of the pollination syndrome concept to date suggested that pollinators of only one-third of plant species can be

predicted via their pollination syndrome, and, further, that very few flowers fall into the traditional morphological definitions of the various pollination syndromes (Ollerton et al. 2009). A prominent argument against pollination syndromes are that they are overly simplistic given that many plant species are visited by more than one functional group of pollinators (Waser et al. 1996; Ollerton et al. 2009). However, this precludes the idea, first proposed by Stebbins (1970), that pollination syndromes reflect selection by the most frequent and effective pollinators; this does not exclude an important role for secondary pollinators (Muchhala 2003; Martén-Rodríguez et al. 2009; Rosas-Guerrero et al. 2014). It has also been argued that specialization to specific pollinators, as predicted by pollination syndromes, increases variance in reproductive success across years and thus should not be evolutionarily favored (Waser et al. 1996). Despite this ongoing discourse, pollination syndromes remain a powerful tool for ecological inference in the absence of empirical pollination studies (Rosas-Guerrero et al. 2014). This is especially true for investigating the macroevolutionary implications of plant-animal mutualisms at the phylogenetic and geographic scale of large groups, such as the centropogonid clade.

Shifts between different pollination syndromes are interesting evolutionary events that have happened frequently during angiosperm diversification and have resulted in widespread convergent evolution in distantly related species that share pollinator types. For example, the bird pollination syndrome, characterized by bright, often red floral pigmentation, long tubular corollas, and production of copious dilute, sucrose-rich nectar from well-protected nectaries, has evolved independently in at least sixty-five plant families (Cronk and Ojeda, 2008). This represents 1% of all angiosperm diversity (Waser and Ollerton, 2006) and includes groups as phylogenetically diverse as *Heliconia* (Stiles 1975; Temeles and Kress 2003), *Aquilegia* (Whittall and Hodges 2007), *Mimulus* (Schemske and Bradshaw 1999), and *Erythrina* (Bruneau

1997). While this broad evolutionary pattern underscores convergent selection pressures operating a deep phylogenetic scales, shifts between pollination syndromes also have an important role in microevolution: they can generate pre-zygotic reproductive isolation between sympatric plant populations, and thus have the potential to drive speciation (Ramsey et al. 2003; Muchhala 2006b; Waterman et al. 2011). Despite this, the effect of repeated, convergent shifts in pollination syndromes with respect to influence on species diversification has been seldom been investigated within narrowly focused plant clade.

Hummingbird and bat pollination are the two major syndromes present in the centropogonid clade, our focal group. Across angiosperms, hummingbird pollination is more common than bat pollination (Fleming and Muchhala 2008; Fleming et al. 2009): bats pollinate species in ~250 genera, as compared to the approximately 500 genera in which bird pollination occurs (Fleming et al. 2009). Together, the two classes of vertebrate pollinators are more costly to the plants than their insect pollinator counterparts: they are large, warm-blooded animals with high energetic demands that require large flowers that produce abundant sugar-rich nectar. However, they also provide distinct pollination benefits: vertebrate pollinators carry large pollen loads over long distances, are relatively long-lived, are generally faithful, and have a higher cognitive capacity than insects (Fleming and Muchhala 2008; Fleming et al. 2009). Thus, despite being more costly, there are many cases in which pollination by vertebrates would be selected for, especially in harsh habitats, such as tropical mountains

With the centropogonid clade, species exhibiting bat and hummingbird pollination syndromes share numerous characteristics, including: tubular corollas, abundant nectar production, a highly specific pollen deposition mechanism, and placement of flowers away from the body of the plant to facilitate hovering pollinators. However, they differ in many important

regards. Bat-pollinated species possess night-blooming, dully colored flowers (e.g., cream colored or green) with wide openings that generally produce a fetid odor and are placed away from the main body of the plant (Muchhala 2006b; Fleming et al. 2009) (Fig. 5.1A–B). These flowers attract nectar-feeding bats of the subfamily Glossophaginae (Phyllostomidae). These glossophagine bats have small body sizes (mean: 7g) and long tongues, tend to hover while feeding from flowers, and visit flowers for less than two seconds per visit (Fleming et al. 2009). In contrast, species displaying the hummingbird pollination syndrome have brightly colored, odorless flowers that are receptive during the day and have long, narrow corolla tubes (Fig. 5.1D–E). These flowers attract a diverse assemblage of hummingbirds (Colwell et al. 1974; Stein 1987; Muchhala and Thomson 2010), including myriad species with straight bills, as well as a specialized subclade of hermit hummingbirds with extremely curved bills— sicklebills in the genus *Eutoxeres* (Stein 1992). Concomitantly, the flowers visited by sicklebill hummingbirds are extremely curved, matching the bill morphology of their obligate pollinators (Stein 1987, 1992) (Fig. 5.1E).

The pollination biology of many centropogonid species has been documented. Pollination syndromes have been shown to reliably predict pollination in *Burmeistera* (Muchhala 2006b) and closely related *Centropogon* species (Muchhala and Thomson 2009): wide, green flowers are most effectively pollinated by bats, while narrow, pink-flowered species are exclusively pollinated by hummingbirds. These results are consistent in species in other genera in the centropogonid clade, including the bird-pollinated species in *Centropogon* subgenus *Eucentropogon* (the eucentropogonid clade *sensu* Lagomarsino et al. [2014]), *C. costaricae*, *C. talamancensis, C. valerioi,* and *S. sulfureus* (Colwell 1973; Colwell et al. 1974; Stein 1987, 1992; Fenster 1991; Sazima et al. 1994). The most important trait in determining effective

pollination by bats versus hummingbirds is the floral aperture width: hummingbird pollinated flowers have a narrow opening, while bat pollinated flowers are wider, facilitating entrance by hummingbird bills and bat snouts, respectively (Muchhala 2006b). While this trait is thought to be an adaptive tradeoff (Muchhala 2007), resulting in the loss of pollination services by one pollinator class by gaining those of the other (Muchhala 2006b), secondary pollination by hummingbirds in bat-pollinated flowers has been documented in a handful of species (e.g., *B. ceratocarpa*, *B. tenuiflora*) (Muchhala 2003, 2006b).

Here, I explore the evolution of pollination syndromes in this species-rich, Andean centered clade. I first use measurements of floral characters, principally derived from herbarium specimens, to test for the presence of pollination syndromes in the centropogonid clade using phylogenetic principal components analysis. I then reconstruct the evolutionary history of pollination syndromes, and many of their constituent characters, along a dated phylogeny of the centropogonid clade. Lastly, I use additional phylogenetic comparative methods to test for correlation between floral traits (as predicted by the pollination syndrome concept) and to determine whether or not these various characters are evolving under adaptive regimes that correspond to pollination syndromes. In this framework, I seek to find patterns of convergent evolution and determine the evolutionary lability of specialized relationships. This is the first study to document the history of pollination syndromes in the centropogonid clade, a very recent, rapid radiation, and is unique in its scale, which includes detailed floral measurements for over 150 species which represent diversity in over 550 closely-related species.

5.3 Materials and Methods

Phylogenetic relationships and floral trait characterization

Our study focuses on the centropogonid clade, which comprises the ~550 species of *Centropogon*, *Burmeistera*, and non-Caribbean *Siphocampylus* (Lagomarsino et al. 2014). The phylogeny of this clade was recently resolved with high support (Lagomarsino et al. 2014, Lagomarsino et al., in revision). Our taxon sampling, which includes 191 species, and phylogenetic methods follow Lagomarsino et al. (2014; in revision). Taxon sampling spans geographic and morphological diversity in the clade and includes representatives of all taxonomic groupings. Phylogenetic relationships were inferred simultaneously with divergence time estimates in BEAST v. 2 (Drummond and Rambaut 2007; Bouckaert et al. 2014) using seven plastid markers (together totaling 11,900 base pairs) and four calibration points for molecular dating as performed in Chapter 4. Upstream phylogenetic comparative analyses used either the maximum clade credibility (MCC) tree or a subset of 100 trees from the posterior distribution of trees, as appropriate.

Fifteen quantitative floral traits were measured from herbarium specimens deposited in the Harvard University Herbaria (herbarium codes: A, GH) or, when not available, from the JSTOR Plants database (http://plants.jstor.org/). Where possible, these specimens were the same as those used for constructing our molecular phylogeny. However, when this was not possible, either because flowers were not present or because no specimen was available, floral measurements were taken from a herbarium specimen of the same species. When material permitted, at least two flowers per specimen were measured, and their trait values were averaged. The traits measured included: corolla length, corolla width at various points, anther size, floral curvature, and ovary size; see Table C.1 for a full list of characters and Fig. C.1 for a visual depiction of many of these measurements. Many of these traits were combined into volume, area, or ratios to capture an integrative measure of floral form. These traits include volume of the

ovary, area of the anthers, and ratio of various measurements of corolla width (i.e., basal, midpoint, and apical measurements).

Flowers of each species were additionally classified by pollination syndrome based on their gross floral morphology (i.e., not using any one of the above qualitative traits as a determinant). Instead, we used traditional descriptions of pollination syndromes (Faegri and van der Pijl 1979), which are bolstered by recent studies of pollination ecology (Muchhala 2006b, 2007), to code this character. Three broad pollination syndromes were represented: bat (Fig. 5.1A–B), hummingbird (Fig. 5.1D–E), and bee (Fig. 5.1C). Furthermore, I recognized two subclasses of hummingbird pollination— pollination by straight-bill hummingbirds (Fig. 5.1D) and by sicklebill hummingbirds (Fig. 5.1E).

Phylogenetic comparative analyses

Ancestral state reconstruction

Ancestral states of pollination syndrome as a categorical trait were reconstructed using both Bayesian inference and maximum likelihood. First, a preliminary ancestral state reconstruction was performed using standard maximum likelihood methods using the equal rates ("ER") and all-rates-different ("ARD") models with the ace function in ape (Paradis et al. 2004). A likelihood-ratio test was subsequently performed to determine the optimal model. Ancestral character states were then estimated along the MCC tree from 1000 iterations of Bayesian stochastic character mapping under the optimal model using the make.simmap function in the phytools package. The Q transition matrix was fixed at the most likely values (i.e., the empirical Bayes method; Q = "empirical"). I then used the *rayDISC* function in the corHMM package of R (Beaulieu et al. 2015) to reconstruct ancestral states using maximum likelihood across 100 trees

from the BEAST posterior. Transitions between each state were counted for each tree and summed across the posterior to generate a mean and range of transitions, allowing for phylogenetic uncertainty. Reconstructed states of each quantitative floral trait were mapped onto the MCC tree using the *contMap* function in the phytools package (Revell 2013).

Validation of pollination syndrome concept using principal components analysis

I tested the validity of the pollination syndrome concept within the centropogonid clade by performing a phylogenetically-corrected principal components analysis (Felsenstein 1985). This analysis was performed in the phytools package of R (Revell 2012) using individual trait means for each species and the MCC tree. Scores from the first three principal components were then used as trait values in a set of comparative analyses described below to test for correlated evolution of traits and pollination syndromes. I hypothesized that the evolution of traits representing significant loadings on PC axes best captured pollination syndromes would similarly be identified in our OU model with adaptive peaks that correspond the pollination syndromes defined by gross morphology.

Identification of correlated character evolution

Identification of correlated evolution of binary traits was conducted using the Discrete function in BayesTraits v2 (Pagel and Meade 2006) in both an ML and Bayesian MCMC framework. Results from models allowing independent and dependent evolution were compared using log likelihood ratios and Bayes Factors. ML analyses used the MCC tree from the BEAST analysis, while the Bayesian analysis was conducted across 100 randomly selected trees from the BEAST posterior distribution.

Identification of correlated evolution of continuous traits was conducted in two ways. First, correlation was tested using the "Continuous" function in BayesTraits by comparing two models, one enforcing correlation and the other enforcing independent evolution ("TestCorrel" with co-variance set to 0). The harmonic means of likelihood values were compared using BayesFactors to determine significance. Pairwise comparisons of all continuous traits, the first four principal component axes, and elevation were conducted.

Phylogenetic generalized linear models (PGLM) were then conducted to determine correlation between floral traits and PC axes using an Orstein-Uhlenbeck (OU) model of trait of evolution. These were performed with a vcv matrix derived from the MCC tree using the function gls in the package nlme (Pinheiro et al. 2015).

Identification of evolutionary regimes associated with pollinator syndrome

I tested the hypothesis that quantitative floral characters evolve towards different evolutionary optima that are dependent on pollination syndrome (i.e., bat, straight-bill hummingbird, sicklebill hummingbird) by evaluating the likelihood of Brownian motion (BM) and various Orstein-Uhlenbeck (OU) models of trait evolution (Butler and King 2004; Beaulieu et al. 2012). I additionally explored the optima for the first four PC axes of the phylogenetic PCA and elevation as dependent on pollination syndrome. All such analyses of trait evolution were conducted using the *OUwie* function in the R statistical package OUwie (Beaulieu and O'Meara 2012) on a sample of 100 trees from a posterior distribution. These input trees had the most likely pollination syndrome reconstructions at the nodes from the *rayDisc* analysis (see above). Because there were two representatives, insect pollinated species were removed from these trees. I tested four models: BM, single-state OU (OU1), two-state OU (OU2), and three-state OU

(OU3). Both the BM and OU1 models imply that there is no relationship between the quantitative trait and pollination syndrome; BM suggests that the evolution of the trait follows a random walk, while stabilizing selection is acting in OU1. For the OU2 model, I collapsed the subclasses of hummingbirds (straight-bill and sicklebill); this model implies that bat and hummingbird pollination syndrome have different trait optima, but there is no difference within subclasses of hummingbird pollination. Finally, the OU3 model infers three separate trait optima for each of the pollination syndromes. Model fit was assessed via AICc.

Trait-dependent species diversification

I modeled the impact of bat versus hummingbird pollination on species diversification rate by concurrently estimating their impact on speciation, extinction, and transition rates using Binary State-Speciation and Extinction (BiSSE, Maddison *et al.* 2007). For this analysis, I combined the two subclasses of hummingbirds (straight-bill and sicklebill) into a single character state; species hypothesized to be bee pollinated were removed from this analysis. I evaluated eight BiSSE diversification models of increasing complexity in which speciation, extinction, and transition rates were allowed to either vary or remain equal between traits (Table 5.1). Analyses were performed using the R package *diversitree* 0.7-6 (FitzJohn 2012). Once the best-fitting model was selected, CIs for each parameter were estimated for the tree. I used an exponential prior following FitzJohn (2012), and began the MCMC with the ML estimates. I ran MCMC for 20,000 generations and applied a burn-in of 2000 steps. I then computed the net diversification rates for each trait based on the combined speciation and extinction rate estimates.

I did not implement a multi-state speciation-extinction model (MuSSE; FitzJohn 2012 because the distribution of our data makes this model inappropriate (Rabosky and Goldberg

2015): sicklebill pollination in the centropogonid clade arose once and defines the majority of a clade, and there are only two putatively bee-pollinated species. Statistical power would be lacking for both of these character states to identify any realistic difference in diversification dynamics for these pollination syndromes (Maddison and FitzJohn 2015).

Table 5.1. Model comparison for the BiSSE analyses for bat and hummingbird taxa, with mean parameter estimates for each model. The best-fitting model is determined via a combination of the lowest corrected Aikake Information Criterion (AICc), a ΔAIC with 2 units of difference with other models, and likelihood ratio tests (LRT) in case where ΔAIC values are close between models. The best model is in red and bold text.

Model	NP	LogL	AICc	ΔAIC	λ_0	λ_1	μ_0	μ_1	q_{01}	q_{10}	Results
Null model ($\lambda_0=\lambda_1$; $\mu_0=\mu_1$; $q_{01}=q_{10}$)	3	-311.69	629.50	2.80	2.13	2.13	1.21	1.21	0.14	0.14	Best model indicates that bat and hummingbird pollinated taxa do not differ in diversification rate, but transitions from hummingbird to bat pollination are more common than the reverse
$\lambda_0\neq\lambda_1$; $\mu_0=\mu_1$; $q_{01}=q_{10}$	4	-311.02	630.26	3.56	1.98	2.20	1.20	1.20	0.15	0.15	
$\lambda_0=\lambda_1$; $\mu_0\neq\mu_1$; $q_{01}=q_{10}$	4	-311.23	630.68	3.98	2.13	2.13	1.34	1.13	0.15	0.15	
$\lambda_0=\lambda_1$; $\mu_0=\mu_1$; $q_{01}\neq q_{10}$	4	-309.25	626.71	0	2.12	2.12	1.20	1.20	0.30	0.05	
$\lambda_0\neq\lambda_1$; $\mu_0\neq\mu_1$; $q_{01}=q_{10}$	5	-310.90	632.13	5.42	1.89	2.26	1.09	1.28	1.28	1.28	
$\lambda_0\neq\lambda_1$; $\mu_0=\mu_1$; $q_{01}\neq q_{10}$	5	-309.04	628.41	1.71	2.01	2.13	1.12	1.12	0.29	0.06	
$\lambda_0=\lambda_1$; $\mu_0\neq\mu_1$; $q_{01}\neq q_{10}$	5	-309.20	628.72	2.02	2.12	2.12	1.19	1.20	0.31	0.05	
$\lambda_0\neq\lambda_1$; $\mu_0\neq\mu_1$; $q_{01}\neq q_{10}$	6	-307.75	627.96	1.25	1.51	2.56	0.35	1.71	0.43	0.04	

5.4 Results

Phylogenetic relationships and floral trait characterization

The concatenated Bayesian phylogenetic analysis using the best-fitting partitioning scheme yielded a highly resolved and strongly supported tree consistent with our ML tree and previously published results (Lagomarsino *et al.* 2014, Lagomarsino et al., in revision). Sequence

divergence, particularly in the centropogonid clade, was low as reflected by the shallow branching pattern toward the tips. Despite short internal branches, indicative of a recent radiation, the phylogeny is well supported: 66% of nodes are recovered with high support (PP>0.90). Our results support the monophyly of the subfamilies Campanuloideae and Lobelioideae and the Neotropical bellflowers (the centropogonids, *Lysipomia*, and Chilean lobelias) with maximum nodal support (PP=1). Phylogenetic results can be found in Fig. B.1.

Floral data collected from herbarium specimens are presented in Table C.1 and will be deposited on Dryad following peer-reviewed publication. The average value for each trait within their putative pollination syndrome is presented in Table 5.2. In total, quantitative measurements were made from 153 species; I was not able to access floral material for the additional 38 species in our centropogonid phylogeny. These taxa were not included in the phylogenetic comparative analyses that relied on quantitative data (i.e., phylogenetic PCA, OU modeling).

Table 5.2. Average values for each quantitative floral trait used in comparative analyses for all species within a pollination syndrome. L= length, values in mm; A= area, values in mm^2; Vol= volume, values in mm^3. Straight bill and sicklebill refer to two subclasses of hummingbirds.

	Ratio—bot:mid	Ratio—mid:top	Ratio—top:bot	Peduncule (L)	Corolla (L)	Corolla tube (L)	Ovary (Vol)	Anther (A)	Curvature (ratio)
Bat	0.561138138	0.8565888	0.4766247	50.574375	41.8888	31.220375	330.11	17.5957	0.9956957
Straight bill	1.409766381	0.5898722	0.7442066	92.8963636	36.9957	19.31209091	1116.9	46.7034	0.9996607
Sicklebill	0.920282521	0.4868263	0.4405152	23.5520833	37.5313	25.47708333	268.86	19.8766	0.902376

Phylogenetic comparative analyses

Validation of pollination syndrome concept using principal components analysis

The first three principal component (PC) axes described 66.5% of the variance in floral traits across species (Fig. 5.2, Table 5.3). The majority of the variation captured by the first PC axis reflected size: length of the peduncle, corolla, corolla tube and stamen, ovary volume and anther size (Table 5.3). There was no clear association between PC1 and pollination syndrome (Fig. 5.2). PC2 captured both size and shape variation and largely separate species according to pollination syndromes (Fig. 5.2). This PC axis' loadings include: ratio of the bottom to the middle of the corolla (i.e., presence of basal corolla constriction), ratio of bottom to top of the corolla (i.e., a distal inflation of the corolla), corolla tube length, and anther area (Table 5.3). PC3 further separated out the sicklebill hummingbird pollinated species (Fig. 5.2). The primary loadings for this PC were corolla curvature and the ratio of the widths at the middle and top of the corolla (i.e. distal inflation of the corolla) (Table 5.3). Overall, our phylogenetic PCA placed species with different pollination syndromes in distinct areas of morphospace. The average PC values for all species within each pollination syndrome is presented in Table 5.4.

Table 5.3. Loadings of each trait for the first three PC axes from a phylogenetic principal components analysis of floral morphology. The most important traits for each PC axes (>0.5) are indicated in bold text.

Trait	PC1 (30.67%)	PC2 (21.87%)	PC3 (13.99%)	PC4 (11.26%)
Corolla curvature	0.03941919	-0.02629041	**0.5627869**	0.2698498
Bottom: middle corolla width	-0.09009557	**-0.75166222**	-0.333315708	-0.4463787
Middle: top corolla width	-0.09009557	0.21038589	**0.876473191**	-0.2103165
Bottom: top corolla width	-0.06978117	**-0.6811523**	0.390677002	**-0.5830456**
Penduncle length	**0.62334715**	-0.43088735	0.182895582	0.3198812
Corolla length	**0.85286744**	0.2745321	-0.042310847	-0.2043441
Corolla tube length	**0.65125302**	**0.56233139**	-0.004615718	-0.2846248
Ovary volume	**0.69292014**	-0.41631094	-0.024961422	0.2508576
Anther area	**0.71800268**	**-0.50972054**	0.086725801	0.1996154
Stamen length	**0.712296**	0.32115021	-0.084692854	-0.3772649

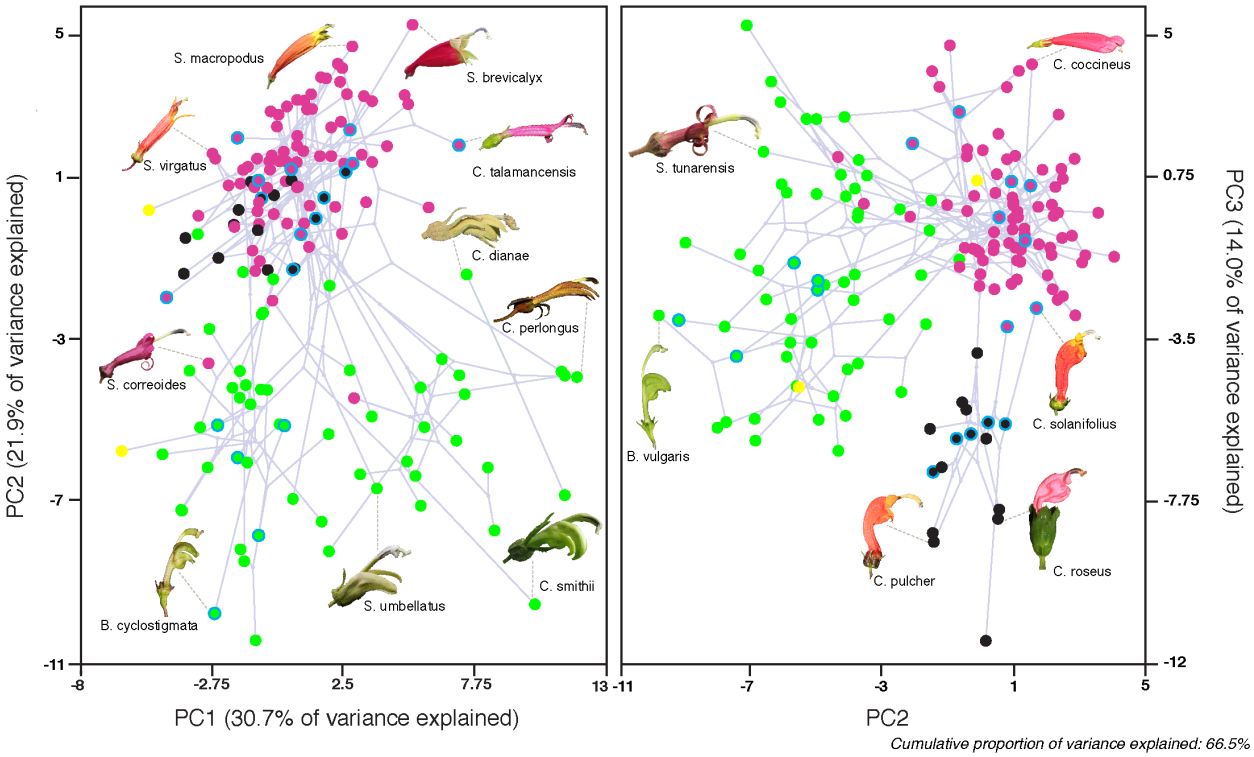


Figure 5.2. Phylogenetic principal components analysis of floral morphology. Scores of the first three principal component axes of floral morphology in 153 species of the centropogonid based on a phylogenetic PCA. Pollination syndrome is indicated by color (green, bat; pink, straight-bill hummingbird; black, sicklebill hummingbird; yellow, bee). Blue circles around the individual point indicate a species whose pollination biology has been studied in the field; pollination syndrome for the remaining species was deducted by gross morphology. MCC topology depicted in light gray lines connecting individual points. Flowers of some of the species are included to show the diversity depicted along the axes. The loadings for the PC axes are provided in Table 5.3. All photos by L. Lagomarsino.

Table 5.4. Average PC values for all species within each pollination syndrome for the first four PC axes from the phylogenetic principal components analysis of floral morphology.

	PC1	PC2	PC3	PC4
Bat	0.169853612	1.501226784	0.300655521	0.152737342
Hummingbird	1.295621187	-5.351052794	-1.338363256	0.319726191
Sicklebill	-1.465407998	-0.024342294	-6.425287144	-1.157330995

Ancestral state reconstruction

Bayesian stochastic character mapping demonstrated that the ancestral pollination syndrome in the centropogonid clade is straight-bill hummingbird (PP=100) (Fig. 5.3). These results were corroborated by maximum likelihood character state reconstruction (Fig. C.2). Further, taking phylogenetic uncertainty into account, I find that evolution of pollination syndrome has been dynamic within the centropogonid clade (Fig. 5.3, Table 5.5): bat pollination has evolved from straight bill hummingbird pollination an average of 13.67 times (range: 5–19), and the reverse, the evolution of straight bill hummingbird pollination from bat-pollinated ancestors, occurred an average of 9.41 times (range: 4–18). Pollination by sicklebills evolved once from straight-bill hummingbird pollinated ancestors, and an average of 2.13 reversions to straight bill pollination occurred from that state (range: 2–4). There were no transitions involving both bat and sicklebill pollination syndromes.

Table 5.5. Number of transitions between pollination syndromes in the centropogonid clade. Values calculated from ancestral state reconstructions on a random subset of 100 trees from the BEAST posterior distribution, performed using an "ARD" model with the rayDISC function in the corHMM package.

Ancestor	Descendant	Mean	Median	Range
Hummingbird	Bat	13.67	14	5–19
Hummingbird	Sicklebill	1	1	1–1
Bat	Hummingbird	9.41	9	4–18
Bat	Sicklebill	0	0	0–0
Sicklebill	Hummingbird	2.13	2	2–4
Sicklebill	Bat	0	0	0–0

.

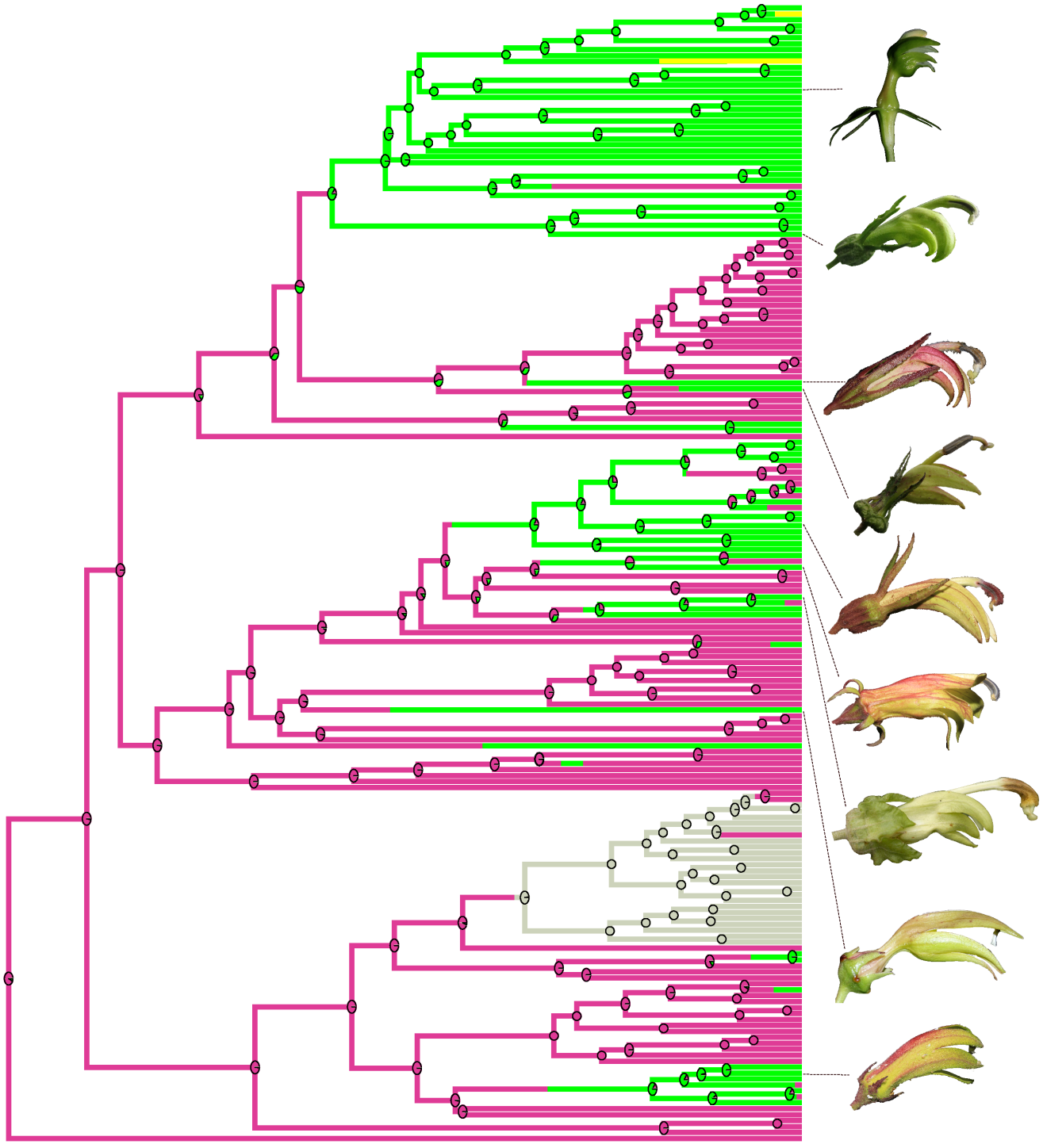


Figure 5.3. Bayesian stochastic character mapping of pollination syndrome evolution.

Figure 5.3 (Continued). Bayesian stochastic character mapping of pollination syndrome evolution. Pie charts at nodes along the MCC chronogram of the centropogonid clade represent ancestral states that were calculated as the marginal posterior probability of bat pollination (green), straight bill hummingbird pollination (pink), and sicklebill hummingbird pollination (grey). Lines connect the phylogenetic terminal and photos (at right) of flowers of species that conform to the bat pollination syndrome, from top to bottom: *Burmeistera tenuiflora* Donn. Sm., *Centropogon smithii* E. Wimm., *Siphocampylus jelskii* Zahlbr., *S. matthiaei* A. DC., *C. viriduliflrous* E. Wimm., *S. rusbyanus* Britton, *S. tunicatus* Zahlbr., *S. smilax* Lammers, and *S. actinothrix* E. Wimm. According to the reconstruction presented, these nine species represent eight independent origins of bat pollination, and they nicely illustrate the repeated evolution of gross morphology while also demonstrating that the end result of this convergent evolution is not identical flowers. Results from a maximum likelihood reconstruction are supplied in Fig. C.2.

Identification of correlated character evolution

The evolution of many quantitative floral traits was found to be significantly correlated with pollination syndrome via phylogenetic generalized linear models and in a Bayesian framework in BayesTraits (Table 5.6, C.2). I find that anther size is correlated with the most traits (two floral width ratios [$p<0.001$, BF=3.82; $p<0.001$, BF=6.3], peduncle length [$p<0.001$, BF=23.96], corolla length [$p<0.001$, BF=8.68], corolla tube length [$p=0.0036$, BF=1.46), and ovary volume [$p<0.001$, BF=30.51]). Within these correlations for anther size, the R^2 value varies from 0.04855 (corolla tube length) to 0.356 (peduncle length). The exception to this general trend of correlated floral trait evolution was floral curvature, which I find is not correlated with a single trait; this is not surprising because the majority of curved flowers are in a single clade (which corresponds to the origin of sicklebill pollination, Fig. 5.3). However, floral curvature was significantly correlated with the PC3 and PC4, which discriminate the sicklebill-pollinated species from the rest of the hummingbird pollinated species. Excluding floral curvature, 19 of the 28 floral traits are significantly correlated, while the remaining nine were not. Total results can be found in Table 5.6, C.2.

Identification of evolutionary regimes in pollination syndrome

Ornstein–Uhlenbeck models of trait evolution were a significantly better fit than simple BM models to all floral traits except corolla curvature (Table 5.7). Fitting our hypothesis of the joint evolution of floral traits and pollination syndrome, OU2 and OU3 models provided the best-fit most often (4/9 traits for both). The OU2 model, in which sicklebill and straight-bill hummingbird pollination were collapsed into a single character state, was the best fit model for the following four characters: ratio of the bottom to top corolla width, corolla length, ovary volume, and anther area (Table 7).

Table 5.6. Correlation between quantitative floral characters from phylogenetic generalized linear model and BayesTraits. R^2 values and their associated p-values from *pgls* in nmls R package implementing a variance-covariance matrix developed from the MCC phylogeny. Significant correlations (P < 0.5) are denoted by bold text. Astericks indicate support for character correlation from BayesTraits. *, positive evidence (BF >2); **, strong evidence (BF 5–10); ***, very strong evidence (BF >10) (see Table C.2).

	Bottom: middle corolla width	Middle: top corolla width	Bottom: top corolla width	Peduncle length	Corolla length	Corolla tube length	Ovary volume	Anther area	Corolla curvature	PC1	PC2	PC3
Middle: top corolla width												
Adjusted R-squared	0.08738											
p-value	**).0001225***											
Bottom: top corolla width												
Adjusted R-squared	0.2205	0.3094										
p-value	**<0.001***	**<0.001***										
Peduncle length												
Adjusted R-squared	-0.005746	0.0188	0.05779									
p-value	0.7173	**0.04973**	**0.001607**									
Corolla length												
Adjusted R-squared	-0.005221	-0.005663	0.01145	0.2476								
p-value	0.6471*	0.7047*	0.0987	**<0.001***								
Corolla tube length												
Adjusted R-squared	0.007958	0.03417	0.01223	0.1095	0.495							
p-value	0.1384*	**0.01259****	0.09164*	**<0.001*****	**<0.001*****							
Ovary volume												
Adjusted R-squared	0.01016	-0.006614	0.02827	0.4662	0.3094	0.1053						
p-value	0.1117	0.9723*	**0.0212**	**<0.001*****	**<0.001*****	**<0.001*****						
Anther area												
Adjusted R-squared	0.09217	0.01117	0.2688	0.356	0.1607	0.04855	0.3302					
p-value	**<0.001*****	0.1013	**<0.001*****	**<0.001*****	**<0.001*****	**0.003582***	**<0.001*****					
Corolla curvature												
Adjusted R-squared	0.01227	0.007164	-0.006427	-0.006172	-0.005471	-0.004166	-0.006536	-0.003954				
p-value	0.0913	0.1497*	0.8642	0.7952	0.6781	0.5442	0.9096	0.5274				
PC1												
Adjusted R-squared	0.00263	-0.006276	0.03278	0.5191	0.7652	0.4651	0.5587	0.4566	-0.006223			
p-value	0.2385	0.82	**0.01423**	**<0.001*****	**<0.001*****	**<0.001*****	**<0.001*****	**<0.001*****	0.8068			
PC2												
Adjusted R-squared	0.3915	-0.001142	0.4723	0.2321	-0.006447	0.04854	0.2149	0.4889	-0.006454	0.04521		
p-value	**<0.001*****	0.3647	**<0.001*****	**<0.001*****	**<0.001****	**0.003586*****	**<0.001*****	**<0.001*****	0.8739	**0.004794**		
PC3												
Adjusted R-squared	0.06991	0.7944	0.3618	0.1048	-0.001156	0.04175	0.01149	0.09391	0.2094	0.01025	0.05601	
p-value	**<0.001*****	**<0.001*****	**<0.001*****	**<0.001*****	0.3653	**0.006481***	0.09827	**<0.001**	**<0.001*****	**0.001875**	**0.001875**	
PC4												
Adjusted R-squared	0.2534	0.05024	0.303	0.07841	0.05911	0.09394	0.03525	-0.005267	0.07649	0.006122	-0.006468	-0.006
p-value	**<0.001*****	**0.003094****	**<0.001*****	**<0.001*****	**.001432****	**<0.001*****	**0.01145***	0.6525	**<0.001****	0.8791	0.8791	0.7603

The OU3 model, which modeled separate trait optima for each of the pollination syndromes (i.e., bat, straight bill hummingbird, and sicklebill), was the best fit model for the following four characters: ratio of the bottom to middle corolla width, ratio of the middle to top corolla width, peduncle length, and corolla tube length (Table 5.7). The BM model was the best fitting model for a single floral trait: corolla curvature.

Additionally, I found that three of the four PC axes that I explored were also fit best by an OU3 model (PC2–4). This is consistent with the results of our phylogenetic PCA: these are the axes that best separated species according to their pollination syndrome (Fig. 5.2). Conversely, PC1, which largely captured size variation, was best modeled in an OU1 framework, suggesting a global optimum for overall floral size across the centropogonid clade, but not within pollination syndromes. Again, this is consistent with our phylogenetic PCA: the first PC axis did not separate species on the basis of pollination syndrome. In this way, OU analyses of our PC axes further validated the presence of pollination syndromes in the centropogonid clade.

Trait-dependent diversification

The best-fitting model for the BiSSE analysis demonstrates that there is no difference in speciation or extinction rate between hummingbird and bat pollinated lineages in the centropogonid clade. This suggests that neither hummingbird and bat pollination syndromes, alone, have driven the rapid rate of diversification characterizes the centropogonid clade, even though vertebrate pollination as a whole seems to explain this phenomenon. However, I see that the transition rates are unequal between the two broad pollination syndromes: transitions rates from hummingbird to bat pollination are approximately 5.6 times higher than transition rates from bat to hummingbird pollination (0.305 vs. 0.0543; Table 5.1). These results corroborate the ancestral state reconstructions of pollination syndrome (Table 5.5).

Table 5.7. Mean corrected Akaike information criterion (AICc) weights representing the relative likelihood of each fitted model of trait evolution. Values were calculated after fitting models to maximum likelihood reconstructions of pollination syndrome on 100 trees. The number of trees supporting each model (i.e., the highest weight for each tree) is presented in parentheses. Bold values indicate the best-fit models for each trait. (BM= Brownian motion; OU= Ornstein-Uhlenbeck model)

Trait	BM	OU1	OU2	OU3
Bottom: middle corolla width	0 (0)	0 (0)	0 (0)	**1 (100)**
Middle: top corolla width	0 (0)	0 (0)	0 (0)	**1 (100)**
Bottom: top corolla width	0 (0)	0 (0)	**0.72 (100)**	0.28 (0)
Peduncle length	0 (0)	0 (0)	0.02 (0)	**0.98 (100)**
Corolla length	0 (0)	0.02 (0)	**0.55 (97)**	0.43 (3)
Corolla tube length	0 (0)	0 (0)	0.14 (0)	**0.86 (100)**
Ovary volume	0 (0)	0.03 (0)	**0.71 (100)**	0.27 (0)
Anther area	0 (0)	0 (0)	**0.62 (99)**	0.38 (1)
Corolla curvature	**0.66 (100)**	0.23 (0)	0.08 (0)	0.03 (0)
PC1	0 (0)	**0.47 (76)**	0.28 (0)	0.25 (24)
PC2	0 (0)	0 (0)	0.06 (1)	**0.94 (99)**
PC3	0 (0)	0 (0)	0(0)	**1 (100)**
PC4	0 (0)	0.26 (21)	0.13 (0)	**0.61 (79)**

5.5 Discussion

Our study provides strong support for the classical bat and hummingbird pollination syndromes in the centropogonid clade. This was demonstrated by the high degree of correlation between floral traits and hypothesized pollinators using phylogenetic PCA. Leveraging these results, I further demonstrate that pollinator-mediated selection has likely played a key role in the evolution of floral diversity in the clade. The degree of lability in pollination syndrome that I document underlies a striking pattern of convergence in floral morphology between closely

related species that comprise a rapid radiation. Our results are consistent with the relatively small, but growing body literature of field-based pollination biology that supports pollination syndromes in the centropogonid clade and further suggests that speciation is driven, or at least reinforced, via floral isolation (Muchhala 2006b, 2008; Muchhala and Potts 2007) . Despite a very dynamic history of pollination syndrome evolution, I demonstrate that there is no significant difference in diversification rate between bat and hummingbird pollinated lineages. Here, I hypothesize that the rapid diversification rates attributed to vertebrate pollination in the centropogonid clade may be maintained by frequent shifts between pollination syndromes.

Support for pollination syndromes in the centropogonid clade

Pollination syndromes are a convenient measure by which to predict effective pollinator visitation, but the concept has received both praise (Fenster et al. 2004; Martén-Rodríguez et al. 2009; Rosas-Guerrero et al. 2014) and criticism (Waser et al. 1996; Smith et al. 2008; Ollerton et al. 2009). Our study provides key support for the pollination syndrome concept within the centropogonid clade via a phylogenetic PCA of floral traits. Here, I demonstrate that species are morphologically well defined within their hypothesized pollination syndromes. These results are consistent with recent studies that have confirmed the predictive capability of pollination syndromes in diverse taxa (Temeles 2000; Martén-Rodríguez et al. 2009; Rosas-Guerrero et al. 2014) and are further bolstered by empirical and field-based pollination studies within the clade (Muchhala 2006b). Furthermore, the syndromes I explored (i.e., bat and hummingbird) have wide support in the literature; of these, the hummingbird pollination syndrome has the most empirical support and is widely accepted (Kay and Schemske 2003; Castellanos et al. 2004; Whittall and Hodges 2007; Martén-Rodríguez et al. 2009).

While pollination syndromes are useful in inferring the primary pollinator of a plant (Stebbins 1970), many studies have shown that floral morphologies conforming to a pollination syndrome do not necessarily prevent pollinators from other guilds from providing pollination services. In fact, visits from such secondary pollinators may be important in the survival of rare species or those whose primary pollinator visits infrequently. I was unable to test the importance of secondary pollinators in our study, although they have been shown to be important to many plant species, both within centropogonid clade (Sazima et al. 1994; Muchhala 2003) and in distantly related taxa (Sanmartin-Gajardo and Sazima 2005; Martén-Rodríguez et al. 2009, 2010; Muchhala et al. 2009). The incomplete separation of bat and bird flowers in morphospace in our phylogenetic PCA may represent morphologies that can be effectively pollinated by both hummingbirds and bats. Species that fall into this region of morphospace are likely key to understanding the relationship between floral morphology and pollinators in the centropogonid clade, and efforts should be made to document theses species' pollination biology in the field.

Further, some pollination syndromes (e.g., butterfly, carrion fly) remain understudied relative to others (e.g., bird, bee). Our delimitation of possible pollination syndromes matches traditional descriptions (Faegri and van der Pijl 1979), as well as the known ecology of the centropogonid clade. However, I cannot completely exclude pollination by non-vertebrates with similar pollination syndromes. The two most similar pollination syndromes involve Lepidoptera: hawkmoth and butterfly flowers have overlapping similarities with bat and hummingbird flowers, respectively (Faegri and van der Pijl 1979). Hawkmoth pollination is likely not important in the flowers I examined; while bat and hawkmoth flowers share light color, strong odor (though it is fetid in bat flowers, not sweet as in hawkmoth flowers), and nocturnal anthesis, the wide corolla opening and lack of a long, narrow nectar spur in centropogonid bat-pollinated

flowers would render pollination by hawkmoths improbable. This has been confirmed in the field: hawkmoth pollination is not effective in *Burmeistera* species because they do not make contact with reproductive parts when visiting flowers (Muchhala 2006a). On the other hand, butterfly visitation has never been documented in the centropogonid clade. While the traditional pollination syndromes for hummingbird and butterflies flowers overlap (including tubular, brightly colored flowers), butterfly flowers have a series of common traits that distinguish them from hummingbird flowers: a distinct rim/landing pad for perching (resulting in funnel or trumpet-shaped flowers, e.g., *Phlox*), flowers that are often grouped into heads (e.g., *Lantana camara*), a sweet odor (Andersson et al. 2002), and the frequent presence of a nectar guide (Faegri and van der Pijl 1979; Andersson et al. 2002). Further, flowers pollinated by butterflies are generally smaller than the hummingbird pollinated flowers in the centropogonid clade, including a much narrower opening that cannot accommodate the full width of a hummingbird bill (Cruden and Hermann-Parker 1979).

Bee pollination is suspected to have evolved at least twice very recently in the centropogonid clade (Muchhala 2006b; Garzón Venegas et al. 2012; Lagomarsino et al. 2014). Our sampling included two such species (*B. parviflora* and *B.* aff. *minutiflora)*, which fall outside of the morphospace of other pollination syndromes, particularly in PC1 (Fig. 5.2, yellow circles). The evolution of this syndrome is very recent (<0.5 Ma) and pollination biology of these species remain to be studied in detail.

Widespread convergence: Lability and bidirectionality in pollination syndrome evolution

Pollination syndrome evolution has been extraordinarily labile in the centropogonid clade: as inferred via ancestral state reconstructions, transitions from hummingbird to bat

pollination and the reverse have both happened numerous times in the clade's history, resulting in average of 26 estimated pollinator shifts. Transitions from hummingbird to bat pollination are most frequent, consistent with evidence suggesting that the bulk of bat-pollinated flowers in the Neotropics evolved from hummingbird-pollinated ancestors (Sanmartin-Gajardo and Sazima 2005; Perret et al. 2007; Tripp and Manos 2008; Fleming et al. 2009; Martén-Rodríguez et al. 2009). However, transitions from bat to hummingbird pollination are frequent: they have occured ca. 9 times (mean= 9, range= 4–18; Table 5.5). Impressively, I have documented more transitions away from bat pollination than in any previous taxon-specific study (Tripp and Manos 2008; Martén-Rodríguez et al. 2009). Further, multiple transitions from sicklebill to straight-bill hummingbird pollination are inferred. The pollinator lability in the centropogonid clade may be related to the intense nature of biological interactions in the tropics, and reflect the heterogeneous environment of the Andes. It may further be facilitated by the relatively minor floral morphological changes needed to make a large ecological impact (Schemske and Bradshaw 1999; Whittall and Hodges 2007; Rausher 2008), especially given that the syndromes share many key characteristics, including tubular corolla, abundant, sucrose-rich nectar production, and generally large, robust stature. The maintenance of specific morphological traits following pollinator shifts despite otherwise rapid morphological evolution is indicative of intense pollinator-mediated selection acting on a deep evolutionary scale (Davis et al. 2014).

Our results suggest that ecological specialization is not an evolutionary dead end, even when that specialization is obligate (i.e., sicklebill pollination). Instead, adaptation to local ecological contexts may drive the evolution of traits that are associated with relationships that change across a landscape. These changes are likely to be abiotic (i.e., temperature, relief),

supporting an interaction of multiple ecological and historical factors in driving diversification, as documented recently in the centropogonid clade (Lagomarsino et al., in revision).

Correlated trait evolution in pollination syndromes elucidates patterns of pollinator-mediated selection

Our results further illuminated the traits that are most important in discriminating flowers that are adapted to pollination by hummingbirds versus those pollinated by bats. The second PC axis of our phylogenetic PCA most effectively separated hummingbird-pollinated taxa from bat-pollinated taxa (Fig. 5.2). The significant PC loadings for this axis represent a series of traits that most strongly separate the bat versus hummingbird pollination syndrome: a basal corolla constriction, distal corolla inflation, corolla tube length, and anther size. Here, I find that bat flowers tend to have inflated corolla openings, large anthers, and short corolla tubes, while hummingbird flowers have basal corolla constrictions, small anthers, and longer corolla tubes (Table 5.2). The third PC axis further separates flowers adapted to a subset of hummingbirds, the sicklebills. These flowers have a curved corolla and an inflated corolla opening (Table 5.2), both characters that morphologically match their specialized pollinator. Results from analyses of the pattern of trait evolution (i.e., OU model testing, pglm, and BayesTraits) further revealed a global pattern of correlated trait evolution. The best-fit OU models suggested that all floral traits except curvature evolve under selective regimes corresponding to pollination syndrome (i.e., OU2 or OU3 models). All traits identified by the phylogenetic PCA and OU analyses have putative adaptive significance and are discussed below.

The width of the corolla opening is a key aspect of both the bat and hummingbird pollination syndromes. Inflated, wide corolla openings are a landmark character of bat

pollination (Martén-Rodríguez et al. 2009), while hummingbird visitation is most effective in flowers with narrow corolla openings (Temeles et al. 2002). Our results confirm the importance of the degree of inflation of the corolla opening across the centropogonid clade: it is a key trait for distinguishing bat-pollinated flowers from hummingbird-pollinated flowers (Table 5.3). I further demonstrate that its evolution is best fit by an OU3 model, with flowers pollinated by bats, straightbill hummingbirds, and sicklebills each having distinct optimal values. The degree of inflation is most extreme in bat-pollinated flowers, followed by sicklebill-pollinated flowers, while it is minimal across straight-bill hummingbird pollinated flowers (Table 5.2). Wide corolla openings match the shape of bat snouts (e.g., Fig. 1 from Muchhala 2006b), and have been empirically shown to be the most important character in determining effective bat pollination to the exclusion of hummingbird pollination within the centropogonid clade (Muchhala 2006b). This characteristic may additionally function in echolocation (Martén-Rodríguez et al. 2009). Sicklebill pollinated flowers share inflated corolla openings with bat flowers. Here, they facilitate the idiosyncratic pollination style of sicklebills, which insert their entire face into the flower while perching on the vegetative body of the plant (Stein 1987, 1992). In contrast, the very narrow corolla apertures that characterize straightbill hummingbird pollinated species facilitate effective pollination not only in the centropogonid clade (Muchhala 2006b), but generally (Temeles et al. 2002): within mechanical constraints, hummingbirds are most precise and most likely to come into contact with reproductive parts of flowers with narrower openings (Temeles et al. 2002; Muchhala 2006b). The difference in corolla inflation between the bat and straightbill hummingbird pollination syndromes is thought to be an adaptive tradeoff via pollinator mismatch that favors specialization to either hummingbirds or bats in the centropogonid clade (Muchhala 2006b). Despite this, some centropogonid species have evolved

a floral morphology with a flexible corolla opening that can be narrow or wide depending on the pressure the pollinator places on flowers during pollination; this ensures efficient pollination by both pollinator guilds (Sazima et al. 1994).

The width of the corolla opening is not the only aspect of corolla morphology that I find to be important in discriminating pollination syndromes in the centropogonid clade: hummingbird pollinated flowers tend to have a basal corolla constriction, which is lacking in bat pollinated flowers (Table 5.2). This trait was also found to be best fit by an OU3 model, with straightbill hummingbirds having the most extreme corolla constrictions and bat flowers generally lacking one. In Antillean Gesneriaceae, such a basal corolla constriction was found to promote effective hummingbird pollination by flowers otherwise demonstrating the bat pollination syndrome in generalist flowers (Martén-Rodríguez et al. 2009, 2010). It is also thought to facilitate hummingbird pollination in *Heliconia* (Wolf and Stiles 1989) and *Drymonia* (Clark et al. 2015). This morphology is hypothesized to perform the dual role of guiding the hummingbird's bill into the flower and protecting against mechanical damage to the ovary during pollination (Cronk and Ojeda 2008). Such damage is likely reduced in bat-pollinated flowers not by corolla shape *per se*, but via the production of longer peduncles. This allows floral display away from the body of the plant, reducing physical damage by these pollinators whose large body size apply significant force on the plant during floral visits. Peduncles of bat-pollinated flowers are likely also thicker; this trait was not measured across species, but thicker peduncles are known to be important in reducing mechanical damage during bat visitation (Muchhala 2006b).

I also identify that bat-pollinated flowers produce larger anthers (and by extension, more pollen) than hummingbird-pollinated flowers (Table 5.2), consistent with their respective

syndromes. Anther size is best fit by an OU2, suggesting that flowers adapted to both subclasses of hummingbirds (straightbill and sicklebill) share an evolutionary optimum that differs from bat-pollinated flowers. This result is consistent with our knowledge of pollination in the centropogonid clade. It has been experimentally shown that bats can hold incrementally more pollen in their fur, thus linearly increasing male-fitness of the plant with linear increases in pollen production. Hummingbird feathers, on the other hand, can only hold modest amounts of pollen and there is no increase in male-fitness to the plant with increased pollen production (Muchhala and Thomson 2010). This is further exacerbated by the different animals' grooming habits: hummingbirds frequently remove excess pollen from their face and bill, when possible, whereas bats do not frequently groom. Anther size may be related to another trait that I find is best fit by an OU2 model: ovary size. Hummingbird pollinated plants tend to have significantly smaller ovaries (i.e., fruit precursors) than bat pollinated plants. This is potentially explained by the lower amount of pollen that is transported by hummingbirds, which selects for fewer seeds per fruit, ultimately resulting in smaller ovaries with fewer ovules. However, it may also be related to fruit type (i.e., berry or capsule): a higher proportion of bat-pollinated species produce berries (associated with larger ovaries than capsules) as compared to hummingbird pollinated species. This fruit type is generally selected for in densely forested understories, where abiotic seed dispersal is ineffective (Smith 2001; Givnish et al. 2005; Givnish 2010; Lagomarsino et al. 2014).

Finally, I find that centropogonid species that are pollinated by hummingbirds tend to have longer corolla tubes than bat-pollinated species (Table 5.2). This is likely a result of the long bills of many hummingbird species that visit centropogonids, though it is important to note that hummingbirds have a large degree in variation in bill length (Temeles et al. 2002). The

corolla length of a particular species, whether or not its bat or bird pollinated, is likely a product of its local pollinator pool (Stiles 1981). The morphological relationship between plants and pollinators, however, can be complex in species-rich communities with a high degree of interspecies interaction, such as the Andean cloud forests where centropogonids thrive, as opposed to insular environments, such as Caribbean islands (Temeles et al. 2002). Long corolla tubes are not an exclusive trait of hummingbird-pollinated flowers: some bat flowers are very long, especially in *Centropogon nigricans*, whose ca. 10 cm long flower is a result of extreme specialization with the nectar bat *Anoura fistulata* (Muchhala 2006a; Muchhala and Thomson 2009). This evolutionary arms race effect, with ecological specialization leading to extreme morphology for both plant and pollinator, is well documented within hummingbird pollination as well (Abrahamczyk et al. 2014). Within the centropogonid clade, extreme specialization within hummingbird pollination is most apparent in those species with abruptly curved flowers that are adapted to sicklebill pollination (Stein 1992). I find that two floral traits are associated with this obligate relationship: a dilated corolla opening and extreme floral curvature (Table 5.3). The floral curvature, as predicted, matches the morphology of their obligate pollinators, while the inflated opening facilitates effective pollination by allowing the sicklebill to place its head inside of the flower during visitation.

I have documented that a few key traits underlie shifts between pollination syndromes, which have been frequent in the evolutionary history of the centropogonids. This combination makes the group ideal for future studies examining the genetic and genomic changes necessary for transitions between vertebrate pollination syndromes. Though many of the floral characters I identified likely have complex genetic underpinnings, there may be relatively few genomic regions that control morphological shifts from bat to bird pollination, as suggested in the

Antillean Gesneriaceae (Alexandre et al. 2015). Future work will seek to determine if evolution of pollination syndrome follows predictable developmental and genomic changes.

The effect of vertebrate pollination syndromes on Andean diversification

Despite the frequency of shifts between bat and hummingbird pollination in the centropogonid clade, I find that there is no difference in species diversification rate (i.e., neither speciation nor extinction rate). This is true even though there is strong evidence that vertebrate pollination, as a whole, is associated with significantly increased diversification rates in the Neotropical bellflowers (Lagomarsino et al, in revision). I argue that shifts between pollination syndromes within this actively diversifying clade may contribute substantially to its overall high rates of diversification, and that the species-richness in this clade may not have been nearly as high if it were exclusively pollinated by only one pollinator guild. The overall high diversification rates concomitant with frequent pollinator shifts may be explained by speciation via floral isolation, in which prezygotic reproductive isolation is achieved via an interplay of floral morphology and pollinator behavior (Fulton and Hodges 1999; Muchhala 2003; Schiestl and Schlüter 2009). In support of this, many centropogonid species have sympatric distributions that appear to have been facilitated by either pollinator shifts (Muchhala 2006b) or character partitioning of floral traits within a pollination syndrome, allowing closely related species to share pollinators (Muchhala and Potts 2007). The frequent shifts between hummingbird and bat pollinators (Fig. 5.3, Table 5.3) and morphological lability within a syndrome (Fig. 5.2) may facilitate the very high speciation rates in the centropogonid clade.

Shifts between specialist pollination syndromes and relationships with vertebrate pollinators may partially explain the high species diversity of the Andes. The evolutionary

histories of many other species-rich clades that characterize the Neotropics, and Andean cloud forests in particular, that are characterized by shifts between pollinators including hummingbirds and bats supports this assertion, and suggests that the pattern I have identified here may apply more broadly. Such groups include Gesneriaceae (Sanmartin-Gajardo and Sazima 2005; Perret et al. 2007; Martén-Rodríguez et al. 2009), Acanthaceae (Tripp and Manos 2008; Tripp 2010), Solanaceae (Knapp 2010 but see Smith et al. 2008), passionflowers (Abrahamczyk et al. 2014), and bromeliads (Sazima et al. 1999). Echoing a common sentiment, I stress that the pollination biology of many plant groups remains understudied, particularly in the tropics. More and better studies of pollination ecology will continue to improve macroevolutionary studies of floral evolution in a pollination context. I emphasize the need for focused pollination work in the montane wet tropics.

5.6 Acknowledgements

I would like to thank members of the Davis Lab for helpful feedback and commentary on this chapter and Nathan Muchhala for helpful discussions about the floral morphology and pollination biology of Neotropical bellflowers. The directors and curators at the following herbaria provided important access to their collections: BOLV, CR, GB, GH, INB, LPB, MO, MOL, NY, PMA, SCZ, SMF, and USZ. Funding was provided by a National Science Foundation Doctoral Dissertation Improvement Grant DEB-1210401 to L.P.L. and C.C.D. and from the Department of Organismic and Evolutionary Biology, the Botanical Society of America, the American Society of Plant Taxonomists, the Arnold Arboretum's Deland Award, the Explorer's Club, and the Rockefeller Center for Latin American Studies to L.P.L.

5.7. References

Abrahamczyk, S., D. Souto-Vilarós, and S. S. Renner. 2014. Escape from extreme specialization: Passionflowers, bats and the sword-billed hummingbird. Proc. R. Soc. B Biol. Sci. 281:20140888.

Alexandre, H., J. Vrignaud, B. Mangin, and S. Joly. 2015. Genetic architecture of pollination syndrome transition between hummingbird-specialist and generalist species in the genus *Rhytidophyllum* (Gesneriaceae). PeerJ 3:e1028.

Andersson, S., L. a a Nilsson, I. Groth, and G. Bergström. 2002. Floral scents in butterfly-pollinated plants: Possible convergence in chemical composition. Bot. J. Linn. Soc. 140:129–153.

Antonelli, A., and I. Sanmartín. 2011. Why are there so many plant species in the Neotropics? Taxon 60:403–414.

Beaulieu, J. M., D. C. Jhwueng, C. Boettiger, and B. C. O'Meara. 2012. Modeling stabilizing selection: Expanding the Ornstein-Uhlenbeck model of adaptive evolution. Evolution (N. Y). 66:2369–2383.

Beaulieu, J., J. C. Oliver, and B. C. O'Meara. 2015. corHMM. R package.

Bouckaert, R., J. Heled, D. Kühnert, T. Vaughan, C. H. Wu, D. Xie, M. a. Suchard, A. Rambaut, and A. J. Drummond. 2014. BEAST 2: A software platform for Bayesian evolutionary analysis. PLoS Comput. Biol. 10:1–6.

Bruneau, A. 1997. Evolution and homology of bird pollination syndromes in *Erythrina*. Am. J. Bot. 84:54–71.

Butler, M. A., and A. A. King. 2004. Phylogenetic compartive analysis: A modeling approach for adaptive evolution. Am. Nat. 164:683–695.

Castellanos, M. C., P. Wilson, and J. D. Thomson. 2004. "Anti-bee" and "pro-bird" changes during the evolution of hummingbird pollination in Penstemon flowers. J. Evol. Biol. 17:876–85.

Clark, J. L., L. Clavijo, and N. Muchhala. 2015. Convergence of anti-bee pollination mechanisms in the Neotropical plant genus Drymonia (Gesneriaceae). Evol. Ecol. 29:355–377. Springer International Publishing.

Colwell, R. K. 1973. Competition and coexistence in a simple tropical community. Am. Nat. 107:737–760.

Colwell, R. K., B. J. Betts, P. Bunnell, F. L. Carpenter, and P. Feinsinger. 1974. Competition for the nectar of *Centropogon valerii* by the hummingbird *Colibri thalassinus* and the flower-piercer *Diglossa plumbea*, and its evolutionary implications. Condor 76:447–452.

Cronk, Q., and I. Ojeda. 2008. Bird-pollinated flowers in an evolutionary and molecular context. J. Exp. Bot. 59:715–27.

Cruden, R., and S. M. Hermann-Parker. 1979. Butterfly pollination of Caesalpinia pulcherrima, with observations on a psychophilous syndrome. J. Ecol. 67:155–168.

Danieli-Silva, A., J. M. T. de Souza, A. J. Donatti, R. P. Campos, J. Vicente-Silva, L. Freitas, and I. G. Varassin. 2012. Do pollination syndromes cause modularity and predict interactions in a pollination network in tropical high-altitude grasslands? Oikos 121:35–43.

Darwin, C. D. 1862. On the various contrivances by which British and foreign orchids are fertilised by insects, and on the good effects of intercrossing. John Murray, London.

Davis, C. C., H. Schaefer, Z. Xi, D. a Baum, M. J. Donoghue, and L. J. Harmon. 2014. Long-term morphological stasis maintained by a plant-pollinator mutualism. Proc. Natl. Acad. Sci. U. S. A. 111:5914–9.

Dodd, M. E., J. Silvertown, and M. W. Chase. 1999. Phylogenetic analysis of trait evolution and species diversity variation among angiosperm families. Evolution (N. Y).

Drummond, A. J., and A. Rambaut. 2007. BEAST: Bayesian evolutionary analysis by sampling trees. BMC Evol. Biol. 7:214.

Eriksson, O., and B. Bremer. 1992. Pollination systems, dispersal modes, life forms, and diversification rates in angiosperm families. Evolution (N. Y). 46:258–266.

Faegri, K., and L. van der Pijl. 1979. The Principles of Pollination Ecology. 3rd ed. Oxford: Pergamon Press.

Felsenstein, J. 1985. Phylogenies and the comparative methods. Am. Nat. 125:1–15.

Fenster, C. B. 1991. Selection on Floral Morphology by Hummingbirds. Biotropica 23:98–101.

Fenster, C. B., W. S. Armbruster, P. Wilson, M. R. Dudash, and J. D. Thomson. 2004. Pollination Syndromes and Floral Specialization. Annu. Rev. Ecol. Evol. Syst. 35:375–403.

Fenster, C. B., S. Martén-Rodriguez, and D. W. Schemske. 2009. Pollination syndromes and the evolution of floral diversity in Iochroma (Solanaceae). Evolution 63:2758–62; discussion 2763–7.

FitzJohn, R. G. 2012. Diversitree: Comparative phylogenetic analyses of diversification in R. Methods Ecol. Evol. 3:1084–1092.

Fleming, T. H., C. Geiselman, and W. J. Kress. 2009. The evolution of bat pollination: A phylogenetic perspective. Ann. Bot. 104:1017–1043.

Fleming, T. H., and N. Muchhala. 2008. Nectar-feeding bird and bat niches in two worlds: Pantropical comparisons of vertebrate pollination systems. J. Biogeogr. 35:764–780.

Fulton, M., and S. A. Hodges. 1999. Floral isolation between Aquilegia formosa and Aquilegia pubescens. Proc. R. Soc. B Biol. Sci. 266:2247–2252.

Garzón Venegas, J., F. González, and J. M. Vélez Puerta. 2012. *Burmeistera minutiflora* (Campanulaceae-Lobelioideae), a new species from the high Andes of Antioquia (Colombia) with the smallest flowers in the genus. An. del Jardín Botánico Madrid 69:243–246.

Givnish, T. J. 2010. Ecology of plant speciation. Taxon 59:1326–1366.

Givnish, T. J., M. H. J. Barfuss, B. Van Ee, R. Riina, K. Schulte, R. Horres, P. a Gonsiska, R. S. Jabaily, D. M. Crayn, J. A. C. Smith, K. Winter, G. K. Brown, T. M. Evans, B. K. Holst, H. Luther, W. Till, G. Zizka, P. E. Berry, and K. J. Sytsma. 2014. Adaptive radiation, correlated and contingent evolution, and net species diversification in Bromeliaceae. Mol. Phylogenet. Evol. 71:55–78.

Givnish, T. J., J. C. Pires, S. W. Graham, M. a McPherson, L. M. Prince, T. B. Patterson, H. S. Rai, E. H. Roalson, T. M. Evans, W. J. Hahn, K. C. Millam, A. W. Meerow, M. Molvray, P. J. Kores, H. E. O'Brien, J. C. Hall, W. J. Kress, and K. J. Sytsma. 2005. Repeated evolution of net venation and fleshy fruits among monocots in shaded habitats confirms a priori predictions: Evidence from an ndhF phylogeny. Proc. R. Soc. B Biol. Sci. 272:1481–1490.

Grant, V., and K. A. Grant. 1965. Flower pollination in the Phlox family. Columbia University Press, New York.

Hodges, S. a., M. L. Arnold, P. B. Sciences, and N. Dec. 1995. Spurring Plant Diversification: Are Floral Nectar Spurs a Key Innovation? Proc. R. Soc. B Biol. Sci. 262:343–348.

Kay, K. M., P. A. Reeves, R. G. Olmstead, and D. W. Schemske. 2005. Rapid speciation and the evolution of hummingbird pollination in Neotropical *Costus* subgenus *Costus* (Costaceae): Evidence from nrDNA ITS and ETS sequences. Am. J. Bot. 92:1899–1910.

Kay, K. M., and D. W. Schemske. 2003. Pollinator Assemblages and Visitation Rates for 11 Species of Neotropical Costus (Costaceae). Biotropica 35:198–207.

Knapp, S. 2010. On “various contrivances”: pollination, phylogeny and flower form in the Solanaceae. Philos. Trans. R. Soc. Lond. B. Biol. Sci. 365:449–60.

Lagomarsino, L. P., A. Antonelli, N. Muchhala, A. Timmermann, S. Mathews, and C. C. Davis. 2014. Phylogeny, classification, and fruit evolution of the species-rich Neotropical bellflowers (Campanulaceae: Lobelioideae). Am. J. Bot. 101:2097–2112.

Lázaro, A., S. J. Hegland, and Ø. Totland. 2008. The relationships between floral traits and specificity of pollination systems in three Scandinavian plant communities. Oecologia 157:249–257.

Maddison, W. P., and R. G. FitzJohn. 2015. The unsolved challenge to phylogenetic correlation tests for categorical characters. Syst. Biol. 64:127–136.

Maddison, W. P., P. E. Midford, and S. P. Otto. 2007. Estimating a binary character’s effect on speciation and extinction. Syst. Biol. 56:701–710.

Martén-Rodríguez, S., A. Almarales-Castro, and C. B. Fenster. 2009. Evaluation of pollination syndromes in Antillean Gesneriaceae: Evidence for bat, hummingbird and generalized flowers. J. Ecol. 97:348–359.

Martén-Rodríguez, S., C. B. Fenster, I. Agnarsson, L. E. Skog, E. A. Zimmer, and S. Marte. 2010. Evolutionary breakdown of pollination specialization in a Caribbean plant radiation. New Phytol. 188:403–417.

Muchhala, N. 2007. Adaptive Trade-Off in Floral Morphology Mediates Specialization for Flowers Pollinated by Bats and Hummingbirds. Am. Nat. 169:494–504.

Muchhala, N. 2003. Exploring the boundary between pollination syndromes: Bats and hummingbirds as pollinators of *Burmeistera cyclostigmata* and *B. tenuiflora* (Campanulaceae). Oecologia 134:373–380.

Muchhala, N. 2008. Functional significance of interspecific variation in Burmeistera flower morphology: Evidence from nectar bat captures in Ecuador. Biotropica 40:332–337.

Muchhala, N. 2006a. Nectar bat stows huge tongue in its rib cage. Nature 444:701–2.

Muchhala, N. 2006b. The pollination biology of *Burmeistera* (Campanulaceae): Specialization and syndromes. Am. J. Bot. 93:1081–1089.

Muchhala, N., A. Caiza, J. C. Vizuete, and J. D. Thomson. 2009. A generalized pollination system in the tropics: bats, birds and Aphelandra acanthus. Ann. Bot. 103:1481–1487.

Muchhala, N., and M. D. Potts. 2007. Character displacement among bat-pollinated flowers of the genus Burmeistera: Analysis of mechanism, process and pattern. Proc. R. Soc. B Biol. Sci. 274:2731–2737.

Muchhala, N., and J. D. Thomson. 2010. Fur versus feathers: Pollen delivery by bats and hummingbirds and consequences for pollen production. Am. Nat. 175:717–726.

Muchhala, N., and J. D. Thomson. 2009. Going to great lengths: Selection for long corolla tubes in an extremely specialized bat-flower mutualism. Proc. R. Soc. B Biol. Sci. 276:2147–2152.

Ollerton, J., R. Alarcón, N. M. Waser, M. V Price, S. Watts, L. Cranmer, A. Hingston, C. I. Peter, and J. Rotenberry. 2009. A global test of the pollination syndrome hypothesis. Ann. Bot. 103:1471–80.

Pagel, M., and A. Meade. 2006. Bayesian analysis of correlated evolution of discrete characters by reversible-jump Markov chain Monte Carlo. Am. Nat. 167:808–825.

Paradis, E., J. Claude, and K. Strimmer. 2004. APE: Analyses of Phylogenetics and Evolution in R language. Bioinformatics 20:289–290.

Pauw, A. 2006. Floral syndromes accurately predict pollination by a specialized oil-collecting bee (Rediviva peringueyi, Melittidae) in a guild of South Afican orchids (Coryciinae). Am. J. Bot. 93:917–926.

Perret, M., A. Chautems, R. Spichiger, T. G. Barraclough, and V. Savolainen. 2007. The geographical pattern of speciation and floral diversification in the neotropics: the tribe Sinningieae (Gesneriaceae) as a case study. Evolution (N. Y). 61:1641–60.

Pinheiro, J., D. Bates, S. DebRob, D. Sarkar, E. Authors, and R-core. 2015. nlme. R package.

Rabosky, D. L., and E. E. Goldberg. 2015. Model inadequacy and mistaken inferences of trait-dependent speciation. Syst. Biol. 64:340–355.

Ramsey, J., H. D. Bradshaw, and D. W. Schemske. 2003. Components of reproductive isolation between the monkeyflowers Mimulus lewisii and M. cardinalis (Phyrmaceae). Evolution (N. Y). 57:1520–1534.

Rausher, M. D. 2008. Evolutionary Transitions in Floral Color. Int. J. Plant Sci. 169:7–21.

Revell, L. J. 2012. phytools: an R package for phylogenetic comparative biology (and other things). Methods Ecol. Evol. 3:217–223.

Revell, L. J. 2013. Two new graphical methods for mapping trait evolution on phylogenies. Methods Ecol. Evol. 4:754–759.

Rosas-Guerrero, V., R. Aguilar, S. Martén-Rodríguez, L. Ashworth, M. Lopezaraiza-Mikel, J. M. Bastida, and M. Quesada. 2014. A quantitative review of pollination syndromes: do floral traits predict effective pollinators? Ecol. Lett. 17:388–400.

Sanmartin-Gajardo, I., and M. Sazima. 2005. Chiropterophily in Sinningieae (Gesneriaceae): Sinningia brasiliensis and Paliavana prasinata are bat-pollinated, but P. sericiflora is not. Not yet? Ann. Bot. 95:1097–1103.

Sazima, M., S. Buzato, and I. Sazima. 1999. Bat-pollinated flower assemblages and bat visitors at two Atlantic Forest sites in Brazil. Ann. Bot. 83:705–712.

Sazima, M., I. Sazima, and S. Buzato. 1994. Nectar by day and night: Siphocampylus sulfureus (Lobeliaceae) pollinated by hummingbirds and bats. Plant Syst. Evol. 191:237–246.

Schemske, D. W., and H. D. Bradshaw. 1999. Pollinator preference and the evolution of floral traits in monkeyflowers (Mimulus). Proc. Natl. Acad. Sci. 96:11910–11915.

Schiestl, F. P., and P. M. Schlüter. 2009. Floral isolation, specialized pollination, and pollinator behavior in orchids. Annu. Rev. Entomol. 54:425–446.

Smith, J. F. 2001. High species diversity in fleshy-fruited tropical understory plants. Am. Nat. 157:646–653.

Smith, S. D., C. Ané, and D. A. Baum. 2008. The role of pollinator shifts in the floral diversification of *Iochroma* (Solanaceae). Evolution (N. Y). 62:793–806.

Stebbins, G. L. 1970. Adaptive radiation of reproductive characteristics in angiosperms, I: Pollination mechanisms. Annu. Rev. Ecol. Syst. 1:307–326.

Stein, B. A. 1992. Sicklebill hummingbirds, ants, and flowers: Plant-animal interactions and evolutionary relationships in Andean Lobeliaceae. Bioscience 42:27–33.

Stein, B. A. 1987. Systematics and evolution of Centropogon subgenus Centropogon (Campanulaceae-Lobelioideae). Washington University.

Stiles, F. G. 1975. Ecology, flowering phenology, and hummingbird pollination of some Costa Rican Heliconia species. Ecology 56:285–301.

Stiles, F. G. 1981. Geographical aspects of bird-flower coevolution, with particular reference to Central American. Ann. Missouri Bot. Gard. 68:323–351.

Temeles, E. J. 2000. Evidence for Ecological Causation of Sexual Dimorphism in a Hummingbird. Science (80-.). 289:441–443.

Temeles, E. J., and W. J. Kress. 2003. Adaptation in a plant-hummingbird association. Science 300:630–3.

Temeles, E. J., Y. B. Linhart, M. Masonjones, and H. D. Masonjones. 2002. The Role of Flower Width in Hummingbird Bill Length – Flower. Biotropica 34:68–80.

Tripp, E. A. 2010. Taxonomic Revision of Ruellia Section Chiropterophila (Acanthaceae): a Lineage of Rare and Endemic Species from Mexico. Syst. Bot. 35:629–661.

Tripp, E. A., and P. S. Manos. 2008. Is floral specialization an evolutionary dead-end? Pollination system transitions in Ruellia (Acanthaceae). Evolution 62:1712–37.

Tripp, E. A., and L. A. Mcdade. 2014. Time-Calibrated Phylogenies of Hummingbirds and Hummingbird-Pollinated Plants Reject a Hypothesis of Diffuse Co-Evolution. 31.

Vamosi, J. C., and S. M. Vamosi. 2011. Factors influencing diversification in angiosperms: at the crossroads of intrinsic and extrinsic traits. Am. J. Bot. 98:460–71.

Waser, N. M., L. Chittka, M. V Price, N. M. Williams, and J. Ollerton. 1996. Generalization in pollination systems, and why it matters. Ecology 77:1043–1060.

Waterman, R. J., M. I. Bidartondo, J. Stofberg, J. K. Combs, G. Gebauer, V. Savolainen, T. G. Barraclough, and A. Pauw. 2011. The effects of above- and belowground mutualisms on orchid speciation and coexistence. Am. Nat. 177:E54–68.

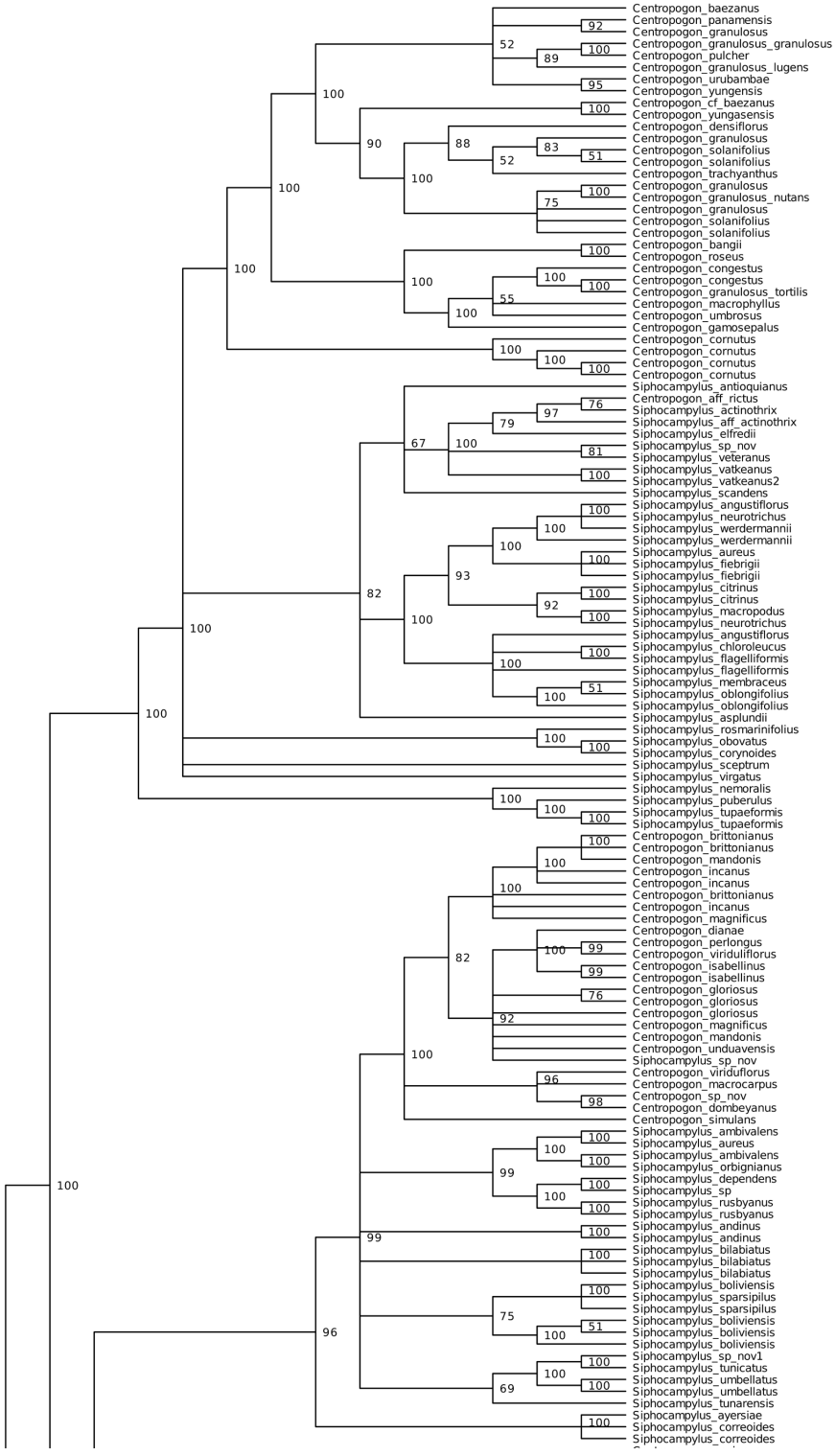
Whittall, J. B., and S. A. Hodges. 2007. Pollinator shifts drive increasingly long nectar spurs in columbine flowers. 447:1–6.

Wolf, L. L., and F. G. Stiles. 1989. Adaptation for the “fail-safe” pollination of specialized ornithophilous flowers. Am. Nat. 121:1–10.

Appendix A:

Supporting material for Chapter I

Figure A.1 (Continued on next page).



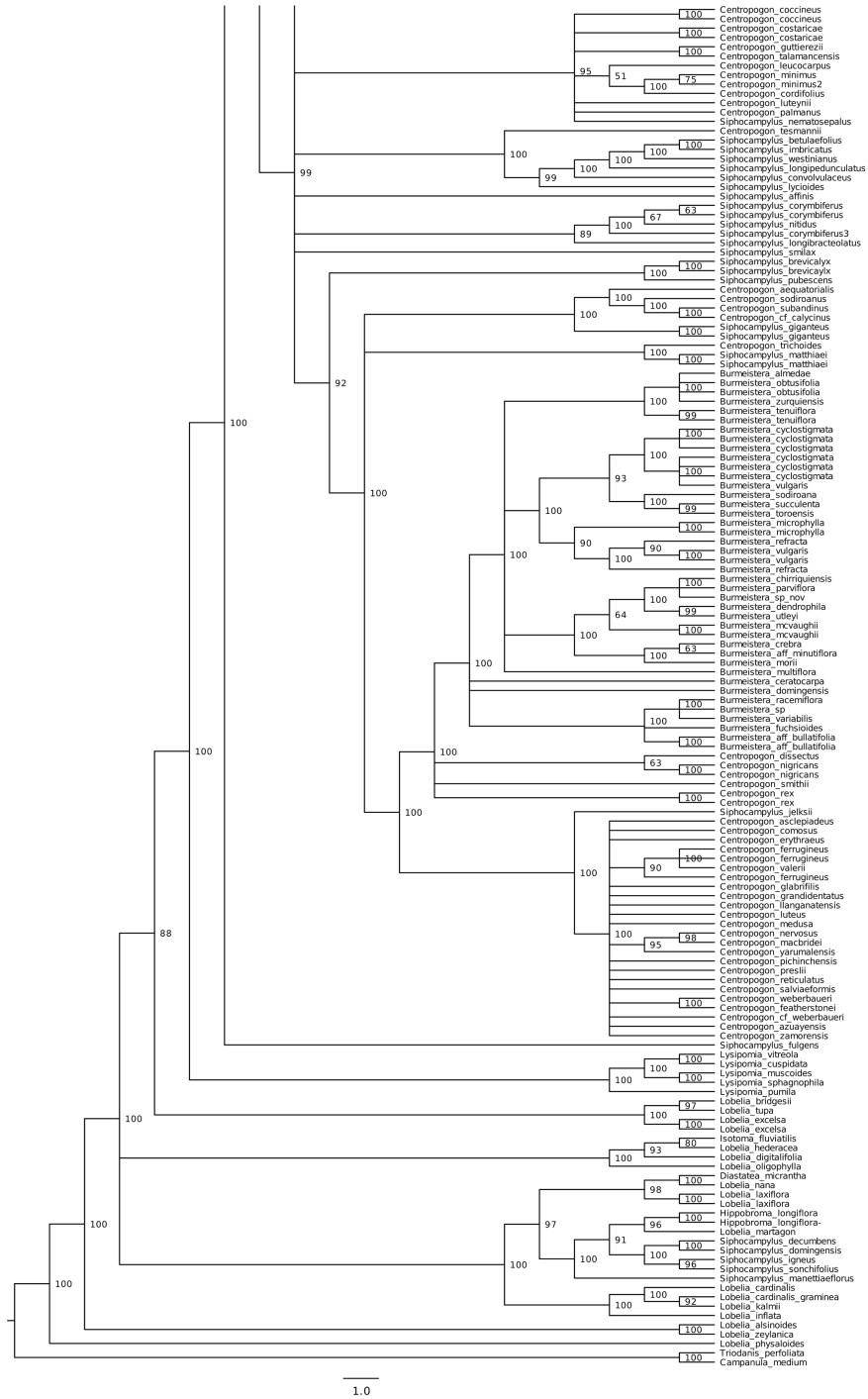


Figure A.1 (Continued). Five locus plastid phylogeny of Neotropical Lobelioideae inferred using MrBayes, excluding gap regions. Bayesian posterior probability percentages >50% shown at nodes. For phylogeny inferred including gap regions see main text Fig. 1.3.

Figure A.2 (Continued on next page).

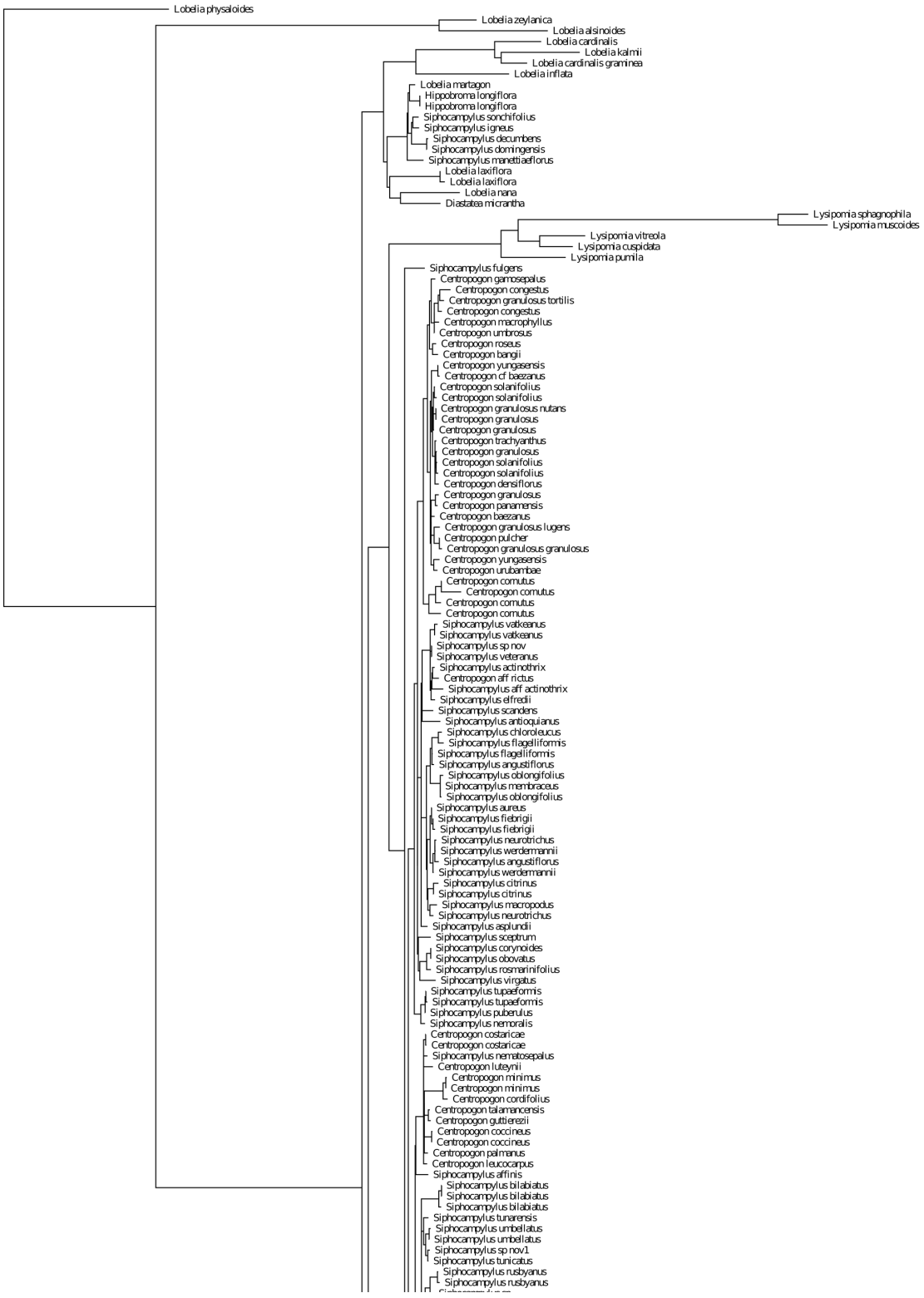
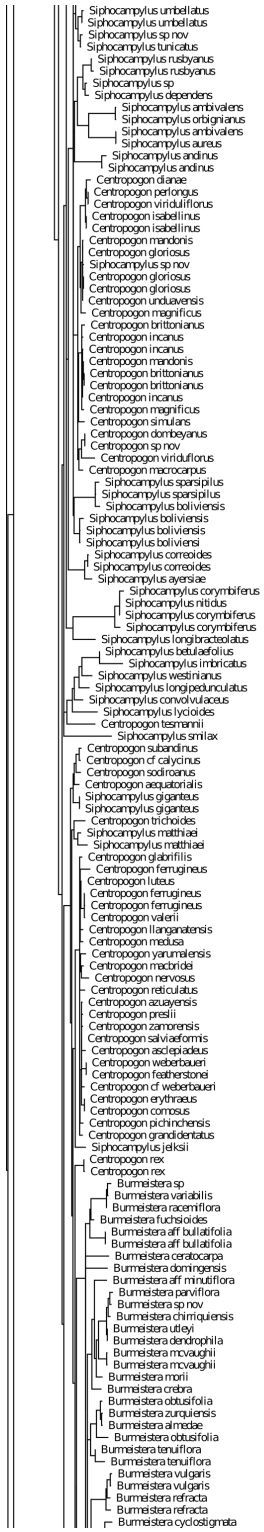


Figure A.2 (Continued on next page).



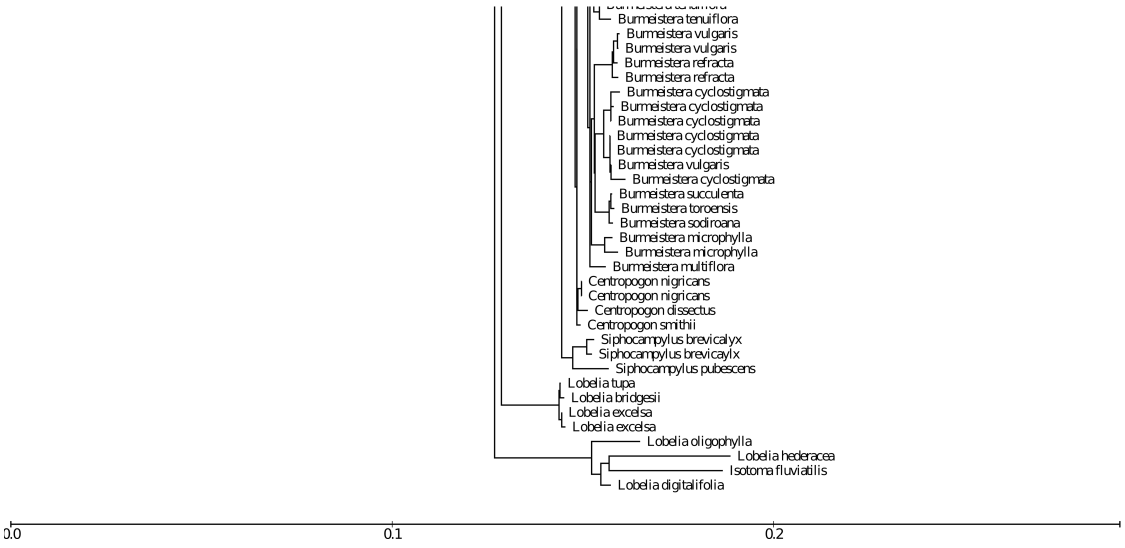


Figure A.2 (Continued). Five locus plastid phylogeny maximum likelihood phylogram of Neotropical Lobelioideae. For cladogram including support values see Figure 1.3.

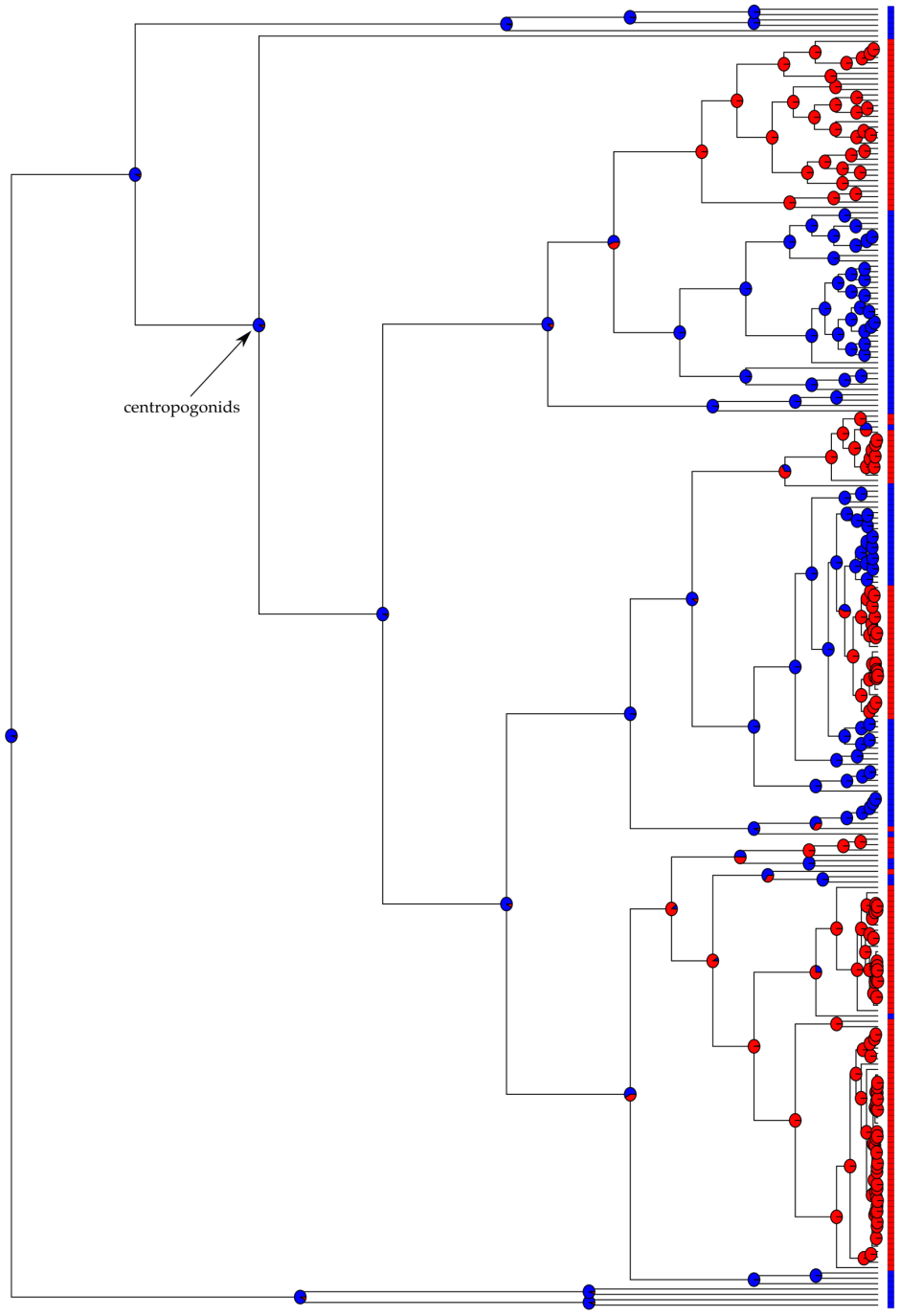


Figure A.3. Maximum likelihood ancestral character reconstruction of fruit evolution. Pie charts at nodes represent ancestral states that were calculated as the marginal likelihood of capsule (blue) and berry (red). For Bayesian stochastic character mapping see Figure 1.4.

Table A.1. Taxa sampled in the five-locus plastid study of Neotropical Lobelioideae, with voucher information, country of origin, and GenBank accession numbers.

Herbarium acronyms follow Index herbariorum (HOLMGREN, P. K., N. H. HOLMGREN, AND L. C. BARNETT. 1990. Index herbariorum. Part 1: The herbaria for the world. New York Botanical Garden, New York).

Taxon	Voucher	Origin	*rpl32-trnL*	*rpl32-trnL*	*rps16-trnK*	*trnG-trnG- trnS*
Burmeistera						
Burmeistera almedae Wilbur	L. Lagomarsino 86 (GH)	Costa Rica	KP014195	KP014848	KP014511	-
Burmeistera aff. bullatifolia J. Garzón & F. Gonzalez	C. D. Bacon 264A (GB)	Colombia	KP014167	KP014861	KP014501	-
Burmeistera aff. bullatifolia J. Garzón & F. Gonzalez	C. D. Bacon 287 (GB)	Colombia	KP014168	KP014862	KP014502	KP014770
Burmeistera ceratocarpa Zahlb.	M. L. Bristol 993 (GH)	Colombia	KP014172	KP014852	KP014343	-
Burmeistera chiriquiensis Wilbur	D. Santamaría 8996 (INB)	Costa Rica	KP014192	KP014858	KP014521	KP014754
Burmeistera crebra McVaugh	L. Lagomarsino 70 (GH)	Costa Rica	KP014234	KP014870	KP014507	KP014758
Burmeistera cyclostigmata J. D. Smith	C. Persson 858 (GB)	Panama	KP014179	KP014873	KP014518	KP014704
Burmeistera cyclostigmata J. D. Smith	L. Lagomarsino 50 (GH)	Costa Rica	KP014182	KP014877	KP014515	KP014695
Burmeistera cyclostigmata J. D. Smith	C. Persson 852 (GB)	Panama	KP014180	KP014874	KP014519	KP014705
Burmeistera cyclostigmata J. D. Smith	L. Lagomarsino 294 (GH)	Panama	KP014178	KP014847	KP014520	-
Burmeistera cyclostigmata J. D. Smith	L. Lagomarsino 45 (GH)	Costa Rica	KP014183	KP014878	KP014516	KP014706
Burmeistera cyclostigmata J. D. Smith	L. Lagomarsino 51 (GH)	Costa Rica	KP014181	KP014876	KP014514	KP014707
Burmeistera dendrophila E. Wimm	L. Lagomarsino 255 (GH)	Panama	KP014163	KP014855	KP014524	KP014750
Burmeistera domingensis Jeppesen	N. Muchhala 102	Ecuador	KP014189	KP014860	KP014532	KP014699
Burmeistera fuchsioides J. Garzón & F. Gonzalez	C. D. Bacon 258 (GB)	Colombia	KP014186	KP014865	KP014503	-
Burmeistera mcvaughii Wilbur	L. Lagomarsino 257 (GH)	Panama	KP014166	KP014853	KP014526	KP014768
Burmeistera mcvaughii Wilbur	L. Lagomarsino 98 (GH)	Panama	KP014233	KP014854	KP014527	KP014769
Burmeistera microphylla J. D. Smith	L. Lagomarsino 34 (GH)	Costa Rica	KP014187	KP014850	KP014350	KP014720
Burmeistera microphylla J. D. Smith	D. Santamaría 6546 (INB)	Costa Rica	KP014188	KP014863	KP014351	KP014717
Burmeistera aff. minutiflora J. Garzón & F. Gonzalez	C. D. Bacon 262 (GB)	Colombia	KP014235	KP014869	KP014508	KP014712
Burmeistera morii Wilbur	L. Lagomarsino 273 (GH)	Panama	KP014165	KP014864	KP014525	KP014771
Burmeistera multiflora Zahlb.	N. Muchhala 114	Ecuador	KP014160	KP014879	KP014530	KP014583
Burmeistera obtusifolia E. Wimm	L. Lagomarsino 61 (GH)	Costa Rica	KP014197	KP014969	KP014510	-
Burmeistera obtusifolia E. Wimm	L. Lagomarsino 163 (GH)	Panama	KP014196	KP014851	KP014513	KP014701
Burmeistera parviflora E. Wimm	L. Lagomarsino 53 (GH)	Costa Rica	KP014236	KP014859	KP014498	KP014752
Burmeistera racemiflora Lammers	M. Madison 7145 (AAU)	Ecuador	KP014170	KP014845	KP014504	KP014760
Burmeistera refracta E. Wimm.	L. Andersson 2464 (GB)	Ecuador	KP014175	KP014871	KP014493	KP014713
Burmeistera refracta E. Wimm.	N. Muchhala 110	Ecuador	KP014176	KP014880	KP014494	KP014711
Burmeistera sodiroana Zahlb.	N. Muchhala 115	Ecuador	KP014239	KP014867	KP014528	-
Burmeistera succulenta H. Karst. & Triana	C. D. Bacon 297 (GB)	Colombia	KP014240	KP014866	KP014529	-
Burmeistera tenuiflora J.D. Smith	L. Lagomarsino 48 (GH)	Costa Rica	KP014194	KP014923	-	KP014757
Burmeistera tenuiflora J.D. Smith	L. Lagomarsino 276 (GH)	Panama	KP014184	KP014881	KP014509	KP014721
Burmeistera toroensis Wilbur	L. Lagomarsino 92 (GH)	Panama	KP014241	KP014868	KP014497	KP014709
Burmeistera utleyi Wilbur	L. Lagomarsino 253 (GH)	Panama	KP014164	KP014856	KP014523	KP014751
Burmeistera variabilis (Gleason) E. Wimm.	C. D. Bacon 298 (GB)	Colombia	KP014169	KP014846	KP014505	KP014759
Burmeistera vulgaris E. Wimm.	C. Persson 867 (GB)	Panama	KP014177	KP014875	KP014517	KP014703
Burmeistera vulgaris E. Wimm.	D. Santamaría S-980 (GB)	Costa Rica	KP014174	KP014872	KP014495	KP014714

Table A.1 (Continued).

Burmeistera vulgaris E. Wimm.	L. Lagomarsino 74 (GH)	Costa Rica	KP014173	-	KP014496	-
Burmeistera zurquiensis Wilbur	L. Lagomarsino 26 (GH)	Costa Rica	KP014193	KP014849	KP014512	KP014702
Burmeistera sp.	C. D. Bacon 283 (GB)	Colombia	KP014171	KP014844	KP014506	KP014638
Burmeistera sp. nov.	D. Santamaría 6640 (INB)	Costa Rica	KP014237	KP014857	KP014522	KP014753
Campanula*						
Campanula medium L.	L. Lagomarsino 422 (GH)	USA	KP014048	-	KP014307	KP014571
Centropogon						
Centropogon aequatorialis E. Wimm.	N. Muchhala 131	Ecuador	KP014206	KP014957	KP014531	KP014767
Centropogon asclepiadeus (Willd.) E. Wimm.	R. E. Weaver, Jr. 1556 (GH)	Colombia	KP014228	KP014927	KP014560	-
Centropogon azuayensis Jeppesen	A. Antonelli 576 (GB)	Ecuador	KP014231	KP014931	KP014558	-
Centropogon baezanus Jeppesen	N. Muchhala 162	Ecuador	KP014141	KP014836	KP014408	KP014624
Centropogon bangii Zahlb.	S. Beck 20763 (OSH)	Bolivia	KP014122	KP014826	KP014409	KP014630
Centropogon brittonianus Zahlb.	A. Timmermann 22 (AAU)	Bolivia	KP014287	KP015005	KP014479	KP014685
Centropogon brittonianus Zahlb.	B. Stein 1416 (MO)	Bolivia	KP014286	KP015015	KP014473	KP014669
Centropogon brittonianus Zahlb.	L. Lagomarsino 196 (GH)	Bolivia	KP014283	KP015004	KP014477	KP014686
Centropogon cf. calycinus Benth.	A. Antonelli 611 (GB)	Ecuador	KP014198	KP014914	KP014570	KP014755
Centropogon coccineus (Hook.) Regel ex B.D. Jacks.	L. Lagomarsino 306 (GH)	Panama	KP014249	KP014954	KP014464	KP014762
Centropogon coccineus (Hook.) Regel ex B.D. Jacks.	D. Santamaría 8218 (INB)	Costa Rica	KP014304	KP014955	KP014465	KP014763
Centropogon comosus Gleason	P. Nuñéz 8162 (AAU)	Ecuador	KP014229	KP014937	KP014546	KP014739
Centropogon congestus Gleason	L. Lagomarsino 40 (GH)	Costa Rica	KP014127	KP014822	KP014406	KP014595
Centropogon congestus Gleason	L. Lagomarsino 95 (GH)	Panama	KP014128	KP014819	KP014410	KP014589
Centropogon cordifolius Benth.	R. Kriebel 5559 (NY)	Guatemala	KP014253	KP014945	KP014457	KP014773
Centropogon cornutus (L.) Druce	C. D. Bacon 219 (GB)	Colombia	KP014129	-	KP014354	-
Centropogon cornutus (L.) Druce	M. Jansen-Jacobs 4955 (GB)	Guyana	KP014124	KP014809	KP014353	KP014637
Centropogon cornutus (L.) Druce	L. Lagomarsino 93 (GH)	Panama	KP014121	KP014810	KP014345	KP014593
Centropogon cornutus (L.) Druce	C. D. Bacon 289 (GB)	Colombia	KP014118	KP014804	KP014355	KP014588
Centropogon costaricae (Vatke) E. Wimm.	D. Santamaría S-966 (GB)	Costa Rica	KP014305	KP014948	KP014469	KP014744
Centropogon costaricae (Vatke) E. Wimm.	L. Lagomarsino 24A (GH)	Costa Rica	KP014306	KP014949	KP014470	KP014742
Centropogon densiflorus Benth.	N. Muchhala 430	Ecuador	KP014146	KP014820	KP014399	-
Centropogon dianae Lammers	L. Lagomarsino 415 (GH)	Peru	KP014267	KP014988	KP014444	-
Centropogon dissectus E. Wimm.	J. Luteyn 5678 (GB)	Ecuador	KP014212	KP014992	KP014561	KP014722
Centropogon dombeyanus E. Wimm	L. Lagomarsino 332 (GH)	Peru	-	KP014986	KP014488	KP014663
Centropogon erythraeus Drake	L. Andersson 2529 (GB)	Ecuador	KP014227	KP014936	KP014559	KP014740
Centropogon featherstonei Gleason	L. Lagomarsino 318 (GH)	Peru	KP014219	KP014933	KP014548	KP014737
Centropogon ferrugineus (L.f) Gleason	D. Santamaría S-902 (GB)	Costa Rica	KP014216	KP014920	KP014543	KP014729
Centropogon ferrugineus (L.f) Gleason	L. Lagomarsino 22 (GH)	Costa Rica	KP014217	KP014925	KP014544	KP014730
Centropogon ferrugineus (L.f) Gleason	L. Lagomarsino 103 (GH)	Panama	KP014203	KP014919	KP014538	KP014696
Centropogon gamosepalus Zahlb.	N. Muchhala 429	Ecuador	KP014130	KP014823	KP014404	KP014627
Centropogon glabrifilis (E. Wimm.) Jeppsen	L. Andersson 2423 (GB)	Ecuador	KP014222	KP014916	KP014542	KP014728
Centropogon gloriosus (Britton) Zahlb.	A. Timmermann 23 (AAU)	Bolivia	KP014292	KP014981	KP014449	KP014668
Centropogon gloriosus (Britton) Zahlb.	A.Timmermann 17 (AAU)	Bolivia	KP014293	KP014980	KP014450	KP014667
Centropogon gloriosus (Britton) Zahlb.	L. Lagomarsino 199 (GH)	Bolivia	KP014294	KP014979	KP014451	KP014670
Centropogon granulosus C. Presl.	C. D. Bacon 306 (GB)	Colombia	KP014136	-	KP014407	-
Centropogon granulosus C. Presl.	L. Lagomarsino 301 (GH)	Panama	KP014140	-	KP014396	KP014616
Centropogon granulosus C. Presl.	L. Lagomarsino 81 (GH)	Costa Rica	KP014144	KP014829	KP014393	KP014622
Centropogon granulosus C. Presl.	L. Lagomarsino 56 (GH)	Costa Rica	KP014147	KP014833	KP014395	KP014625
Centropogon granulosus subsp lugens Stein (ined)	C. D. Bacon 303 (GB)	Colombia	KP014123	KP014840	KP014416	KP014618

Table A.1 (Continued).

Centropogon granulosus subsp. granulosus Stein (ined.)	L. Lagomarsino 330 (GH)	Peru	KP014142	KP014841	KP014413	KP014614
Centropogon granulosus subsp. nutans Stein (ined.)	D. Santamaría S-962 (GB)	Costa Rica	KP014145	KP014830	KP014394	KP014623
Centropogon granulosus subsp. tortilis Stein (ined.)	C. Persson 829 (GB)	Panama	KP014126	KP014821	KP014411	KP014605
Centropogon gutierrezii (Planch & Oerst.) E. Wimm.	L. Lagomarsino 19 (GH)	Costa Rica	KP014301	KP014950	KP014466	KP014745
Centropogon incanus (Britton) Zahlb.	S. Acha 207 (MO)	Bolivia	KP014279	KP014998	KP014480	KP014659
Centropogon incanus (Britton) Zahlb.	L. Lagomarsino 200 (GH)	Bolivia	KP014284	KP014996	KP014474	KP014684
Centropogon incanus (Britton) Zahlbr..	L. Lagomarsino 223 (GH)	Bolivia	KP014285	KP014997	KP014476	KP014662
Centropogon isabellinus Wimm	L. Lagomarsino 406 (GH)	Peru	KP014280	KP014983	KP014445	KP014679
Centropogon isabellinus Wimm	L. Lagomarsino 405 (GH)	Peru	-	KP014982	KP014446	KP014680
Centropogon leucocarpus McVaugh	L. Lagomarsino 280 (GH)	Panama	KP014162	KP014951	KP014462	KP014743
Centropogon llanganatensis Jeppsen	N. Muchhala 139	Ecuador	KP014226	KP014926	KP014556	KP014727
Centropogon luteus E. Wimm.	L. Andersson 2411 (GB)	Ecuador	KP014214	KP014922	KP014555	KP014731
Centropogon luteynii Wilbur	L. Lagomarsino 259 (GH)	Panama	KP014161	KP014911	KP014432	KP014747
Centropogon macbridei Gleason	L. Lagomarsino 337 (GH)	Peru	KP014208	KP014917	KP014540	KP014732
Centropogon macrocarpus Zahlb.	L. Valenzuela 858 (OSH)	Peru	KP014289	-	KP014460	-
Centropogon macrophyllus (G. Don.) E. Wimm	L. Lagomarsino 345 (GH)	Peru	KP014120	KP014824	KP014405	KP014629
Centropogon magnificus Zahlb.	A. Fuentes 10044 (LPB)	Bolivia	KP014288	KP014995	KP014475	KP014658
Centropogon magnificus Zahlb.	N. Paniagua 5740 (MO)	Bolivia	KP014291	KP015003	KP014455	KP014656
Centropogon mandonis Zahlb.	A. Timmermann 1 (AAU)	Bolivia	KP014282	KP014999	KP014478	KP014687
Centropogon mandonis Zahlb.	L. Lagomarsino 243 (GH)	Bolivia	KP014295	KP014977	KP014452	KP014666
Centropogon medusa E. Wimm.	N. Muchhala 174	Ecuador	KP014223	KP014930	KP014549	KP014692
Centropogon minimus McVaugh	C. D. Bacon 264B (GB)	Colombia	KP014254	KP014947	KP014458	KP014698
Centropogon minimus McVaugh	C. D. Bacon 257 (GB)	Colombia	KP014255	KP014946	KP014459	-
Centropogon nervosus Wimm	L. Lagomarsino 407 (GH)	Peru	KP014202	KP014915	KP014539	KP014724
Centropogon nigricans Zahlb.	J. Ramos 7097 (OSH)	Ecuador	KP014209	-	KP014565	-
Centropogon nigricans Zahlb.	N. Muchhala 118	Ecuador	KP014210	KP015007	KP014566	KP014723
Centropogon palmanus (J. D. Smith) E. Wimm.	L. Lagomarsino 193a (GH)	Costa Rica	KP014303	KP014843	KP014746	KP014746
Centropogon panamensis Wilbur	L. Lagomarsino 308 (GH)	Panama	KP014131	KP014828	KP014403	KP014613
Centropogon perlongus Gleason	L. Lagomarsino 409 (GH)	Peru	KP014265	KP014989	KP014447	KP014681
Centropogon pichinchensis Zahlb.	Luteyn 14284 (OSH)	Ecuador	KP014220	-	KP014550	-
Centropogon preslii E. Wimm.	L. Andersson 2503 (GB)	Ecuador	KP014225	KP014929	KP014553	KP014734
Centropogon pulcher Zahlb.	L. Lagomarsino 344 (GH)	Peru	KP014143	KP014842	KP014415	KP014615
Centropogon reticulatus Drake	M. Merello 1099 (MO)	Peru	KP014185	KP014921	KP014557	KP014718
Centropogon rex E. Wimm.	C. D. Bacon 288 (GB)	Colombia	KP014201	KP014972	KP014564	-
Centropogon rex E. Wimm.	C. D. Bacon 288A (GB)	Colombia	KP014200	KP014971	KP014563	KP014774
Centropogon roseus Rusby	L. Lagomarsino 372 (GH)	Peru	KP014119	KP014827	KP014412	KP014628
Centropogon salviaeformis Zahlb.	N. Muchhala 173	Ecuador	KP014230	KP014932	KP014554	KP014726
Centropogon simulans Lammers	L. Lagomarsino 402 (GH)	Peru	KP014281	KP014974	KP014461	KP014646
Centropogon smithii E. Wimm.	L. Lagomarsino 68 (GH)	Costa Rica	KP014211	KP015008	KP014562	KP014772
Centropogon sodiroanus Zahlb.	N. Muchhala 106	Ecuador	KP014204	KP015011	KP014568	-
Centropogon solanifolius Benth.	D. Santamaría S-904 (GB)	Costa Rica	KP014133	KP014834	KP014397	KP014621
Centropogon solanifolius Benth.	L. Lagomarsino 25 (GH)	Costa Rica	KP014132	KP014832	KP014398	KP014626
Centropogon solanifolius Benth.	N. Muchhala 104	Ecuador	KP014139	KP014837	KP014400	KP014749
Centropogon solanifolius Benth.	C. D. Bacon 261 (GB)	Colombia	KP014134	KP014839	KP014402	-
Centropogon subandinus Zahlb.	N. Muchhala 475	Ecuador	KP014207	KP014913	KP014569	KP014756
Centropogon talamancensis Wilbur	L. Lagomarsino 140 (GH)	Costa Rica	KP014302	KP014953	KP014467	KP014748
Centropogon tessmannii E. Wimm.	N. Muchhala 168	Ecuador	KP014150	KP014882	KP014344	KP014700
Centropogon trachyanthus E. Wimm.	N. Muchhala 138	Ecuador	KP014137	KP014838	KP014401	KP014606
Centropogon trichodes E. Wimm.	L. Andersson 2546 (GB)	Ecuador	KP014213	KP014970	KP014535	KP014766

Table A.1 (Continued).

Centropogon umbrosus E. Wimm	L. Lagomarsino 349 (GH)	Peru	KP014125	KP014825	-	KP014631
Centropogon unduavensis (Britton) Zahlb.	J. Solomon 15418 (LPB)	Bolivia	KP014290	KP014978	KP014453	-
Centropogon urubambae E. Wimm	L. Lagomarsino 347 (GH)	Peru	KP014148	KP014831	KP014414	KP014617
Centropogon valerii Standley	D. Santamaría S-977 (GB)	Costa Rica	KP014215	KP014924	KP014545	KP014733
Centropogon viriduliflorus Wimm	L. Lagomarsino 370 (GH)	Peru	KP014268	KP015006	KP014487	KP014665
Centropogon viriduliflorus Wimm	L. Valenzuela 712 (OSH)	Peru	KP014266	-	KP014448	-
Centropogon weberbaueri Zahlb.	L. Lagomarsino 317(GH)	Peru	KP014218	KP014934	KP014547	KP014736
Centropogon cf. weberbaueri Zahlb.	L. Lagomarsino 351 (GH)	Peru	KP014232	KP014935	KP014552	KP014735
Centropogon yarumalensis E. Wimm.	C. D. Bacon 263 (GB)	Colombia	KP014221	KP014918	KP014541	KP014725
Centropogon yungasensis Britton	L. Lagomarsino 392 (GH)	Peru	KP014149	KP014818	KP014391	KP014619
Centropogon yungasensis Britton	A. Araujo-Murakami 3893 (LPB)	Bolivia	KP014138	KP014835	KP014359	-
Centropogon cf. yungasensis Britton	L. Lagomarsino 380 (GH)	Peru	KP014135	-	KP014390	KP014620
Centropogon zamorensis Jeppesen	L. Andersson 2542 (GB)	Ecuador	KP014224	KP014928	KP014551	KP014738
Centropogon sp. nov. (Lagomarsino & Santamined.)	L. Lagomarsino 354 (GH)	Peru	KP014269	KP014987	KP014489	KP014664
Centropogon sp. nov. (Lagomarsino & Santamined.)	L. Lagomarsino 190 (GH)	Bolivia	KP014296	KP014976	KP014454	-
Diastatea						
Diastatea micrantha (Kunth) McVaugh	L. Lagomarsino 44	Costa Rica	KP014066	KP014803	KP014327	KP014581
Hippobroma						
Hippobroma longiflora (L.) G. Don	Cultivated, University of Aarhus, no voucher	Clutivated	KP014071	-	KP014336	KP014781
Hippobroma longiflora (L.) G. Don	L. Lagomarsino 346	Peru	KP014072	-	KP014337	KP014782
Isotoma						
Isotoma fluviatilis F. Muell. Ex Bentham	Cultivated, University of Aarhus, no voucher	Clutivated	KP014054	KP014790	KP014321	KP014783
Lobelia						
Lobelia alsinoides Lam.	Larsen 34131 (AAU)	Thailand	KP014050	KP014785	KP014309	KP014572
Lobelia bridgesii Hook & Arn.	M. Gustafsson 1019 (AAU)	Cultivated	KP014077	KP014800	KP014338	KP014584
Lobelia cardinalis L.	L. Lagomarsino 423 (GH)	USA	KP014060	KP014794	KP014314	-
Lobelia cardinalis subsp. graminea (Lam.) McVaugh	R. Kriebel 5570 (NY)	Guatemala	KP014061	KP014795	KP014315	-
Lobelia digitalifolia (Griseb.) Urb.	R. A. Howard 19407 (NY)	Guadeloupe	-	-	KP014324	-
Lobelia excelsa Bonpland	Schlatzer 1966.04.26 (AAU)	China	KP014075	-	KP014340	-
Lobelia excelsa Bonpland	L. Lagomarsino 426 (GH)	Cultivated	KP014078	KP014801	KP014341	KP014586
Lobelia hederacea Cham.	A. Schinini 12141 (AAU)	Argentina	KP014053	KP014797	KP014323	KP014578
Lobelia inflata L.	H. Schmidt 1531 (MO)	USA	KP014062	-	KP014320	-
Lobelia kalmii L.	L. Lagomarsino 424 (GH)	USA	KP014059	KP014793	KP014316	KP014577
Lobelia laxiflora Kunth.	L. Lagomarsino 289 (GH)	Panama	KP014065	KP014799	KP014326	KP014777
Lobelia laxiflora Kunth.	A. Antonelli 631 (GB)	Mexico	KP014064	KP014798	KP014325	KP014776
Lobelia martagon Hitchc.	W. Judd 5375 (NY)	Jamaica	KP014073	-	KP014335	-
Lobelia nana Kunth.	L. Lagomarsino 228 (GH)	Bolivia	KP014063	KP014796	KP014328	KP014775
Lobelia oligophylla (Wedd.) Lammers	C. M. Taylor 11210 (NY)	Argentina	KP014055	-	KP014322	KP014784
Lobelia physaloides A. Cunn.	Cameron s.n. (AAU)	New Zealand	-	-	KP014311	KP014574
Lobelia tupa L.	Cultivated, University of Aarhus, no voucher	Cultivated	KP014076	KP014802	KP014339	KP014585
Lobelia zeylanica L.	D. Boufford 24898 (GH)	Taiwan	-	-	KP014310	KP014573
Lysipomia						
Lysipomia cuspidata McVaugh	L. Andersson 2559 (GB)	Ecuador	KP014057	-	KP014318	KP014579
Lysipomia muscoides Hook f.	L. Lagomarsino 325 (GH)	Peru	KP014051	-	KP014312	KP014575
Lysipomia pumila (Wedd.) E. Wimm.	L. Lagomarsino 238 (GH)	Bolivia	KP014056	KP014791	KP014317	KP014580
Lysipomia sphagnophila Griseb. Ex Wedd.	L. Andersson 2444 (GB)	Ecuador	KP014052	-	KP014313	KP014576
Lysipomia vitreola McVaugh	A. Antonelli 581 (GB)	Ecuador	KP014058	KP014792	KP014319	-

Table A.1 (continued)

Siphocampylus						
Siphocampylus actinothrix E. Wimm.	L. Lagomarsino 403 (GH)	Peru	KP014086	KP014812	KP014367	KP014643
Siphocampylus aff. actinothrix E. Wimm.	L. Lagomarsino 361 (GH)	Peru	KP014086	KP014812	KP014367	KP014643
Siphocampylus affinis (Mirb.) McVaugh	B. Lojtnant 11426 (GB)	Ecuador	KP014270	-	KP014456	KP014661
Siphocampylus ambivalens Lammers	J. Wood 9986	Bolivia	KP014151	KP014806	KP014421	KP014650
Siphocampylus ambivalens Lammers	A. Timmermann 8 (AAU)	Bolivia	KP014243	KP014912	KP014417	KP014647
Siphocampylus andinus Britton	A. Timmermann 12 (AAU)	Bolivia	KP014259	KP014985	KP014499	KP014653
Siphocampylus andinus Britton	L. Lagomarsino 226 (GH)	Bolivia	KP014260	KP014984	KP014500	KP014654
Siphocampylus angustiflorus Schlechtend.	A. Timmermann 16 (AAU)	Bolivia	KP014101	KP014892	KP014385	KP014600
Siphocampylus angustiflorus Schlechtend.	L. Lagomarsino 417 (GH)	Peru	KP014097	KP014887	KP014379	KP014633
Siphocampylus antioquianus E. Wimm.	C. D. Bacon 242 (GB)	Colombia	KP014090	KP014943	KP014364	-
Siphocampylus asplundii Jeppesen	E. Narvaez 539 (MO)	Ecuador	KP014092	-	KP014366	-
Siphocampylus aureus Rusby	A. Acebey 634 (OSH)	Bolivia	KP014244	-	KP014418	-
Siphocampylus aureus Rusby	J. Wood 14956	Bolivia	KP014105	KP014898	KP014383	-
Siphocampylus ayersiae Lammers	L. Lagomarsino 212 (GH)	Bolivia	KP014297	KP014965	KP014437	KP014648
Siphocampylus betulaefolius (Cham.) G. Don.	S. Godoy 3000 (UEC)	Brazil	KP014153	KP014904	KP014420	KP014694
Siphocampylus bilabiatus Zahlb.	S. Beck 22873 (OSH)	Bolivia	KP014257	KP015017	KP014425	-
Siphocampylus bilabiatus Zahlb.	A. Araujo-Murakami 4230 (MO)	Bolivia	KP014256	KP015016	KP014423	KP014677
Siphocampylus bilabiatus Zahlb.	L. Lagomarsino 227 (GH)	Bolivia	KP014258	KP015018	KP014424	KP014678
Siphocampylus boliviensis Zahlb.	J. Solomon 19044 (OSH)	Bolivia	KP014276	-	KP014490	KP014651
Siphocampylus boliviensis Zahlb.	L. Lagomarsino 377 (GH)	Peru	KP014251	KP014959	KP014482	KP014682
Siphocampylus boliviensis Zahlb.	L. Lagomarsino 239 (GH)	Bolivia	KP014252	KP014960	KP014483	KP014673
Siphocampylus boliviensis Zahlb.	L. Lagomarsino 376 (GH)	Peru	KP014250	KP014961	KP014484	KP014683
Siphocampylus brevicalyx E. Wimm.	B. Lojtnant 11826 (GB)	Ecuador	KP014246	KP014902	KP014439	KP014716
Siphocampylus brevicalyx E. Wimm.	N. Muchhala 480	Ecuador	KP014245	KP014901	KP014433	KP014715
Siphocampylus chloroleucus E. Wimm	Asplund 13060 (S)	Ecuador	KP014098	KP014903	KP014377	KP014611
Siphocampylus citrinus Wimm	L. Lagomarsino 368 (GH)	Peru	KP014115	KP014896	KP014374	KP014604
Siphocampylus citrinus Wimm	L. Lagomarsino 369 (GH)	Peru	KP014114	KP014897	KP014375	KP014591
Siphocampylus convolvulaceus (Cham.) G. Don.	F. M. Souza 104 (UEC)	Brazil	KP014159	KP014907	KP014481	KP014645
Siphocampylus correoides Zahlb.	A. Timmermann 3 (AAU)	Bolivia	KP014298	KP014967	KP014436	KP014657
Siphocampylus correoides Zahlb.	A. Timmermann 11 (AAU)	Bolivia	KP014299	KP014966	KP014438	-
Siphocampylus corymbifer Pohl	A. Timmermann 9 (AAU)	Bolivia	KP014155	KP014941	KP014347	-
Siphocampylus corymbifer Pohl	A. Glaziou s.n.		KP014156	KP014940	KP014348	-
Siphocampylus corymbiferus Pohl	L. Lagomarsino 216 (GH)	Bolivia	KP014157	KP014942	KP014346	KP014693
Siphocampylus corynoides E. Wimm	L. Lagomarsino 353 (GH)	Peru	KP014117	KP014910	KP014361	KP014610
Siphocampylus decumbens (Rich.) Juss & A. DC.	P. Acevedo-Rodriguez 14172 (NY)	Dominican Republic	KP014067	-	KP014330	-
Siphocampylus dependens (Ruiz & Pavon) G. Don	L. Lagomarsino 316 (GH)	Peru	KP014261	KP015000	KP014485	KP014690
Siphocampylus domingensis A. DC.	A. Veloz 2001 (JBSD)	Dominican Republic	KP014068	KP014787	KP014331	KP014582
Siphocampylus elfriedii E. Wimm	L. Lagomarsino 387 (GH)	Peru	KP014084	KP014813	KP014371	KP014641
Siphocampylus fiebrigii E. Wimm	S. Beck 11587 (OSH)	Bolivia	KP014104	KP014899	KP014384	KP014598
Siphocampylus fiebrigii E. Wimm	S. Beck 31446 (LPB)	Bolivia	KP014100	KP014900	KP014382	KP014599
Siphocampylus flagelliformis Zahlb.	E. Garcia 2006 (GB)	Bolivia	KP014096	KP014883	KP014378	KP014612
Siphocampylus flagelliformis Zahlb.	L. Lagomarsino 220 (GH)	Bolivia	KP014099	KP014888	KP014380	KP014632
Siphocampylus fulgens Hort.	Hatschbacch 44995 (GB)	Ecuador	KP014081	KP015014	KP014434	KP014719
Siphocampylus giganteus (Cav.) G. Don.	L. Andersson 2432 (GB)	Ecuador	-	KP015002	KP014533	KP014761
Siphocampylus giganteus (Cav.) G. Don.	N. Muchhala 101	Ecuador	KP014205	KP015001	KP014534	-

Table A.1 (continued)

Siphocampylus igneus Urb.	J. R. Abbott 21003 (FLAS)	Dominican Republic	KP014069	KP014788	KP014332	KP014779
Siphocampylus imbricatus (Cham.) G. Don.	P. Nuñéz 8182 (AAU)	Brazil	-	-	KP014329	-
Siphocampylus jelskii Zahlb.	L. Lagomarsino 321 (GH)	Peru	KP014199	KP014956	KP014567	KP014764
Siphocampylus longepedunculatus Pohl	A. Antonelli 299 (GB)	Brazil	KP014238	KP014905	KP014471	KP014697
Siphocampylus longibracteolatus E. Wimm	B. Stein 3155 (AAU)	Colombia	KP014158	-	-	-
Siphocampylus lycioides (Cham.) G. Don.	R. Romero 3805 (UEC)	Brazil	KP014247	KP014808	KP014352	KP014710
Siphocampylus macropodus (Billb.) G. Don.	A. Antonelli 298 (GB)	Brazil	KP014107	KP014890	KP014365	KP014639
Siphocampylus manettiaeflorus Hook.	Cultivated, Marbury Bot. Garden, no voucher	Cultivated	KP014074	KP014786	KP014334	KP014780
Siphocampylus matthiaei A. DC.	L. Lagomarsino 313 (GH)	Peru	KP014190	KP014968	KP014536	KP014765
Siphocampylus matthiaei A. DC.	J. Boeke 1929 (AAU)	Peru	KP014191	KP014891	KP014537	-
Siphocampylus membraceus Britton	A. Gentry 44,526 (MO)	Bolivia	KP014094	KP014885	KP014388	-
Siphocampylus nematosepalus (Donn. Smith) E. Wimm	L. Lagomarsino 164 (GH)	Costa Rica	KP014300	KP014952	KP014463	KP014741
Siphocampylus nemoralis Griseb.	D. Spooner 6605	Bolivia	KP014112	KP014944	KP014426	-
Siphocampylus neurotrichus E. Wimm	S. Beck 22756 (OSH)	Bolivia	KP014102	KP014894	KP014386	KP014596
Siphocampylus neurotrichus E. Wimm	M. Nee 42251 (NY)	Bolivia	KP014108	KP014889	KP014381	KP014603
Siphocampylus nitidus Pohl	J. Pirani 689 (UEC)	Brazil	-	-	KP014349	-
Siphocampylus oblongifolius Rusby	J. L. Clark 6687 (OSH)	Bolivia	KP014093	KP014884	KP014358	KP014636
Siphocampylus oblongifolius Rusby	S. Beck 30201 (LPB)	Bolivia	KP014095	KP014886	KP014389	-
Siphocampylus obovatus (G. Don) E. Wimm	L. Lagomarsino 350 (GH)	Peru	KP014116	-	KP014360	KP014609
Siphocampylus orbignianus A. DC.	L. Lagomarsino 217 (GH)	Bolivia	KP014152	KP014807	KP014422	KP014655
Siphocampylus puberulus E. Wimm	Vargas 226 (LPB)	Bolivia	KP014109	KP014964	KP014427	-
Siphocampylus pubescens Benth.	B. √òllgaard 74216 (GH)	Ecuador	KP014080	-	KP014419	-
Siphocampylus aff. rictus Lammers	L. Lagomarsino 341 (GH)	Peru	KP014082	KP014811	KP014363	KP014640
Siphocampylus rosmarinifolius G. Don.	L. Lagomarsino 331 (GH)	Peru	KP014113	KP014909	KP014362	KP014634
Siphocampylus rusbyanus Britton	L. Lagomarsino 395 (GH)	Peru	KP014263	KP015013	KP014430	KP014688
Siphocampylus rusbyanus Britton	A. Fuentes 4760 (MO)	Bolivia	KP014264	KP015012	KP014431	KP014689
Siphocampylus scandens (HBK) G. Don.	L. Andersson 2515 (GB)	Ecuador	KP014248	KP014973	KP014356	KP014592
Siphocampylus sceptrum Decaisne apud Linden	L. Dorr 20513	Venezuela	KP014242	KP015009	KP014392	KP014597
Siphocampylus smilax Lammers	L. Lagomarsino 250 (GH)	Bolivia	KP014079	KP014908	KP014342	KP014649
Siphocampylus sonchifolius (Sw.) McVaugh	T. Clase 3048 (JBSD)	Dominican Republic	KP014070	KP014789	KP014333	KP014778
Siphocampylus sparsipilus E. Wimm	L. Lagomarsino 197 (GH)	Bolivia	KP014278	KP014939	KP014492	KP014652
Siphocampylus sparsipilus E. Wimm.	A. Timmermann 15 (AAU)	Bolivia	KP014277	KP014938	KP014491	KP014660
Siphocampylus tunarensis Zahlb.	L. Lagomarsino 232 (GH)	Bolivia	KP014271	KP014975	KP014435	KP014674
Siphocampylus tunicatus Zahlb.	L. Lagomarsino 235 (GH)	Bolivia	KP014272	KP014991	KP014443	KP014676
Siphocampylus tupaeformis Zahlb.	L. Lagomarsino 225 (GH)	Bolivia	KP014110	KP014963	KP014428	KP014594
Siphocampylus tupaeformis Zahlb.	A. Timmermann 7 (LPB)	Bolivia	KP014111	KP014962	KP014429	KP014708
Siphocampylus umbellatus (HBK) G. Don.	S. Beck 17837 (OSH)	Bolivia	KP014273	KP014993	KP014441	KP014671
Siphocampylus umbellatus (HBK) G. Don.	L. Lagomarsino 193 (GH)	Bolivia	KP014275	KP014994	KP014442	KP014672
Siphocampylus vatkeanus Zahlb.	N. Paniagua 5774 (MO)	Bolivia	KP014088	KP014816	KP014369	KP014608
Siphocampylus vatkeanus Zahlb.	A. Fuentes 8571 (LPB)	Bolivia	KP014089	KP014817	KP014370	KP014590
Siphocampylus veteranus Wimm	L. Lagomarsino 388 (GH)	Peru	KP014087	KP014815	KP014373	KP014644
Siphocampylus virgatus A. DC.	L. Lagomarsino 343 (GH)	Peru	KP014091	KP014958	KP014357	KP014607
Siphocampylus werdermannii E. Wimm	J. Schmit 138 (OSH)	Bolivia	KP014103	KP014895	KP014387	KP014601
Siphocampylus werdermannii E. Wimm	L. Lagomarsino 245 (GH)	Bolivia	KP014106	KP014893	KP014376	KP014602
Siphocampylus westinianus (Billb.) Pohl	A. Antonelli 308 (GB)	Brazil	KP014154	KP014906	KP014472	KP014587
Siphocampylus sp.	L. Lagomarsino 333 (GH)	Peru	KP014262	KP015010	KP014486	KP014691
Siphocampylus antonelli (Lagom. & Santam.)	L. Lagomarsino 400 (GH)	Peru	KP014085	KP014814	KP014372	KP014642
Siphocampylus siberiensis (Lagom & Santam)	L. Lagomarsino 241 (GH)	Bolivia	KP014274	KP014990	KP014440	KP014675

Table A.1 (continued)

Triodanis						
Triodanis perfoliata (L.) Nieuwl.	L. Lagomarsino 425 (GH)	USA	KP014049	-	KP014308	-

Table A.2. Fruit coding for character state reconstruction. Berry = 0; capsule =1. * indicates outgroup taxon.

Taxon	Fruit Coding
Burmeistera	
Burmeistera almedae Wilbur	0
Burmeistera aff. *bullatifolia* J. Garzón and F. González	0
Burmeistera aff. *bullatifolia* J. Garzón and F. González	0
Burmeistera ceratocarpa Zahlb.	0
Burmeistera chiriquiensis Wilbur	0
Burmeistera crebra McVaugh	0
Burmeistera cyclostigmata J. D. Smith	0
Burmeistera cyclostigmata J. D. Smith	0
Burmeistera cyclostigmata J. D. Smith	0
Burmeistera cyclostigmata J. D. Smith	0
Burmeistera cyclostigmata J. D. Smith	0
Burmeistera cyclostigmata J. D. Smith	0
Burmeistera dendrophila E. Wimm	0
Burmeistera domingensis Jeppesen	0
Burmeistera fuchsioides J. Garzón & F. González	0
Burmeistera mcvaughii Wilbur	0
Burmeistera mcvaughii Wilbur	0
Burmeistera microphylla J. D. Smith	0
Burmeistera microphylla J. D. Smith	0
Burmeistera aff. *minutiflora* J. Garzón and F. González	0
Burmeistera morii Wilbur	0
Burmeistera multiflora Zahlb.	0
Burmeistera obtusifolia E. Wimm	0
Burmeistera obtusifolia E. Wimm	0
Burmeistera parviflora E. Wimm	0
Burmeistera racemiflora Lammers	0
Burmeistera refracta E. Wimm.	0
Burmeistera refracta E. Wimm.	0
Burmeistera sodiroana Zahlb.	0
Burmeistera succulenta H. Karst. & Triana	0
Burmeistera tenuiflora J.D. Smith	0
Burmeistera tenuiflora J.D. Smith	0
Burmeistera toroensis Wilbur	0
Burmeistera utleyi Wilbur	0
Burmeistera variabilis (Gleason) E. Wimm.	0
Burmeistera vulgaris E. Wimm.	0
Burmeistera vulgaris E. Wimm.	0
Burmeistera vulgaris E. Wimm.	0
Burmeistera zurquiensis Wilbur	0
Burmeistera sp.	0
Burmeistera sp. nov. (Lagomarsino & Santam. ined.)	0

Table A.2 (Continued).

*Campanula**	
Campanula medium L.	1
Centropogon	
Centropogon aequatorialis E. Wimm.	0
Centropogon asclepiadeus (Willd.) E. Wimm.	0
Centropogon azuayensis Jeppesen	0
Centropogon baezanus Jeppesen	0
Centropogon bangii Zahlb.	0
Centropogon brittonianus Zahlb.	0
Centropogon brittonianus Zahlb.	0
Centropogon brittonianus Zahlb.	0
Centropogon cf. *calycinus* Benth.	0
Centropogon coccineus (Hook.) Regel ex B.D. Jacks.	0
Centropogon coccineus (Hook.) Regel ex B.D. Jacks.	0
Centropogon comosus Gleason	0
Centropogon congestus Gleason	0
Centropogon congestus Gleason	0
Centropogon cordifolius Benth.	0
Centropogon cornutus (L.) Druce	0
Centropogon cornutus (L.) Druce	0
Centropogon cornutus (L.) Druce	0
Centropogon cornutus (L.) Druce	0
Centropogon costaricae (Vatke) E. Wimm.	0
Centropogon costaricae (Vatke) E. Wimm.	0
Centropogon densiflorus Benth.	0
Centropogon dianae Lammers	0
Centropogon dissectus E. Wimm.	0
Centropogon dombeyanus E. Wimm	0
Centropogon erythraeus Drake	0
Centropogon featherstonei Gleason	0
Centropogon ferrugineus (L.f) Gleason	0
Centropogon ferrugineus (L.f) Gleason	0
Centropogon ferrugineus (L.f) Gleason	0
Centropogon gamosepalus Zahlb.	0
Centropogon glabrifilis (E. Wimm.) Jeppsen	0
Centropogon gloriosus (Britton) Zahlb.	0
Centropogon gloriosus (Britton) Zahlb.	0
Centropogon gloriosus (Britton) Zahlb.	0
Centropogon grandidentatus (Schlechtd.) Zahlb.	0
Centropogon granulosus C. Presl.	0
Centropogon granulosus C. Presl.	0
Centropogon granulosus C. Presl.	0
Centropogon granulosus C. Presl.	0
Centropogon granulosus subsp *lugens* Stein (ined)	0
Centropogon granulosus subsp. *granulosus* Stein (ined.)	0
Centropogon granulosus subsp. *nutans* Stein (ined.)	0
Centropogon granulosus subsp. *tortilis* Stein (ined.)	0
Centropogon gutierrezii (Planch & Oerst.) E. Wimm.	0

Table A.2 (Continued).

Centropogon incanus (Britton) Zahlb.	0
Centropogon incanus (Britton) Zahlb.	0
Centropogon incanus (Britton) Zahlbr..	0
Centropogon isabellinus Wimm	0
Centropogon isabellinus Wimm	0
Centropogon leucocarpus McVaugh	0
Centropogon llanganatensis Jeppsen	0
Centropogon luteus E. Wimm.	0
Centropogon luteynii Wilbur	0
Centropogon macbridei Gleason	0
Centropogon macrocarpus Zahlb.	0
Centropogon macrophyllus (G. Don.) E. Wimm	0
Centropogon magnificus Zahlb.	0
Centropogon magnificus Zahlb.	0
Centropogon mandonis Zahlb.	0
Centropogon mandonis Zahlb.	0
Centropogon medusa E. Wimm.	0
Centropogon minimus McVaugh	0
Centropogon minimus McVaugh	0
Centropogon nervosus Wimm	0
Centropogon nigricans Zahlb.	0
Centropogon nigricans Zahlb.	0
Centropogon palmanus (J. D. Smith) E. Wimm.	0
Centropogon panamensis Wilbur	0
Centropogon perlongus Gleason	0
Centropogon pichinchensis Zahlb.	0
Centropogon preslii E. Wimm.	0
Centropogon pulcher Zahlb.	0
Centropogon reticulatus Drake	0
Centropogon rex E. Wimm.	0
Centropogon rex E. Wimm.	0
Centropogon roseus Rusby	0
Centropogon salviaeformis Zahlb.	0
Centropogon simulans Lammers	0
Centropogon smithii E. Wimm.	0
Centropogon sodiroanus Zahlb.	0
Centropogon solanifolius Benth.	0
Centropogon solanifolius Benth.	0
Centropogon solanifolius Benth.	0
Centropogon solanifolius Benth.	0
Centropogon talamancensis Wilbur	0
Centropogon tessmannii E. Wimm.	0
Centropogon trachyanthus E. Wimm.	0
Centropogon trichodes E. Wimm.	0
Centropogon umbrosus E. Wimm	0
Centropogon unduavensis (Britton) Zahlb.	0
Centropogon urubambae E. Wimm	0
Centropogon valerii Standley	0

Table A.2 (Continued).

Centropogon viriduliflorus Wimm	0
Centropogon viriduliflorus Wimm	0
Centropogon weberbaueri Zahlb.	0
Centropogon cf. *weberbaueri* Zahlb.	0
Centropogon yarumalensis E. Wimm.	0
Centropogon yungasensis Britton	0
Centropogon yungasensis Britton	0
Centropogon cf. *yungasensis* Britton	0
Centropogon zamorensis Jeppesen	0
Centropogon sp. nov. (Lagomarsino & Santam ined.)	0
Centropogon sp. nov. (Lagomarsino & Santam ined.)	0
Diastatea	
Diastatea micrantha (Kunth) McVaugh	1
Hippobroma	
Hippobroma longiflora (L.) G. Don	1
Hippobroma longiflora (L.) G. Don	1
Isotoma	
Isotoma fluviatilis F. Muell. Ex Bentham	1
Lobelia	
Lobelia alsinoides Lam.	1
Lobelia bridgesii Hook & Arn.	1
Lobelia cardinalis L.	1
Lobelia cardinalis subsp. *graminea* (Lam.) McVaugh	1
Lobelia digitalifolia (Griseb.) Urb.	1
Lobelia excelsa Bonpland	1
Lobelia excelsa Bonpland	1
Lobelia hederacea Cham.	1
Lobelia inflata L.	1
Lobelia kalmii L.	1
Lobelia laxiflora Kunth.	1
Lobelia laxiflora Kunth.	1
Lobelia martagon Hitchc.	1
Lobelia nana Kunth.	1
Lobelia oligophylla (Wedd.) Lammers	1
Lobelia physaloides A. Cunn.	1
Lobelia tupa L.	1
Lobelia zeylanica L.	1
Lysipomia	
Lysipomia cuspidata McVaugh	1
Lysipomia muscoides Hook f.	1
Lysipomia pumila (Wedd.) E. Wimm.	1
Lysipomia sphagnophila Griseb. Ex Wedd.	1
Lysipomia vitreola McVaugh	1
Siphocampylus	
Siphocampylus actinothrix E. Wimm.	1
Siphocampylus aff. *actinothrix* E. Wimm.	1
Siphocampylus affinis (Mirb.) McVaugh	1
Siphocampylus ambivalens Lammers	1

Table A.2 (Continued).

Siphocampylus ambivalens Lammers	1
Siphocampylus andinus Britton	1
Siphocampylus andinus Britton	1
Siphocampylus angustiflorus Schlechtend.	1
Siphocampylus angustiflorus Schlechtend.	1
Siphocampylus antioquianus E. Wimm.	1
Siphocampylus asplundii Jeppesen	1
Siphocampylus aureus Rusby	1
Siphocampylus aureus Rusby	1
Siphocampylus ayersiae Lammers	1
Siphocampylus betulaefolius (Cham.) G. Don.	1
Siphocampylus bilabiatus Zahlb.	1
Siphocampylus bilabiatus Zahlb.	1
*Siphocampylus bilabiatus Z*ahlb.	1
Siphocampylus boliviensis Zahlb.	1
Siphocampylus boliviensis Zahlb.	1
Siphocampylus boliviensis Zahlb.	1
*Siphocampylus boliviensi*s Zahlb.	1
Siphocampylus brevicalyx E. Wimm.	1
Siphocampylus brevicalyx E. Wimm.	1
Siphocampylus chloroleucus E. Wimm	1
Siphocampylus citrinus Wimm	1
Siphocampylus citrinus Wimm	1
Siphocampylus convolvulaceus (Cham.) G. Don.	1
Siphocampylus correoides Zahlb.	1
Siphocampylus correoides Zahlb.	1
Siphocampylus corymbiferus Pohl	1
Siphocampylus corymbiferus Pohl	1
Siphocampylus corymbiferus Pohl	1
Siphocampylus corynoides E. Wimm	1
Siphocampylus domingensis A. DC.	1
Siphocampylus elfriedii E. Wimm	1
Siphocampylus fiebrigii E. Wimm	1
Siphocampylus fiebrigii E. Wimm	1
Siphocampylus flagelliformis Zahlb.	1
Siphocampylus flagelliformis Zahlb.	1
Siphocampylus fulgens Hort.	1
Siphocampylus giganteus (Cav.) G. Don.	1
Siphocampylus giganteus (Cav.) G. Don.	1
Siphocampylus igneus Urb.	1
Siphocampylus imbricatus (Cham.) G. Don.	1
Siphocampylus jelskii Zahlb.	1
Siphocampylus longepedunculatus Pohl	1
Siphocampylus longibracteolatus E. Wimm	1
Siphocampylus lycioides (Cham.) G. Don.	1
Siphocampylus macropodus (Billb.) G. Don.	1
Siphocampylus manettiaeflorus Hook.	1

Table A.2 (continued).

Siphocampylus matthiaei A. DC.	1
Siphocampylus matthiaei A. DC.	1
Siphocampylus membraceus Britton	1
Siphocampylus nematosepalus (Donn. Smith) E. Wimm	1
Siphocampylus nemoralis Griseb.	1
Siphocampylus neurotrichus E. Wimm	1
Siphocampylus neurotrichus E. Wimm	1
Siphocampylus nitidus Pohl	1
Siphocampylus oblongifolius Rusby	1
Siphocampylus oblongifolius Rusby	1
Siphocampylus obovatus (G. Don) E. Wimm	1
Siphocampylus orbignianus A. DC.	1
Siphocampylus puberulus E. Wimm	1
Siphocampylus pubescens Benth.	1
Siphocampylus aff. *rictus* Lammers	1
Siphocampylus rosmarinifolius G. Don.	1
Siphocampylus rusbyanus Britton	1
Siphocampylus rusbyanus Britton	1
Siphocampylus scandens (HBK) G. Don.	1
Siphocampylus sceptrum Decaisne apud Linden	1
Siphocampylus smilax Lammers	1
Siphocampylus sonchifolius (Sw.) McVaugh	1
Siphocampylus sparsipilus E. Wimm	1
Siphocampylus sparsipilus E. Wimm.	1
Siphocampylus tunarensis Zahlb.	1
Siphocampylus sp. nov. (Lagomarsino & Santam. ined.)	1
*Triodanis**	
Triodanis perfoliata (L.) Nieuwl.	1

Appendix B:

Supporting material for Chapter IV

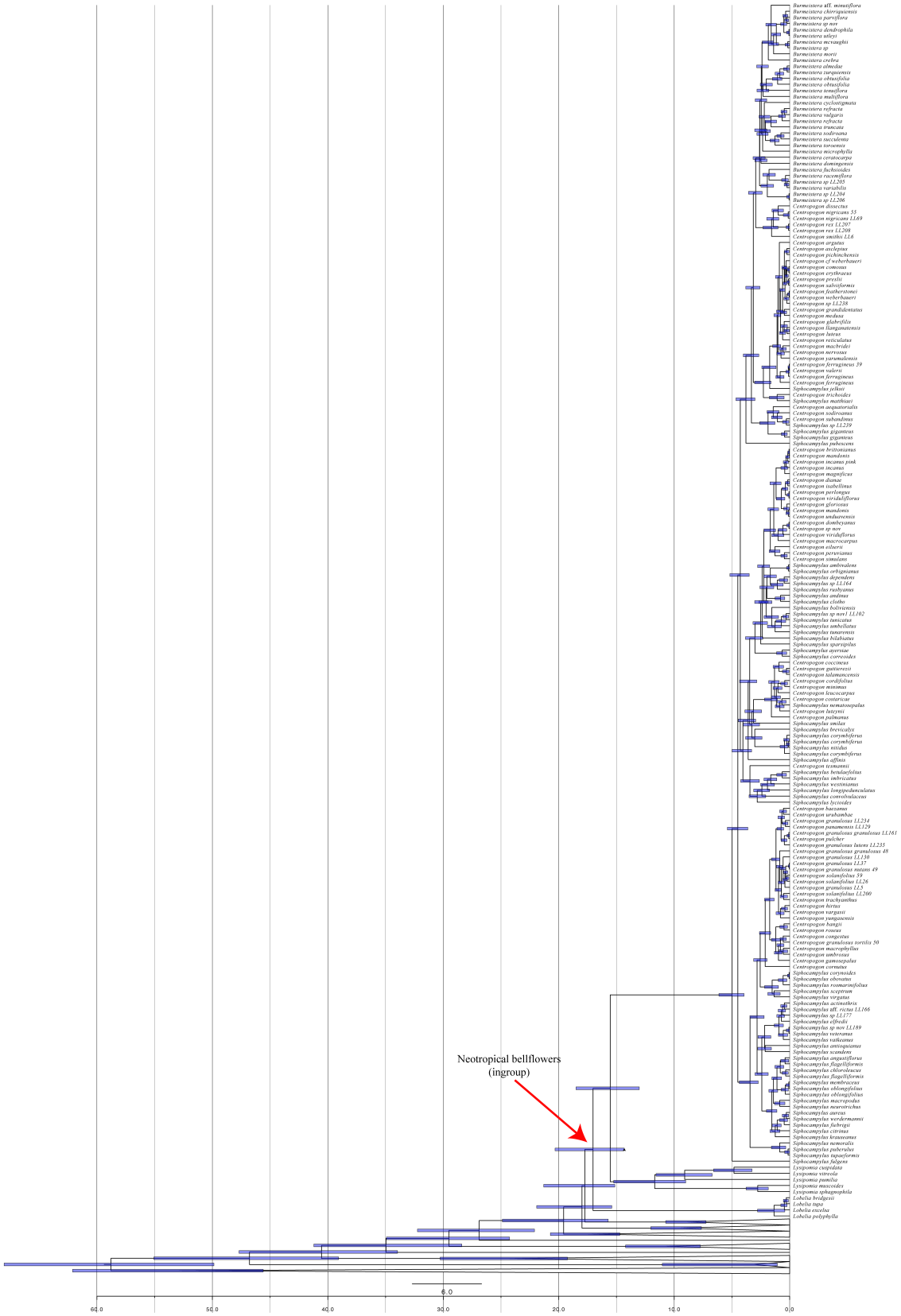


Figure B.1 (Continued on next page).

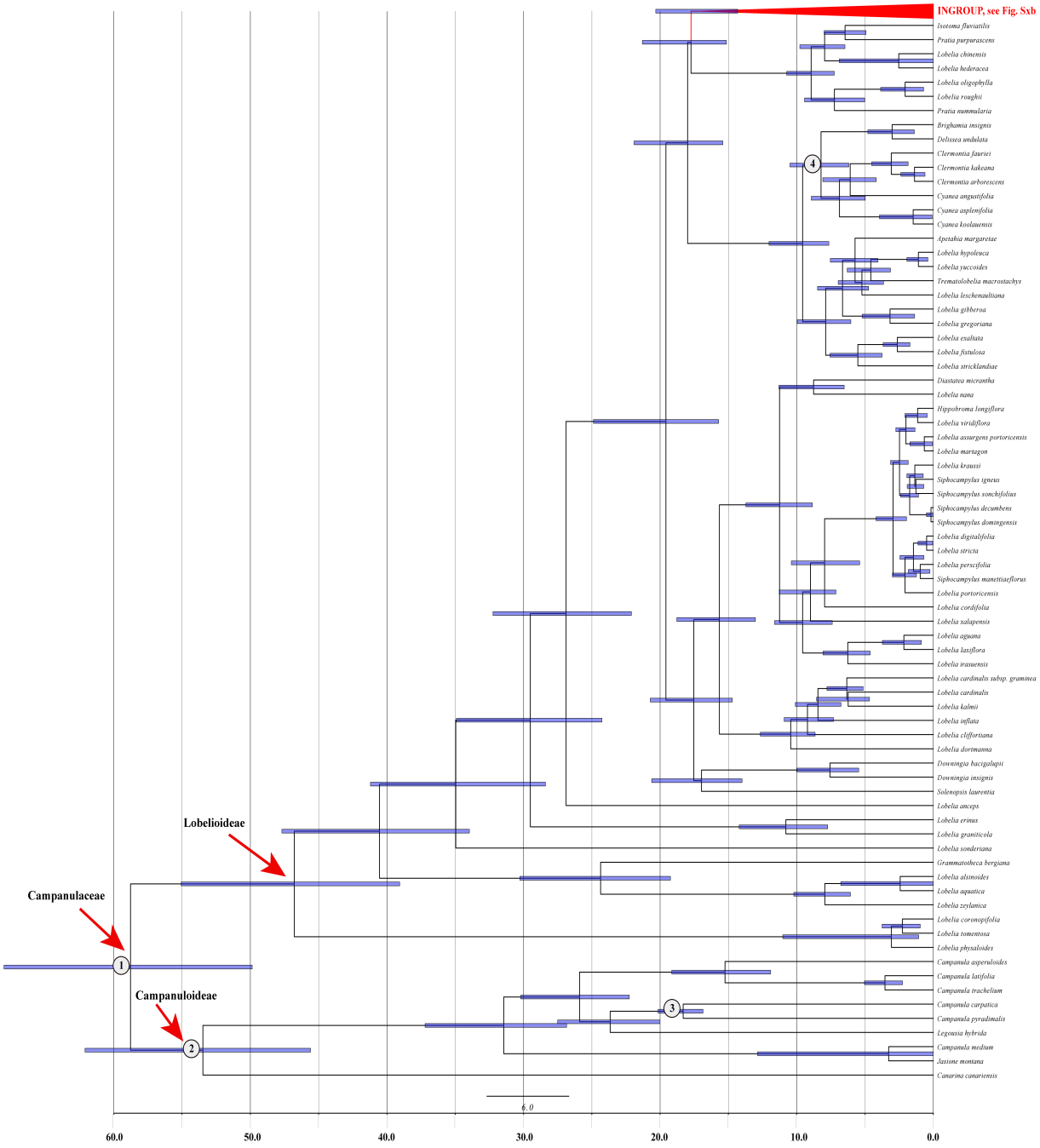


Figure B.1 (Continued).

Figure B.1 (Continued). Time-calibrated phylogeny of Neotropical Campanulaceae, including representatives of Lobelioideae and Campanuloideae. Phylogeny represents a maximum clade credibility tree resulting from BEAST2 analysis with four calibration points and implementing a lognormal relaxed molecular clock for the Neotropical bellflowers (ingroup; page 193) and outgroup species (page 194). The posterior distribution used to summarize this chronogram was applied in all subsequent diversification analyses. Bars at nodes represent the 95% highest posterior density (HPD) of inferred ages. Geological time series below the chronogram is in Ma. Page 193: Ingroup relationships, with outgroup clades collapsed. Red arrow marks the ingroup, the Neotropical bellflowers. Page 194: Outgroup relationships, with ingroup collapsed (in red, at top). Red arrows denote major taxonomic groups: Campanulaceae, Campanuloideae, and Lobelioideae. Numbers circled at nodes correspond to the four calibration points used to infer ages: 1) secondary age constraint for crown group Campanulaceae; 2) secondary age constraint for crown group Campanuloideae; 3) the fossil, *Campanula paleopyramidalis* at most recent common ancestor of *C. pyramidalis* Gilib. and *C. carpatica* Jacq.; and 4) the geological age constraint for the oldest island of the Hawaiian Ridge. See methods in Chapter 4 for additional details.

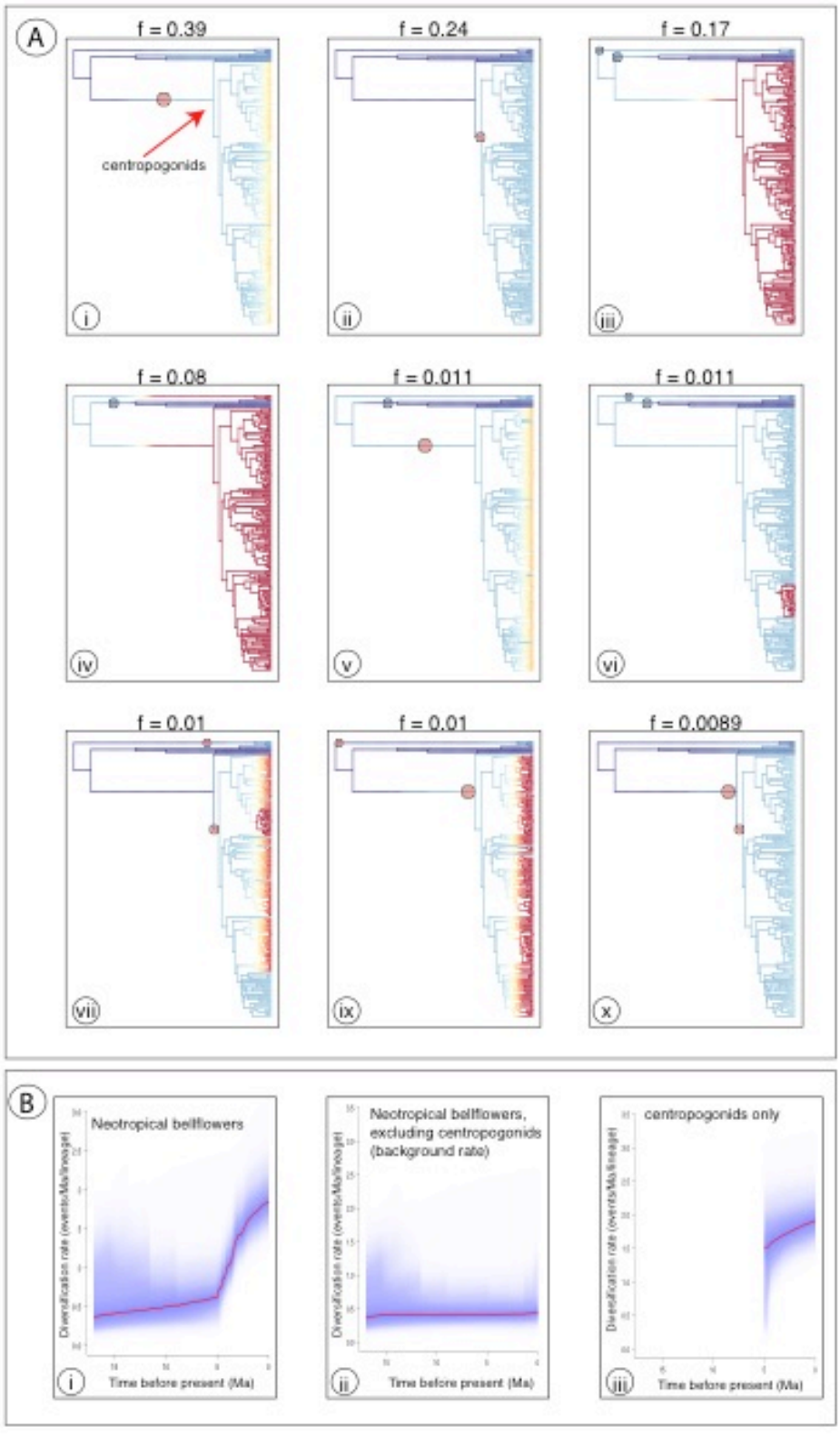


Figure B.2 (Continued on next page).

Figure B.2 (Continued). Diversification rate analysis using BAMM. A. 95% credible set of shift configurations from a BAMM analysis. Circles on branches denote inferred shift in evolutionary rates: red (increase), blue (decrease). Colors of branches denote directionality and strength of rate change, cooler and warmer colors designate slower and faster rates, respectively. Significant rate changes are designated by a circle along the branch at which this shift takes place. Note that among the 95% credible set of shift configurations, the majority (~67% of the shift configurations) indicate a significant increase in diversification rate at or near the origin of the centropogonid clade (highlighted with red arrow, Ai). Bi–iii. Diversification rates (in events/Ma/lineage) through time for the Neotropical bellflower clade (i), Neotropical bellflowers minus the centropogonid clade (ii), and the centropogonid clade alone (iii). Shading in B denotes confidence interval in rate reconstructions.

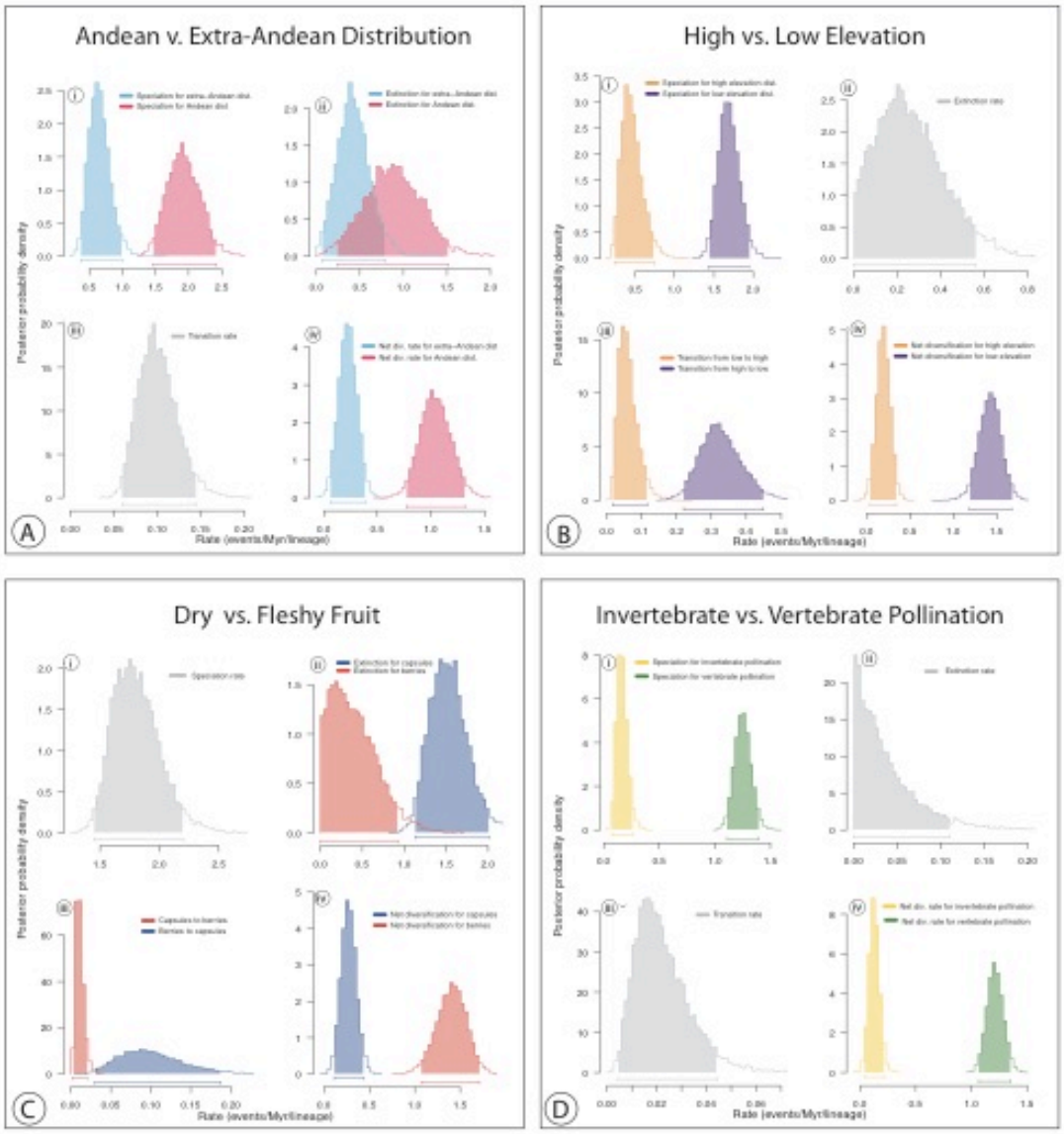


Figure B.3. Posterior distributions of trait-dependent speciation (i), extinction (ii), transition (iii), and net diversification rates (iv) as estimated by BiSSE. Histogram colors correspond to Fig. 1 in the main text for each trait, except when the parameter is indistinguishable between the two traits (in which case it is colored gray). A. Andean vs. extra-Andean parameter estimates. B. High vs. low elevation parameter estimates. C. Dry capsule vs. fleshy berry parameter estimates. D. Vertebrate vs. invertebrate pollination parameter estimates.

Table B.1. Divergence time estimation to assess sensitivity to dating method, calibration selection, and branch length heterogeneity. Analysis in boldface denoted with an asterisk is the one presented in the main text and used in subsequent diversification analyses. Age estimates reported for major clades relevant to the study reported in million years (Ma). Root node = crown group Campanulaceae.

	Campanulaceae	Campanul-oideae	Lobelioideae	Neotropical Lobelioideae	*Lobelia* section *Tupa*	*Lysipomia*	centropogonid clade
treePL dates from RAxML bootstrap trees:							
All priors	58.19 (55.89-61.62)	56.13 (55.87-57.0)	54.98 (51.71-56.00)	20.15 (18.06-22.04)	1.07 (0.36-1.35)	13.05 (11.13-14.36)	5.12 (4.24-5.83)
Three priors (fossil and secondary ages)	57.15 (55.90–61.76)	55.93 (55.87–56.0)	55.03 (51.72–56.0)	20.24 (18.09–22.04)	0.86 (0.34–1.33)	13.08 (11.13–14.37)	5.32 (4.22–5.86)
Two priors (fossil and root age)	66.89 (66.88–67.0)	65.41 (60.64–66.95)	64.65 (56.13–66.94)	24.73 (20.74–25.40)	1.01 (0.15–1.20)	15.21 (13.01–16.38)	6.22 (4.76–6.67)
One prior (root age only)	66.69 (66.88–67.0)	65.34 (60.65–66.96)	63. 66 (56.13–66.93)	23.58 (21.19–25.25)	1.01 (0.147–1.20)	15.3 (12.85–16.38)	6.24 (4.76–6.68)
All priors, *Lysipomia* removed	60.17 (55.98–62.09)	56 (55.87–56.0)	53.42 (50.96–56.12)	17.33 (13.97–18.31)	0.34 (0.31–1.31)	N/A	4.62 (4.14–5.45)
BEAST dates, all with expanded outgroup							
All priors, exponential relaxed clock	57.1 (44-69.55)	46.57 (36.28-56.39)	49.8 (35.88-65.20)	16.26 (9.44-22.51)	0.9 (0.18-2.63)	8.2 (4.70-13.06)	5.94 (3.32-9.54)
All priors, lognormal relaxed clock*	**58.78 (49.87-68.04)**	**53.48 (45.60-62.11)**	**46.79 (39.07-55.07)**	**17.74 (14.32-20.32)**	**1.35 (0.42-2.78)**	**11.69 (9.00-15.24)**	**4.98 (3.95-6.13)**
Three priors (fossil and secondary ages), lognormal relaxed clock	59.2 (46.81-72.03)	48.55 (38.38-59.31)	51.78 (37.87-66.55)	16.07 (10.54-22.32)	0.95 (0.22-2.75)	8.97 (5.08-13.83)	6.55 (3.74-9.95)
Two priors (fossil and root age), lognormal relaxed clock	62.47 (48.31-76.38)	53.23 (39.67-68.62)	51.52 (34.62-69.17)	17.78 (9.69-24.49)	0.97 (0.30-2.90)	9.24 (5.03-13.89)	6.71 (3.87-10.46)
One prior (root age only), lognormal relaxed clock	53.4 (35.61-69.51)	20.33 (9.69-34.34)	43.62 (19.68-57.10)	12.11 (6.27-18.80)	0.68 (0.10-2.17)	6.37 (2.84-9.89)	4.77 (2.25-7.67)
All priors, *Lysipomia* removed	58.77 (47.0-71.94)	49.16 (37.82-59.07)	50.05 (35.34-66.99)	11.8 (6.93-17.63)	0.85 (0.15-0.86)	N/A	6.11 (3.78-9.47)

Table B.2. Trait codings for the traits used in our BiSSE analyses. Character states: Andean distribution 0=extra-Andean, 1= Andean; Elevation– 0= Low (<1900m), 1= High (>1900 m); Fruit– 0= Capsule, 1= Berry; Pollinator– 0– Invertebrate, 1– Vertebrate

	Andean Distribution	Elevation	Fruit	Pollinator
Burmeistera almedae Wilbur	0	1	1	1
Burmeistera aff. *bullatifolia* J. Garzón & F. Gonzalez	1	1	1	1
Burmeistera aff. *bullatifoli*a J. Garzón & F. Gonzalez	1	1	1	1
Burmeistera ceratocarpa Zahlb.	1	0	1	1
Burmeistera chiriquiensis Wilbur	0	1	1	1
Burmeistera crebra McVaugh	0	1	1	1
Burmeistera cyclostigmata J. D. Smith	0	1	1	1
Burmeistera dendrophila E. Wimm	0	1	1	1
Burmeistera domingensis Jeppesen	1	0	1	1
Burmeistera fuchsioides J. Garzón & F. Gonzalez	1	1	1	1
Burmeistera mcvaughii Wilbur	0	1	1	1
Burmeistera mcvaughii Wilbur	0	1	1	1
Burmeistera microphylla J. D. Smith	0	0	1	1
Burmeistera aff. *minutiflora* J. Garzón & F. Gonzalez	1	1	1	0
Burmeistera morii Wilbur	0	0	1	1
Burmeistera multiflora Zahlb.	1	0	1	1
Burmeistera obtusifolia E. Wimm	0	1	1	1
Burmeistera obtusifolia E. Wimm	0	1	1	1
Burmeistera parviflora E. Wimm	0	1	1	0
Burmeistera racemiflora Lammers	1	0	1	1
Burmeistera refracta E. Wimm.	1	0	1	1
Burmeistera refracta E. Wimm.	1	0	1	1
Burmeistera sodiroana Zahlb.	1	1	1	1
Burmeistera succulenta H. Karst. & Triana	1	0	1	1
Burmeistera tenuiflora J.D. Smith	0	0	1	1
Burmeistera toroensis Wilbur	0	0	1	1
Burmeistera truncata Zahlbr.	1	0	1	1
Burmeistera utleyi Wilbur	0	1	1	1
Burmeistera variabilis (Gleason) E. Wimm.	1	0	1	1
Burmeistera vulgaris E. Wimm.	0	0	1	1
Burmeistera zurquiensis Wilbur	0	1	1	1
Burmeistera sp.	1	1	1	1
Burmeistera sp. nov.	0	1	1	0
Centropogon aequatorialis E. Wimm.	1	1	1	1
Centropogon argutus E. Wimm.	1	1	1	1
Centropogon asclepiadeus (Willd.) E. Wimm.	1	1	1	1
Centropogon azuayensis Jeppesen	1	1	1	1
Centropogon baezanus Jeppesen	1	1	1	1
Centropogon bangii Zahlb.	1	0	1	1
Centropogon brittonianus Zahlb.	1	1	1	1
Centropogon coccineus (Hook.) Regel ex B.D. Jacks.	0	0	1	1
Centropogon comosus Gleason	1	1	1	1
Centropogon congestus Gleason	0	0	1	1
Centropogon cordifolius Benth.	0	0	1	1
Centropogon cornutus (L.) Druce	0	0	1	1
Centropogon costaricae (Vatke) E. Wimm.	0	1	1	1
Centropogon dianae Lammers	1	1	1	1
Centropogon dissectus E. Wimm.	1	1	1	1
Centropogon dombeyanus E. Wimm	1	1	1	1
Centropogon eilersii Lammers & M.O. Dillon	1	1	1	1
Centropogon erythraeus Drake	1	1	1	1
Centropogon featherstonei Gleason	1	1	1	1
Centropogon ferrugineus (L.f) Gleason	0	1	1	1
Centropogon ferrugineus (L.f) Gleason	0	1	1	1
Centropogon ferrugineus (L.f) Gleason	0	1	1	1

Table B.2 (Continued).

Centropogon foetidus (Kunth) E. Wimm.	1	1	1	1
Centropogon gamosepalus Zahlb.	1	0	1	1
Centropogon glabrifilis (E. Wimm.) Jeppsen	1	1	1	1
Centropogon gloriosus (Britton) Zahlb.	1	1	1	1
Centropogon grandidentatus (Schltdl.) Zahlbr.	0	0	1	1
Centropogon granulosus subsp. *granulosus* Stein (ined.) 1	1	0	1	1
Centropogon granulosus subsp. *granulosus* Stein (ined.) 2	1	0	1	1
Centropogon granulosus subsp. *lugens* Stein (ined)	1	0	1	1
Centropogon granulosus subsp. *nutans* Stein (ined.)	0	0	1	1
Centropogon granulosus subsp. *tortilis* Stein (ined.)	0	0	1	1
Centropogon granulosus C. Presl. 1	1	0	1	1
Centropogon granulosus C. Presl. 2	0	0	1	1
Centropogon granulosus C. Presl. 3	0	0	1	1
Centropogon granulosus C. Presl. 4	0	0	1	1
Centropogon gutierrezii (Planch & Oerst.) E. Wimm.	0	1	1	1
Centropogon hirtus (Cav.) C. Presl.	1	1	1	1
Centropogon incanus (Britton) Zahlb.	1	1	1	1
Centropogon incanus (Britton) Zahlbr..	1	1	1	1
Centropogon isabellinus E. Wimm.	1	1	1	1
Centropogon leucocarpus McVaugh	0	1	1	1
Centropogon llanganatensis Jeppsen	1	1	1	1
Centropogon luteus E. Wimm.	1	1	1	1
Centropogon luteynii Wilbur	0	1	1	1
Centropogon macbridei Gleason	1	1	1	1
Centropogon macrocarpus Zahlb.	1	1	1	1
Centropogon macrophyllus (G. Don.) E. Wimm	1	0	1	1
Centropogon magnificus Zahlb.	1	1	1	1
Centropogon mandonis Zahlb.	1	1	1	1
Centropogon mandonis Zahlb.	1	1	1	1
Centropogon medusa E. Wimm.	1	1	1	1
Centropogon minimus McVaugh	1	1	1	1
Centropogon nervosus Wimm	1	1	1	1
Centropogon nigricans Zahlb.	1	1	1	1
Centropogon nigricans Zahlb.	1	1	1	1
Centropogon palmanus (J. D. Smith) E. Wimm.	0	0	1	1
Centropogon panamensis Wilbur	0	0	1	1
Centropogon perlongus Gleason	1	1	1	1
Centropogon peruvianus (E. Wimm.) McVaugh	1	1	1	1
Centropogon pichinchensis Zahlb.	1	1	1	1
Centropogon preslii E. Wimm.	1	1	1	1
Centropogon pulcher Zahlb.	1	0	1	1
Centropogon reticulatus Drake	1	1	1	1
Centropogon rex E. Wimm.	1	1	1	1
Centropogon roseus Rusby	1	0	1	1
Centropogon salviaeformis Zahlb.	1	1	1	1
Centropogon simulans Lammers	1	1	1	1
Centropogon smithii E. Wimm.	0	1	1	1
Centropogon sodiroanus Zahlb.	1	1	1	1
Centropogon solanifolius Benth. 1	1	1	1	1
Centropogon solanifolius Benth. 2	0	1	1	1
Centropogon solanifolius Benth. 3	0	1	1	1
Centropogon subandinus Zahlb.	1	1	1	1
Centropogon talamancensis Wilbur	0	1	1	1
Centropogon tessmannii E. Wimm.	1	0	1	1
Centropogon trachyanthus E. Wimm.	1	1	1	1
Centropogon trichodes E. Wimm.	1	1	1	1
Centropogon umbrosus E. Wimm	1	1	1	1
Centropogon unduavensis (Britton) Zahlb.	1	1	1	1
Centropogon urubambae E. Wimm	1	0	1	1
Centropogon valerii Standley	0	1	1	1
Centropogon vargasii B. A. Stein (ined.)	1	1	1	1
Centropogon viriduliflorus Wimm	1	1	1	1
Centropogon viriduliflorus Wimm	1	1	1	1
Centropogon weberbaueri Zahlb.	1	1	1	1
Centropogon cf. *weberbaueri* Zahlb.	1	1	1	1
Centropogon yarumalensis E. Wimm.	1	1	1	1

Table B.2 (Continued).

Centropogon yungasensis Britton	1	1	1	1
Centropogon sp. nov. (Lagom. & Santam. ined.)	1	1	1	1
Centropogon sp.	1	1	1	1
Lobelia bridgesii Hook & Arn.	1	0	0	1
Lobelia excelsa Bonpland	1	0	0	1
Lobelia polyphylla Hook. & Arn.	1	0	0	1
Lobelia tupa L.	1	0	0	1
Lysipomia cuspidata McVaugh	1	1	0	0
Lysipomia muscoides Hook f.	1	1	0	0
Lysipomia pumila (Wedd.) E. Wimm.	1	1	0	0
Lysipomia sphagnophila Griseb. Ex Wedd.	1	1	0	0
Lysipomia vitreola McVaugh	1	1	0	0
Siphocampylus actinothrix E. Wimm.	1	1	0	1
Siphocampylus aff. *actinothrix* E. Wimm.	1	1	0	1
Siphocampylus affinis (Mirb.) McVaugh	1	1	0	1
Siphocampylus ambivalens Lammers	1	1	0	1
Siphocampylus andinus Britton	1	1	0	1
Siphocampylus angustiflorus Schlechtend.	1	1	0	1
Siphocampylus antioquianus E. Wimm.	1	1	0	1
Siphocampylus aureus Rusby	1	0	0	1
Siphocampylus ayersiae Lammers	1	1	0	1
Siphocampylus betulaefolius (Cham.) G. Don.	0	0	0	1
Siphocampylus bilabiatus Zahlb.	1	0	0	1
Siphocampylus boliviensis Zahlb.	1	1	0	1
Siphocampylus brevicalyx E. Wimm.	1	1	0	1
Siphocampylus chloroleucus E. Wimm	1	1	0	1
Siphocampylus citrinus E. Wimm	1	1	0	1
Siphocampylus clotho E. Wimm.	1	1	0	1
Siphocampylus convolvulaceus (Cham.) G. Don.	0	0	0	1
Siphocampylus correoides Zahlb.	1	1	0	1
Siphocampylus corymbifer Pohl	1	0	0	1
Siphocampylus corymbifer Pohl	1	0	0	1
Siphocampylus corymbifer Pohl	1	0	0	1
Siphocampylus corynoides E. Wimm	1	1	0	1
Siphocampylus dependens (Ruiz & Pavon) G. Don	1	1	0	1
Siphocampylus elfriedii E. Wimm	1	1	0	1
Siphocampylus fiebrigii E. Wimm	1	0	0	1
Siphocampylus flagelliformis Zahlb.	1	1	0	1
Siphocampylus flagelliformis Zahlb.	1	1	0	1
Siphocampylus fulgens Hort.	0	0	0	1
Siphocampylus giganteus (Cav.) G. Don.	1	1	0	1
Siphocampylus giganteus (Cav.) G. Don.	1	1	0	1
Siphocampylus imbricatus (Cham.) G. Don.	0	0	0	1
Siphocampylus jelskii Zahlb.	1	1	0	1
Siphocampylus krauseanus E. Wimm.	1	1	0	1
Siphocampylus longipedunculatus Pohl	0	0	0	1
Siphocampylus lycioides (Cham.) G. Don.	0	0	0	1
Siphocampylus macropodus (Billb.) G. Don.	0	0	0	1
Siphocampylus matthiaei A. DC.	1	1	0	1
Siphocampylus membraceus Britton	1	0	0	1
Siphocampylus nematosepalus (Donn. Smith) E. Wimm	0	1	0	1
Siphocampylus nemoralis Griseb.	1	1	0	1
Siphocampylus neurotrichus E. Wimm	1	0	0	1
Siphocampylus nitidus Pohl	0	0	0	1
Siphocampylus oblongifolius Rusby	1	0	0	1
Siphocampylus oblongifolius Rusby	1	0	0	1
Siphocampylus obovatus (G. Don) E. Wimm	1	1	0	1
Siphocampylus orbignianus A. DC.	1	0	0	1
Siphocampylus puberulus E. Wimm	1	1	0	1
Siphocampylus pubescens Benth.	1	1	0	1
Siphocampylus aff. *rictus* Lammers	1	1	0	1
Siphocampylus rosmarinifolius G. Don.	1	1	0	1
Siphocampylus rusbyanus Britton	1	1	0	1
Siphocampylus scandens (HBK) G. Don.	1	1	0	1
Siphocampylus sceptrum Decaisne apud Linden	1	1	0	1
Siphocampylus smilax Lammers	1	0	0	1

Table B.2 (Continued).

Siphocampylus sparsipilus E. Wimm	1	1	0	1
Siphocampylus tunarensis Zahlb.	1	1	0	1
Siphocampylus tunicatus Zahlb.	1	1	0	1
Siphocampylus tupaeformis Zahlb.	1	1	0	1
Siphocampylus umbellatus (HBK) G. Don.	1	1	0	1
Siphocampylus vatkeanus Zahlb.	1	1	0	1
Siphocampylus veteranus Wimm	1	1	0	1
Siphocampylus virgatus A. DC.	1	0	0	1
Siphocampylus werdermannii E. Wimm	1	1	0	1
Siphocampylus westinianus (Billb.) Pohl	0	0	0	1
Siphocampylus sp.	1	1	0	1
Siphocampylus siberiensis (Lagom. & Santam. ined.)	1	1	0	1
Siphocampylus antonelli (Lagom. & Santam. ined.)	1	1	0	1

Table B.3. Paleoenvironmental-dependent diversification analyses using paleoaltimetry and Cenozoic climate data. Mean parameter estimates presented for each model. Best-fitting model, as determined via a combination of the Aikake Information Criterion and likelihood ratio tests (see main text methods) highlighted in red and boldface. In our best fit paleoaltitude-dependent model, speciation is positively exponentially correlated to Andean orogeny over time; adding extinction as a parameter did not improve model fit. Likewise, extinction is positively linearly correlated to temperature variation over time; allowing speciation to vary with temperature did not improve model fit. λ = speciation rate (in events/Ma/lineage); μ = extinction rate (in events/Ma/lineage); α = rate of variation of the speciation according to the relevant paleoenvironmental variable; β = rate of variation of the extinction according to the paleoenvironmental variable; NP: number of parameters in each model.

Table B.3 (Continued).

Paleoaltitude Dependence

Model	Mode of dependency	NP	logL	AICc	ΔAIC	P (LRT)	λ	α	μ	β
λ Alti.; no μ	**Exponential**	**2**	**-267.358**	**538.78**	**0**	**Best**	**0.0010**	**0.0025**	**-**	**-**
λ Alti; μ constant	Exponential	3	-266.863	539.85	1.07	0.320	0.0004	0.0026	0.0184	-
λ constant; μ Alti.	Exponential	3	-271.228	548.58	9.80	0.999	2.3894	-	6.1267	-0.0003
λ Alti.; μ Alti.	Exponential	4	-266.523	541.25	2.47	0.434	0.0016	0.0021	0.0611	-0.0331
λ Alti.; no μ	Linear	2	-281.176	566.41	27.64	0.999	2.1972	-0.0008	-	-
λ Alti.; μ constant	Linear	3	-268.544	543.21	4.44	0.999	2.3254	-0.0009	0.9437	-
λ constant; μ Alti.	Linear	3	-271.499	549.12	10.34	0.999	2.1654	-	4.1010	-0.0007
λ Alti.; μ Alti.	Linear	4	-270.284	548.77	9.99	0.999	2.7205	0.0001	1.7161	-0.0001

Temperature Dependence

Model	Mode of dependency	NP	logL	AICc	ΔAIC	P (LRT)	λ	α	μ	β
λ Temp.; no μ	Exponential	2	-268.613	541.29	5.24	0.999	2.7463	-0.4332	-	-
λ Temp.; μ constant	Exponential	3	-265.353	536.83	0.79	0.999	2.5085	-0.1436	1.0536	-
λ constant; μ Temp.	Exponential	3	-265.248	536.62	0.58	0.999	2.2038	-	1.2030	0.10578
λ Temp.; μ Temp.	Exponential	4	-264.955	538.11	2.07	0.913	2.2776	-0.0552	1.0695	0.07642
λ Temp.; no μ	Linear	2	-272.381	548.82	12.78	0.999	1.6588	-0.2392	-	-
λ Temp.; μ constant	Linear	3	-265.748	537.62	1.57	0.999	2.1378	-0.2623	0.6189	-
λ constant; μ Temp.	Linear	3	-264.961	536.044	0	Best	2.1238	-	0.9730	0.20179
λ Temp.; μ Temp.	Linear	4	-264.575	537.355	1.310	0.3796	1.7996	0.28453	0.7834	0.47501

Table B.4. Model comparison for the four BiSSE analyses presented in the main text. Best-fitting model, as determined via a combination of the Aikake Information Criterion and likelihood ratio tests (LRT), is in red and bold text. The best model is first identified with the lowest AICc and then compared to other models with ΔAIC and LRT. The best-fitting models show that there is higher net diversification in the Andes (vs. extra-Andes), at high elevation (vs. low elevation), in berry-producing lineages (vs. capsular lineages), and in vertebrate-pollinated lineages (vs. invertebrate-pollinated lineages). Our second and third best models in each scenario also support these conclusions. λ = speciation rate (in events/Ma/lineage); μ = extinction rate (in events/Ma/lineage); q = transition rate between states; NP, number of parameter in each model.

Table B.4 (Continued).

Andes (0: extra-Andean; 1: Andean)											
Model	**NP**	**LogL**	**AICc**	**ΔAIC**	**P (LRT)**	**λ_0**	**λ_1**	**μ_0**	**μ_1**	**q_{01}**	**q_{10}**
Null model ($\lambda_0=\lambda_1$; $\mu_0=\mu_1$;$q_{01}=q_{10}$)	3	-361.737	729.597	15.332	0.99	2.932	2.932	2.592	2.592	0.084	0.084
$\lambda_0\neq\lambda_1$; $\mu_0=\mu_1$; $q_{01}=q_{10}$	4	-354.666	717.537	3.271	0.99	1.908	2.541	1.818	1.818	0.089	0.089
$\lambda_0=\lambda_1$; $\mu_0\neq\mu_1$; $q_{01}=q_{10}$	4	-357.126	722.457	8.192	0.99	2.713	2.713	2.621	2.164	0.102	0.102
$\lambda_0=\lambda_1$; $\mu_0=\mu_1$; $q_{01}\neq q_{10}$	4	-359.261	726.726	12.460	0.99	2.924	2.924	2.583	2.583	0.273	0.077
$\lambda_0\neq\lambda_1$; $\mu_0\neq\mu_1$; $q_{01}=q_{10}$	**5**	**-351.978**	**714.266**	**0**	**Best**	**1.267**	**2.975**	**1.152**	**2.275**	**2.275**	**2.275**
$\lambda_0\neq\lambda_1$; $\mu_0=\mu_1$; $q_{01}\neq q_{10}$	5	-352.912	716.133	1.867	0.99	1.690	2.477	1.636	1.636	0.043	0.109
$\lambda_0=\lambda_1$; $\mu_0\neq\mu_1$; $q_{01}\neq q_{10}$	5	-354.944	720.197	5.931	0.99	2.348	2.348	2.305	1.510	0.031	0.123
$\lambda_0\neq\lambda_1$; $\mu_0\neq\mu_1$; $q_{01}\neq q_{10}$	6	-351.892	716.219	1.953	0.678	1.292	2.938	1.184	2.224	0.081	0.088
Elevation (0: low; 1: high)											
Model	**NP**	**LogL**	**AICc**	**ΔAIC**	**P (LRT)**	**λ_0**	**λ_1**	**μ_0**	**μ_1**	**q_{01}**	**q_{10}**
Null model ($\lambda_0=\lambda_1$; $\mu_0=\mu_1$; $q_{01}=q_{10}$)	3	-370.173	746.468	16.468	0.99	2.994	2.994	2.656	2.656	0.175	0.175
$\lambda_0\neq\lambda_1$; $\mu_0=\mu_1$; $q_{01}=q_{10}$	4	-365.927	740.060	10.060	0.99	2.554	2.973	2.465	2.465	0.209	0.209
$\lambda_0=\lambda_1$; $\mu_0\neq\mu_1$; $q_{01}=q_{10}$	4	-367.173	742.551	12.551	0.99	2.944	2.944	2.822	2.480	0.206	0.206
$\lambda_0=\lambda_1$; $\mu_0=\mu_1$; $q_{01}\neq q_{10}$	4	-367.360	742.924	12.924	0.99	2.989	2.989	2.650	2.650	0.353	0.119
$\lambda_0\neq\lambda_1$; $\mu_0\neq\mu_1$; $q_{01}=q_{10}$	5	-360.316	730.942	0.942	0.99	0.963	3.566	0.740	2.876	2.876	2.876
$\lambda_0\neq\lambda_1$; $\mu_0=\mu_1$; $q_{01}\neq q_{10}$	**5**	**-359.845**	**730.000**	**0**	**Best**	**1.418**	**2.427**	**1.349**	**1.349**	**0.034**	**0.274**
$\lambda_0=\lambda_1$; $\mu_0\neq\mu_1$; $q_{01}\neq q_{10}$	5	-362.785	735.880	5.880	0.99	2.244	2.244	2.193	1.177	0.024	0.300
$\lambda_0\neq\lambda_1$; $\mu_0\neq\mu_1$; $q_{01}\neq q_{10}$	6	-358.759	729.952	*-0.048*	0.141	1.079	2.956	0.965	2.037	0.064	0.227

** the lowest AIC is the model with 6 parameters, but it has a small ΔAIC as compared to simplest models*

Table B.4 (Continued).

Fruit type (0: capsule; 1: berry)											
Model	**NP**	**LogL**	**AICc**	**ΔAIC**	**P (LRT)**	**λ_0**	**λ_1**	**μ_0**	**μ_1**	**q_{01}**	**q_{10}**
Null model ($\lambda_0=\lambda_1$; $\mu_0=\mu_1$; $q_{01}=q_{10}$)	3	-319.636	645.395	22.804	0.99	2.815	2.815	2.469	2.469	0.037	0.037
$\lambda_0\neq\lambda_1$; $\mu_0=\mu_1$; $q_{01}=q_{10}$	4	-310.059	628.324	5.733	0.99	1.954	2.666	1.692	1.692	0.024	0.024
$\lambda_0=\lambda_1$; $\mu_0\neq\mu_1$; $q_{01}=q_{10}$	4	-310.192	628.588	5.998	0.99	2.280	2.280	2.044	1.186	0.018	0.018
$\lambda_0=\lambda_1$; $\mu_0=\mu_1$; $q_{01}\neq q_{10}$	4	-319.270	646.745	24.155	0.99	2.814	2.814	2.467	2.467	0.030	0.052
$\lambda_0\neq\lambda_1$; $\mu_0\neq\mu_1$; $q_{01}=q_{10}$	5	-309.859	630.028	7.437	0.99	2.055	2.498	1.804	1.460	1.460	1.460
$\lambda_0\neq\lambda_1$; $\mu_0=\mu_1$; $q_{01}\neq q_{10}$	5	-307.565	625.438	2.848	0.99	1.937	2.715	1.701	1.701	0.014	0.067
$\lambda_0=\lambda_1$; $\mu_0\neq\mu_1$; $q_{01}\neq q_{10}$	**5**	**-306.141**	**622.591**	**0**	**Best**	**2.220**	**2.220**	**2.018**	**1.017**	**0.009**	**0.081**
$\lambda_0\neq\lambda_1$; $\mu_0\neq\mu_1$; $q_{01}\neq q_{10}$	6	-305.982	624.400	1.809	0.573	2.364	2.111	2.170	0.875	0.008	0.085
Pollinator class (0: invertebrate; 1: vertebrate)											
Model	**NP**	**LogL**	**AICc**	**ΔAIC**	**P (LRT)**	**λ_0**	**λ_1**	**μ_0**	**μ_1**	**q_{01}**	**q_{10}**
Null model ($\lambda_0=\lambda_1$; $\mu_0=\mu_1$;$q_{01}=q_{10}$)	3	-290.715	587.553	37.753	0.99	2.847	2.847	2.501	2.501	0.013	0.013
$\lambda_0\neq\lambda_1$; $\mu_0=\mu_1$;$q_{01}=q_{10}$	**4**	**-270.798**	**549.800**	**0**	**Best**	**0.998**	**1.943**	**0.970**	**0.970**	**0.011**	**0.011**
$\lambda_0=\lambda_1$; $\mu_0\neq\mu_1$; $q_{01}=q_{10}$	4	-272.780	553.766	3.966	0.99	2.051	2.051	2.045	1.144	0.007	0.007
$\lambda_0=\lambda_1$; $\mu_0=\mu_1$; $q_{01}\neq q_{10}$	4	-290.087	588.379	38.579	0.99	2.844	2.844	2.498	2.498	0.001	0.015
$\lambda_0\neq\lambda_1$; $\mu_0\neq\mu_1$; $q_{01}=q_{10}$	5	-269.357	549.023	*-0.777*	0.089	0.351	2.093	0.255	1.155	1.155	1.155
$\lambda_0\neq\lambda_1$; $\mu_0=\mu_1$; $q_{01}\neq q_{10}$	5	-270.113	550.534	0.734	0.242	0.990	1.952	0.968	0.968	0.007	0.021
$\lambda_0=\lambda_1$; $\mu_0\neq\mu_1$; $q_{01}\neq q_{10}$	5	-271.390	553.089	3.289	0.99	1.992	1.992	1.998	1.037	0.004	0.022
$\lambda_0\neq\lambda_1$; $\mu_0\neq\mu_1$; $q_{01}\neq q_{10}$	6	-269.330	551.094	1.294	0.23	0.377	2.083	0.288	1.140	0.016	0.019

** the lowest AIC is the model with 5 parameters, but it has a small ΔAIC as compared to simplest models*

Table B.5. Correlated evolution of binary traits using BayesTraits. Results of likelihood ratio test (above) and Bayes factor of harmonic means from MCMC (below) for the correlated evolution of 6 pairs of binary characters. Tests were performed by comparing fit of a dependent v. independent model of trait evolution in BayesTraits. Asterisks mark traits whose evolution was found to be significantly correlated. LH: log-likelihood; df: degrees of freedom.

Maximum Likelihood					
Pair of Characters	**LH (Dependent)**	**LH (Independent)**	**χ^2 statistic**	**df**	**p-value**
Pollination: Fruit	-56.583684	-60.354574	7.54178	4	0.109881
Pollination: Elevation	-104.072122	-107.581998	7.019752	4	0.1348481
Pollination: Andean	-88.546479	-92.452286	7.811614	4	0.09872793
Fruit: Elevation	-130.009089	-133.796692	7.575206	4	0.1084384
Fruit: Andean	-118.2341643	-122.1769823	7.8856359	4	0.09585848
Elevation: Andean	-159.696796	-168.894404	18.395216	4	0.001032828*

Bayesian Inference			
Pair of Characters	**Harmonic Mean (Dependent)**	**Harmonic Mean (Independent)**	**Bayes Factor**
Pollination: Fruit	-66.279838	-64.657858	3.24396
Pollination: Elevation	-111.382757	-111.797966	-0.830418
Pollination: Andean	-98.023314	-97.954698	0.137232
Fruit: Elevation	-138.288508	-138.146294	0.284428
Fruit: Andean	-127.542706	-126.737234	1.610944
Elevation: Andean	-229.079744	-172.277752	113.603984*

Table B.6. Model comparison for the two diversity-dependence analyses presented, with mean parameter estimates for each model. Both models show that the group has not reached its ecological carrying capacity, suggesting that there currently is no limit to species diversity. λ = speciation rate (in events/Ma/lineage); μ = extinction rate (in events/Ma/lineage); K = carrying capacity; NP, number of parameter in each model.

Diversity Dependence							
Model	**Mode of dependency**	**NP**	**logL**	**AICc**	**λ**	**μ**	**K**
λ depends on diversity (no extinction)	Exponential	2	-1056.37	2108.68	0.0598	-	31190.11
λ depends on diversity and μ constant	Exponential	3	-958.066	1910.01	0.0768	3.041e-05	5873.402

Appendix C:

Supporting material for Chapter V

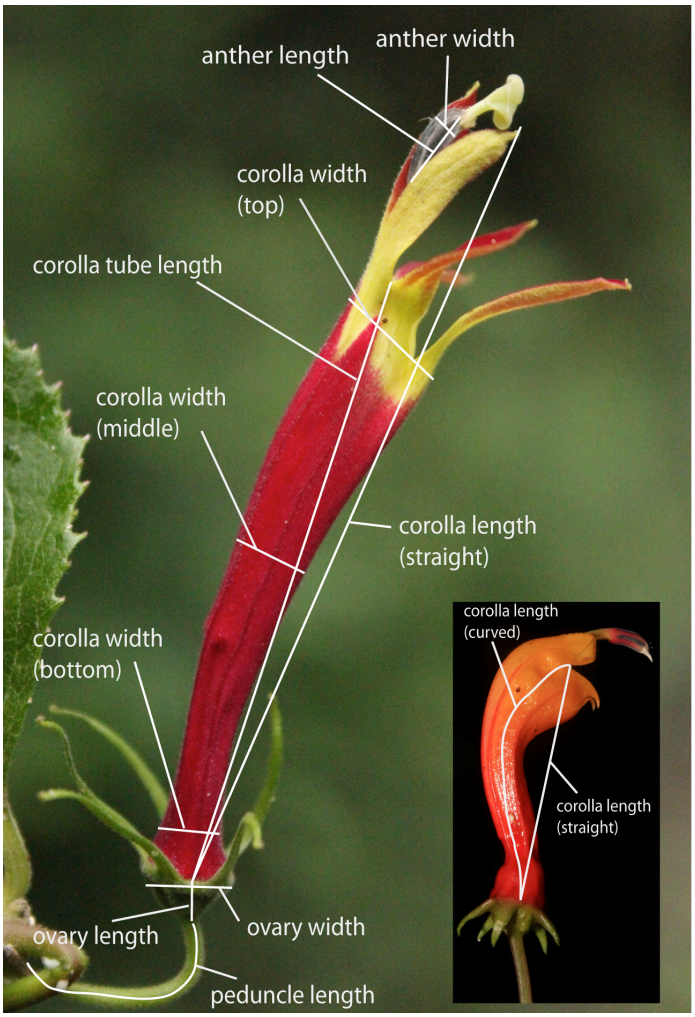


Figure C.1. Depiction of measurements of floral traits taken herbarium specimens. Species values for many of these traits are given in Table C.1. The remaining traits were combined to provide more informative values (i.e., volumes, areas, and ratios that provide shape information), and these values are presentd in Table C.1. The combined characters include: include ovary length and ovary width (together, ovary volume); anther length and anther width (together, anther area); the three values of corolla width (combined into three separate ratios); and corolla length (curved) (combined with corolla length straight to determine the curvature ratio). Photos are of *Siphocampylus orbignianus* A. DC. and *Centropogon yungasensis* Britton (inset) by L. Lagomarsino.

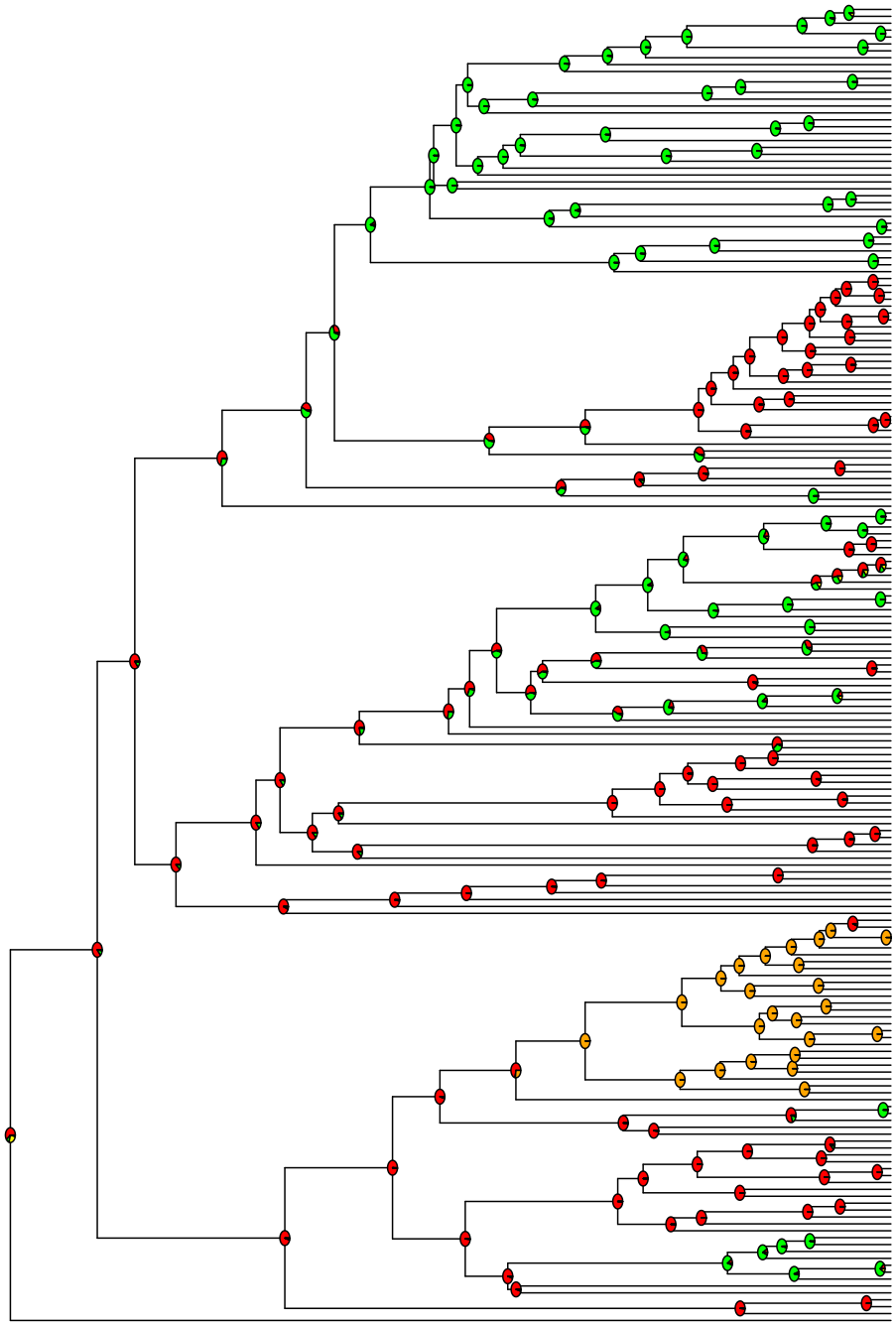


Figure C.2. Maximum likelihood reconstruction of pollination syndromes in the centropogonid clade. Pie charts at nodes represent ancestral states that were calculated as the marginal likelihood of each pollination syndrome: straight-bill hummingbird (red), bat (green), bee (yellow), and sicklebill hummingbird (orange). For Bayesian stochastic character mapping see Figure 5.3.

Table C.1. Trait values of floral characters for all species sampled. L= length, measurements in mm; A= area, measurements in mm^2;Vol, measurements in mm^3; PC= principal component, values given for the first four principal component axes. A visual representation of these measurements is given in Figure C.1.

Species	Corolla width (Ratio-bot:mid)	Corolla width (Ratio-mid:top)	Corolla width (Ratio-top:bot)	Peduncule (L)	Corolla (L)	Corolla tube (L)	Ovary (Vol)	Anther (A)	Curvature (ratio)	PC1	PC2	PC3	PC4	Pollination Syndrome
Burmeistera almedae	1.730769	0.433333	0.75	30	37	14	180	18	0.9900391	-2.3	-4.183	-3.9	-2.08	bat
Burmeistera ceratocarpa	1.517241	0.58	0.88	43	25	9	144	24	1	-3.54	-5.219	-1.5	-1.13	bat
Burmeistera chirriquiensis	1.5	0.266667	0.4	100	28	12	324	24	1	-2.09	-4.68	-4.6	2.99	bat
Burmeistera crebra	1.666667	0.257143	0.4285714	65	26	14	52.938	22.605	1	-2.89	-4.252	-5.1	1.546	bat
Burmeistera cyclostigmata	2.75	0.5	1.375	35	33	7	216	20	1	-3.68	-10.08	-2.6	-6.23	bat
Burmeistera dendrophila	2.142857	0.3	0.6428571	51	32	18	225	29.25	1	-0.81	-5.193	-5.2	-2.11	bat
Burmeistera domingensis	1.2	0.487013	0.5844156	37	20	20	94.299	17.94	1	-3.9	-2.733	-2.6	0.981	bat
Burmeistera mcvaughii	1.826087	0.383333	0.7	70	25	8	96	21	1	-3.98	-6.312	-3.6	0.511	bat
Burmeistera microphylla	2.02381	0.35	0.7083333	30	7	15	48	12	1	-5.97	-5.971	-4.3	-0.54	bat
Burmeistera morii	2.458333	0.3	0.7375	37	20	11	100	15	1	-5.11	-7.429	-5.2	-1.44	bat
Burmeistera obtusifolia	2.9	0.307692	0.8923077	43	35	15	441	24.5	1	-2.37	-8.734	-5.4	-3.85	bat
Burmeistera parviflora	1.823009	0.338323	0.6167665	25	9.5	3.5	12.5	3	1	-7.77	-5.887	-4.4	1.279	hb
Burmeistera racemiflora	1	0.480769	0.4807692	48.4	34	21.2	168.54	28.7	1	-1.09	-1.447	-2.7	1.073	bat
Burmeistera refracta	2.583333	0.296296	0.7654321	45	25	9	252	42	1	-2.53	-8.426	-5.3	-2.06	bat
Burmeistera sodiroana	2.521739	0.418182	1.0545455	66	32	18	250	24	1	-1.74	-8.067	-3.5	-4.29	bat
Burmeistera sp.	2.583333	0.282353	0.7294118	14	20	11	392	12	1	-5.15	-7.407	-5.8	-2.03	bat
Burmeistera succulenta	1.517241	0.527273	0.8	98	35	14	162	33	1	-0.6	-5.231	-1.8	-0.55	bat
Burmeistera tenuiflora	1.6	0.588235	0.9411765	85	24	14.5	192	24	1	-2.66	-6.055	-1	-1.02	bat
Burmeistera toroensis	1.266667	0.545455	0.6909091	93	28	16	275	30	1	-1.35	-4.31	-1.6	0.818	bat
Burmeistera truncata	1.657143	0.402299	0.6666667	80	45	20	145	66	1	1.349	-5.449	-3.2	-0.06	bat
Burmeistera ulleyi	1.72	0.396825	0.6825397	100	28	10	150	28	1	-2.24	-6.185	-3.2	0.798	bat
Burmeistera variabilis	1.333333	0.315789	0.4210526	44	31.5	22	151.25	28	1	-1.54	-2.31	-4.5	1.102	bat
Burmeistera vulgaris	2.285714	0.411765	0.9411765	125	25	15	432	60	1	-1.87	-10.78	-2.5	0.645	bat
Burmeistera zurquiensis	2.152778	0.248276	0.5344828	25	33	19	294	15	1	-2.57	-4.508	-6.1	-1.32	bat
Centropogon aequatorialis	0.733333	1.090909	0.8	65.5	37.2	32	328.56	21.96	1	0.127	-0.286	2.97	-1.78	hummingbird
Centropogon argutus	0.5	0.75	0.375	20	45	37	500	12	1	0.393	2.9419	-0.8	0.15	hummingbird
Centropogon asclepius	0.583333	0.888889	0.5185185	23	34	30	320	12	1	-1.26	1.6052	0.57	-0.31	hummingbird
Centropogon baezanus	1.307692	0.5	0.6538462	20	45	35	320	27.3	0.8932011	-0.23	-1.198	-6.6	-3.7	sicklebill
Centropogon bangii	0.697674	0.518072	0.3614458	16.5	21	14	128.56	11	0.9087262	-4.96	-0.382	-5.7	1.246	sicklebill
Centropogon brittonianus	1	1	1	124	33.42	21	1859	90	1	5.172	-6.529	3.23	-0.13	bat
Centropogon cf. weberbaueri	0.615385	0.8125	0.5	75	54	41	720	16	1	2.807	1.772	0.17	-0.38	hummingbird
Centropogon coccineus	0.404255	1.342857	0.5428571	60	46	30	250	15	0.9947668	-0.03	2.2567	4.24	-0.65	hummingbird
Centropogon comosus	0.961538	0.670968	0.6451613	37	47	35	864	27	1	1.933	-0.274	-1.2	-1.51	hummingbird
Centropogon congestus	0.807692	0.594966	0.4805492	35	42	35	405	15	0.8405557	-0.29	1.1115	-7.6	-3.09	sicklebill
Centropogon cordifolius	0.461538	0.866667	0.4	55	40	31	245	17.5	0.977598	-0.04	1.9969	-0.3	0.481	hummingbird
Centropogon cornutus	0.647059	1.036585	0.6707317	50	45	35	180	30	0.9747256	2.025	1.5402	1.12	-2.96	hummingbird
Centropogon costaricae	0.320988	0.94186	0.3023256	35	35	24	72	12	1	-2.67	2.2055	1.01	2.449	hummingbird

Table C.1 (Continued).

Centropogon dianae	0.814815	0.75	0.6111111	85	60	45	2880	45	1	7.423	-1.324	-0.2	0.139	bat
Centropogon dombeyanus	0.831325	0.754545	0.6272727	147.5	50.5	24	3364	94.5	1	8.362	-6.312	0.82	3.877	bat
Centropogon eilseri	0.9	0.526316	0.4736842	150	62	45	2343.8	119	1	11.75	-3.937	-1.4	2.482	bat
Centropogon erythraeus	0.82	0.735294	0.6029412	28.5	40.2	34	874.64	15.8	0.9812441	0.514	0.4533	-1.4	-1.36	hummingbird
Centropogon featherstonei	0.721154	0.8125	0.5859375	50	34	25	245	21	1	-2	-0.71	0.5	1.003	hummingbird
Centropogon ferrugineus 1	0.375	0.625	0.234375	77	36	38.5	90.75	10.5	0.9913338	0.422	2.9776	-1.8	1.985	hummingbird
Centropogon ferrugineus 2	0.461538	0.722222	0.3333333	60	36	20	311.04	14	0.9969891	-1.36	0.9157	-0.7	2.533	hummingbird
Centropogon glabrifilis	0.4	0.769231	0.3076923	32	35	29	320	13	1	-0.93	2.4979	-0.6	1.529	hummingbird
Centropogon grandidentatus	0.359375	0.888889	0.3194444	32	32	27	245	16	0.9521768	-0.86	2.8032	-1.4	0.13	hummingbird
Centropogon granulosus 1	0.9	0.5	0.45	15	38	33	180	20	0.9316213	-1.06	0.7252	-5.3	-1.24	sicklebill
Centropogon granulosus 2	0.930233	0.52439	0.4878049	32	46	40	320	28.8	0.9264228	2.101	1.3229	-5.3	-2.86	sicklebill
Centropogon granulosus 3	1.047619	0.475831	0.4984894	20	48	36	320	33	0.9289392	0.783	0.1233	-5.6	-1.99	sicklebill
Centropogon granulosus 4	1	0.454545	0.4545455	45	44	39	500	18	0.9302185	1.142	0.6581	-5.7	-1.73	sicklebill
Centropogon guttierezii	0.466667	0.8	0.3733333	61	60	42.5	1024	19.8	1	4.689	3.3097	-0.4	-0.54	hummingbird
Centropogon incanus (white)	1	0.95	0.95	153	50	27	1936	78	1	6.975	-5.621	2.78	-0.27	bat
Centropogon incanus (pink)	1	0.9	0.9	77	42	22	1635.9	55	1	2.466	-4.52	1.77	-0.32	hummingbird
Centropogon isabellinus	1.079545	0.475676	0.5135135	150	65	30	4725	96	1	11.75	-7.028	-2	4.435	bat
Centropogon leucocarpus	0.533333	0.75	0.4	30	37	25	100	10	1	-2.21	1.4557	-0.5	1.395	hummingbird
Centropogon anganatensis	0.480769	0.702703	0.3378378	49.5	19.5	14.5	81.648	5.95	1	-4.39	0.1919	-0.7	3.463	hummingbird
Centropogon luteus	0.589286	0.691358	0.4074074	59	42	36	600	12	1	0.963	1.7309	-1	0.67	hummingbird
Centropogon luteynii	0.571429	0.76087	0.4347826	50	36	26	125	10	1	-1.92	0.9318	-0.2	1.485	hummingbird
Centropogon macbridei	0.53125	0.780488	0.4146341	74	54	41.5	661.25	34	1	3.918	1.9914	-0.1	0.167	hummingbird
Centropogon macrocarpus	1.709091	0.388235	0.6635294	164	27	11.5	1470.3	48	1	1.362	-8.478	-2.7	2.838	bat
Centropogon macrophyllus	0.534884	0.5375	0.2875	30	31	16.5	405	17.875	0.9675442	-2.62	0.3436	-3.5	2.717	sicklebill
Centropogon magnificus	0.7875	0.833333	0.65625	128	44	30	1611.5	81.25	1	6.334	-3.511	1.28	1.237	bat
Centropogon mandonis	0.758242	0.8125	0.6160714	183	44.4	28	2704.5	58.5	1	7.339	-4.418	1.3	2.893	bat
Centropogon mandonis	1	0.777778	0.7777778	151	51	32	1454.8	70	1	7.103	-3.928	0.93	-0.24	bat
Centropogon minimus	0.426667	0.9375	0.4	14.5	13.9	12.31	29.403	3.92	1	-6.57	0.3366	1.14	3.123	bee
Centropogon nervosus	0.333333	1	0.3333333	70	57	35	180	30	1	2.899	3.283	1.45	0.364	hummingbird
Centropogon palmanus	0.65	0.689655	0.4482759	65	35	25	137.5	8.75	1	-1.79	0.3082	-0.7	1.662	hummingbird
Centropogon panamensis	1.222222	0.406015	0.4962406	20	35	31	400	27	0.8731769	-1.34	-1.21	-8.2	-2.23	sicklebill
Centropogon perlongus	1.117647	0.53125	0.59375	135	75	38	3920	68	1	12.28	-3.975	-2	0.629	bat
Centropogon peruvianus	1	0.8	0.8	110	29	14	2704	55	1	2.736	-6.488	1.05	2.307	bat
Centropogon pichinchensis	0.666667	1.193182	0.7954545	62.5	30.5	27.5	650.25	15.75	0.992227	-1.69	-0.979	3.64	-0.63	hummingbird
Centropogon prestii	0.381818	0.774648	0.2957746	104	37	32	700	14	0.9599845	1.461	1.7317	-1.5	1.676	hummingbird
Centropogon pulcher	1.315789	0.361905	0.4761905	15	46	18	320	27	0.8897579	-0.15	-1.171	-8.5	-2.95	sicklebill
Centropogon reticulatus	0.558824	0.607143	0.3392857	75	49	34	576	24	1	2.405	1.5415	-1.6	1.338	hummingbird
Centropogon rex	1.655172	0.437736	0.7245283	139	49	25	1089	63	1	4.798	-6.158	-2.5	-0.11	bat
Centropogon roseus	0.714286	0.425676	0.3040541	15	42	21	245	12	0.88	-2.07	1.0675	-7.9	-0.38	sicklebill
Centropogon salviiformis	0.595238	0.730435	0.4347826	50.2	26	22.5	356.4	12.9375	0.992345	-2.8	-0.096	-0.6	2.231	hummingbird
Centropogon simulans	1	0.592308	0.5923077	120	38	11	3600	75	0.991298	5.404	-7.299	-1.3	4.363	bat
Centropogon smithii	1.217009	0.554472	0.6747967	200	43	20	3757	120	1	10.43	-9.849	-0.5	4.66	bat

Table C.1 (Continued).

Centropogon sodiroanus	0.477273	0.721311	0.3442623	41	49	47	324	10	1	1.95	4.0081	-1	-0.41	hummingbird
Centropogon solanifolius	0.55	0.707965	0.3893805	21.5	47	40	433.5	40	0.9670385	2.285	2.4136	-2.3	-0.78	hummingbird
Centropogon solanifolius	0.64	0.646552	0.4137931	35	38	30	256	19.6	0.9639471	-0.31	1.3918	-2.7	-0.11	hummingbird
Centropogon sp	0.545455	0.733333	0.4	57	34.2	29	786.5	14.4	1	-0.05	0.9281	-0.6	1.583	hummingbird
Centropogon sp. nov.	1.022727	0.55	0.5625	160	43	23	3375	112.5	1	8.651	-7.94	-0.8	5.048	bat
Centropogon subandinus	0.7	0.645161	0.4516129	143	54	42.5	729	35	1	5.748	0.4068	-0.8	0.625	hummingbird
Centropogon talamancensis	0.711111	0.762712	0.5423729	70.5	74	49	1378.1	31.9	1	7.085	2.0165	-0.5	-1.91	hummingbird
Centropogon tesmannii	0.5	0.571429	0.2857143	16	48	42	324	12	1	1.013	3.7717	-2.4	0.249	hummingbird
Centropogon trachyanthus	1	0.488636	0.4886364	12	35.5	28.8	66.27	17.05	0.7764471	-1.61	0.6444	-11	-4.93	sicklebill
Centropogon trichoides	0.454545	0.859375	0.390625	56	32.75	29	158.4	17.92	0.9587629	-0.63	1.8488	-1	0.319	hummingbird
Centropogon umbrosus	0.825	0.56338	0.4647887	38.333333	39	19.3333	300.93	12	0.9259259	-1.77	-0.181	-4.8	-0.39	sicklebill
Centropogon unduavensis	0.555556	0.825688	0.4587156	59	30	23	814.31	21.45	1	-0.48	-0.008	0.33	1.677	hummingbird
Centropogon urubambae	1.025	0.444444	0.4555556	13	32	17	147	12	0.9123768	-3.51	-0.898	-6.5	-0.59	sicklebill
Centropogon valerii	0.407407	0.80597	0.3283582	69	27	23	245	13.2	1	-1.74	1.1071	0.17	2.719	hummingbird
Centropogon vargasii	0.625	0.533333	0.3333333	25	30	15	196	24	0.9266263	-2.83	-0.04	-5	1.406	sicklebill
Centropogon viriduflorus	1	0.807292	0.8072917	85	60	25	2535	55	1	5.395	-4.245	0.72	0.136	bat
Centropogon weberbaueri	0.692308	0.866667	0.6	45	36.5	29.5	496.38	13	1	-1.07	0.2367	0.73	0.011	hummingbird
Centropogon yarumalensis	0.533333	0.882353	0.4705882	36	36	30	405	17.25	0.9878021	-0.51	1.5913	0.12	0.035	hummingbird
Centropogon yungasensis	0.771429	0.460526	0.3552632	25	26	9	48	16	0.9264755	-5.03	-1.305	-5.5	2.205	sicklebill
Siphocampylus actinothrix	1	1	1	75	30	11	108	40	1	-1.64	-4.295	2.84	-1.23	bat
Siphocampylus aff. rictus	1	0.869565	0.8695652	120	51	21	891	36.9	1	2.279	-3.801	1.69	-0.37	bat
Siphocampylus affinis	0.552941	0.790698	0.4372093	85	28	22	405	24	1	-2.42	-1.262	0.61	3.797	bat
Siphocampylus andinus	0.460526	0.8	0.3684211	47	52.05	39.5	64	15.4	1	1.847	3.6531	-0.3	-0.49	hummingbird
Siphocampylus angustiflorus	0.4	0.75	0.3	7	32	20	24	15	1	-3.65	1.6702	-0.6	2.652	hummingbird
Siphocampylus antioquianus	0.273333	0.920245	0.2515337	108	52	43	900	30.4	1	4.85	3.0769	0.97	1.615	hummingbird
Siphocampylus aureus	0.4375	0.738462	0.3230769	53.25	53	42.5	67.2	6.75	1	1.749	4.1189	-0.8	-0.16	hummingbird
Siphocampylus aversiae	1.272727	1	1.2727273	30.5	20.575	8	222.35	17.845	1	-4.31	-5.275	2.78	-3.62	bat
Siphocampylus betulaefolius	0.454545	0.982143	0.4464286	46	46	40	36	12	0.9966415	0.573	3.3343	1.19	-0.73	hummingbird
Siphocampylus bilabiatus	0.844444	0.681818	0.5757576	65	58	32	405	27	1	2.996	0.5433	-1	-1.32	hummingbird
Siphocampylus boliviensis	0.468085	0.839286	0.3928571	79	50	40	180	16	1	1.458	2.4759	0.44	0.749	hummingbird
Siphocampylus brevicalyx	0.375	0.733333	0.275	80	60	52	108	18	1	5.04	5.1267	-0.9	-0.81	hummingbird
Siphocampylus chloroleucus	0.638889	0.692308	0.4423077	10.7	23.5	12.5	44.55	16.32	1	-4.42	-0.285	-1	2.024	bat
Siphocampylus citrinus	0.446809	1.044444	0.4666667	29	38	20.5	256	12	1	-1.81	1.669	1.8	0.508	hummingbird
Siphocampylus clotho	0.571429	0.602151	0.344086	40	67	37	98	27	1	3.261	3.1534	-2	-0.44	hummingbird
Siphocampylus convolvulaceus	0.361111	0.947368	0.3421053	100	48	40	144	21	1	1.888	2.6236	1.43	1.399	hummingbird
Siphocampylus correoides	1.25	0.8	1	25	28	14	190.13	10	1	-3.94	-3.619	0.52	-2.34	hummingbird
Siphocampylus corymbiferus 1	0.388889	0.870968	0.3387097	45	44	32	75	14	1	0.272	3.1662	0.29	0.539	hummingbird
Siphocampylus corymbiferus 2	0.625	1	0.625	37	41	30	88	8.25	1	-1.24	1.3852	1.71	-1.09	hummingbird
Siphocampylus corynoides	1.244444	1.144068	1.4237288	110	35	30	1296	60	1	1.042	-7.71	5.28	-2.26	bat
Siphocampylus dependens	0.725	0.615385	0.4461538	75	47	30	567	21	0.9944017	1.64	0.4207	-1.7	0.666	hummingbird
Siphocampylus elfredii	0.742424	1	0.7424242	45	45	30	384	24	1	0.268	-0.006	1.98	-1.6	hummingbird
Siphocampylus fiebrigii	0.361702	1.037528	0.3752759	62	47	40	125	12	1	1.236	3.7444	1.72	-0.13	hummingbird

Table C.1 (Continued).

Siphocampylus flagelliformis	0.566667	0.909091	0.5151515	19	30	21	55.688	11	1	-3.06	0.9762	0.81	0.445	hummingbird
Siphocampylus fulgens	0.421053	1.1875	0.5	37	44	35	200	10	1	-0.04	3.1862	2.9	-1.06	hummingbird
Siphocampylus giganteus	0.873239	0.751323	0.6560847	115	77	40	4000	80	1	11.61	-3.834	0.16	1.166	bat
Siphocampylus jelksii	0.875	0.727273	0.6363636	160	53	22	1573	80	1	5.563	-5.27	0.79	3.175	bat
Siphocampylus krauseanus	0.461538	0.962963	0.4444444	25	31	21	45.375	24	1	-2.54	1.0232	1.31	1.339	hummingbird
Siphocampylus longipedunculatus	0.6	0.769231	0.4615385	80	53	40	700	24	1	3.262	1.5797	-0.2	0.049	hummingbird
Siphocampylus lycioides	0.571429	1	0.5714286	66	35	25	182.25	8	1	-1.73	0.5376	1.95	0.496	hummingbird
Siphocampylus macropodus	0.384615	0.928571	0.3571429	45	55	49	108	17.5	0.9881531	2.389	4.5697	0.28	-0.97	hummingbird
Siphocampylus matthiaei	0.571429	0.538462	0.3076923	120	37.5	21	180.5	56	1	1.394	-1.615	-1.4	4.403	bat
Siphocampylus nematosepalus	0.454545	0.611111	0.2777778	35	51	38	144	28	1	2.156	3.3354	-1.9	0.508	hummingbird
Siphocampylus nemoralis	0.789474	1	0.7894737	22	22	10	84.609	4.2	1	-5.79	-1.919	2.13	0.102	hummingbird
Siphocampylus nitidus	0.68	0.740741	0.5037037	26	43	35	90.75	19.6	1	0.232	1.8647	-0.7	-0.9	hummingbird
Siphocampylus oblongifolius	0.581395	0.86	0.5	23	39	28	56	15	1	-1.16	1.7482	0.32	-0.32	hummingbird
Siphocampylus obovatus	1.2	0.782609	0.9391304	12.2	17.5	9.5	130.7	18	1	-4.78	-3.812	0.28	-1.65	bat
Siphocampylus orbignianus	0.681818	0.897959	0.6122449	30	41	31	108	15	1	-0.06	1.5749	0.69	-1.77	hummingbird
Siphocampylus pubescens	0.311828	0.93	0.29	39	39	30	364.5	14	0.9855145	-0.49	3.0173	0.2	1.243	hummingbird
Siphocampylus rosmarinifolius	0.442308	1.238095	0.547619	40	36	22.5	73.938	13	1	-2.42	1.3791	3.63	0.242	hummingbird
Siphocampylus rusbyanus	0.846154	0.764706	0.6470588	90	42	12	175	18	1	-1.6	-2.356	0.38	1.303	bat
Siphocampylus scandens	0.47619	0.777778	0.3703704	10	39	30	101.53	10.5	1	-1.21	2.8898	-0.6	0.265	hummingbird
Siphocampylus sceptrum	0.793651	1.211538	0.9615385	45.5	41.2	18	130.93	13.64	1	-1.88	-1.234	4.06	-2.62	hummingbird
Siphocampylus smilax	1.540541	0.402174	0.6195652	23	28.5	16.965	303.07	28.875	1	-2.56	-3.821	-3.7	-0.22	bat
Siphocampylus sp	0.826923	1.268293	1.0487805	55	41	39	320	24	1	0.483	-0.613	4.75	-4	hummingbird
Siphocampylus sp. nov. 1	0.818182	0.611111	0.5	40	45	31	225	12	1	0.004	0.9419	-1.8	-0.41	hummingbird
Siphocampylus sp. nov. 2	1	0.75	0.75	84	37	22	128	12.75	1	-1.13	-2.002	0.18	-0.56	hummingbird
Siphocampylus sparsipilus	0.4	0.918367	0.3673469	15	46	30	294	27	1	0.611	2.9516	0.5	0.094	hummingbird
Siphocampylus tunarensis	1.4375	0.833333	1.1979167	129	28	15	700	32	1	-0.23	-7.124	1.91	-1.92	bat
Siphocampylus tupaeformis	0.666667	1	0.6666667	25	35	22	320	21	1	-1.72	-0.02	1.79	-0.63	hummingbird
Siphocampylus umbellatus	1.3375	1	1.3375	145	47.37	22	440.64	63	1	3.474	-6.855	3.78	-3.54	bat
Siphocampylus vatkeanus	1.316667	0.526316	0.6929825	135	43	17	845	50	1	3.249	-4.994	-1.6	0.496	bat
Siphocampylus virgatus	0.338983	1.311111	0.4444444	40	30	19	32	6	1	-3.77	1.7979	4.07	1.32	hummingbird
Siphocampylus werdermannii	0.471698	1.06	0.5	85	41	22.63	81	12	1	-0.54	1.0839	2.39	0.741	hummingbird
Siphocampylus westinianus	0.47619	0.857143	0.4081633	40	41	30	108	24	1	-0.82	1.603	0.49	1.258	hummingbird

Table C.2. Results of analysis of correlated floral trait evolution using Bayesian MCMC. The harmonic mean of MCMC chains from two separate models, one enforcing correlated evolution of the trait pair and the other allowing independent evolution, were used to generate Bayes factors to assess the strength of correlation between the pairs of traits shown at left. Analyses were run in BayesTraits across a random subset of 100 trees from the posterior distribution from BEAST. Asteriks next to Bayes factor values indicate strength of support: *, positive evidence (BF >2); **, strong evidence (BF 5–10); ***, very strong evidence (BF >10).

		Harmonic mean of Log Likelihood			
Trait A	Trait B	Correlated	Independent	Δharmonic mean of log likelihood	log Bayes Factor
Bottom: middle corolla width	Middle: top corolla width	-25.881374	-35.518483	9.637109	19.274218***
Bottom: middle corolla width	Bottom: top corolla width	-27.954571	-56.737992	28.783421	57.566842***
Bottom: middle corolla width	Peduncle length	-848.4945231	-848.6918014	0.197278349	0.394556697
Bottom: middle corolla width	Corolla length	-643.8745612	-645.4038166	1.529255405	3.05851080910338*
Bottom: middle corolla width	Corolla tube length	-643.8874291	-645.4169548	1.529525683	3.05905136689648*
Bottom: middle corolla width	Ovary volume	-1264.874922	-1266.006781	1.13185857	1.250661616
Bottom: middle corolla width	Anther area	-730.8440877	-737.7537135	6.909625834	13.8192516683625***
Bottom: middle corolla width	Corolla curvature	304.0269212	303.2669076	0.760013612	1.520027223
Bottom: middle corolla width	PC1	-464.8757094	-465.1023333	0.226623872	0.453247744
Bottom: middle corolla width	PC2	-376.4345692	-422.2803855	45.84581627	91.6916325483783***
Bottom: middle corolla width	PC3	-402.0666896	-407.9525461	5.885856509	11.7717130188909***
Bottom: middle corolla width	PC4	-373.749048	-394.5520306	20.80298257	41.6059651367071***
Middle: top corolla width	Bottom: top corolla width	64.0368	48.455739	15.581061	31.162122***
Middle: top corolla width	Peduncle length	-760.8698346	-761.1225476	0.252712902	0.505425804
Middle: top corolla width	Corolla length	-577.556927	-578.630175	1.073248	2.14649600000007*
Middle: top corolla width	Corolla tube length	-562.176677	-566.739957	4.56328	9.12655999999993**
Middle: top corolla width	Ovary volume	-1175.471343	-1177.304135	1.832792062	3.66558412335417*
Middle: top corolla width	Anther area	-637.399627	-637.241343	-0.158284	-0.316568
Middle: top corolla width	Corolla curvature	366.330402	364.434583	1.895819	3.79163800000003*
Middle: top corolla width	PC1	-378.170964	-379.032148	0.861184	1.722368
Middle: top corolla width	PC2	-331.296727	-332.200952	0.904225	1.80845
Middle: top corolla width	PC3	-219.460703	-319.771669	100.310966	200.621932***

Table C.2 (Continued).

Middle: top corolla width	PC4	-317.548777	-320.537032	2.988255	5.97651000000008**
Bottom: top corolla width	Peduncle length	-777.7897936	-778.170888	0.381094397	0.762188795
Bottom: top corolla width	Corolla length	-594.746239	-595.562829	0.81659	1.63318
Bottom: top corolla width	Corolla tube length	-583.196465	-585.374031	2.177566	4.35513199999991*
Bottom: top corolla width	Ovary volume	-1194.374844	-1194.440562	0.065718058	0.131436115
Bottom: top corolla width	Anther area	-648.827144	-655.195446	6.368302	12.7366039999999**
Bottom: top corolla width	Corolla curvature	345.224565	345.289566	-0.065001	-0.130002
Bottom: top corolla width	PC1	-397.553426	-398.06267	0.509244	1.018488
Bottom: top corolla width	PC2	-309.947821	-348.242526	38.294705	76.58941***
Bottom: top corolla width	PC3	-324.226425	-338.875785	14.64936	29.29872***
Bottom: top corolla width	PC4	-311.494673	-336.191672	24.696999	49.393998***
Peduncle length	Corolla length	-1393.408504	-1405.726251	12.31774713	24.6354942582975***
Peduncle length	Corolla tube length	-1379.326742	-1386.550075	7.223333218	14.4466664361485***
Peduncle length	Ovary volume	-1975.569377	-2005.5938	30.02442275	60.0488455054756***
Peduncle length	Anther area	-1440.837866	-1464.795392	23.95752644	47.9150528835921***
Peduncle length	Corolla curvature	-457.854758	-456.7155236	-1.139234426	-2.278468852
Peduncle length	PC1	-1163.836156	-1203.270056	39.43389974	78.8677994874779***
Peduncle length	PC2	-1147.893145	-1158.872105	10.97896038	21.9579207598085***
Peduncle length	PC3	-1143.612932	-1148.945807	5.332875428	10.6657508569606***
Peduncle length	PC4	-1128.531554	-1146.384988	17.85343365	35.706867295713***
Corolla length	Corolla tube length	-1128.086156	-1187.020439	58.93428324	117.868566489147***
Corolla length	Ovary volume	-1792.251247	-1816.933071	24.68182351	49.3636470174151***
Corolla length	Anther area	-1273.034532	-1281.718264	8.683732086	17.3674641710218***
Corolla length	Corolla curvature	-263.638019	-263.22123	-0.416789	-0.833578
Corolla length	PC1	-905.0693395	-1011.486767	106.4174274	212.834854817654***
Corolla length	PC2	-969.3848801	-972.4001979	3.015317795	6.03063558996178**
Corolla length	PC3	-962.0724929	-962.2274671	0.154974192	0.309948383
Corolla length	PC4	-944.398255	-948.4587868	4.06053176	8.12106352022374**
Corolla tube length	Ovary volume	-1783.15807	-1793.271904	10.1138339	20.2276677921191***
Corolla tube length	Anther area	-1270.481666	-1271.938235	1.456569344	2.91313868741418*
Corolla tube length	Corolla curvature	-239.696728	-239.889673	0.192945	0.38589
Corolla tube length	PC1	-934.8256911	-988.5368877	53.71119667	107.42239333558***
Corolla tube length	PC2	-937.1384277	-949.5683789	12.4299512	24.8599023950846***
Corolla tube length	PC3	-936.9113719	-938.3626756	1.451303625	2.90260725063013*
Corolla tube length	PC4	-918.1082013	-924.7707016	6.662500289	13.3250005777315***
Ovary volume	Anther area	-1850.813144	-1881.327559	30.51441486	61.0288297168818***
Ovary volume	Corolla curvature	-869.0100392	-868.8802182	-0.129820997	-0.259641994
Ovary volume	PC1	-1559.868469	-1617.340281	57.47181247	114.943624936822***
Ovary volume	PC2	-1561.399278	-1575.816552	14.4172737	28.8345474022267***
Ovary volume	PC3	-1565.438902	-1565.645499	0.206596591	0.413193181
Ovary volume	PC4	-1552.079354	-1554.51424	2.434886367	4.86977273376306*
Anther area	Corolla curvature	-344.463541	-345.222262	0.758721	1.517442
Anther area	PC1	-1040.6217	-1084.073658	43.45195823	86.9039164603932***
Anther area	PC2	-1010.804725	-1034.466234	23.66150869	47.3230173890431***
Anther area	PC3	-1023.883966	-1024.73569	0.851724	1.703448
Anther area	PC4	-1021.213159	-1021.697528	0.484369498	0.968738997
Corolla curvature	PC1	-65.319383	-65.661331	0.341948	1.025513714
Corolla curvature	PC2	-23.171408	-22.416708	-0.7547	-1.5094
Corolla curvature	PC3	10.844387	-8.018329	18.862716	37.725432***

Table C.2 (Continued).

Corolla curvature	PC4	9.058493	5.66248	3.396013	6.792026**
PC1	PC2	-770.2839574	-770.4829371	0.198979705	0.39795941
PC1	PC3	-762.8844157	-763.4759607	0.591544989	1.183089978
PC1	PC4	-749.0087894	-749.2844619	0.275672547	0.551345094
PC2	PC3	-718.4525459	-718.8476971	0.395151233	0.790302466
PC2	PC4	-708.6613541	-709.0419805	0.380626351	0.761252702
PC3	PC4	-698.8161655	-699.2017543	0.385588758	0.771177516

Appendix D:

Lectotypification of Peruvian Campanulaceae names associated with collections made by Augusto Weberbauer

The contents of this appendix are reprinted from Lagomarsino LP, Santamaría-Aguilar, DA. Lectotypification of Peruvian Campanulaceae names associated with collections made by Augusto Weberbauer. *Harvard Papers in Botany* 20(1): 77–79. Copyright 2015 with permission from the Harvard University Herbaria.

D.1 Abstract

We designate lectotypes for thirteen Peruvian *Centropogon* and *Siphocampylus* (Campanulaceae: Lobelioideae) names associated with type collections made by Augusto Weberbauer.

D.2 Introduction

Augusto Weberbauer (1871--1948) was an explorer and botanist who made many important contributions to the understanding of the flora and phytogeography of Peru (Weberbauer 1911, 1936, 1945). He amassed more than 8,000 specimens over the course of 35 years of active collecting in the early 20th century (Velarde 1968, 1969; León 2002; Luteyn et al. 2008). His principal set of specimens was deposited at Berlin-Dahlem (B), and from there, duplicates were sent to other major European and American herbaria, including F, GH, K, NY, and US (Velarde 1968; León 2002). In addition, a few hundred of his specimens remained in Peru, where they are currently housed in the Weberbauer Herbarium (MOL) at the Universidad Nacional Agraria La Molina in Lima (Velarde 1968; Luteyn et al. 2008). More than 20% of the specimens Weberbauer collected were recognized as new to science. Most of these new species were described from collections at Berlin (Luteyn et al. 2008). Unfortunately, many of these type specimens were destroyed during World War II. While many of the associated names have since been lectotypified (León et al., 2006; Luteyn et al., 2008; Burke and Michelangeli, 2013), the majority likely still require treatment.

Here, we designate lectotypes for thirteen names associated with type collections made by Weberbauer in *Siphocampylus* Pohl and *Centropogon* C. Presl (Campanulaceae: Lobelioideae), genera included in the centropogonid clade (Lagomarsino et al. 2014). Many specimens cited herein can be viewed on the JSTOR Global Plants website (https://plants.jstor.org/). Where possible, we designate specimens at MOL as lectotypes as they are in good condition and have the most complete label information available, sometimes including detailed descriptions of the plant and/or locality; specimens outside of Peru typically have a truncated version of this information. We place the names that we treat into two groups.

The first comprises names erected by A. Zahlbruckner (1906), who did not designate herbaria in his original species descriptions. The second comprises names erected by Franz Elfried Wimmer (1924, 1929, 1935, 1943, 1953, 1968), who sometimes designated holotypes in his protologues, though frequently listed a series of syntypes. Some of these holotypes and syntypes were destroyed during the bombing of Berlin. We choose lectotypes for these names. We note that the majority of Weberbauer type specimens of Campanulaceae are extant, likely because they had been loaned to F. E. Wimmer, who was based in Vienna, Austria (W).

D.3 Typification

LECTOTYPIFICATION OF TAXA DESCRIBED BY A. ZAHLBRUCKNER (1906)

Centropogon grandicephalus Zahlbr. Bot. Jahrb. Syst. 37(4): 454. 1906 [24 Apr 1906]

TYPE: PERU. Departamento Amazonas: Östl. von Chachapoyas: zwischen den Tambos Almirantes und Incatambo, 1800--1900 m, 31 July 1904 (fl), *A. Weberbauer 4461*. Lectotype (designated here): *A. Weberbauer 4461* (B [10 0244141-barcode, digital image], negative of B sheet: F 30218).

Centropogon macrocarpus Zahlbr. Bot. Jahrb. Syst. 37(4): 452. 1906 [24 Apr 1906]

TYPE: PERU. Departamento Huánuco: Provincia Huamalíes, Berge südwestlich von Monzon, gesträuch stellenweise unterbrochen durch moor und grassteppe, 3400--3500 m, 1906 (fl), *A. Weberbauer 3344*. Lectotype (designated here): *A. Weberbauer 3344* (G [00236661-barcode, digital image]).

Homotypic synonyms: *Burmeistera macrocarpa* E.Wimm. Repert. Spec. Nov. Regni Veg. 30: 41. 1932.

Centropogon pulcher Zahlbr. Bot. Jahrb. Syst. 37(4): 451. 1906 [24 Apr 1906].

TYPE: PERU. Departamento Junín: Provincia Tarma, cerros al Oeste de Huacapistana, monte bajo compuesto de arbustos, 14 January 1903 (fl), 2000 m, *A. Weberbauer 2164* Lectotype (designated here): *A. Weberbauer 2164* (MOL [00209]; Isolectotypes: B-2 sheets [10 0244119, 10 0244121-barcode, digital image], G [006035, digital image], negative of B sheet: F 30221).

This name was invalidly lectotypified in the unpublished dissertation thesis of Bruce A. Stein (1987). While he had intended to designate a Berlin specimen with a photo negative available at F (30221) as the lectotype, we instead chose the MOL specimen as it is more complete and has been verified.

Centropogon weberbaueri Zahlbr. Bot. Jahrb. Syst. 37(4): 453. 1906 [24 Apr 1906]

TYPE: PERU. Departamento Huánuco: Provincia Huamalíes, Berge südwestlich von Monzon, 3400--3500 m, 11 July 1903 (fl), *A. Weberbauer 3347*. Lectotype (designated here): *A. Weberbauer 3347* (B [10 0244102-barcode, digital image]); Isolectotype: B [10 0244103-barcode, digital image], negative of B sheet: F 30230).

Siphocampylus floribundus Zahlbr. Bot. Jahrb. Syst. 37(4): 460. 1906 [24 Apr 1906]

TYPE: PERU. Departamento Huánuco: Provincia Huamalies, cerros al Sudoeste de Monzon, monte bajo tupido, siempreverde compuesto de arbustos y escasos arbolitos,

predominando el follaje rígido, 2400--2500 m, s.d. (fl), *A. Weberbauer 3421*. Lectotype (designated here): *A. Weberbauer 3421* (MOL [00206]).

Siphocampylus macropodoides Zahlbr. Bot. Jahrb. Syst. 37(4): 458. 1906 [24 Apr 1906]

TYPE: PERU. Departamento Áncash: Provincia Huaylas, Abajo de la Had. Cajamba, estepa de gramíneas con arbustos esparcidos, 3500 m, 30 May 1903 (fl), *A. Weberbauer 3201*. Lectotype (designated here): *A. Weberbauer 3201* (MOL [00205]; Isolectotype: B [10 024258-barcode, digital image]).

Siphocampylus sanguineus Zahlbr. Bot. Jahrb. Syst. 37(4): 456. 1906 [24 Apr 1906].

TYPE: PERU. Departamento Amazonas: Provincia Chachapoyas, vertientes Orientales del valle del Marañón, encima de Balsas, monte bajo, siempreverde, compuesto de arbustos y pequeños árboles, predominando el follaje rígido, 3200 m, s.d. (fl), *A. Weberbauer 4285*. Lectotype (designated here): *A. Weberbauer 4285* (MOL [00204]; Isolectotypes: B [10 0242553-barcode, digital image], G [00237858-barcode, digital image], negative of B sheet: F 30245).

Siphocampylus superbus Zahlbr. Bot. Jahrb. Syst. 37(4): 455. 1906 [24 Apr 1906].

TYPE: PERU. Departamento Cajamarca: Hualgayoc, 3600 m, 11 May 1904 (fl), *A. Weberbauer 3983*. Lectotype (designated here): *A. Weberbauer 3983* (B [10 0242547-barcode, digital image]; Isolectotype: B [10 0242548-barcode, digital image], negative of B sheet: F 30212).

Siphocampylus tortuosus Zahlbr. Bot. Jahrb. Syst. 37(4): 459. 1906 [24 Apr 1906].

TYPE: PERU. Departamento Loreto: Moyobamba, 1500 m, 28 August 1904 (fl), *A. Weberbauer 4646.* Lectotype (designated here): *A. Weberbauer 4646* (B [10 0242546-barcode, digital image]; Isolectotype: B [10 0242545-barcode, digital image], negative of B sheet: F 30247).

Siphocampylus weberbaueri Zahlbr. -- Bot. Jahrb. Syst. 37(4): 456. 1906 [24 Apr 1906].

TYPE: PERU. Departamento Cajamarca: Provincia Hualgayoc, encima de la Hacienda La Tahona, estepa de gramíneas con arbustos esparcidos, 3100--3300 m, 04 May 1904 (fl),), *A. Weberbauer 4019* . Lectotype (designated here): *A. Weberbauer 4019* (MOL [00203]; Isolectotypes: B-2 sheets [10 0242533, 10 0242534 -barcode, digital image], G [00237944, digital image], negative of B sheet: F 30213).

LECTOTYPIFICATION OF TAXA DESCRIBED BY WIMMER (1929, 1935)

Siphocampylus albus E.Wimm. Repert. Spec. Nov. Regni Veg. 26: 17, pl. 72, fig. 15. 1929

TYPE: PERU. Departamento Piura: Provincia Ayavaca, Ayavaca, 2700--2800 m, 1909--1914 (fl), *A. Weberbauer 6383* (Holotype: B, most likely destroyed; Lectotype (designated here): *A. Weberbauer 6383* (F [628514, digital image]; Isolectotype: GH [00033376-barcode]).

Siphocampylus citrinus E.Wimm. Repert. Spec. Nov. Regni Veg. 38: 75. 1935

TYPE: PERU. Departamento Cuzco: Provincia Quispicanchi, Marcapata valley, Chaupichaca, mixed formation, 1700 m, 19--20 February (fl), *A. Weberbauer 7829.* Lectotype

(designated here): *A. Weberbauer 7829* (US [1496787, digital image]; Isolectotypes: F [605331, digital image], K [000329901-barcode, digital image]).

Wimmer noted three herbaria in the description of this species: B, F, and W. We have chosen the specimen at US as the lectotype as it is in the best condition.

Siphocampylus nobilis E.Wimm. Repert. Spec. Nov. Regni Veg. 26: 12, pl. 72, fig. 23. 1929

TYPE: PERU. Departamento Cajamarca: Provincia Jaen, above Shumaya, 2200--2300 m, 07 May 1912 (fl), *A. Weberbauer 6291*. Lectotype (designated here): *A. Weberbauer 6291* (F [548771, digital image]; Isolectotypes: GH, NY-2 sheets [00547290, 00547291-barcode, digital image], US [1496196, digital image]).

Wimmer noted two herbaria in the description of this species: B and W. We have chosen the specimen at F as the lectotype as it is in the best condition.

D.4 Acknowledgements

I acknowledge the following herbaria and their staff for access to relevant collections: A, GH, MO, MOL, NY, and USM. A visit to MOL was supported by an NSF Doctoral Dissertation Improvement Grant (DEB-1210401) and Arnold Arboretum's Deland Award for Student Research to LPL. I would additionally like to thank Kanchi Gandhi for nomenclatural advice and the staff of the Harvard University Herbaria Botany Libraries for helping to locate necessary literature. Images of many type specimens were accessed via JSTOR Global Plants (https://plants.jstor.org/).

D.5 References

Burke, J. M., and F. A. Michelangeli. 2013. Lectotypification of Peruvian Melastomataceae described by Cogniaux from Weberbauer collections. Phytotaxa 125:10–16.

Lagomarsino, L. P., A. Antonelli, N. Muchhala, A. Timmermann, S. Mathews, and C. C. Davis. 2014. Phylogeny, classification, and fruit evolution of the species-rich Neotropical bellflowers (Campanulaceae: Lobelioideae). Am. J. Bot. 101:2097–2112.

León, B. 2002. Significance of August Weberbauer's plant collecting for today's Rio Abiseo. Taxon 51:167–170.

León, B., A. Granda, G. José Roque, and G. Vilcapoma. 2006. A review of Peruvian Phoradendron (Viscaceae) species names published by Paczoski and typified by material collected by Augusto Weberbauer. Taxon 55:513–514.

Luteyn, J. L., E. M. Ortiz, and B. León. 2008. Notes on and lectotypification of Augusto Weberbauer's collections of Peruvian Ericaceae. Rev. Peru. Biol. 15:127–134.

Stein, B. A. 1987. Systematics and evolution of Centropogon subgenus Centropogon (Campanulaceae-Lobelioideae). Washington University.

Velarde, N. O. 1968. Catálogo de isótipos de la colección de plantas peruanas de A. Weberbauer que se conserva en el herbario de la Universidad Agraria del Perú. Raymondiana 1:89–104.

Velarde, N. O. 1969. Catálogo de isótipos de la colección de plantas peruanas de A. Weberbauer que se conserva en el herbario de la Universidad Agraria del Perú. Raymondiana 2:115–147.

Weberbauer, A. 1911. Die Pflanzenwelt der peruanischen Anden. Pp. 1–355 *in* A. Engler and O. Drude, eds. Die Vegetation der Erde, vol. 12. Wilhelm Engelmann, Leipzig.

Weberbauer, A. 1945. El Mundo Vegetal de los Andes Peruanos. Ministerio de Agricultra, Lima.

Weberbauer, A. 1936. Phytogeography of the Peruvian Andes. Pp. 18–36 *in* J. F. Macbridge, ed. Flora of Peru, Part I.

Wimmer, F. E. 1968. Campanulaceae-Lobelioideae supplementum et Campanulaceae-Cyphiodeae. Pp. 815–1024 *in* S. Danert, ed. Das Pflanzenreich IV.276c. Akademie-Verlag, Berlin.

Wimmer, F. E. 1953. Campanulaceae-Lobelioideae, II. Teil. Pp. 261–814 *in* R. Mansfeld, ed. Das Pflanzenreich IV.276b. Akademie-Verlag, Berlin.

Wimmer, F. E. 1943. Campanulaceae-Lobelioideae. I. Teil. Pp. 1–260 *in* R. Mansfeld, ed. Das Pflanzenreich IV.276b. Wilhem Engelmann, Leipzig.

Wimmer, F. E. 1935. Lobelioideae Novae. II. Repert. Specierum Nov. Regni Veg. 38:75–87.

Wimmer, F. E. 1924. Lobelioideae. II. Repert. Specierum Nov. Regni Veg. 19:211–265.

Wimmer, F. E. 1929. Studien zu einer Monographie der Lobelioïdeen (Lobelioïdeae IV). Repert. Specierum Nov. Regni Veg. 26:1–20.

Zahlbruckner, A. 1906. Campanulaceae andinae in Plantae novae andinae imprimis Weberbauerianae. I. Bot. Jahrbücher für Syst. Pflanzengeschichte und Pflanzengeographie 37:451–463.